Examination of the Role of the K-*ras* Isoforms in Development and Neoplasia

Sarah J. Plowman

PhD

University of Edinburgh

2002

Declaration

This thesis and the research described herein is solely my own work. Any collaborative work or assistance from others is explicitly acknowledged at the relevant point within the text.

Sarah J. Plowman, September 2002

List of Figures

List of Tables

Abstract

The results detailed in this thesis were aimed at elucidating further the role of the isoforms of the proto-oncogene K-Ras in development and the implications of deregulated K-*ras* isoform function in tumorigenesis.

In order to investigate the role of K-*ras* isoforms *in vitro* ES cells with the genotype K-*ras*$^{+/tm\Delta 4A}$ were generated by gene targeting of ES cells by homologous recombination using a targeting vector that deleted the K-*ras* exon 4A, and hence homozygous ES cells of genotype K-*ras*$^{tm\Delta 4A/tm\Delta 4A}$ were derived. These cells enabled the dissection of the role of K-*ras* 4A in cellular functions including proliferation, differentiation and apoptosis, highlighting functional differences between the K-Ras isoforms. Analysis of cell cycle parameters in ES cell cultures showed that both K-Ras protein isoforms were dispensable for proliferation and regulation of cell cycle checkpoints. However, K-Ras 4B was critical for the differentiation of ES cells following LIF withdrawal. Inactivation of both K-*ras* isoforms together in ES cells resulted in a reduced requirement for LIF and maintenance of the ability to undergo stem cell renewal, while deletion of K-*ras* 4A alone did not do so. The K-Ras 4A protein was found to be critical for initiation of apoptosis. Whilst K-*ras*$^{tm\Delta 4A/tm\Delta 4A}$ ES cells do undergo apoptosis following treatment with etoposide they suffer a delay. Investigation in to the pathways involved suggested that this might be due to the failure of the K-Ras 4A protein to generate appropriate pro-apoptotic signals *via* pathways such as the MAPK pathway to counteract the anti-apoptotic signals generated via the PI-3Kinase pathway in these cells.

The K-*ras* gene products are critical for mouse development, since K-*ras*$^{-/-}$ mice are unable to complete embryogenesis. To examine the role of K-*ras* 4A in mouse development K-*ras* $^{+/tm\Delta 4A}$ mice were produced by blastocyst injection of the targeted ES cells. These mice are viable and fertile with no overt abnormalities. Breeding for animals homozygous for the *tmΔ4A* mutation is on going at the time of writing. This will provide a powerful tool to investigate the requirement of the K-Ras 4A protein during embryonic development.

Investigation of the expression of the K-Ras proteins in human tumours showed that the K-Ras 4A and K-Ras 4B proteins are expressed in colon adenocarcinomas with known K-*ras* mutations. In particular K-Ras 4A protein expression was up-regulated in these tumours compared to normal colon. In cervical intraepithelial neoplasia the expression of the K-Ras isoforms is lost.

The expression of the K-Ras 4B protein was investigated during mouse development. This investigation highlighted tissue specific regulation during embryonic development and regulation was found to continue in neonatal and adult tissues.

These studies provide insight into the possible differential regulation of cellular functions by the K-Ras proteins, since activating mutations occur within codons shared by the K-Ras isoforms these findings highlight the possibility of the synergistic interaction of protein function in the development of cancer.

Acknowledgements

I would like to acknowledge the Medical Research Council and the Melville Trust who jointly funded this research, and to whom I am grateful for the support of this project. I would like to thank my supervisors Professor Martin Hooper, Dr Charles Patek and Dr Mark Arends for all their help and guidance over the years and more recently for their helpful comments during the writing of this thesis.

I would like to thank Professor David Melton for the gift of the wonderful HM-1 ES cells, and for his help and advice on matters regarding ES cells and gene targeting.

For those in the lab my special thanks go to Rachel for all her help with too many things to mention. To Jennifer, whose expertise in the form of microinjection was fundamental to this project. Ann-Marie, for her help and advice with ES cell culture and flow cytometry, and to Paul for looking after my special babies while I have been busy writing this thesis. Also to Marion, Roberta, Derek, Andrew, CarolAnne, Yvonne and everyone else for making the lab a great place to come to work every day.

I would also like to say a special thank you to Julie for putting up with me over this last year. I haven't been much fun to live with, but she stuck in there and has been a great flatmate, always ready with a bottle of wine at a moments notice! Also Satoko and Anna for being great friends and understanding exactly what it's all about.

Finally, my heart felt gratitude goes out to my parents for supporting me in all my decisions over the years, even when it looked like I would never leave university! They gave me my strength to carry on by believing in me and were always willing to listen for hours at a time to my ups and downs, living every anxious moment with me. Thank you again.

List of Abbreviations

ABC	Avidin Biotin Complex
ACF	Aberrant Crypt Foci
AJ	Adherens junction
AMP	Ampillicin
AP-1	Activator Protein-1
APC	Adenomatous Polyposis Coli
BSA	Bovine Serum Albumin
bp	base pair
CaM	Calmodulin
Cav^{DGV}	Caveolin dominant negative mutation
CDI	Cyclin Dependent Kinase Inhibitor
cDNA	Complimentary Deoxyribonucleic Acid
CDK	Cyclin Dependent Kinase
CEA	Carcinoembryonic Antigen
CIN	Cervical Intraepithelial Neoplasia
cpm	counts per minute
CREB	cAMP Response Element Binding Protein
DAB	Diaminobenzidine
dCTP	Deoxycytosine Triphosphate
DEPC	Diethylpyrocarbonate
DMSO	Dimethyl Sulfoxide
DNA	Deoxyribonucleic Acid
dNTP	Deoxynucleotide Triphosphate
DTT	Dithiotheitol
E	Embryonic day of development
EC	Embryonal Carcinoma Cells
EDTA	Diaminoethanetetra-Acetic Acid
EGF	Epidermal Growth Factor
ER	Endoplasmic Reticulum
ERF	Ets Repressor Factor
ERK	Extracellular-signal-Regulated Kinase
ES cells	Embryonic Stem cells
FasL	Fas Ligand
FasMAb	Fas Monoclonal Antibody
FCS	Fetal Calf Serum
FGF	Fibroblast Growth Factor
FTI	Farnesyltransferase Inhibitors
G418	Geneticin
GAP	GTPase Activating Proteins
GDP	Guanine Nucleotide Diphosphate
GEF	Guanine Nucleotide Exchange Factors
GFP	Green Fluorescent Protein
GGTI	Geranylgeranyltransferase I Inhibitors
Grb2	Growth Factor Receptor Bound Protein 2
GSK-3	Glycogen Synthease Kinase 3
GTP	Guanine Nucleotide Triphosphate
H-*ras*	Harvey-*ras*

HCG	Human Chronic Gonadotrophin
HOME	Highly Optimised Microscope Environment
HRPO	Horse Radish Peroxidase
HPRT	Hypoxanthine Phosphoribosyltransferase
HSV-*tk*	Herpes Simplex Virus-*thymidine kinase*
HVR	Hypervariable Region
IEG	Immediate Early Gene
IGF-1	Insulin-like Growth Factor-1
IgG	Immunoglobulin G
IKKα	IκB Kinase complex
IL-3	Interleukin-3
JNK	c-Jun NH2-terminal Kinase
K-*ras*	Kirsten-*ras*
Kb	Kilobases
KDa	KiloDaltons
LI	Large Intestine
LIF	Leukaemia Inhibitory Factor
LIFR	Leukaemia Inhibitory Factor Receptor
LOH	Loss Of Heterozygosity
LoxP	Locus of crossover of P1
MAPK	Mitogen-Activated Protein Kinase
MEF	Mouse Embryonic Fibroblasts
MEK	Mitogen-Activated Protein Kinase/ERK
MMP	Matrix Metalloproteinase
mRNA	messenger RNA
MTT	3[4,5-Dimethylthizol-2-oyl]-2,5-diphenyltetrazdium bromide
MuSV	Murine Sarcoma Virus
NCS	New born Calf Serum
neo^r	neomycin resistance cassette
NF1	Neurofibromatosis Type 1
NF-κB	Nuclear Factor κ B
NGF	Nerve Growth Factor
NIK	NF-κB-Inducing Kinase
OD	Optical Density
PA	Phosphatidic Acid
PAK	p21 Activated Kinase
PAS	Periodic Acid-Schiff stain
PBS	Phosphate Buffered Saline
PC	Phosphatidylcholine
PCR	Polymerase Chain Reaction
PDGF	Platelet Derived Growth Factor
PE	Parietal Endoderm
PGK	Phosphoglycerate Kinase
PI	Propidium Iodide
PI-3Kinase	Phosphoinositol-3-Kinase
PK	Proteinase K
PKB	Protein Kinase B
PKC	Protein Kinase C
PLD1	Phospholipase D1
PMS	Pregnant Mares Serum

polβ	Polyermase β
pp	postpartum
PrE	Primitive Endoderm
PS	Phosphatidyl Serine
RA	all trans Retinoic Acid
Rb	Retinoblastoma
RE	Restriction Enzyme
RFLP	Restriction Fragment Length Polymorphism
RNA	Ribonucleic Acid
rpm	revolutions per minute
RT	Reverse Transcriptase
RT-PCR	Reverse Transcriptase-Polymerase Chain Reaction
SDS	Sodium Dodecyl Sulphate
sem	standard error of the mean
SH domains	Src Homology domains
mSos	mammalian Son of sevenless
smg GDS	small G protein GDP Dissociation Stimulator
SRF	Serum Response Factor
St	Stomach
SV-40 TAg	Simian Virus-40 T antigen
TBE	Tris Boric acid EDTA
TCA	Trichloroacetic Acid
TE	Tris EDTA
TNFα	Tumour Necrosis Factor α
TNFR	Tumour Necrosis Factor Receptor
TPA	12-O-tetradecanoylphorbol-13-acetate
TRIZMA	Tris(hydroxymethyl)aminomethane
U	Units
UTR	Untranslated Region
U.V-c	Ultra-Violet light -c
VEGF	Vascular Endothelial Growth Factor

Chapter 1

Introduction

The research detailed here was aimed at elucidating the role of the K-*ras* gene products in development and neoplasia. This took the form of investigations into the differences between the isoforms of K-*ras* to highlight the functional differences of these two proteins.

The Ras superfamily is a diverse group of guanine nucleotide binding proteins, which function as important switches in cellular signalling events, by binding guanine nucleotides, which determine the activity of the protein. Although they are known to function in the growth and differentiation of cells their exact physiological functions are still poorly understood. However, it is known that *ras* gene mutations are present in approximately 30% of all cancers, supporting the view that inappropriate activation of these genes is an important step in the path of cancer development.

1.1 The *ras* gene family

The *ras* genes encode 21KDa proteins, which are present in all eukaryotes including yeast, and have a high degree of conservation between species. Humans and rodents encode three functional *ras* genes K-, H-, and N-*ras*. These three genes share a large degree of structural homology. Functional homology between species has also been demonstrated, since human *ras* genes are able to rescue *ras* deficient yeast cells (reviewed Lowy and Willumsen, 1993). Other members of the Ras protein family include R-Ras, TC21 (R-Ras2) and M-Ras (R-Ras3), which are believed to constitute a subfamily (Kimmelman *et al.*, 1997) and also genes that encode the Ral, Rap, and Rho families of proteins (reviewed Denhardt, 1996).

The mutated *ras* genes were identified by their ability to transform NIH/3T3 cells after DNA transfection (reviewed Bos *et al.*, 1989). Viral oncogenes of certain acute transforming retroviruses were the first to be identified (v-*ras*). The H- and K-*ras* genes were identified as human homologs of the v-H-*ras* of Harvey (Ha) and the v-K-*ras* of Kirsten (Ki) murine sarcoma viruses (MuSV) respectively. N-*ras* was found in a

neuroblastoma cell line as a transforming gene with homology to the other *ras* genes. The genes are unlinked and map to different chromosomes: H-*ras* maps to chromosome 11, K-*ras* to chromosome 12 and N-*ras* to chromosome 1 in humans and these genes map to chromosomes 7, 6 and 3 respectively in the mouse (reviewed Barbacid, 1987).

Although the *ras* genes differ in their overall gene size due to variations in intron length, the arrangement of the exons is very similar. The mammalian *ras* genes have a 5' non-coding exon and four coding exons. The fourth exon encodes the heterogeneous region, and the exons encode the same part of the protein for each gene (reviewed Lowy and Willumsen, 1993). Initiation of transcription occurs at multiple start sites within a GC-rich promoter region that lacks a TATA or CCAAT box in common with other housekeeping genes (Hoffman *et al.*, 1987). H-*ras* has an alternative splice site, which results in the translation of a protein called p19 and it has been hypothesised that this may have an inhibitory function (Codony *et al.*, 2001). K-*ras* is unique, as it contains two alternative fourth coding exons 4A and 4B respectively. This leads to the production of two proteins K-Ras 4A and K-Ras 4B by alternative splicing (Capon *et al.*, 1983; McGrath *et al.*, 1983). The diagrammatic representation of the gene structure and resulting mRNA following alternative splicing are depicted in figure 1.1.

Two separate K-*ras* homologues exist in the human genome c-K-*ras* 1 and c-K-*ras* 2. c-K-*ras* 1 is a pseudogene and appears to be a processed version of c-K-*ras* 2 probably generated *via* a mature c-K-*ras* 2 mRNA intermediate (McGrath *et al.*, 1983). The c-K-*ras* 1 pseudogene has a high degree of homology to the K-*ras* 4B sequence, whereas the sequence of the K-*ras* 4A product is highly homologous to v-K-*ras*, there is in fact only a single conservative amino acid difference distinguishing the two within the sequence derived from exon 4A (McGrath *et al.*, 1983). The complete murine K-*ras* gene sequence, which is approximately ~38Kb is available as part of the mouse genome project (http://www.ncbi.nlm.nih.gov accession number AC019026).

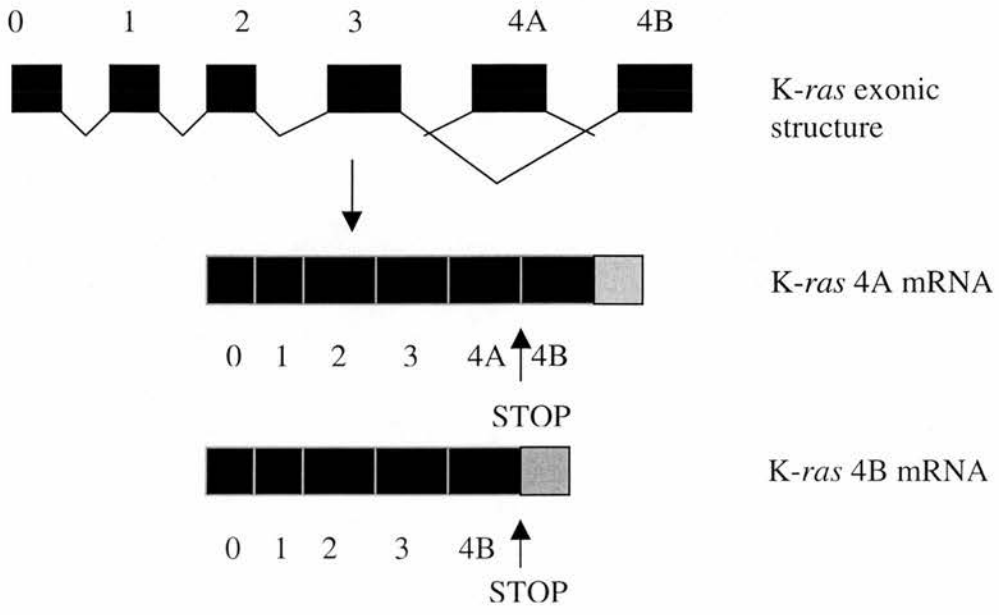

Figure 1.1. Diagrammatic representation of the exonic structure of the K-*ras* gene. The K-*ras* gene encodes five coding exons. The diagram shows the alternative splicing to the two fourth coding exons. The K-*ras* 4A mRNA is larger than that of the K-*ras* 4B mRNA, as it contains the transcribed exon 4B sequence. However, a translation stop site at the end of the exon 4A means that this sequence is not translated. Both transcripts also contain a 3' untranslated region (UTR) downstream of exon 4B.

1.2 Ras Proteins

The K-Ras 4A, N-Ras and H-Ras proteins are all 189 amino acids long, the K-Ras 4B protein is one amino acid shorter at 188 amino acids long. (Lowy and Willumsen, 1993). Analysis of the amino acid sequence encoded by these genes suggests that they show a high degree of homology in their first 164 amino acids (figure 1.2). This region contains the effector, exchange factor and guanine nucleotide binding domains. Based on primary sequence comparisons, Ras proteins can be viewed as consisting of three contiguous regions. The first region encompasses the N-terminal 86 amino acids, which are 100% identical among different Ras proteins. Within this region lies the Ras effector domain (amino acids 32 to 40), which is the critical interaction site with all known downstream targets of Ras. The next 80 amino acids define a second region where mammalian Ras proteins diverge only slightly from each other, exhibiting an 85% homology between any protein pair. The third region shows significant divergence and is the last 24/25 amino acids of the protein. This region is termed the hypervariable region (HVR). There appears to be strong selective influences operating in this heterogeneous C-terminal region, as this shows strong conservation between species (Lowy and Willumsen, 1993). The heterogeneity in the C-terminal may be important in explaining observed functional differences between Ras proteins. This region undergoes posttranslational modifications and is important for membrane localisation; it is therefore possible that this could result in unique membrane localisation sites for the individual isoforms.

1.3 Posttranslational modifications

The Ras protein is synthesised in the cytoplasm as pro-p21, which then undergoes post-translational modifications. The modification of the Ras proteins increases the hydrophobicity of the molecule and therefore membrane binding affinity, which is essential for their activity (Jackson *et al.*, 1994). Until recently it was thought that to be biologically active, Ras proteins must be located at the inner surface of the plasma membrane, where they effectively interact with their upstream activators and downstream targets. However, recent research has challenged this hypothesis showing Ras signalling can occur on other membranes as well, which is associated with signalling pathway specificity (Chiu *et al.*, 2002).

The HVR contains two signal sequences that cooperate to target the proteins to the plasma membrane. The first of these is the CAAX (C cysteine; A aliphatic acid; X serine or methionine) motif at the carboxyl terminal. The CAAX motif is modified sequentially: the cysteine residue is farnesylated, the AAX sequence removed by proteolysis and the now C-terminal cysteine is carboxymethylated. The carboxyl methylation of the isoprenylcysteine is important for the correct localisation of the Ras proteins to the plasma membrane (Bergo *et al.*, 2000). In cells deficient for the isoprenylcysteine carboxyl methyltransferase the Ras proteins remain trapped in the cytoplasm. In addition, K-Ras 4A, H-Ras and N-Ras are then palmitoylated at upstream cysteine residues (cysteine 181 of N-Ras, cysteines 181 and 184 of H-Ras and cysteine 180 of K-Ras 4A) (Hancock *et al.*, 1989). Whilst polyisoprenylated but non-palmitoylated H-Ras proteins are biologically active and associate weakly with cell membranes, palmitoylation increases the avidity of this binding (Hancock *et al.*, 1989). These cysteine residues in the K-Ras 4B sequence are substituted by a polybasic domain consisting of six lysine residues (175-180) (Hancock *et al.*, 1990, 1991). This polylysine domain acts as the second signal sequence of K-Ras 4B. These signals alone are sufficient to target the Ras proteins to the plasma membrane (Hancock *et al.*, 1991). An important consequence of this is that the membrane anchors of these Ras protein isoforms are all different, and correct membrane localisation is important for biological activity of these proteins.

The K-Ras 4B isoform has been shown to be a substrate for geranylgeranylation as well as farnesylation *in vitro* and possibly also *in vivo* (James *et al.,* 1995, 1996; Lerner *et al.*, 1995). More recently it has been shown that K-Ras 4B can be geranylgeranylated *in vivo* when cells are subjected to specific farnesyltransferase inhibitors (FTIs) (Rowell *et al.*, 1997), although under normal circumstances K-Ras 4B was shown to be farnesylated. H-Ras however does not undergo geranylgeranylation when treated with FTIs (Rowell *et al.*, 1997).

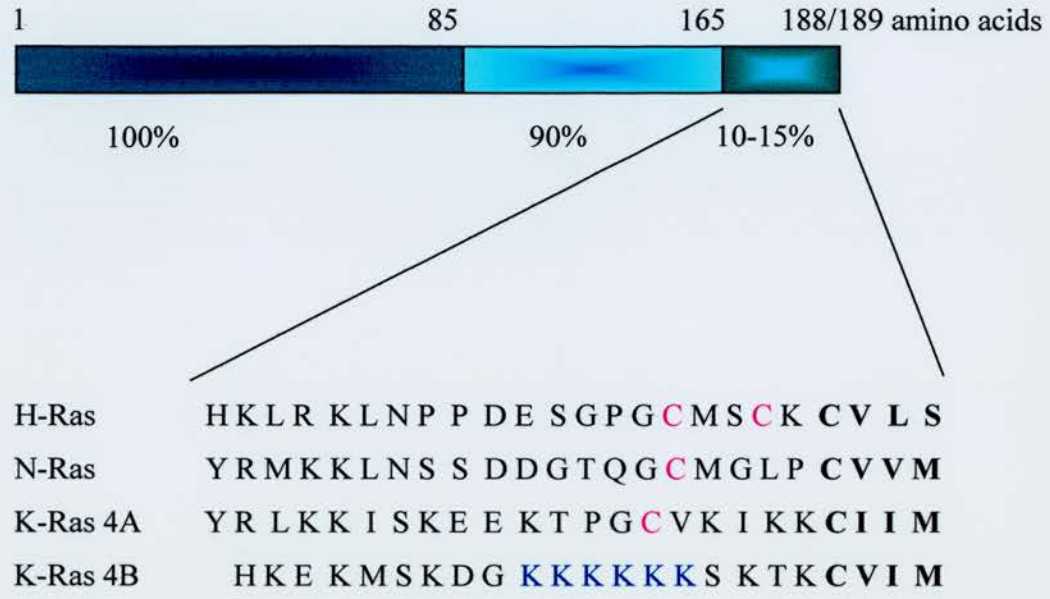

Figure 1.2. Diagrammatic representation of the Ras protein showing regions of homology and the sequence of the HVR for the Ras isoforms. The consensus CAAX sequence directs posttranslational modifications. H-Ras, N-Ras and K-Ras 4A then undergo additional palmitoylation at the downstream cysteine residues, which mediates membrane localisation and anchoring. K-Ras 4B interacts with the plasma membrane *via* its polybasic region.

1.4 Membrane Trafficking

The current view of Ras membrane trafficking is that the Ras proteins are prenylated in the cytosol and then translocated to the endoplasmic reticulum (ER) for further processing, as the protein prenyltransferases are cytosolic, and both the endoprotease and the Ras methyltransferase are located in the ER (Ashby *et al.*, 1998; Dai *et al.*, 1998; Schmidt *et al.*, 1998). Since methylesterification is the final CAAX modification, this suggests that CAAX processing is completed on the cytoplasmic leaflet of the ER membrane. Ras proteins are then targeted to the plasma membrane. However, K-Ras 4B is diverted from the classical exocytic pathway proximal to the Golgi apparatus, unlike the other Ras proteins (Choy *et al.*, 1999; Apolloni *et al.*, 2000). The second signal in the form of the polybasic region appears to be required for the clearing K-Ras 4B from the ER and excluding it from the Golgi apparatus, whereas the palmitoylation signal of N-Ras and H-Ras appears to be responsible for their trafficking through the Golgi apparatus to the plasma membrane (Choy *et al.*, 1999; Apolloni *et al.*, 2000). Therefore, the second membrane signal is not important for endomembrane association, but for the subsequent trafficking out of the endomembrane system. Importantly, when taken together these two studies show that the C-terminal motifs of the HVR contain all the appropriate signals for correct membrane localisation of these proteins. Moreover, they demonstrate that the palmitoylated proteins H-Ras and N-Ras use the same trafficking pathway, but that the polybasic region of K-Ras 4B appears to direct this protein to an alternative trafficking pathway.

A search for factors involved in the intracellular trafficking of K-Ras identified a specific and prenylation-dependent interaction between K-Ras 4B and tubulin/microtubules. This association is specific to K-Ras 4B, since H-Ras and other prenylated proteins do not bind. The location of newly synthesised K-Ras 4B was disrupted by the treatment of the cells with either paclitaxel or taxol, leading to an accumulation of the protein intracellularly, rather than at the plasma membrane as seen in untreated cells (Thissen *et al.*, 1997, Apolloni *et al.*, 2000). The localization of H-Ras was not disrupted by this treatment, nor was that of N-Ras, which still showed the predominant plasma membrane localization (Chen *et al.*, 2000). The polylysine domain immediately upstream of the prenylation site is important for this interaction, since the loss of this region meant that K-Ras 4B trafficking was no longer susceptible to

disruption by treatment with paclitaxel (Chen *et al.*, 2000). Therefore, the intact microtubule network is necessary for K-Ras 4B to transit the cell, apparently uniquely so for this protein. This could imply that K-Ras 4B has a direct interaction with the microtubule network, although there is not a consensus for this (Chen *et al.*, 2000; Apolloni *et al.*, 2000). Whilst the trafficking of the K-Ras 4A protein was not explored in this series of experiments, it seems likely that this protein would traffic in a manner similar to N-Ras and H-Ras *via* the ER due to its palmitoylation modifications.

1.5 Membrane Localisation (Plasma membrane microdomains)

The plasma membrane can be divided simplistically into lipid raft and non-raft compartments. Evidence has shown that H-Ras is localised to caveolae and non-caveolae lipid rafts and K-Ras 4B to an unidentified, non-caveolae region (Roy *et al.*, 1999; Prior *et al.*, 2001). Motility studies using GFP-K-Ras with a codon 12 activating mutation (G12V) (see section 1.6) also confirm that K-Ras is unlikely to be restricted to such regions (Niv *et al.*, 1999). The use of dominant-negative caveolin mutants (Cav^{DGV}) showed that whilst the activation of membrane recruited Raf by H-RasG12V was blocked by Cav^{DGV} little effect was seen on K-RasG12V-catalysed Raf activity (Roy *et al.*, 1999). This appears to be the result of depletion of cholesterol from the plasma membrane. The interaction of H-Ras with lipid rafts is GTP-dependent, since GTP binding causes H-Ras to disassociate with the lipid raft (Prior *et al.*, 2001). Raf activation by H-Ras occurs more potently in non-raft fractions. Association of H-Ras with cholesterol rich microdomains has been shown to be important for MAPK activation following stimulation with insulin (Rizzo *et al.*, 2001) and that endocytosis and activation of the MAPK pathway are coupled. Following insulin stimulation internalisation of cholesterol rich regions of the plasma membrane with which Ras, Raf and MAPK are associated occurs (Rizzo *et al.*, 2001). The association of Ras with endocytosis following insulin stimulation is dependent upon C-terminal modifications, as GFP- tagged C-terminal amino acids mimic the response of the full-length protein (Rizzo *et al.*, 2001). However, it must be noted that Raf can be activated when targeted to either raft or non-raft regions of the plasma membrane (Chen *et al.*, 2001), suggesting that Raf activation is not dependent upon membrane microdomains. ERK activation was not correlated to raft localisation. Therefore, while H-Ras has a relatively tightly controlled although dynamic association with specific cholesterol-rich regions of the

plasma membrane, K-Ras appears to have no such restrictions upon its lateral movement within the plasma membrane. Therefore, differential membrane localisation may be one of the physiological mechanisms underlying biological differences between Ras proteins.

1.6 Biochemical Activity

The Ras proteins are members of the small guanine nucleotide binding protein family and as such Ras proteins bind guanine nucleotide triphosphates (GTP) and guanine nucleotide diphosphates (GDP) with high affinity. The activity of the Ras proteins is determined by the guanine nucleotide with which they are associated and they can cycle between active and inactive forms. Ras proteins are in an active conformation if they are bound to GTP and become inactivated when bound to GDP (reviewed Bollag & McCormick, 1991). The guanine nucleotide bound to the Ras protein is determined by at least two groups of proteins, the guanine nucleotide exchange factors (GEF) and the GTPase activating proteins (GAP). In cells most Ras proteins are in the Ras.GDP conformation. The disassociation of Ras from the GDP nucleotide is facilitated by the interaction of Ras with guanine nucleotide exchange factors (GEF). The mammalian homologue of the Drosophila Son of sevenless (mSos) is the archetypal GEF. Since GTP is present at greater concentrations in the cell compared to GDP, once Ras is unbound GTP will bind preferentially (reviewed Bollag & McCormick, 1991).

Regulation of specific Ras protein signal transduction can occur at the level of the GEF. The small G protein GDP dissociation stimulator (smg GDS) has been shown to function as a guanine nucleotide exchange factor (GEF) on a subset of GTPases, including K-Ras 4B (Mizuno *et al.*, 1991; Orita *et al.*, 1993). This GEF has been shown to translocate K-Ras 4B from the membrane to the cytoplasm (Kawamura *et al.*, 1993; Nakanishi *et al.*, 1994). However, recent analysis has shown that smg GDS can interact with H- and N-Ras, although this interaction was exclusive to the nucleotide free form of these proteins and smg GDS was unable to promote nucleotide exchange (Vikis *et al.*, 2002). This suggests that the interaction of smg GDS with K-Ras is qualitatively different from that of H- and N-Ras and may reflect two distinct modes of binding. Furthermore, H-Ras has been shown to interact with the GEF Ras-GRF2, but neither K-, or N- or R-Ras are activated by this GEF (Jones and Jackson, 1998; Gotoh *et al.*,

2001), whereas Ras-GRF1 activates both H-Ras and R-Ras in cells (Gotoh *et al.*, 2001). The signalling specificity of Ras-GFR1 and Ras-GRF2 is mediated by the sequences of the HVR (Gotoh *et al.*, 2001). Therefore, differences in affinity for GEFs may enable H-Ras and K-Ras 4B to associate with a set of molecules distinct from those shared by the other Ras proteins and hence have unique biological outcomes.

Ras proteins have an intrinsic GTPase activity, which limits the activity of the Ras proteins by reducing the length of time the Ras.GTP association lasts. This hydrolysis of GTP to GDP returns the protein to the inactive state. Levels of the Ras.GTP bound form only rise above basal levels under certain circumstances, for example if a cell is stimulated by a growth factor (reviewed Bollag & McCormick, 1991a). Association with GAPs increases the hydrolysis of GTP to GDP dramatically and therefore the transition from active to inactive form. Thus, GAPs are important regulators of the duration of Ras signal transduction. Five mammalian GAPs have been described (Boguski and McCormick, 1993) including $p120^{GAP}$, the archetype for this class of protein and NF1 (the product of the type 1 neurofibromatosis gene). The crystal structure of the Ras-GAP complex has been analysed (Scheffzej *et al.*, 1997). GAPs have been shown to be negative regulators of Ras activity in several cell types (Yao and Cooper, 1995). Specificity between Ras proteins is not limited to positive regulators but also occurs with negative regulators. NF1 exhibits a four-fold greater affinity for H-Ras than N-Ras (Bollag and McCormick, 1991b). The $p190^{GAP}$, which mediates signalling *via* Rho, Rac and CDC42 binds to the $p120^{GAP}$ (Wang *et al.*, 1997), thereby linking the regulation of these two pathways.

Other proposed regulators of Ras biochemical activity include the Ca^{2+}- binding protein calmodulin (CaM). This protein has been shown to have a regulatory effect upon the Ras/Raf/MEK/ERK signalling cascade. In cultured fibroblasts Ca^{2+} and CaM were important for inactivating this pathway (Bosch *et al.*, 1998). The activation of Ras induced by CaM inhibition preferentially leads to the activation of the Ras/Raf/MEK/ERK pathway. It has further been shown that the binding of CaM to Ras is GTP dependent and K-Ras 4B specific (Villalonga *et al.*, 2001). K-Ras 4A, H-Ras and N-Ras were unable to bind to CaM in pull down experiments. This evidence suggests a mechanism by which differential down-regulation of the K-Ras 4B signalling pathways may occur.

Mutational activation of the Ras proteins is associated with point mutations in a number of codons most frequently 12, 13, 59, and 61(reviewed Bollag and McCormick, 1991). Mutations at codon 12 frequently result in an amino acid substitution from glycine to valine (G12V). The mutations in codons 12, 13, 59 and 61 are associated with impaired GTPase activity. These point mutations result in the Ras protein becoming constitutively active, leading to inappropriate signal transduction. Altered nucleotide exchange rates are associated with mutations in codons 16, 17, 116, 119, 144, and 146 (reviewed Bollag and McCormick, 1991). The mutation occurring at codon 17 (RasN17) resulting from a single substitution leads to a dominant inhibitory effect, since RasN17 binds GDP with preferential affinity over GTP, which results in inhibition of endogenous Ras activation by sequestering guanine nucleotide exchange factors. This mutant has been used extensively to study Ras protein function; some of these studies are discussed as part of this literature review.

1.7 Signal transduction pathways

The Ras family members are key regulators of signal transduction pathways connecting cell surface receptors to the nucleus. Ras activates multiple downstream pathways; including Raf-1 and the MAPK cascade, RalGDS and Ral proteins and PI-3Kinase and Rac1. Alterations in the balance of the activity of the pathways may contribute to the differential cellular responses elicited by Ras (figure 1.3).

The most extensively studied of the Ras signalling pathways is the Ras/Raf/MEK (mitogen-activated protein kinase/ERK)/ERK (extracellular-signal-regulated kinase) cascade (reviewed Kolch, 2000). Extracellular or intracellular signals generate the Ras.GTP form. Activated Ras then functions as an adapter that binds to the Raf serine/threonine kinase with high affinity and causes their translocation to the inner surface of the plasma membrane where Raf activation takes place. Raf activation leads to the initiation of a mitogen activated protein kinase (MAPK) cascade that carries signals to the nucleus (McCormick, 1994) and plays a leading role in the mitogenic signal transduction. Raf acts as the MAPKKK (MAPK kinase kinase) and transfers the mitogenic signal by phosphorylation of MEK (MAPKK (MAPK kinase)), which in turn phosphorylates ERK (MAPK). In mammals, there are three isoforms of Raf; c-Raf-1,

A-Raf and B-Raf. Ras proteins have been shown to bind to different Raf isoforms with different affinities, which leads to different levels of activation of the Raf kinase (Weber *et al.*, 2000). However, Raf activation of MEK is not necessary for activation of ERK to occur (Huser *et al.*, 2000), suggesting that the classical idea of the Ras/Raf/MEK/ERK pathway being a linear progression may not be correct. K-Ras 4A and K-Ras 4B have been shown to differ in their abilities to activate the Raf-1 effector protein, with K-Ras 4B activating Raf-1 more efficiently than K-Ras 4A and the other Ras family members (Yan *et al.*, 1998; Voice *et al.*, 1999). Additionally, H-Ras and N-Ras were shown to regulate MAPK activity by different mechanisms *in vivo* (Hamilton and Wolfman, 1998). One of the ultimate targets of the signalling pathway is the nuclear transcriptional machinery, particularly transcription factors such as c-Jun, which is part of the AP-1 transcription factor, c-Myc and Ets (Westwick *et al.*, 1994; Yang *et al.*, 1996; Kerkhoff *et al.*, 1998; Paumelle *et al.*, 2002). Ras can also modulate functional repression of transcription factors for example; the activity of the TTF-1 transcription factor in thyroid cells is repressed *via* direct phosphorylation of TTF-1 at three serine residues by ERK (Missero *et al.*, 2000).

Phosphatidylinositol-3-OH kinase (PI-3Kinase) is a heterodimeric lipid kinase consisting of a p85 regulatory subunit and a p110 catalytic subunit. Multiple forms of PI-3Kinase with distinct mechanisms of regulation and different substrate specificities exist in mammalian cells (reviewed Carpenter and Cantley, 1996). This lipid kinase is responsible for converting phosphatidylinositol (4,5)-bisphosphate to phosphatidylinositol (3,4,5)-triphosphate. Ras directly targets PI-3Kinase in a GTP dependent manner through its effector region, which interacts with the p110 catalytic subunit (Rodrigez-Viciana *et al.*, 1994). The crystal structure of the Ras/PI-3Kinase has been analysed (Pacold *et al.*, 2000). One well-characterised downstream effector of PI-3Kinase is the serine/threonine kinase PKB (protein kinase B)/Akt (reviewed Franke *et al.*, 1997). In quiescent or serum-starved cells, catalytically inactive PKB/Akt resides within the cytosol. Upon stimulation of cells with growth factors and cytokines, PKB/Akt is recruited to the plasma membrane by second messengers in the form of phosphorylated phosphoinositides, which are generated by the phosphorylation of inositol lipids by PI-3Kinase (as described above).

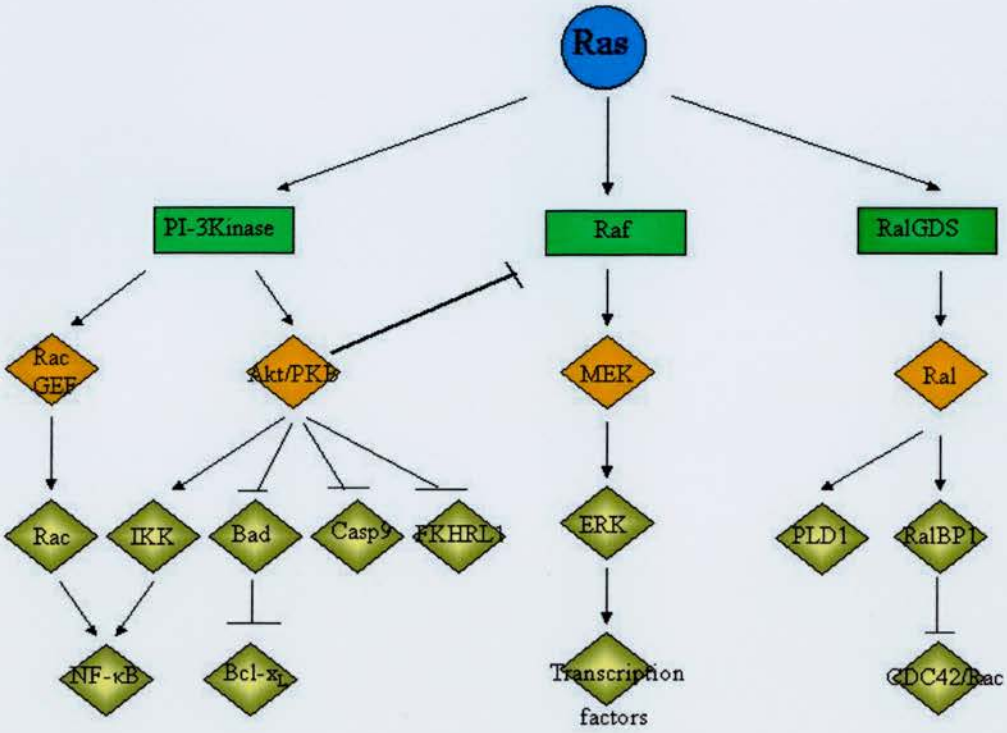

Figure 1.3. Diagrammatic representation of the downstream effectors of Ras signal transduction pathways. RalGDS is activated by direct interaction with Ras and activates Ral A/B proteins by stimulating guanine nucleotide exchange. Ral proteins act as GAPs for Rac and CDC42 and therefore negatively regulate their activity. Ral can also interact with phospholipase D1 (PLD1). Following activation by Ras, Raf phosphorylates and activates the dual specificity kinases MEK1/2, which in turn phosphorylate and activate the ERK1/2 (MAPK), which translocate into the nucleus where they phosphorylate and activate transcription factors such as Elk 1, c-Myc, and c-Jun. Ras interacts with the p110 catalytic subunit of PI-3Kinase, to stimulate its activity. Akt/PKB serine/threonine kinase phosphorylates multiple targets including FKHRL1 a member of the forkhead transcription factor family, the pro-apoptotic protein Bad, and caspase 9 (casp 9) leading to their inactivation. It activates IKK that inactivates IκB resulting in activation of NFκB. PI-3Kinase can also cause activation of Rac and Rac can activate NFκB. Furthermore cross talk can occur between Akt/PKB and the MAPK pathway at various points including phosphorylation and downregulation of Raf activity by Akt/PKB.

At the plasma membrane PKB/Akt is catalytically activated by phosphorylation at threonine^{308} and serine^{473} (Alessi *et al.*, 1996; Stokoe *et al.*, 1997; Stephens *et al.*, 1998; Alessi *et al.*, 1997; Kohn et al., 1996). PI-3Kinase can also activate the Rho GTPases family member Rac (reviewed Scita *et al.*, 2000), which together with Akt facilitates Ras activation of the NF-κB transcription factor (reviewed Shields *et al.*, 2000). Stimulation of cells with tumour necrosis factor (TNF) activates the TNF receptor (TNFR1) and induces tyrosine phosphorylation of the p85 subunit of PI-3Kinase and activation of Akt/PKB, which activates NF-κB by phosphorylation of IκB kinase complex (IKKα), leading to the phosphorylation of IκB and its dissociation from NF-κB, which allows NF-κB to translocate to the nucleus (Ozes *et al.*, 1999). Platelet derived growth factor (PDGF) has also been shown to activate NF-κB *via* Akt/PKB phosphorylation of IKK (Romashkova and Makarov, 1999). Insulin induced the phosphorylation of the forkhead transcription factor AFX by way of both PI-3Kinase Atk/PKB and Ras/Ral signalling pathway *in vitro* and *in vivo* inhibiting its transcriptional activity following growth factor stimulation (Kops *et al.*, 1999). Other targets of Atk/PKB include glycogen synthease kinase-3 (GSK-3) and p70^{S6kinase} (reviewed Franke *et al.*, 1997). Signalling *via* the PI-3Kinase pathway is important for transformation of mammalian cells by activated Ras and essential for Ras-induced cytoskeletal re-organisation (Rodriguez-Viciana *et al.*, 1997). H-Ras is a more potent activator of PI-3Kinase than K-Ras (Yan *et al.*, 1998), this differential activation of pathways may lead to functional differences between these proteins.

The Ras/Raf/MEK/ERK and PI-3Kinase/Akt signalling pathways are further complicated by the observations that cross-talk between these pathways exists. The PI-3Kinase pathway can interact with the Ras/Raf/MEK/ERK at several different levels. PKB/Akt can negatively regulate B-Raf activity through phosphorylation of several residues in its amino terminal regulatory domain (Guan *et al.*, 2000). Raf-Akt cross-talk is regulated in a concentration- and ligand-dependent manner (Moelling *et al.*, 2002). In the presence of high, but not low concentrations IGF-1, PKB/Akt can inhibit Raf kinase activity in MCF-7 cells (Moelling *et al.*, 2002). However, PI-3Kinase can also have a dual inhibitory role up-stream of Ras and ERK activation by low levels of EGF, but not high doses (Wennstrom and Downward, 1999). Furthermore, p21 activated kinase (PAK); a downstream target of PI-3Kinase *via* activation of Rac can

promote stimulation of MEK by phosphorylation on serine[298] (Frost *et al.*, 1996; Frost *et al.*, 1997). K-RasG12V is a more potent activator of Rac-1 *in vivo* then H-RasG12V (Walsh and Bar-Sagi, 2001). The differential activation was elegantly demonstrated to be the result of the Ras HVR. Chimaeric H-Ras proteins generated with the K-Ras C-terminal region caused cells to undergo K-RasG12V responses in terms of membrane ruffling.

Ras also activates a family of guanine nucleotide exchange factors (GEF) for the Ral family of proteins (RalGDS, RGL and Rlf). RalGDS, RGL and Rlf all bind to and are activated by Ras.GTP, which in turn cause the activation of Ral proteins by promoting the release of GDP allowing GTP to bind in its place (reviewed Shields *et al.*, 2000). Activated Ral proteins can influence a variety of cellular processes by interacting with a distinct set of down stream target proteins. These include RalBPI (RLIP) (Cantor *et al.*, 1995; Jullien-Flores *et al.*, 1995; Park and Weinberg, 1995), which binds to a family of related EH domain proteins, Rep 1 (Yamaguchi *et al.*, 1997), POB1 (Ikeda *et al.*, 1998) and the AP2 complex (Jullien-Flores *et al.*, 2000). These associations have implicated Ras function through Ral activation in the regulation of endocytosis (Nakashima *et al.*, 1999). RalBPI also negatively regulates Rac and CDC42 activity, since it can act as a GAP for these proteins and Ral.GTP binds to the actin cross-linking protein filamin (Ohta *et al.*, 1999). Therefore, Ral proteins are likely to be involved in the regulation of the cytoskeleton. Ras proteins are important regulators of phospholipase D (PLD), *via* the RalGDS/Ral A pathway (Voss *et al.*, 1999; Lucas *et al.*, 2000). PLD catalyses formation of phosphatidic acid (PA) from the membrane phospholipid, phosphatidylcholine (PC), linking the RalGDS pathway to the control of vesicular trafficking and cell growth and differentiation. Furthermore, transformation of human cell lines by expression of constitutively active Ras has been associated with signal transduction *via* the RalGDS/Ral pathway, but not the Raf or PI-3Kinase pathways (Hamad *et al.*, 2002).

Furthermore, Chiu and co-workers have recently hypothesised that far from being restricted to the plasma membrane Ras signalling can occur on other membranes including the endoplasmic reticulum and Golgi apparatus and that this may confer signalling specificity to Ras proteins (Chiu *et al.*, 2002). Golgi tethered Ras was more efficient at activating ERK and Akt than c-Jun NH_2-terminal kinase (JNK). In contrast,

Ras tethered to the endoplasmic reticulum activated JNK more efficiently than ERK and Akt.

Mutations within the Ras proteins effector domain, which spans amino acids 32-40 have been characterised, and used extensively for analysis of Ras signal transduction pathways to elucidate the downstream effectors of the signal transduction pathways described above, but also to define the cellular outcomes associated with these pathways. (Joneson *et al.*, 1996; Matsuguchi *et al.*, 1998). These Ras effector mutants are able to signal by only one specific pathway as follows: Ras T35S, couples almost exclusively to the Raf/ERK pathway; Ras Y40C, couples exclusively to the PI-3Kinase pathway and Ras E37G, results in signal transduction *via* RalGDS.

1.8 Regulation of the Cell Cycle by *ras* gene products

The progression of the mammalian cell cycle is controlled by complexes of cyclins and cyclin dependent kinases (CDK). The progression through the G1 phase of the cell cycle is mediated by the sequential activation of D-type cyclins (D1, D2 or D3) in complexes with, either CDK4, or CDK6 and the cyclin E-CDK2 complex. In G0 and early G1 the Rb protein (product of the retinoblastoma susceptibility gene) is hypophosphorylated and functionally active, forming a complex with the E2F-DPI transcription factor, thereby inhibiting the expression of E2F-DPI responsive genes (reviewed by Takuwa and Takuwa, 2001). The Rb protein is phosphorylated by cyclin D-CDK4/CDK6 during mid-G1, finally becoming hyperphosphorylated by cyclin E-CDK2 later in G1, resulting in its inactivation and release of the E2F-DPI transcription factor, leading to the expression of E2F-DPI responsive genes which are required for S phase entry (reviewed in Takuwa and Takuwa, 2001).

Seminal experiments have demonstrated that Ras is essential for the progression of quiescent cells through the G1 phase of the cell cycle into S phase (Mulcahy *et al.*, 1985; Feig and Cooper, 1988; Cai *et al.*, 1990). Following the microinjection of NIH3T3 cells with monoclonal antibodies against cellular Ras proteins, cells were unable to enter S phase following mitogenic stimulation. Closer examination of the requirement for Ras during the G1 phase of the cell cycle indicated that Ras activity was necessary at multiple points during G1 progression, almost until entry into S phase

(Dobrowolski *et al.*, 1994; Aktas *et al.*, 1997). Expression of dominant negative Ras N17 blocked the activation of cyclin D1 and cyclin E dependent kinases and prevented the appearance of the hyperphosphorylated form of Rb in serum stimulated cells, preventing their entry into S phase (Leone *et al.*, 1997), which was associated with inhibition of EF2 mediated gene transcription. The Ras proteins regulate cyclin D1 and cyclin E activity through the downregulation of the CDK inhibitor $p27^{kip1}$ (Aktas *et al.*, 1997) and its dissociation from cyclin E-Cdk2 complexes, which results in phosphorylation of Rb. However, Ras activity was not required for progression through the G1/S phase restriction point in the absence of Rb indicating that the regulation of Rb activity by Ras was a critical target for cell cycle progression to occur (Leone *et al.*, 1997). Nevertheless, the regulation of Rb activity by Ras has an added level of complexity, since the Rb protein has a regulatory role in the activation of Ras proteins *in vitro.* In the absence of Rb, N-Ras and K-Ras had significantly increased activity following serum stimulation of quiescent MEF (Lee *et al.*, 1999). Therefore, Rb may function to downregulate Ras activity *in vitro* in response to serum stimulation.

The requirement of *ras* gene products during the G1 phase of the cell cycle has been intensively studied. Ras activation following growth factor stimulation of quiescent cells is biphasic (Gille and Downward, 1999). The first peak occurring ~30mins after simulation, this is associated with ERK activity. The second peak occurring 2-4hrs after exit from quiescence and is associated with PI-3Kinase activity mediated *via* Akt/PKB, Ral activity and to a lesser extent Rac, which are required for expression of endogenous cyclin D1, E2F activity and S phase entry of NIH 3T3 fibroblasts (Gille and Downward, 1999).

However, the expression of activated *ras* genes in primary cell lines; including primary rat Schwann cells, pheochromocytoma cells, rodent fibroblasts and primary mouse keratinocytes (Bar-Sagi and Feramisco, 1985; Benito *et al.*, 1991; Franza *et al.*, 1986; Ridley *et al.*, 1988; Lin and Lowe, 2001) led to premature G1 cell cycle arrest (figure 1.4).

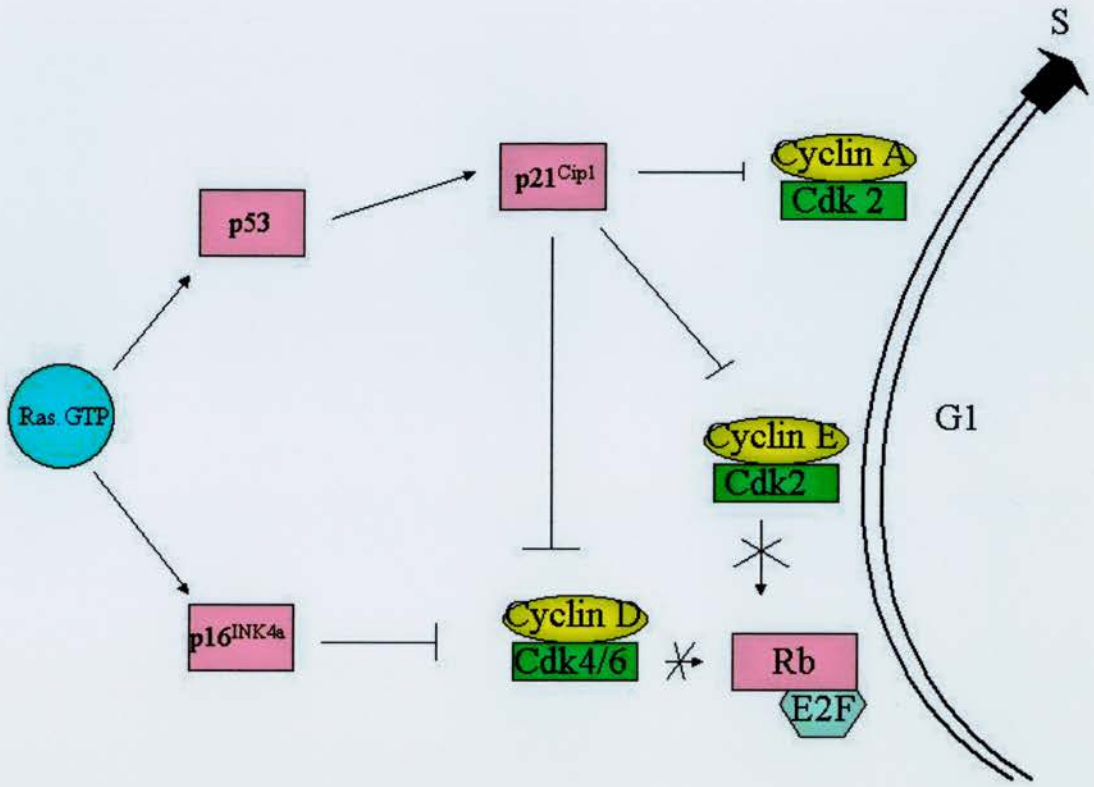

Figure 1.4 Diagram showing the mechanism by which activated Ras induces senescence in non-immortalised cell lines. The expression of activated *ras* genes in non-immortalised cell lines leads to cellular senescence *via* the up-regulation of $p16^{INK4a}$, p53 and $p21^{Cip1}$, which inhibit cyclin D/CDK4/CDK6, cyclin E/CDK2 and cyclin A/CDK2 complexes, preventing phosphorylation of Rb. The hypophosphorylated Rb remains complexed with E2F, preventing E2F dependent transcription and G1/S transition.

The expression of oncogenic *ras* in either primary human or rodent cells resulted in G1 arrest associated with an accumulation of p53, $p21^{cip1}$, $p16^{INK4a}$ and $p19^{ARF}$ and a decline in the levels of hyperphosphorylated Rb, cyclin A and CDK2 kinase activity (Serrano *et al.*, 1997; Lin and Lowe, 2001). Whilst decreases in the abundance of hyperphosphorylated Rb, cyclin A and CDK2 activity are characteristic of G0/G1 cell cycle arrest associated with quiescence, p53, $p21^{cip1}$ and $p16^{INK4a}$ accumulation are not. The up-regulation of these proteins is associated with cellular senescence, suggesting that activated *ras* may be inducing cell-cycle arrest through mechanisms associated with replicative senescence. Cell cycle arrest induced by activated *ras* could be overcome in the absence of either p53 or $p16^{INK4a}$. The introduction of activated H-*ras* into *INK4a*-deficient fibroblasts resulted in neoplastic transformation (Serrano *et al.*, 1996; Serrano *et al.*, 1997). This effect was also abrogated in the absence of $p19^{ARF}$ presumably because the activated Ras protein was unable to efficiently activate p53 (Lin and Lowe, 2001). Further analysis of the mechanisms underlying this growth arrest showed that this it was mediated in part *via* an induction of the CDK inhibitor (CDI) $p21^{cip1}$ by Raf and the subsequent inhibition of cyclin D and cyclin E-dependent kinases and an accumulation of hypophosphorylated Rb protein (Lloyd *et al.*, 1997; Sewing *et al.*, 1997; Woods *et al.*, 1997). Increased $p21^{cip1}$ protein synthesis induced by *ras* expression occurred *via* the MAPK pathway by transcriptional and posttranscriptional mechanisms, in a p53-independent manner (Kivinen *et al.*, 1999; Gartel *et al.*, 2000). Whilst activated Ras leads to increase in $p21^{cip1}$ and cell cycle arrest, Rho acts to down regulate $p21^{cip1}$ in a transcriptional dependent way (Olson *et al.*, 1998). Importantly cellular fate was determined by the intensity of the signal strength, as only higher Raf activity elicited cell cycle arrest, whereas moderate levels of Raf activity led to activation of cyclin D1/CDK4 and cyclin E/CDK2 complexes and cell cycle progression (Sewing *et al.*, 1997; Woods *et al.*, 1997). Whilst the Rb and p107 proteins are both separately dispensable for Ras induced cellular senescence, the absence of both these genes leads to unrestrained proliferation (Peeper *et al.*, 2001) despite the activation of the $p19^{ARF}$/p53 pathway, suggesting that redundancy may exist between members of the Rb family. Another mechanism through which Ras mediates cellular senescence appears to be ubquitin mediated degradation of cyclin D1 (Shoa *et al.*, 2000). Escape from *ras* induced premature senescence requires cooperating mutations in the genes described, such mutations are often present in immortalised cell lines, which leads to the transformation of these cell lines. Therefore, cell cycle arrest is a natural defence to

counter uncontrolled mitogenic signalling, and elimination of this mechanism by the occurrence of additional mutations is critical for transformation and presumably tumour progression.

The expression of activated *ras* genes in immortalised cell lines is associated with a shortening of the G1 phase and acceleration of cell cycle progression (Lui *et al.*, 1995; Winston *et al.*, 1996; Fan and Bertino, 1997) and a reduced requirement for growth factor stimulation. This acceleration in G1 progression is associated with an increased expression of cyclin D1, and accumulation of cyclin D1/CDK4 complexes (Liu *et al.*, 1995; Winston *et al.*, 1996). Activated *ras* induced acceleration of G1 progression could be mimicked by over-expression of cyclin D1 alone (Liu *et al.*, 1994), as cyclin D1 together with its respective CDK phosphorylate Rb and thus inactivate the G1 restriction point control. Examination of the effect of the specific activation of the K-*ras* gene on cell cycle stimulators and inhibitors in a human breast carcinoma line showed that the cell cycle stimulators cyclin A, D3 and E and the E2F family of transcription factors were up-regulated (Fan & Bertino, 1997). Down-regulation of $p27^{kip1}$ and up-regulated p53, which was accompanied by up-regulation $p21^{waf1/cip1}$ and Gadd45 two negative regulators, were also seen. Additionally, up-regulation of Bcl2 was also seen, supporting a role for K-*ras* in apoptosis suppression (Fan & Bertino, 1997). The effect of K-*ras* on the cell cycle therefore appears to rely upon a balance between opposing factors, which may be deregulated in cancer.

Ras may mediate these effects by signal transduction pathways that result in cell cycle dependent alteration of either transcription factor or repressor activity. The Ets repressor factor (ERF) is a ubiquitously expressed transcriptional repressor and member of the Ets family. It is a direct target of ERK, which binds to and phosphorylates ERF at multiple sites (Gallic *et al.*, 1999). ERK-dependent phosphorylation of ERF determines its cellular localisation: upon mitogenic stimuli ERF is immediately phosphorylated and exported from the nucleus to the cytoplasm. Conversely upon serum withdrawal ERF is rapidly dephosphorylated and imported into the nucleus. Mutated ERF proteins that were phosphorylation deficient displayed a predominantly nuclear localisation and resulted in G0/G1 cell cycle arrest (Gallic *et al.*, 1999). This suggests that ERF may be a Ras responsive transcriptional repressor that is important for the control of cellular proliferation. AFX-like Forkhead transcription factors appear

to mediate cell-cycle regulation by Ras through $p27^{kip1}$ (Medema *et al.*, 2000). AFX-mediated transcription is negatively regulated through PI-3Kinase-Akt/PKB and Ras/Ral signalling (Kops *et al.*, 1999).

1.8.1 Cell cycle control in stem cell populations

ES cells, unlike somatic cells, do not undergo exit from the cell cycle following serum withdrawal, but continue to proliferate (Schratt *et al.*, 2001). In the absence of a quiescent state, activation of the immediate early gene (IEG) response by serum response factor (SRF) following signal transduction through the MAPK pathway is dispensable for ES cell growth. This may be explained by the observations that ES cells are not regulated by the normal cell cycle controls. ES cells cycle quickly and have a short G1 phase with an absence of hypophosphorylated Rb protein and an apparent reduction in the overall level of this protein following the exit from mitosis (Savatier *et al.*, 1994). Indeed, the Rb protein is detected mainly in its hyperphosphorylated form in ES cells. In addition, ES cells express very low levels of cyclin E/CDK2 complexes, $p21^{cip1}$ and $p27^{kip1}$ CDIs (Savatier *et al.*, 1996). Cyclin D/CDK 4-associated kinase activity was undetectable and only low levels of cyclin D1 and no cyclin D2 or cyclin D3 were detectable. Furthermore, over-expression of $p16^{INK4a}$, which is associated with activated *ras* induced cell cycle arrest (Serrano *et al.*, 1997) did not cause growth arrest in ES cells (Savatier *et al.*, 1996). Therefore, ES cells are not regulated by the normal cell cycle controls characteristic of somatic cells, but maintain a continuously proliferating population, which is growth factor independent. This has been shown recently to be associated with differential requirement for Ras/MEK/ERK and PI-3Kinase signal transduction pathways (Jirmanova *et al.*, 2002). ERK activity was dispensable for ES cell proliferation and G1 to S phase transition. However, following differentiation of ES cells by retinoic acid (RA) ERK activity was found to be necessary for proliferation. Signal transduction *via* the PI-3Kinase pathway was critical for the proliferation of ES cells and in ES cells induced to differentiate by RA (Jirmanova *et al.*, 2002).

1.9 Differentiation

Ras proteins have been implicated as key regulators of proliferation and differentiation. Ras may be important for the maintenance of a proliferative or stem cell compartment as shown by the role of Ras in the maintenance of ES cell renewal. Activation of the MAPK pathway following cytokine stimulation of the gp130 receptor (Boulton *et al.*, 1994; Ernst *et al.*, 1996; Sheng *et al.*, 1997; Yin and Yang, 1994), suggested that *ras* might be important for the maintenance of ES cell renewal. This was demonstrated directly by the observation that expression of v-H-*ras* reduced ES cell requirement for LIF by approximately 8 fold (Ernst *et al.*, 1996).

A marked inhibition of morphological differentiation induced by nerve growth factor (NGF) and fibroblast growth factor (FGF) is seen in PC12 cells expressing a mutant H-Ras protein (Szeberenyl *et al.*, 1990). High levels of the mutant H-Ras, also inhibited induction of early response genes (fos, jun, and zif268) by NGF and FGF, but not 12-O-tetradecanoylphorbol-13-acetate (TPA).

Approximately day 4.5 post coitum one of the first differentiation processes during mouse embryogenesis takes place in the blastocyst. Some of the cells of the inner cell mass differentiate into primitive endoderm (PrE) and subsequently differentiate into parietal endoderm (PE). Using the F9 embryonal carcinoma (EC) cell line as a model system both of these differentiation processes were found to be mediated by Ras signal transduction. Differentiation to PrE was associated with increased endogenous Ras and ERK activity, whilst differentiation to PE was accompanied by a decrease in endogenous Ras and ERK activity (Verheijen *et al.*, 1999a). Expression of activated *ras* was sufficient to cause differentiation to a PrE-like morphology, but prevented further differentiation to a PE-like morphology following treatment with parathyroid hormone. However, further analysis of the pathways associated with Ras induced differentiation to PrE using Ras effector mutants, showed this this occurred *via* an interdependent action of RalGEFs and ERK (Verheijen *et al.*, 1999b).

Appropriate expression of *ras* genes in the epidermis is also important for correct differentiation. Normal epidermis is a self-renewing tissue composed of stratified epithelium, containing a basal layer of mitotically active cells. Expression of a dominant-negative mutant Ras (N17) by the specific basal layer keratin 14 promoter in

mice caused these animals to have extremely thin skin, which was characterised by terminally differentiated cells (Dajee *et al.*, 2002). However, the expression of activated RasG12V by this same promoter resulted in hyperplasia, and an absence of differentiation. This clearly indicated that spatial localisation of Ras signalling is important for appropriate epidermal tissue proliferation and differentiation. Therefore, it appears that expression of Ras proteins is important for proliferation and controls differentiation at least in part by the appropriate cessation of signalling. Inappropriate signalling as described above overrides the differentiation signals and maintains a proliferative population.

1.10 Regulation of Apoptosis by Ras signalling cascades

Apoptosis is a normal physiological process of programmed cell death that is essential for embryonic development and homeostasis of adult tissues. Disorders of the apoptotic process cause various pathologies, including autoimmune and neurodegenerative diseases (Rinkenberger and Korsmeyer, 1997). The abrogation of apoptotic pathways is vital for cancer development and may influence the tumour's net growth and accumulation of further mutation due to the retention of mutated cells, which would normally undergo apoptosis. Apoptosis is characterised by its morphological features of cell shrinkage and nuclear chromatin condensation and the formation of apoptotic bodies (Kerr *et al.*, 1972), which distinguishes it from other forms of cell death such as necrosis.

One of the early events of apoptosis is the exposure of phosphatidyl serine (PS) upon the surface of apoptotic cells, which triggers specific recognition and removal by macrophages and is important for clearage of apoptotic cells before they rupture (Fadok *et al.*, 1992). PS externalisation is a widespread event during apoptosis regardless of the initiating event (Martin *et al.*, 1995). This underlies one of the most important characteristics of apoptosis: the dying cells are removed quickly without the generation of an inflammatory response. In necrosis however, the dying cell swells and ruptures releasing its contents, which induce an inflammatory response.

Apoptosis is executed by a family of proteins called caspases, which are an evolutionarily conserved class of cysteine proteases that cleave after asparate residues in

target proteins, with homology to the *C. elegans ced-3* gene (reviewed Meier and Evan, 1998). Caspases are produced as inactive zymogen precursors and are activated by cleavage at sites that conform to caspase substrate consensus sequences. Activation of apical caspases appears to occur by an autocatalytic process, these activated caspases then cleave downstream effector caspases, which implement apoptosis by cleaving cellular substrates (reviewed Meier and Evan, 1998).

Another family of proteins exist in vertebrates that are structurally and functionally related to the *C. elegans* death suppressor *ced-9*, the archetypal member of this family being the Bcl-2 protein (reviewed Meier and Evan, 1998). However, this family has been shown to have members that interact with each other to either promote or inhibit apoptosis. The pro-apoptotic Bad in its unphosphorylated state antagonises the anti-apoptotic function of Bcl-2 and Bcl-x_L by forming inactivating Bad-Bcl-2 and Bad-Bcl-x_L heterodimers (Zha *et al.*, 1996), thereby neutralising their protective effect and promoting cell death. Following stimulation with the survival signal IL-3 Bad is phosphorylated, causing Bad to be sequestered to the cytoplasm bound to 14-3-3 (Zha *et al.*, 1996). When uncomplexed with Bad, Bcl-2 and Bcl-x_L are capable of abrogating Bax-mediated apoptosis through the formation of Bax-Bcl-2 and Bax-Bcl-x_L heterodimers (Zha *et al.*, 1996; Reed *et al.*, 1998). In addition, members of this family have been shown to suppress caspase 9 activation through direct interaction with Apaf-1 (Pan *et al.*, 1998). Apaf-1 is the mammalian homologue of the *C-elegans ced-4* gene and acts as an adapter protein for formation of the apoptosome with cytochrome c and caspase 9.

Apoptosis can be initiated by many different stimuli, including death receptors, which are members of the tumour necrosis factor receptor superfamily (Nagata, 1997). These death receptors can induce apoptosis triggered by binding of their ligands and are characterised by the presence of death domains within their cytoplasmic regions, which can interact physically with caspases and receptor oligmerisation by ligand directly initiates the caspase proteolytic cascade (Cohen, 1997). Alternatively apoptosis can be initiated by stimuli that indirectly activate caspases, included in this lists are treatments that induce DNA damage such as etoposide (reviewed McConkey *et al.*, 1998).

1.10.1 Identification of Ras pathways involved in apoptosis

Several lines of investigation suggest that Ras proteins may have an important function in the control of apoptotic pathways. However, there is a great deal of conflicting evidence to whether this is a pro- or anti-apoptotic role. Some of the Ras apoptotic pathways are shown diagrammatically in figure 1.5.

The use of Ras effector-loop mutants has helped to identify those pathways that are involved in pro- and anti-apoptotic Ras-mediated signalling. Expression of activated RasG12V is an effective promoter of apoptosis induced by c-Myc, through the Raf pathway in fibroblasts (Kauffman-Zeh *et al.*, 1997). However, specific activation of the PI-3Kinase pathway alone by a Ras effector loop mutant suppresses apoptosis induced by c-Myc *via* the activation of Akt/PKB in the same cells. This apparently contradictory finding has also been demonstrated in rat thyroid cells. Transformation with RasG12V sensitises the cells to apoptosis induced by matrix detachment, compared to parental cells (Cheng and Meinkoth, 2001). A Ras effector loop mutant that could only signal *via* the Raf/MEK pathway was similarly sensitive, but cells expressing activated Ras able to signal only *via* the PI-3Kinase pathway were no longer sensitive to matrix detachment induced apoptosis (Cheng and Meinkoth, 2001). Thus, demonstrating that RasG12V activates multiple intracellular pathways in response to apoptotic stimuli. Therefore, it can be postulated that the determination of cellular fate results from the synergistic outcome of signalling by these opposing pathways, determined by other unknown modulators. However, it should be noted that in rat fibroblasts Ras activation has been reported to cooperate with activation of c-Myc to cause cellular transformation by inhibiting apoptosis in a Raf/MEK dependent manner (Tsuneoka and Mekada, 2000).

Furthermore, in fibroblasts, treated with FasL expression of K-Ras G12V suppressed apoptosis. The use of effector loop mutants showed that this suppression was mediated by specific signalling *via* the Raf/MEK pathway, and neither the PI-3Kinase nor the RalGDS pathway were capable of mimicking this response (Kazama and Yonehara, 2000).

Therefore, the cell fates determined by these pathways also appear to be dependent upon the cell type, apoptotic stimulus and possibly experimental conditions. Activated Ras

has been shown to promote cell survival in various cell types by signalling through both the Raf/MEK and PI-3Kinase pathways; including sympathetic neurons (Mazzoni *et al.*, 1999, Xue *et al.*, 2000) and murine haematopoietic cells (Kinoshita *et al.*, 1995; Kuribara *et al.*, 1999; Terada *et al.*, 2000). Rat sympathetic neurons are dependent upon Ras signalling for NGF mediated survival. Expression of RasG12V in these cells protects them from apoptosis induced by NGF withdrawal (Xue *et al.*, 2000). However, only signalling *via* the PI-3Kinase pathway protects from apoptosis induced by NGF withdrawal. The Raf/ERK pathway protects from araC induced apoptosis in these cells. Therefore, these two pathways both mediate survival in response to different stimuli with no functional overlap. However, another group showed that Ras suppression of sympathetic neuron survival in the absence of NGF was mediated mainly by PI-3Kinase, but also by Raf-1 (Mazzoni *et al.*, 1999). This survival was as a result of activated Ras suppression of the increases in c-jun, p53 and Bax proteins normally associated with NGF withdrawal.

1.10.2 Regulation of anti-apoptotic signals *via* the PI-3Kinase pathway

Whilst signal transduction through the Raf/MEK pathway can apparently mediate either pro- or anti-apoptotic signals, to date signal transduction *via* the PI-3Kinase pathway has only been implicated in anti-apoptotic responses. The PI-3Kinase effector PKB/Akt has been shown to regulate apoptosis by direct phosphorylation of several components of the apoptotic machinery. PKB-Akt can directly phosphorylate pro-caspase-9 at ser^{196} thereby preventing its activation by the Apaf-1/cytochrome c oligmeric complex (Cardone *et al.*, 1998). PKB/Akt also regulates the activity of FKHRL1, a member of the Forkhead family of transcription factors (Brunet *et al.*, 1999). In the presence of survival signals phosphorylation by PKB/Akt results in association of FKHRL1 with 14-3-3 proteins leading to its sequestering in the cytoplasm, thereby inhibiting FKHRL1-dependent transcription. Withdrawal of survival factors results in dephosphorylation of FKHRL1 and translocation to the nucleus leading to apoptosis possibly by activating transcription from the *fas* ligand gene (Brunet *et al.*, 1999).

Ras can also mediate cell survival signals through PI-3Kinase activation of Akt and/or Rac/Cdc42, which stimulates Pak and leads to phosphorylation of the pro-apoptotic factor BAD (Tang *et al.*, 2000). Furthermore, the PI-3Kinase and Raf/MAPK pathways have been postulated to phosphorylate distinct serine residues of the BAD protein. The

PI-3Kinase pathway phosphorylates BAD at ser^{136} and the Raf/MAPK pathway phosphorylates BAD at ser^{112} (Bonni *et al.*, 1999; Fang *et al.*, 1999). This phosphorylation allows the 14-3-3 protein to interact with and sequester BAD in the cytoplasm resulting in its inactivation (Datta *et al.*, 1997; Zha *et al.*, 1996). Activation by phosphorylation of the cAMP response element binding (CREB) protein by the Raf/MAPK pathway also promoted cell survival; a known transcriptional target of CREB is Bcl-2 (Bonni *et al.*, 1999). Activated Ras has previously been shown to regulate the expression of Bcl-2 and its related survival proteins (Kinoshita *et al.*, 1995). These findings suggest that Ras proteins may promote cell survival by transcription-dependent and -independent mechanisms. The PI-3Kinase pathway can also delay the onset of p53-mediated apoptosis in BRK epithelial cells but cannot prevent it (Sabbatin and McCormick, 1999).

In rat fibroblasts, the pro-apoptotic effects of activated Ras are mediated by concerted activation of the ERK and JNK MAP kinase cascades (Joneson and Bar-Sagi, 1999). However, Rac-mediated signals are necessary and sufficient to protect against Ras-induced apoptosis through a pathway that involves NF-κB activation (Joneson and Bar-Sagi, 1999). PI-3Kinase *via* Akt stimulates NF-κB predominantly by up-regulating the transactivation potential of the p65 subunit in response to H-RasG12V (Madrid *et al.*, 2000). H-RasG12V and constitutively active MEKK1 can stimulate nuclear translocation of NF-κB by increased activity of IκB kinase (IKK) complex and degradation of IκB, but PI-3Kinase does not in this cell type. However, other groups reported that PI-3Kinase activation of NF-κB *via* Akt following stimulation with TNF and PDGF was associated with mechanisms involving IKK-dependent phosphorylation and subsequent degradation of IκB (Ozes *et al.*, 1999; Romashkova and Makarov, 1999). Furthermore, activated K-*ras* has been reported to induce the nuclear translocation and activation of NF-κB through the NIK-IKKβ-IκBα signalling pathway (Kim *et al.*, 2002).

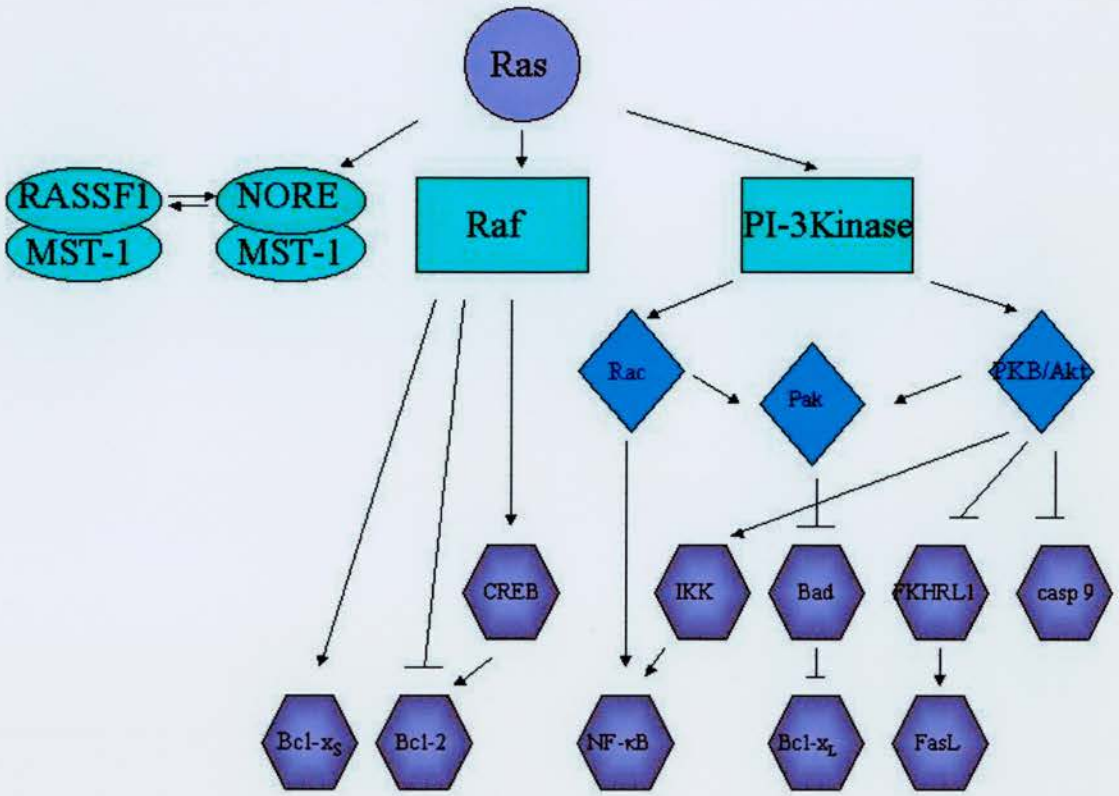

Figure 1.5. The downstream effectors of Ras that regulate both pro- and anti-apoptotic signals. The activation of PI-3Kinase pathway generates anti-apoptotic signals via phosphorylation and inactivation of pro-apoptotic targets such as pro-caspase 9, FKHRL1 and Bad by the serine/threonine kinase Akt/PKB. PI-3Kinase also activates NF-κB regulated gene transcription through Rac and Akt/PKB. The Raf/MEK/ERK pathway can promote either pro- or anti-apoptotic signals possibly though positive and/or negative regulation of members of the Bcl-2 family. The RASSF1/MST1 and NORE/MST1 effectors promote pro-apoptotic pathways although the downstream effects of this pathway have yet to be established.

1.10.3 Ras regulation of the Bcl-2 family of proteins

Ras has also been investigated as an important mediator of murine interleukin-3 (IL-3) mediated cell survival of haematopoietic cells. Activation of Ras resulted in a rapid up-regulation of Bcl-2 and Bcl-x_L in haematopoietic cells (Kinoshita *et al.*, 1995). The survival effects of activated Ras were mediated *via* the MEK and PI-3Kinase pathways (Kuribara *et al.*, 1999). The survival signalling effects of these pathways seem to be associated with suppression of activation of the pro-apoptotic protease caspase-3 upon IL-3 removal (Terada *et al.*, 2000). Other pathways are also postulated to be involved because although the MEK and PI-3Kinase pathways are partly responsible activated Ras still causes suppression of apoptosis even when these pathways are inhibited (Terada *et al.*, 2000).

The expression of a constitutively active *ras* gene in Jurkat T cells renders them susceptible to apoptosis caused by withdrawal of protein kinase C (PKC) (Chen and Faller, 1995), which may be regulated by direct interaction of Ras and Bcl-2 (Chen and Faller, 1996). PKC/Ras mediated apoptosis was cell cycle dependent and required expression of G1/S cyclins (Chen *et al.*, 1998). Further analysis showed that Fas-independent, FADD/caspase-8 signalling is involved in PKC/Ras-mediated apoptosis, and JNK may be an upstream effector of caspase activation (Chen *et al.*, 2001).

K-Ras, H-Ras and N-Ras have all been found to associate with Bcl-2 in the mitochondria (Rebollo *et al.*, 1999). However, their mitochondrial localisation is differentially regulated. In addition, Ras and Raf were also found to be associated with phosphorylated Bcl-2 protein following induction of apoptosis by withdrawal of serum from Ras transformed brown adipocytes (Navarro *et al.*, 1999). Activated H-*ras* sensitised these cells to apoptosis induced by serum withdrawal in a Raf-dependent, but MEK-independent fashion (Navarro *et al.*, 1999). This response was associated with the up-regulation of the pro-apoptotic Bcl-x_S and a down-regulation of the anti-apoptotic Bcl-2.

1.10.4 Novel Ras apoptotic pathway

RASSF1, which is a putative tumour suppressor, binds to Ras in a GTP dependent manner and appears to mediate pro-apoptotic signals generated by activated Ras (Vos *et*

al., 2000). NORE is a non-catalytic protein that binds Ras and several other GTPases in the Ras subfamily in a GTP-dependent manner *in vitro* and *in vivo* and is homologous to RASSF1. Serum and EGF can stimulate the binding of NORE to both endogenous and recombinant Ras in several cell types, clearly demonstrating that NORE is amongst Ras' physiological effectors. MST-1 has the ability to engage in a ternary complex with Ras-GTP and NORE. NORE-MST1 complex has been implicated as a pro-apoptotic effector of constitutively active forms of Ras. In HEK 293 cells over-expression of K-RasG12V efficiently induced cell death. In contrast, over-expression of H-RasG12V did not result in significant cell death. This may be due to the greater activation of PI-3Kinase by H-Ras, since an effector loop mutant of H-Ras, which was unable to bind to either Raf-1 or PI-3Kinase elicited substantial cell death in 293 cells (Khokhlatchev *et al.*, 2002).

1.10.5 Specificity of response by Ras family members to apoptotic stimuli

The evidence cited above clearly indicates that there are important differences in the cellular fate determined by a complex interaction of multiple Ras effector pathways, which is further complicated by cell type and stimulus differences. However, the evidence cited below indicates that an additional level of complexity exists, since the different Ras proteins appear to differentially mediate these responses. K-*ras* can function to promote apoptosis in response to DNA damaging agents. This is best seen in K-*ras* knockout cells, where K-*ras*$^{-/-}$ ES cells and K-*ras*$^{-/-}$ mouse embryonic fibroblasts (MEFs) are more resistant to apoptosis induced by treatment with, either etoposide, or cisplatin, or TNFα in the presence of cycloheximide, compared to their wild-type counterparts (Brooks *et al.*, 2001; Wolfman and Wolfman, 2000). This is further evidenced by rescue strategies introducing, either wild-type K-*ras,* or K-*ras* G12V minigenes into K-*ras*$^{-/-}$ ES cells, which results in sensitivity to apoptotic stimuli comparable to wild-type levels and above respectively (Brooks *et al.*, 2001). Thereby showing that oncogenic K-*ras* G12V in this system is responsible for an increased sensitivity to apoptosis. This maybe as a result of a p53 dependent mechanism, since increased p19^{arf} mRNA levels accompanied the apoptotic response of K-*ras*$^{-/-}$ ES cells expressing the K-*ras* G12V mingene to etoposide treatment (Brooks *et al.*, 2001). In contrast, N-*ras* homozygous null MEFs are more sensitive to apoptotic stimuli than wild-type MEFs (Wolfman and Wolfman, 2000). Therefore, N-*ras* may have an opposing anti-apoptotic function. Analysis of the role of N-*ras* in apoptosis has

revealed that there are several anti-apoptotic mechanisms involved, which provide more than one survival signal (Wolfman *et al.*, 2002). N-*ras*$^{-/-}$ cell lines had elevated JNK and p38 activity. Therefore, it appears that N-Ras provides a second survival signal in addition to up-regulating Akt and Bad levels, by specifically attenuating the magnitude and duration of JNK and p38 activation in response to the induction of apoptosis by down-regulating the upstream kinase activator of JNK and p38 (Wolfman and Wolfman, 2000; Wolfman *et al.*, 2002). H-*ras* appears to be similar to K-*ras,* as transformation of brown adipocytes, leads to increased apoptosis, compared to wild-type cells following serum starvation (Navarro *et al.*, 1999).

This subject is further complicated as it appears that the method of apoptotic induction and the cell system used lead to different results. Oncogenic K-*ras* G12V and v-H-*ras* have been shown to negatively regulate Fas-mediated killing. K-*ras* G12V strongly inhibits Fas mediated apoptosis in Balb3T3 cells *via* the MAPK pathway (Kazama & Yonehara, 2000) and v-H-*ras* inhibits Fas action in NIH3T3 cells and an established mouse mammary epithelial cell line by down-regulating the expression of Fas (Peli *et al.*, 1999). However, Chen and co-workers show that by increasing *ras* activity by either expressing v-*ras* or by inhibiting GAPs with antisense oligonucleotides leads to an acceleration of Fas mediated apoptosis (Chen *et al.*, 1998) in Jurkats and mouse LF cells. Although these results were found in v-H-*ras* transfected cells the authors report that identical results were seen with v-K-*ras* transfected cells, suggesting that functional overlap may occur between these proteins.

1.10.6 Caspase cleavage of downstream components of the Ras signal transduction pathways

One of the clearest indications of the importance of Ras mediated signalling pathways for the suppression of apoptosis is the observation that several of the downstream Ras effectors are substrates for caspase cleavage. Following FasL induced apoptosis Cdc42 and Rac were cleaved by caspase-3 and caspase-7 (Tu and Cerione, 2001). However, Ras itself and Rho were not cleaved. Other Ras effectors cleaved by caspases following apoptotic stimulation by FasL, etoposide and UV c were RasGAP, Raf-1 and Akt (Widmann *et al.*, 1998). The cleavage of RasGAP was also observed in Fas induced apoptosis of Jurkat T cells (Wen *et al.*, 1998). This result clearly demonstrates the importance of turning off Ras-mediated survival signals for appropriate apoptosis.

1.10.7 Ras and apoptosis: implications for tumorigenesis

As detailed above expression of activated *ras* genes in many different cell type results in reduced sensitivity to different types of apoptotic stimuli. This is further supported by observations made by Arends and co-workers showing that the transfection of mutant H-*ras* genes into immortalised rat fibroblasts resulted in reduced levels of apoptosis (Arends *et al* 1993). In addition, following doxorubicin incubation a rat cell line stably transfected with v-H-*ras* also showed reduced apoptosis (Nooter *et al.*, 1995), implying that expression of mutant *ras* genes may promote survival during treatment and therefore lead to a selection of cells harbouring *ras* mutants which have gained a growth advantage. These observations appear to have clinical relevance following the observation that tumours with K-*ras* mutations have a significantly lower apoptotic index than those tumours, which have the wild type allele (Ward *et al.*, 1997), suggesting that K-*ras* has a role in inhibiting apoptosis *in vitro* and *in vivo*. Therefore, K-*ras* mutations potentially drive cancer development by promoting survival of mutant cells.

However, clearly this is not the complete picture, since in an *in vivo* system co-expression of K-Ras G12V and SV-40 T antigen (TAg) in postmitotic villus enterocytes of the small intestine caused cells to undergo apoptosis in a p53-independent manner (Coopersmith *et al.*, 1997). Expression of SV-40 TAg caused the cells to re-enter the cell cycle, since expression of K-RasG12V alone did not cause apoptosis, this indicated that the apoptosis was cell cycle dependent. Furthermore, there is data to indicate that oncogenic Ras elicits an anti-tumorigenic response mediated by the up-regulation of both $p19^{ARF}$ and $p16^{INK4a}$, which in turn activate the tumour suppressors p53 and retinoblastoma respectively (Palmero *et al.*, 1998).

1.11 Gene Targeting and transgenic animal models

The ability to manipulation the genome of an animal for the creation of targeted gene mutations, allows the investigation of proteins *in vivo*. The use of such technology has led to massive steps forward in our understanding of the roles of certain proteins during development and in the maintenance of adult tissues.

Embryonic stem (ES) cells are an integral part of the ability to manipulate the mouse genome. ES cells were first isolated in 1981 (Evans and Kauffman, 1981; Martin, 1981). They were derived from the inner cell mass of preimplantation blastocysts by direct culture *in vitro* and had a pluripotent capacity, which could be maintained despite long term culturing when grown on a layer of STO fibroblasts. Pluripotency was confirmed by their ability to differentiate into a wide variety of cell types either *in vitro* or *in vivo* after inoculation into a mouse as a teratoma. Recent progress has shown that ES cells originate from the epiblast (primitive ectoderm) and isolation of early epiblasts yielded ES cells at a higher frequency than culture of intact blastocysts (Brook and Gardiner, 1997). Further advances were made following the realisation that conditioned medium from Buffalo rat liver cells (BRL) containing an agent differentiation-inhibiting activity (DIA) could substitute for feeders (Smith and Hooper, 1987). The purified cytokine leukaemia inhibiting factor (LIF) maintains the ES cell's ability to contribute to the germline of chimaeric mice (Smith *et al.*, 1988; Williams *et al.*, 1988).

The successful isolation of ES cell paved the way for attempts to alter the mouse genome by homologous recombination. Homologous recombination allows the insertion of foreign DNA into the genome between two arms of homologous DNA. Using a replacement vector chromosomal sequences can be replaced by the vector sequences by a double crossover event involving the flanking homologous regions. The first successful example of this was achieved for the selectable hypoxanthine phosphoribosyl transferase (HPRT) gene locus (Doetschman *et al.*, 1987; Thomas and Cappecchi, 1987). The development of strategies to enrich for homologous recombination such as the integration of the *neomycin* resistance gene (*neo*^{r}) under the control of a strong promoter, subsequently allowed the targeting of non-selectable genes such as int-2 and c-abl (Mansour *et al.*, 1988; Schwartzberg *et al.*, 1989). This type of selection is known as positive selection. The selection can then be enriched for clones that have undergone homologous recombination as opposed to those that have undergone random integration by a strategy known as "positive/negative selection" (Mansour *et al* 1988). In addition to the *neo*^{r} (positive selection) a *thymidine kinase* (*tk*) gene from the Herpes simplex virus (HSV) is inserted at the end of the linearised targeting construct. The cells that have undergone homologous recombination will have lost the HSV-*tk* cassette and therefore will be unaffected by treatment with the nucleoside analogue ganciclovir, whereas cells that have the targeting vector integrated

randomly will retain the HSV-*tk* cassette and therefore will be sensitive to the toxic affects of ganciclovir (negative selection) (figure 1.6). The DNA used to construct the homology arms of non-isogenic targeting vectors is derived from a different mouse strain than the ES cells to be targeted. This leads to a reduced frequency of homologous recombination, which results from strain specific differences in the DNA sequence of the homology arms, compared to the genome. In this scenario, the enrichment resulting from positive/negative selection is particularly important for targeting strategies, to enrich for the low frequency of homologous recombination occurring. However, isogenic targeting vectors do not require this additional selection method, since the efficiency of homologous recombination is much greater.

A potential drawback of this technology could be that the phenotype of the knockout is so severe that it results in an embryonic lethality, making assessment of the function in adult tissues impossible. This has led to the generation of technology to enable tissue specific deletion of a gene of interest at a specific time point, this technology is known as Cre-Lox technology. Cre is the product of the *cre* gene of the bacteriophage P1 (Sternberg, 1978) and is a site-specific DNA recombinase. Cre recognises a 34 base pair site on the P1 genome called locus of X-over of P1 (*loxP*) and catalyses reciprocal conservative DNA recombination between pairs of *loxP* sites (Austin *et al.*, 1981). Cre mediated recombination between two directly repeated *loxP* sites results in the excision of the DNA between them as a covalently closed circle, since it requires no accessory factors or DNA topological requirements Cre-mediated DNA recombination is a useful tool for genomic manipulation of eukaryotic cells (Sauer, 1988). The implementation of this strategy is similar in many ways to that described above, since the target gene is modified by homologous recombination in ES cells so that two loxP sites flank it. Importantly, the offspring resulting from the injection of these ES cells into blastocyst are phenotypically normal. They are then crossed to mice that expression Cre in the tissue of interest and Cre-mediated excision results in the tissue specific ablation of the target gene. This strategy was first reported by Gu and co-workers using a mouse in which the promoter and first exon of the DNA Polymerase β gene (*polβ*) were flanked by *loxP* sites. When crossed with a transgenic mouse, which specifically expressed Cre in T cells the *polβ* gene was inactivated in the T cell population, but not in any other tissue (Gu *et al.*, 1994).

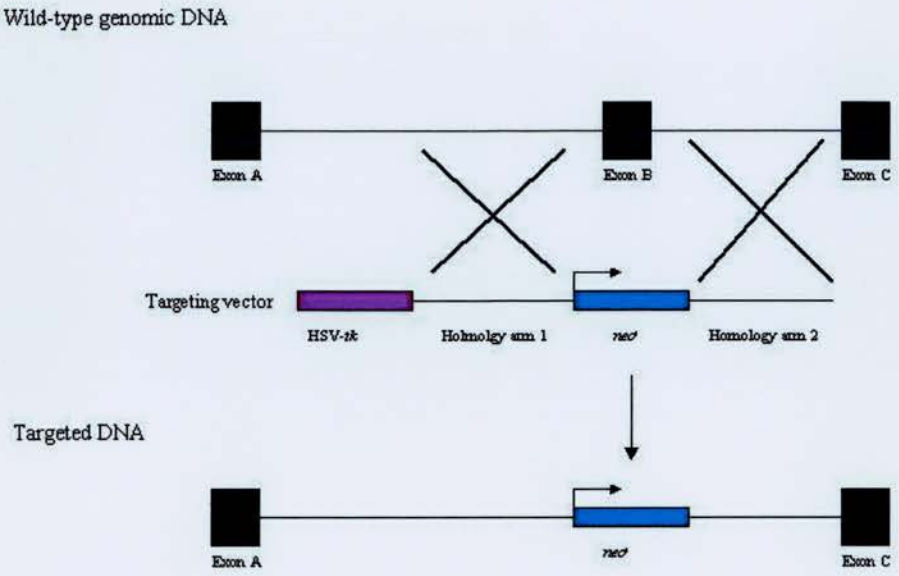

Figure 1.6. Homologous recombination using positive/negative selection. Homologous recombination occurs between the homology arms and the genomic DNA, which results in the integration of the *neo*^{r} cassette into the genome deleting the sequence of interest and allowing selection for clones with the targeting vector integrated by G418 (positive selection). The HSV-*tk* cassette is not integrated into the genome following homologous recombination. However, if random integration of the targeting vector has occurred then these clones can be selected against using the nucleoside analogue ganciclovir, since only those clones with the HSV-*tk* cassette will be killed by this treatment (negative selection).

This is a powerful strategy and there are currently many Cre transgenic mice available; including liver (Kellendonk *et al.*, 2000) and pancreas specific strains (Ray *et al.*, 1999). However, this system requires identification of tissue–specific promoters which restrict its usefulness. The generation of synthetic inducible systems provides an attractive alternative. The tetracycline-regulated transcription systems (Gossen *et al.*, 1992 and 1995) allow the induction of *cre* expression at a desired time, either by simply dosing an animal with tetracycline, or by withdrawing animals from tetracycline administration. Alternatively, viral-mediated gene transfer of Cre recombinase can be utilised (Anton and Graham, 1995). Parts of the viral genome are replaced with a Cre expression construct, leading to replication deficient viruses, which are still capable of host cell infection. This is a highly efficient method of gene targeting and has been utilised *in vivo* for amongst other purposes the analysis of inducible K-*ras* mutations in the mouse lung (Jackson *et al.*, 2001).

The generation of homozygous null ES cell for a particular mutation can be achieved by several methods. Firstly, the sequential gene targeting of both alleles using a targeting vector that contains a *neo*^{r} cassette, followed by a second round of targeting with a targeting vector containing a different selectable marker such as *hygromycin* B-resistance gene (Mortensen *et al.*, 1991). Alternatively, it is possible to generate homozygous null ES cell line using a single targeting construct, by high G418 selection (Mortensen *et al.*, 1992). Here heterozygous null ES cells that have been generated by a targeting vector containing a *neo*^{r} cassette are grown in high concentrations of the selectable agent G418. Following this selection many of the surviving cells have undergone loss of heterozygosity (LOH) at the targeted locus and contain two copies of the *neo*^{r} cassette. This process selects for those cells that have undergone spontaneous LOH, which occurs at a frequency of approximately 10^{-5}, as only those cells with a duplicated *neo*^{r} can survive higher doses of G418 (Lefebvre *et al.*, 2001). This spontaneous LOH is believed to result either by chromosome loss and duplication, or mitotic recombination.

1.12 Role in development

1.12.1 Ras RNA expression in embryonic and adult tissues

Analysis of the expression of cellular oncogenes during the development of the mouse, showed that these oncogenes participated in normal development (Muller *et al.*, 1982). Furthermore, the H-*ras* and K-*ras* transcripts were found to be ubquitiously expressed in all embryonic stages and adult tissues examined (Muller *et al.*, 1983), although differences in the level of expression were noted. Closer examination of RNA levels showed that there was a differential expression pattern of the *ras* gene family in mice (Leon *et al.*, 1987). H-*ras* was more prevalent in the brain, muscle and skin and the highest levels of expression for K-*ras* were seen in gut, lung and thymus. N-*ras* was expressed most strongly in the thymus and testis (Leon *et al.*, 1987). Analysis of expression of *ras* genes during development by Northern blot experiments showed that the *ras* family members were temporally regulated during embryonic development. Levels of K-*ras* and N-*ras* RNA were high at E10, but decreased towards late gestation, H-*ras* RNA levels were found to remain relatively constant (Muller *et al.*, 1983; Leon *et al.*, 1987).

Differential expression of the K-*ras* isoforms was detected by analysis of the RNA expression (Pells *et al.*, 1997). The pattern of the K-*ras* 4A isoform mRNA was greatly restricted, compared to that of the K-*ras* 4B, which was found ubquitiously. The K-*ras* 4A isoform mRNA was not detected in embryonic stem (ES) cells, but during the differentiation stage there was a marked induction (Pells *et al.*, 1997). A rapid induction of K-*ras* 4A was seen in the yolk sac at E12 and is detectable in the gut at E15, however K-*ras* 4B was ubquitiously expressed from the earliest embryonic stage examined (E9) (Pells *et al.*, 1997). The level of the K-*ras* 4A isoform mRNA did not exceed that of the K-*ras* 4B isoforms even in those tissues where it was most strongly expressed. The highest levels of expression of the K-*ras* 4A isoform were detected in the kidney, stomach and large intestine. The large intestine was found to have levels of K-*ras* 4A expression comparable to those of the K-*ras* 4B isoform, but the K-*ras* 4A isoform was a minor species in the liver (Pells *et al.*, 1997). Analysis of the isoforms' expression by Northern blot hybridisation (Wang *et al.*, 2001) confirmed the previous findings showing the same restricted pattern of K-*ras* 4A RNA expression.

Therefore, *ras* genes are regulated in a complex manner with differences in expression occurring through pre- and postnatal development and with certain adult tissues showing preferential expression of one of the family members.

1.12.2 Ras protein expression in embryonic and adult tissues

Immunohistochemistry on histological samples from normal foetal and adult human tissues using a pan-Ras monoclonal antibody showed that significant quantities of Ras are expressed not only by cells in the proliferative compartments, but also by certain mature cells carrying out specialised functions, such as neurons and the epithelial cells of endocrine glands (Furth *et al.*, 1987). This suggests a role for Ras in both cellular proliferation and specialised cellular functions. A wide range of normal human tissues express Ras, but within these tissues expression is often sharply restricted to cells at specific stages of differentiation. Garin Chesa and colleagues showed that terminally differentiated cells generally showed a stronger reactivity to pan-Ras antibodies than did rapidly proliferating cells in human tissues (Garin Chesa *et al.*, 1987). Fetal and adult tissues were also found to have corresponding patterns of Ras expression, and that the distribution of Ras in neoplasms paralleled the pattern in the normal tissue from which they were derived (Garin Chesa *et al.*, 1987). Detection of Ras in early rat embryos shows that there is evidence of expression from day E6.5. The expression appeared to be temporally and spatially regulated, with expression in the visceral and parietal endoderm not becoming obvious until development was proceeding through the primitive streak stages (Brewer *et al.*, 1992). By day E10 of development all the tissues were positive for Ras staining, strong staining was seen in the heart and neural elements. Therefore, Ras does not appear to be ubquitiously expressed in the rat conceptus prior to gastrulation, but shows differential distribution, appearing later in endodermal derivatives. Possibly Ras is involved in determination of the ectodermal and endodermal lineages (Brewer *et al.*, 1992).

1.12.3 Transgenic models of Ras

The differential expression of members of the Ras family during embryonic development suggested that these proteins might be important regulators of embryonic development.

Ras activity is essential for mouse embryos to develop through the two-cell stage (Yamauchi *et al.*, 1994). As demonstrated by microinjection of neutralising antibodies, antisense oligonucleotides and constructs expressing the dominant negative RasN17 mutant into fertilised eggs, which inhibited development through the two-cell stage. Inhibition of development through the two-cell stage could be overcome by simultaneous injection of an activated *raf* oncogene, suggesting that the Ras/Raf pathway was important for this progression to occur. This effect was specific to progression through the two-cell stage, as microinjection of late two-cell stage eggs with RasN17 did not affect subsequent cleavages and development to morulae and blastocysts (Yamauchi *et al.*, 1994).

More recent gene targeting experiments have demonstrated that, neither N-*ras,* nor H-*ras* are essential for, either mouse development, or fertility. Tissues from N-*ras*$^{-/-}$ mice were analysed for either pathological or abnormal histological features, but these where found to be indistinguishable from their heterozygous and wild-type siblings (Umanoff *et al.*, 1995). Even in haematopoietic cells where N-*ras* is expressed at high levels there were no obvious abnormalities. Furthermore, recent studies have shown that mice lacking both the H-*ras* and N-*ras* loci are still capable of developing normally (Esteban *et al.*, 2001). Characterisation of lymphocyte subsets in the spleen and thymus and neuronal markers in the brain. showed no significant differences between wild-type and H-*ras*$^{-/-}$ mice. Crossing of H-*ras*$^{-/-}$ and N-*ras*$^{-/-}$ mice gave rise to viable double knockout offspring. Therefore, with regards to the Ras family, mice containing only a functional K-*ras* gene are capable of normal growth, development and fertility.

This confirms the observations based on transgenic studies of the K-*ras* gene (Johnson *et al.*, 1997; Koera *et al.*, 1997). K-*ras*$^{-/-}$ embryos die progressively between embryonic day 12.5 (E12.5) and term. Both studies noted that K-*ras*$^{-/-}$ embryos exhibited smaller size and delayed growth, compared to wild-type littermates, although Johnson and co-workers additionally noted features consistent with anaemia, without gross external abnormalities. Johnson and colleagues found the liver to be the only consistently defective tissue in the K-*ras*$^{-/-}$ embryos. K-*ras*$^{-/-}$ livers were reported to contain typically 2- to 8-fold fewer cells than control livers, with apparent cell death detected (Johnson *et al.*, 1997). K-Ras has recently been reported to be important for E-cadherin-based adherens junction (AJ) formation in fetal hepatocyte culture (Matsui *et*

al., 2002). AJ formation was defective in fetal hepatocytes from K-*ras*$^{-/-}$ mice, but not from either H- or N-*ras*$^{-/-}$ mice and was rescued by expression of K-*ras,* but not H- or N-*ras*, which may explain the abnormalities observed in the fetal liver of K-*ras*$^{-/-}$ mice (Johnson *et al.*, 1997). However, it should be noted that Koera and co-workers reported that the liver of K-*ras*$^{-/-}$ embryos appeared almost histologically normal.

Reduced thickness of the ventricular myocardium was also reported in K-*ras*$^{-/-}$ embryos at E15.5, possibly due to reduced proliferation (Koera *et al.*, 1997). By E11.5 K-*ras*$^{-/-}$ mice showed increased cell death of motorneurons in the medulla and cervical spinal cord. Thus, neuronal apoptosis appears to be influenced by K-*ras*, suggesting a possible role for K-*ras* in the development of the nervous system (Koera *et al.*, 1997). However, Johnson and co-workers reported neither of these findings. Therefore, these studies attribute the lethality of the K-*ras*$^{-/-}$ embryos to different mechanisms.

Analysis of chimaeras generated by the microinjection of blastocysts with K-*ras*$^{-/-}$ ES cells revealed that there was also a low contribution of K-*ras*$^{-/-}$ cells to the liver and also the spleen, lung and multiple haematopoietic lineages (Johnson *et al.*, 1997), indicating that K-*ras* has a role in the development of these tissues. In their series of experiments Johnson and co-workers also showed that the survival of N-*ras* knockout mice was due to rescue by wild-type K-*ras* by crossing to K-*ras*$^{+/-}$ animals. Interestingly, deletion of both of these *ras* gene resulted in a much more severe phenotype, with K-*ras*$^{-/-}$/N-*ras*$^{-/-}$ offspring undetectable at E9, suggesting that there may be cooperative effects.

Although the growth and differentiation of many tissues can proceed normally in the absence of K-*ras,* in a subset of tissues K-*ras* is essential for the completion of embryogenesis. However, the tissues dependent upon K-Ras protein function during embryonic development cannot be clearly defined due to conflicting data. Furthermore, since residual Ras proteins in the form of H- or N-Ras are unable to rescue the effects of the K-*ras* knockout, these studies suggest that K-Ras may have unique functions during mouse development. Therefore, with regard to the *ras* genes, K-*ras* is essential and sufficient for mouse embryonic development. The role of K-*ras* in development is still to be fully elucidated. However, the use of transgenic models to study this has increased the level of understanding of the role of K-*ras* in mouse development.

1.13 Role in Neoplasia

Mutations in the *ras* genes can be found in a variety of human tumours. The highest incidence of *ras* gene mutations have been reported in adenocarcinoma of the pancreas (90%), high incidences have also been reported in cancers of the colon (40-50%), lung (30%), thyroid (30%) and myeloid leukaemia (30%) (Bos *et al.*, 1989). Overall, *ras* mutations are associated with approximately 30% of all cancers.

However, mutations in the different *ras* gene family members seem to be specifically associated with certain types of cancers. For example over 90% of pancreatic adenocarcinomas contain mutations in the K-*ras* gene, but mutations in N- or H-*ras* are rarely seen. In colon cancers, roughly 40-50% of cases exhibit K-*ras* activating mutations, yet only a few percent contain N-*ras* mutations and H-*ras* mutations are very uncommon (Bos *et al.*, 1989). The reason for this selectivity is still unknown, but it may be due to the level of contribution that each particular gene makes to the cell types involved.

Support for this hypothesis also comes from *in vitro* analysis of the transforming potentials of the different *ras* family members. It was demonstrated that the different members of the *ras* family had different transforming potentials *in vitro* (Maher *et al.*, 1995). Furthermore, these differences appear to be cell-type specific. In Rat-2 and NIH3T3 fibroblasts, transformation assays showed that H-Ras was more transforming than either N-Ras or K-Ras. However, in the human haematopoietic cell line, TF-1, N-Ras had the greater transforming potential. In rat intestinal epithelial cells H-Ras and K-Ras 4A induced transformed foci with greater efficiency than K-Ras 4B and N-Ras (Voice *et al.*, 1999). When anchorage independent growth was analysed K-Ras 4A expression enabled a greater number of foci to form than the other Ras proteins.

An alternative mechanism of *ras* activation may occur through the increased production of the normal gene product. Quantitative alterations of the *ras* gene product are known to induce neoplastic transformation of cells of various species including humans (Chang *et al.*, 1982; Schwab *et al.*, 1983; DeBortoli *et al.*, 1985). Amplification of the K-*ras* gene has also been detected in some human tumours including renal clear cell adenocarcinoma (Kozma *et al.*, 1997) and Kaposi's sarcoma (Nicolaides *et al.*, 1994).

In addition, high levels of *ras* mRNA and p21 are found in a wide variety of human tumours; including colonic tumours (Slamon *et al.*, 1984; Gallick *et al.*, 1985). Previous studies have found that high expression of Ras, independent of mutational activation, is a common feature of carcinomas with poor prognosis (Horan Hand *et al.*, 1987).

1.13.1 Colorectal Cancer

Clinical and histopathological observation that many if not all carcinomas arise in pre-existing adenomas has led to the concept that colorectal cancer progresses in a stepwise manner, known as the adenoma-carcinoma sequence (reviewed Leslie *et al.*, 2002). This sequence encompasses the progression from normal to dysplastic epithelium to carcinoma, through sequentially worsening degrees of adenomatous dysplasia. It is widely accepted that this is associated with a progressive accumulation of mutations in both sporadic and familial colonic cancers, leading to the clonal evolution of the descendents of a single cell initiated by a somatic mutation. Additional mutations may lead to a subset of daughter cells forming, which acquire a growth advantage. Further proliferation of this clone may ultimately lead to the appearance of a microscopic adenoma or polyp. This concept led to attempts to determine the mutational events associated with this progression. Four somatic events in particular have been highlighted in this sequence, mutation of K-*ras*, inactivation of Adenomatous Polyposis Coli (APC), inactivation of p53 and allelic losses of occurring on chromosome 18q. A series of non-invasive and invasive adenomas and carcinomas were analysed for the presence of these somatic events (Vogelstein *et al.*, 1988), which led to the generation of a model for the genetic basis of colorectal neoplasia (Fearon and Vogelstein, 1990). The model proposed that either mutation or loss of APC was probably the earliest event, leading to hyperproliferative epithelium. Hypomethylation is also present in very small adenomas. Mutations in the K-*ras* gene were proposed to be associated with the progression of pre-existing small adenomas to larger more dysplastic tumours. Allelic deletions of chromosome 17p (associated within activation of p53) and 18q were proposed to occur at later stages of tumorigenesis. However, Vogelstein and co-workers observed that it was the accumulation of these mutational events, rather than the order of their accumulation that was of importance in this model (Vogelstein *et al.*, 1988). The allelic loss at 18q was originally thought to be important for the inactivation of the gene DCC (Deleted in Colorectal Cancer), but recent evidence suggests that it is

SMAD4, which also resides in this region that is involved in the allelic losses of chromosome 18q (reviewed Arends, 2000). Intense investigation in the ten years since this model was proposed has led to a considerable elaboration of the molecular events involved in colorectal tumorigenesis, including the identification of other mutations that occur at a high frequency, which has resulted the emergence of a much more complex picture of interactions (reviewed Houlston, 2001, Leslie *et al.*, 2002). Furthermore, a recent analysis of 106 colorectal tumours found that the progressive accumulation of mutations in APC, K-*ras* and p53 was not a prerequisite for colorectal tumour development (Smith et al., 2002). Indeed, the occurrence of mutations in all three genes was extremely rare in the cases examined, clearly indicating that alternative mechanisms of tumour progression exist.

As described above, one of the earliest events in this progression is believed to be the mutation of the K-*ras* gene. These mutations have been identified in high frequencies in aberrant crypt foci (ACF), which have been identified as putative pre-neoplastic lesions in the colon, and not in morphologically normal crypt areas from the same patients (Pretlow *et al.*, 1993). Increased levels of Ras protein and mRNA have been seen in aberrant crypts in rats (Stopera *et al.*, 1992). K-*ras* mutations have been found with equal frequency in dysplastic and non-dysplastic polyps unlike mutations in the APC gene, which is also closely linked to the development of colorectal cancer (Jen *et al.*, 1994; Smith *et al.*, 1994). Furthermore, a high frequency of K-*ras* codon 12 mutations has been identified in histologically normal mucosa found adjacent to areas of tumour in patients who have K-*ras* mutation positive colorectal cancers (Zhu *et al.*, 1997). This and other evidence (reviewed Arends, 2000), suggests that K-*ras* gene mutations may be involved in the actual initiation of colorectal tumorigenesis, rather than progression as previously proposed (Vogelstein *et al.*, 1988).

Nevertheless, K-*ras* gene mutations were analysed in 738 adenomas and found to be associated with 17.2% of these (Maltzman *et al.*, 2001). The K-*ras* mutations were found to be more commonly associated with adenomas with villous histology and in adenomas with high-grade dysplasia, which corresponds well with the Fearon and Vogelstein model of colorectal tumorigenesis, since these observations suggest that K-*ras* mutations were associated with the histologic features of adenoma progression (Maltzman *et al.*, 2001). However the examination of benign adenomas and adenomas

with focal carcinoma, suggest that the K-*ras* gene mutations occur during the late stage of adenoma progression (Ohnishi *et al.*, 1997). However, there is some evidence to suggest that heterogeneity with regard to K-*ras* mutations may exist within carcinomas. Some primary carcinomas with K-*ras* mutations have been shown to also contain areas in which only the wild-type gene is present. This implies that the K-*ras* gene mutation even when present may not have been necessary for the establishment of the malignant phenotype within these primary carcinomas (Al-Mulla *et al.*, 1998).

Finally, evidence suggests that K-*ras* mutations may be associated with certain types of colorectal cancer, since a preferential association of the K-*ras* oncogene with the polypoid type of colorectal cancer, compared to the ulcerative type of colorectal cancer has been demonstrated (Chiang *et al.*, 1998). This observation may be indicative of the existence of different pathways of tumour progression.

1.13.2 Mouse models of cancer

Using a hit and run gene targeting strategy a mouse model has been generated that expresses activated K-*ras* (Johnson *et al.*, 2001). The expression of the oncogenic K-*ras* gene occurs randomly following spontaneous somatic recombination within the targeted K-*ras* allele. These mice were highly predisposed to developing a range of tumours, predominantly early onset lung cancers, but tumours were also seen in the thymus and the skin (Johnson *et al.*, 2001). This model interestingly did not show the development of pancreatic or colon carcinomas despite the high rate of tumours seen in these sites in humans with associated K-*ras* mutations. Significantly however all of the mutant mice examined did have ACF of the colon, whereas wild-type littermates did not. When these mice were crossed on to the $p53^{+/-}$ background the lung tumours showed more malignant features, suggesting that the p53 mutation contributes to the development of these lung tumours. Crossing to the Apc^{min} strain did not alter the intestinal polyp phenotype (Johnson *et al.*, 2001). This was an exciting development as this model more closely represents the spontaneous oncogenic activation seen in human tumours. Additional work from two groups has further pointed to an intimate relationship between K-*ras* gene mutations and lung cancer initiation. Jackson and co-workers showed that by using an adeno-Cre inducible K-*ras* mutant that numerous surface lung lesions were apparent after only 4 weeks post treatment. The number of lung adenomas was directly proportional to the amount of virus used for infection

(Jackson *et al.*, 2001). Fisher and co-workers also using an inducible system showed the development of lung tumours following expression of mutant K-Ras, but most interestingly that these tumours regressed following the withdrawal of the inducing agent. The tumours were found to arise faster in the absence of tumour suppressors p53 or Ink4a/Arf, but tumours in these bitransgenic mice did not persist following removal of the inducer either (Fisher *et al.*, 2001).

Recently a mouse model of K-*ras* intestinal tumorigenesis has been developed, by the expression of K-*ras* G12V under the control of the mouse villin promoter in epithelial cells of the large and small intestine (Janssen *et al.*, 2002). This model was found to closely recapitulate the progression of tumour formation associated with human disease, including the detection of spontaneous mutations in the tumour suppressor gene p53 in a proportion of lesions examined. However, associated mutations in the APC gene were not detected.

1.13.3 Mechanisms underlying tumorigenesis

The literature discussed in previous sections indicates that activated *ras* genes can inhibit apoptosis under certain circumstances and in the presence of co-operating mutations can cause uncontrolled cellular proliferation and transformation of cell lines *in vitro* and the prevention of appropriate differentiation. All these features of activated *ras* genes are hypothesised to be the mechanisms by which activated *ras* genes drive tumorigenesis. Other mechanisms by which activated *ras* may contribute to tumorigenesis include: inappropriate angiogenesis and alterations in cell adhesion.

Angiogenesis is the normal physiological process that produces new blood vessels. However it can also become part of the pathological processed involved in diseases such as cancer. Mutant *ras* oncogene dependent vascular endothelial growth factor (VEGF) expression has been shown to be necessary, but not sufficient for tumour growth *in vivo* (Okada *et al.*, 1998). This has been shown for H-*ras* and for two colorectal carcinoma cell lines known to carry a single mutant K-*ras* allele. Signalling through K-Ras up-regulated VEGF in a PI-3K dependent manner and also appeared to enhance Wnt signalling, which has been shown to strongly up-regulate VEGF (Zhang *et al.*, 2001).

The development of metastases is perhaps one of the most significant steps in the progression of cancers into more aggressive lesions with a markedly worse prognosis. The intercellular adhesion molecule carcinoembryonic antigen (CEA), which is important for the establishment of basolateral polarity in colon epithelial cells is up-regulated by the mutant K-*ras* gene but not H-*ras* (Yan *et al.*, 1997b). Oncogenic K-*ras* but not H-*ras* also prevented normal glycosylation of the integrin β1-chain of the collagen receptor, blocking its maturation and preventing the apicobasal polarization of colon epithelial cells (Yan *et al.*, 1997a). Clinical evidence has linked alterations in the ratio of the β1 integrin precursor to the mature form of β1 integrin in invasive and metastatic colorectal cancers (Yan *et al.*, 1997a). By the up-regulation of CEA, K-*ras* may prevent lateral adhesion of adjacent colon epithelial cells and the selective effects of mutant K-*ras* on integrin β1-chains also affecting adhesion may have important implications, partly accounting for the selection of K-*ras* mutants in human tumours. Activated K-*ras* reduced the cell surface expression of the α1β1 collagen/laminin receptor and the α5β1 fibronectin receptor, both of which are implicated in maintenance of a non-transformed phenotype (Schramm *et al.*, 2000). It also increased cell surface expression of the α3β1 laminin/collagen/fibronectin receptor and the αvβ5 vitronectin receptor, which may also have a role to play in metastatic behaviour (Schramm *et al.*, 2000).

Epithelial cell scattering is likely to play an important role in the process of carcinoma cell invasion and metastasis. It has been shown that Ras has a positive role in epidermal growth factor (EGF) induced cell scattering. It was also able to induce cell dispersion in the absence of the growth factor (Boyer *et al.*, 1997), implicating Ras as a potential regulator of epithelial cell scattering.

The production of proteases is associated with invasion and metastasis. Colorectal carcinomas with mutant forms of *ras* have significantly higher expression levels of cathespin B or L cysteine protease than carcinomas in which these alterations were not detected (Kim *et al.*, 1998). Additionally, an association between activated *ras* oncogenes and an increase in matrix metalloproteinase (MMP) activity has been reported (Meade-Tollin *et al.*, 1998).

1.13.4 Prognostic factors

Since the importance of K-*ras* mutations in colorectal cancer became apparent research has strived to find ways of using this knowledge for the benefit of the patient. It is possible that the detection of K-*ras* mutations using molecular methods such as PCR of tissues or fluids may be helpful in the early detection of primary cancers and micrometastases, also in the assessment of tumour burden and efficacy of treatment regimens (Nomoto *et al.*, 1998; Urban *et al.*, 1993; Yamada *et al.*, 1998), although large clinical trials are needed to ascertain the true benefit of these measures.

K-*ras* activating mutations have also been investigated as a potential prognostic marker for colorectal cancer. However, there are conflicting reports regarding the relevance of this approach. The presence of K-*ras* mutation has been demonstrated to have no affect on patients' prognosis (Kressner *et al.*, 1998). However, others report that mutations in the K-*ras* gene correlate with prognosis, with *ras* over expression predicting a poor prognosis independent of Duke's stage, DNA ploidy and S-phase fractions (Sun *et al.*, 1998).

In addition, the type of mutation present appears to determine the phenotype of the tumour, with some mutations being associated with decreased overall survival and increased risk of disease recurrence, suggesting these mutations may confer a more aggressive phenotype to cancers (Al-Mulla *et al.*, 1998; Cerottini *et al.*, 1998). However, these studies all suffer from a lack of numbers and this may explain the conflicting observations. A large multicentre study (RASCAL) with nearly 3000 patients showed that K-*ras* mutations were associated with increased risk of relapse and death, and that some mutations conferred a more aggressive phenotype that others. In particular, any mutation of guanine to thymine, but not to adenine or to cytosine increased the risk of recurrence and death. However, only the specific valine codon 12 mutation was independently associated with increased risk of recurrence and death (Andreyev *et al.*, 1998).

Therefore, K-*ras* mutations may prove to be useful biomolecular markers, and in combination with histopathological parameters may help to identify colorectal cancer patients with an increased risk of disease recurrence and/or death and therefore help with the choice of appropriate treatment regimens.

1.13.5 Therapeutic approaches

The activity of Ras proteins is dependent upon specific post-translational modifications that occur at the C-terminus. These modifications namely farnesylation and geranylgeranylation increase the hydrophobicity of the proteins and cause them to be located at the inner surface of the plasma membrane. Drug therapies have been developed to specifically target the enzymes responsible for these modifications. The anti-tumour effects of a farnesyltransferase inhibitor (FTIs) have been tested on mammary and lymphoid tumour models over-expressing N-Ras and were found to be an effective treatment (Mangues *et al.*, 1998). However, due to the nature of K-Ras post-translational modifications it is necessary to use both FTIs and geranylgeranyltransferase I inhibitors (GGTIs) to prevent K-Ras 4B processing, MAP kinase activation and growth in nude mice of K-Ras 4B transformed NIH3T3 cells (Sun *et al.*, 1998). Although, FTIs effectively inhibit the farnesylation of H-Ras, they do not completely inhibit the prenylation of K-Ras, as it remains prenylated in FTI treated cells due to modification by the related prenyltransferase, geranylgeranyltransferase I. Hence, cells transformed with K-*ras* tend to be more resistant to FTIs than H-*ras*. Therefore, to investigate methods to overcome this, cells were treated with FTIs, GGTIs and dual prenylation inhibitors that have both FTI and GGTI activity, but problems of toxicity were associated with this treatment. (Lobell *et al.*, 2001)

In murine cells, the MAPK pathway is clearly critical for tumorigenesis and is also commonly activated in human tumours (Hoshino *et al.*, 1999). As a consequence this pathway has been extensively investigated as a potential target for therapeutic approaches. A variety of pharmacological and antisense approaches have been developed to block the activities of Raf and MEK and are now under clinical investigation. (reviewed Sebolt-Leopold *et al.*, 2000). Inhibition of MEK with the orally active small molecule PD184352, suggested that tumours containing high-level expression of phosphorylated ERK are the most sensitive to treatment with this agent (Sebolt-Leopold *et al.*, 1999). PD184352 was found to significantly inhibit the growth of colon carcinomas of both mouse and human origin at doses that were well tolerated. In addition to impairing tumour proliferation PD184352 was found to block the disruption of cell adhesion contact and motility required for invasion (Sebolt-Leopold *et al.*, 1999).

Another therapeutic strategy currently being researched is the use of peptide aptamers. Peptide aptamers have been identified that preferentially bind to the activated allelic form of H-Ras. Transfection of mammalian cells with these peptide aptamers resulted in abolition of Raf kinase activity stimulated by EGF (Xu and Lou, 2002).

1.14 Aims and objectives

As outlined above there are many conflicting sets of data concerning the role of Ras proteins in certain cellular processes, such as differentiation, proliferation and apoptosis. Depending upon the experimental settings *in vitro*, Ras can induce opposite effects, making assessment and extrapolation of the physiological role of Ras in any given tissue or cell type extremely difficult, underscoring the need for *in vivo* studies.

The aim of this project is three fold. The first of these is to elucidate the contribution of the individual K-*ras* isoforms during mouse development. This is to be addressed by the development of mice homozygous for the deletion of exon 4A, which can be used to investigate whether expression of both isoforms is essential for normal embryonic development. In addition, immunohistochemical analysis of embryonic stages will be performed to detail the tissues and cell lineages that express the K-Ras isoforms, to investigate whether differential protein expression occurs during embryonic development.

The second aim is to assess the expression of the individual isoforms in adenocarcinomas of the colon with known K-*ras* mutations. To investigate whether the K-*ras* activating mutations are associated with increased expression of both isoforms and to contrast this analysis with the expression pattern detected in cervical intraepithelial neoplasia, the progression of which is not normally associated with K-*ras* mutations.

The third aim of this study is to develop ES cells homozygous null for the deletion of the K-*ras* 4A exon by gene targeting and to characterise these by examining *in vitro* the effect of this mutation upon growth, differentiation and apoptosis, in order to identify those cellular functions that are differentially regulated by the individual K-Ras protein isoforms.

Chapter 2

Materials and Methods

2.1 Maintenance of Embryonic Stem Cell lines

2.1.1 Routine Embryonic Stem Cell Culture

Embryonic stem (ES) cells were routinely cultured on gelatinised tissue culture plastic (Costar, Corning), in a humidified 37°C incubator with 5% CO_2 injection (Sanyo). All ES cell work was carried out in a class 2 biological safety cabinet (Microflow), using aseptic techniques.

Gelatinised plastics for ES cell culture were prepared at least one hour before use, by covering the growth surface with 0.1% gelatin (w/v) (Sigma) made up in sterile water. The residual gelatin was removed just prior to the use of the plastics. ES cells were routinely cultured in BHK-21 Glasgow modified eagles medium (Life Technologies), which was supplemented with 5% (v/v) new born calf serum (NCS) (Life Technologies, selected batches), 5% (v/v) foetal calf serum (FCS) (Life Technologies, selected batches), 1% non-essential amino acids (Life Technologies) and 10mM sodium pyruvate (Life Technologies). β-mercaptoethanol (Sigma) was added at 0.01% (v/v) and leukaemia inhibiting factor (LIF) conditioned medium was added at 0.005% (v/v). The LIF-conditioned medium was produced by culturing Cos 7 cells containing the pC10 plasmid expressing the recombinant LIF protein. This medium was used in all cases unless otherwise stated.

2.1.2 Thawing cells after cryopreservation

When cells were raised from liquid nitrogen storage the thawing process was carried out quickly to maintain cell viability. Vials were defrosted at 37°C, the cell suspension removed into 10ml of pre-warmed medium in a 50ml falcon tube, which was then centrifuged at 1,000rpm 5 min (MSE Mistral 1000). The supernatant was removed and cells were resuspended in 6ml of fresh medium and transferred to a 25cm^2 tissue culture flask and cultured at 37°C with 5% CO_2. The medium was aspirated the following day

to remove any cellular debris and remaining traces of dimethyl sulfoxide (DMSO), and replaced with 7ml of fresh pre-warmed medium. Medium was replenished at least every second day, to avoid serum starvation. When the cells were approximately 80% confluent they were sub-cultured to avoid over acidification of the medium as described below.

2.1.3 Sub-culturing of ES cells

When the cells reached a state of approximately 80% confluence observed microscopically (Leica) they were, either sub-cultured into fresh gelatinised flasks, or prepared for cryopreservation. The medium was removed and the monolayer was washed with 1X phosphate buffered saline Ca^{2+}/Mg^{2+} free (PBS) (Life Technologies) to remove any excess medium, which if not removed inhibited the trypsin. Trypsin-EDTA (appendix I) was added and incubated at 37°C until the cells started to detach from the surface. The flask was given a sharp tap to detach the cells and medium added to approximately 10X the volume to neutralise the trypsin, then transferred to a falcon tube and centrifuged at 1,000rpm for 5 min (MSE Mistral 1000). The supernatant was discarded and the cells resuspended in an appropriate volume of fresh medium to give the required dilution. The cell suspension was then added to a fresh gelatinised tissue culture flask or plate.

2.1.4 Cryopreservation of ES cell stocks

Cryopreservation medium was complete medium supplemented, with additional FCS to give a total of 15% (v/v) and 10% (v/v) DMSO (Sigma). Cells were harvested in the manner used for routine sub-culture and then centrifuged at 1,000rpm for 5 min, (MSE Mistral 1000) the supernatant was removed and the cells resuspended in cryopreservation medium to give the required concentration of cells per ml of medium. Then 1ml aliquots of cell suspension were added to freezer vials (Nunc) and these were frozen slowly overnight at -70°C in plastic racks (Nunc). The vials were then transferred to the liquid nitrogen freezer and stored in the gaseous phase.

2.1.5 Analysis of chromosome number

Cells for analysis were subcultured two days before they were needed and grown to approximately 70% confluence in 75cm^2 tissue culture flasks. The growth medium was removed and replaced with medium containing 1% (v/v) Colchicine (Life technologies)

and cells were incubated for 3hrs at 37°C in a 5% CO_2 incubator. Cells were trypsinised and centrifuged at 1,000 rpm for 5 min (MSE Mistral 1000) and then resuspended in 10ml of hypotonic solution (0.075M KCl). The cells were incubated for 15 min at 37°C to allow them to swell, then centrifuged at 800rpm for 5 min (MSE Mistral 1000) and resuspended in 10ml freshly prepared ice-cold fixative (3:1 (v/v) methanol, glacial acetic acid), which was added drop wise to avoid cell clumping and allowed to fix for an hour at -20°C. The cells were then centrifuged at 1,000 rpm for 5 min (MSE Mistral 1000) and resuspended in a further 1ml of fixative. The cell suspension was dropped on to slides that had been prepared by emersion in absolute alcohol overnight at 4°C. The slides were allowed to dry and stained with 5% (v/v) giemsa (Sigma). Coverslips were mounted with DPX (BDH) and the chromosome numbers counted using the highly optimised microscope environment (HOME) (Axial) (Brugal *et al.*, 1992). The HOME microscope was used to ensure accuracy and reproducibility of counting. Minimums of 25 metaphase spreads were counted for each cell line. Spreads that had obviously been damaged in the preparation process were not included in the counts.

2.1.6 Differentiation of ES cells with Retinoic acid

ES cells were seeded at a density of approximately $2x10^5$ cells in 90mm diameter petri dishes (Geiner) and allowed to plate down in normal ES cell medium overnight. All trans-retinoic acid (Sigma) was dissolved in DMSO (stock concentration of 10mM) and added to the medium, which lacked LIF at final concentrations of 1μM, 5μM, and 10μM. All treatments, including control plates had DMSO added to the same final concentration (0.05%). The control medium also lacked LIF to control for possible differentiation effects seen in the absence of LIF and presence of DMSO that were not attributable to retinoic acid. The cells were grown for five days and the medium replenished each day to maintain the retinoic acid concentration.

2.1.7 Mitomycin C treatment of STO Fibroblasts

Fibroblasts were grown in non-gelatinised $125cm^2$ tissue culture flasks. In ES cell medium, but lacking LIF and β-mercaptoethanol. Mitomycin C (Sigma) was made up to a stock solution of 1mg/ml with sterile PBS. Cells were then treated with mitomycin C at a final concentration of 10μg/ml in tissue culture medium, for 2-3 hrs at 37°C. The

mitomycin C medium was removed and cells washed three times with 1X PBS, trypsinised and frozen away as described above for cryopreservation of ES cells. To prepare a feeder layer 1 vial of fibroblasts was raised from liquid nitrogen storage and added to a $25cm^2$ flask as previously described. The fibroblasts were allowed to attach to the surface before the ES cells were added.

2.2 Manipulation of Plasmid DNA

2.2.1 Transformation of bacteria with plasmid vectors

Library efficiency ®DH5α ™ Competent cells (Life Technologies) were used for the transformation. The competent cells were thawed on ice, gently mixed, and aliquots of 100µl were put into pre-chilled Eppendorf tubes. To the competent cells 1µl (1-10ng) of DNA to be transformed was added. The cells were incubated for 30 minutes on ice, heat-shocked for 45 seconds in a 42°C water bath, placed on ice for a further 2 minutes, then 0.9ml of room temperature S.O.C medium (Life Technologies) was added. The cells were then shaken at 225rpm for 1 hour at 37°C. The experimental reaction was diluted as necessary and 100-200µl of this dilution was spread on L broth plates containing 50µg/ml ampicillin (L Amp) (appendix I), and then incubated overnight at 37°C to allow colony growth.

2.2.2 Plasmid Miniprep

Bacterial colonies were picked from plates and used to create a culture by inoculating 10ml of L Amp broth. The bacterial cultures were grown at 37°C overnight, shaking at 180rpm. Wizard Plus minipreps (Promega) were used, as per manufacturers instructions. In brief, 1.5ml of the bacterial culture was used for each miniprep. The supernatant was removed following centrifugation and the Eppendorf tubes blotted to remove excess liquid. The pellet was resuspended in 200µl of cell resuspension solution (Promega) and cells lysed by the addition of 200µl of cell lysis solution (Promega). After mixing by inverting and addition of 200µl of neutralisation solution (Promega) the suspension was centrifuged at 10,000rpm for 5 min (MSE Microcentaur). Syringe barrels were attached into columns and inserted into a vacuum source (Vaccman, Promega). DNA purification resin (Promega) was added to each barrel with

the cleared lysates and the resin and lysate were pulled into the column by vacuum pump. Columns were washed with column wash solution and the vacuum was continued for a further 30 seconds to dry the resin. Finally, the columns were transferred to new Eppendorf tubes and the DNA was eluted from the columns into a volume of 30µl TE buffer by centrifugation for 20 seconds at 10,000rpm (MSE Microcentaur).

2.2.3. Plasmid Maxi Preps

This procedure used the Hybaid Maxi-prep system. Starter cultures were established by inoculating 8ml of L Amp broth with 100µl of bacterial stock containing the plasmid of interest. The culture was grown for a minimum of 8 hrs but usually overnight at 37°C shaking at 180rpm. The culture was then used to inoculate 500ml of L Amp broth and grown overnight as before. The maxi-prep was performed according to manufacturers instructions. The culture was centrifuged at 6,000rpm for 30 min at 4°C (Sorvall), and the supernatant removed. The bacterial cell pellet was resuspended in 20ml of resuspension solution (Hybaid) and the cells lysed with 20ml of cell lysis solution (Hybaid). Following incubation at room temperature for 5 min the lysate was neutralised with 10ml of neutralising solution (Hybaid) and then centrifuged at 20°C for 20 min at 6,000rpm (Sorvall). Columns were equilibrated using 30ml of equilibration solution (Hybaid) and the cleared lysate added and allowed to flow through by gravity. Columns were washed with 2X 30ml of wash solution (Hybaid) and the DNA eluted with 15ml of elution solution (Hybaid), and precipitated with 10.5ml of room temperature isopropanol. The tube was centrifuged at 4°C for 30 min at 6,000rpm (Sorvall) to pellet the DNA, which was then washed with 70% ethanol and centrifuged at 13,000rpm for 5 min (MSE Microcentaur). The DNA was air dried and resuspended in of TE buffer.

2.2.4 Restriction digest of Plasmid DNA

Plasmid DNA was digested with the appropriate restriction endonuclease in the presence of the ionic strength buffer recommended by the manufacturer (the restriction enzymes were supplied by either Life Technologies or New England Biolabs). The digests were carried out in 10µl reaction volumes. Restriction enzymes were used at the volume required to give complete digestion of the target DNA, where 1unit of enzyme

is enough to digest 1μg of λ DNA in 1 hour. Enzymes were used in volumes of <10% of the final reaction volume, since an excess of glycerol (the enzyme solution is composed of 50% glycerol) has an inhibitory effect on the reaction. The 10X stock ionic strength buffer solution was diluted 1:10 in the reaction volume to give a final 1X buffer concentration and 1μl plasmid DNA was added. Some enzymes required addition of bovine serum albumin (BSA), which was provided by the manufacturers in these cases as a 100X stock solution, which was diluted to give a 1X concentration in the reaction volume. Water was added to make the final volume up to 10μl. Digests were carried out at 37°C for a minimum of 1 hour.

2.2.5 Agarose gel electrophoresis

Agarose gels were routinely used at 0.8% (w/v) for minigels, but concentrations of up to 2% (w/v) were used if small fragments needed to be separated. Agarose (Sigma) was added to a 1X Tris, boric acid, EDTA (TBE) solution (appendix I) diluted from a 10X stock, to give the final concentration of agarose (w/v), and this was heated in a microwave oven to dissolve the agarose. Ethidium bromide (Sigma) was added (0.5μg/ml) and the molten agarose poured into a mould and allowed to set. Once set the gel was place into a gel tank (Anachem) containing running buffer (1X TBE) to a level above the gel and the samples loaded into the wells using a TBE based loading buffer containing bromophenol blue (Appendix I). Current was supplied by an electrophoresis power supply (Amersham Pharmacia Biotech Inc). The fragments were visualised using an ultraviolet transilluminator and the images were captured using the GelDoc 1000 system (Bio-rad) and molecular analyst software.

2.2.6 Isolation of DNA from agarose gels

The band corresponding to the fragment size of interest was cut out of the gel with a clean scalpel blade, and weighed. The extraction used Glassmax spin columns (Life Technologies). For each 0.1g of agarose, 0.45ml of DNA binding solution was added and 20μl of TBE enhancing buffer. The tubes were heated to 50°C until the agarose melted. The solution was added to the spin column and centrifuged at 13,000rpm for 20 seconds (MSE Microcentaur). The flow through was discarded. To the spin column 0.4ml of cold wash buffer was then added and centrifuged as above and this procedure was repeated twice more. The column was centrifuged at 13,000rpm for 1min (MSE

Microcentaur) to ensure that all residual wash buffer was removed. The spin cartridge was transferred to a new tube and 40µl of TE buffer (appendix I) preheated to 65°C added. The cartridge was then centrifuged at 13,000rpm for 20 seconds (MSE Microcentaur) to elute the DNA. The product was then run on a minigel to confirm the size, purity and integrity of the DNA band. Products were then stored at -20°C in small aliquots.

2.3 Genetic Manipulation of ES cells

2.3.1 Preparation of the pPTKiNKiΔ4A targeting vector

Approximately 150µg of the pPTKiNKiΔ4A targeting vector plasmid was linearised by restriction digest with the *EcoR1* enzyme (see digestion of plasmid DNA 2.2.4). To ensure that the plasmid was completely linearised, a small aliquot of digested plasmid DNA was run on an agarose minigel against undigested plasmid DNA. The linearised plasmid DNA was precipitated with ½ volume 7.5M ammonium acetate and 2 volumes of absolute ethanol at -70°C for 1 hour, and then centrifuged at 13,000rpm for 10 min (MSE Microcentaur). The DNA was sterilised by washing with 750µl of cold 80% ethanol and centrifuged as above. The supernatant was removed under sterile conditions, and the DNA pellet air-dried. The pellet was then resuspended in 600µl sterile PBS.

2.3.2 Electroporation of ES cells with the pPTKiNKiΔ4A targeting vector

Cells for electroporation were grown to subconfluence in a 125cm^2 tissue culture flask (approximately 10^8 cells). The cells were dissociated with ES cell trypsin, resuspended in fresh medium, and centrifuged, the pellet washed with 1X PBS. The cell pellet was then resuspended in the 600µl DNA/PBS mixture (prepared as described 2.4.1). This suspension was incubated for 10 min at room temperature. The cells were transferred to a sterile cuvette and electroporated at 0.8kV and 3µF capacitance with a time constant of 0.1 seconds (Bio-Rad Gene –Pulser). The cells were resuspended in 100ml of non-selective tissue culture medium and added to ten 75cm^2 gelatinised tissue culture petri dishes. The selection with 150µg/ml geneticin (G418) (Life Technologies) started the following day. The selection with 2µM ganciclovir (Sigma) started four days after

electroporation. Selection continued for approximately 14 days or until colonies became visible. The surviving clones were then picked. The colonies to be picked were ringed with a marker pen and detached from the surface of the petri dish using a p200 pipette tip. The colony was then taken up into the tip with a small volume of medium and pipetted into ES cell trypsin. The colony was left to dissociate for a few minutes at 37°C. The colony was then transferred to a single well of a 24 well plate (Nunc), containing non-selective medium. Medium was changed the following day and when the well became confluent the cells were sub-cultured into the adjacent well to expand the colonies. Cells from these colonies were then either prepared for cryopreservation or used for DNA extraction when both wells became confluent.

2.3.3 Selection for transgene homozygosity in ES cells

This method was adapted from Mortensen *et al.*, (1992). Heterozygous ES cells were plated at $1.25x10^5$ cells per $75cm^2$ gelatinised petri dish and allowed to attach for 24 hours in normal growth medium. The medium was then replaced with medium containing different concentrations of geneticin G418 (Life Technologies). There were duplicate petri dishes for each concentration. The G418 was kept as a stock of 20mg/ml in ES cell medium and diluted to a final concentration of 1mg/ml, 1.5mg/ml, 2mg/ml, 2.5mg/ml and 3mg/ml in cell culture medium. The medium was changed every day initially to maintain selective pressure. The selection was maintained for approximately 14 days; at which time the surviving clones were picked as above and transferred to 24 well plates. Cells were harvested for DNA extraction or prepared for cryopreservation.

2.3.4 Single Cell Cloning

Single cell cloning was performed using flat-bottomed 96 well plates (Corning, Costar). Cells were trypsinised and counted. Then aliquots calculated to have on average less than 1 cell were added to the wells, which ensured that as many of the wells as possible had only single cell colonies. Cells were grown for approximately 14 days then the single colonies were picked and transferred into 24 well plates for expansion as described above (2.3.2).

2.4 Manipulation of Genomic DNA

2.4.1 DNA Extraction

DNA extraction from either cell pellets or tissue samples was performed as follows. To the sample 500µl of DNA lysis buffer (appendix I) and 40µl of proteinase K (PK) (20mg/ml) (ICN) was added. The pellet was incubated overnight at 37°C, shaking at 180rpm.

To the lysate 500µl of phenol (Sigma) was added, the phases were mixed by inverting the tube and then centrifuged 13,000rpm 5 min (MSE Microcentaur). The aqueous phase was transferred to a fresh tube containing an additional 500µl of phenol. The phases were again mixed by inversion, and centrifuged as above. The aqueous phase was removed to a fresh tube containing 500µl of chloroform (Fisher). The phases were again mixed and centrifuged as above. The upper layer was transferred into a fresh tube to which an equal volume of isopropanol (Fisher) was added to precipitate the DNA. The solution was mixed vigorously and centrifuged at 13,000rpm for 10 min (MSE Microcentaur). The supernatant was removed and the pellet allowed to air dry for a few minutes. The pellet was then resuspended in an appropriate volume of TE buffer.

2.4.2 Estimation of DNA concentration and purity

Spectrophotometric analysis and ethidium bromide fluorescent quantification were used for analysis of genomic DNA concentration and digested plasmid DNA concentration respectively. Concentrations were measured on a spectrophotometer (Biomate 3, Thermo Spectronic, Fisher Scientific) initially. Optical densities (OD) of double stranded DNA solutions diluted 1:500 were measured at λ = 260nm. The ratio of measurements made at ODs of 260nm and 280nm gave a measure of the purity of the DNA sample.

Ethidium bromide fluorescent quantitation was performed by running a small sample of DNA for analysis, against known quantities of λ DNA ladder (Life Technologies) on an agarose gel. The gel was visualised by ultraviolet transilluminator and the DNA

concentration was estimated by comparing the fluorescent intensity of the sample against the λ DNA control.

2.4.3 Restriction digest of genomic DNA

A 50µl reaction mix was made up using the required enzyme at 10% of the total reaction volume. The 10X stock ionic strength buffer recommended for use with the enzyme by the manufacturer was diluted to a IX solution in the reaction volume. Spermidine was used at a concentration of 2mM and deionised water was added to make up the final volume taking into account the volume of DNA to be added. The digest was incubated at 37°C overnight. Aliquots were analysed on minigels prior to proceeding to ensure that complete digestion had occurred.

2.4.4 Southern Analysis

Restriction digest products for Southern analysis were run on large agarose gels. The DNA digested with *Hind III* to be probed with the internal probe was run on a 0.8% gel and that for the external probe on a 1% agarose gel. This ensured that proper separation of the DNA fragments would occur. The samples were loaded and run overnight at 4°C. A λ *Hind III* DNA ladder (Life Technologies) was run along side the samples to identify the size position of the DNA fragments. Once the DNA size marker showed that the product sizes of interest had separated sufficiently the gel was photographed and cut to size.

The DNA was then transferred to a membrane by capillary action. Firstly, the gel was soaked in denaturing buffer (0.5M NaOH, 1.5M NaCl) for 2X 30min with constant agitation. This made the DNA single stranded, which was important to enable the probe to bind to its target sequence. The gel was then placed onto the blotting apparatus, which was arranged as follows. Two pieces of Whatman's filter paper (cut to the width of the gel) placed on top of each other were used as a wick from the reservoir of transfer buffer (denaturing buffer). The gel was placed upon the wick making sure that there were no air bubbles between the wick and the gel, as this would impair transfer. The nylon membrane (Hybond H+, Amersham) was cut to size and soaked in deionised water for 5mins followed by transfer buffer for 5 mins and placed on top of the gel, ensuring that there were no air bubbles. Three pieces of Whatman's filter paper cut to

size were soaked in buffer and also placed on top of the membrane. Finally, layers of paper towel were placed on top with a weight to encourage the capillary action. The DNA was left to transfer overnight. Next day the membrane was removed and air-dried.

2.4.5 Radioactive probing of Southern Blots

2.4.5.1 Radiolabelling of Probe DNA

Probe DNA was labelled using a random primer labelling kit (Stratagene), which provided tubes containing freeze dried primers. An aliquot of DNA was added to the probe labelling mixture to give a final concentration of between 25-50ng in a total volume of 42µl made up with deionised water. The primer/DNA mix was incubated at room temperature for a few minutes to ensure that the constituents were properly resuspended. The primer/DNA mixture was then boiled for 10 min to denature the DNA and centrifuged briefly to collect the entire volume. To the primer/DNA mixture 3µl of magenta polymerase and 5µl (50µCi) of α^{32}P dCTP (ICN) were then added in a safety cabinet behind a Perspex shield, to give a final reaction volume of 50µl. The reaction was incubated for approximately 1 hour at 37°C, to allow maximum incorporation of the radioactive isotope in to the probe, after which time the reaction was stopped with 2µl stop mix.

2.4.5.2 Probe purification

The probes were purified using Sephadex Nick translation columns (Amersham Pharmacia Biotech). The columns were washed through with TE buffer prior to use. To the tube containing the radioactively labelled probe 20µl of 10mg/ml sonicated salmon sperm DNA was added. The probe solution was added to the column and washed through with 2X 400µl of TE buffer. The second eluate was collected and the level of radioactivity incorporated checked using a Geiger counter. Unincorporated isotope remained in the column. As a rough guide, if the amount of radioactivity in the probe eluate was greater than that remaining in the column the probe was used for the hybridisation. For more accurate analysis of isotope incorporation TCA precipitation was used.

2.4.5.3 Trichloroacetic precipitation

Trichloroacetic acid (TCA) precipitation was used to measure the incorporation of radioactive isotope into probe DNA. To 1ml of pre-chilled distilled water 10µl of carrier DNA (either salmon sperm or herring sperm DNA) and 1µl of sample DNA were added. This was mixed and then 1ml of 10% TCA was added and the mixture was incubated on ice for 3mins. The apparatus arranged as follows: A glass filter holder was placed into a conical flask with a vacuum attachment. A Whatman 2.4cm glassmicrofibre filter was placed on to the holder and a Pyrex 15ml Millipore funnel was placed on top and the apparatus clamped together. The vacuum was applied and the funnel was wet with a squirt of 10% TCA. The sample was added to the funnel and the tube rinsed with 10% TCA, which was then poured on to the filter. The filter was rinsed with 10% TCA followed by absolute alcohol. The filter was removed with forceps, dried under a heat lamp, then placed in a scintillation vial with 5ml of scintillation fluid (Ultima gold, Packard Biosciences), and the radioactivity was counted by liquid scintillation counting (TRI-CARB 2100TR Liquid scintillation analyser, Packard Biosciences). Samples of probe DNA were analysed before and after purification, with and without TCA precipitation. This allowed analysis of the total counts/minute (cpm) incorporated into the reaction and the cpm that were precipitated with the purified probe DNA. This was necessary to assess the effectiveness of the labelling reaction described above.

2.4.5.4 Pre-hybridisation of membranes

Membranes were washed in 2X SSC (appendix I) and placed into hybridisation tubes (Hybaid). Large membranes were rolled up with gauze, to separate overlapping edges of the membrane. The hybridisation solution (appendix I) was preheated to 65°C. Sonicated salmon sperm DNA (10mg/ml stock) was denatured by boiling for 10min and 200µg/ml was added to 25ml of hybridisation solution. This was enough for one membrane. The hybridisation solution was then added to the tube and the membrane was pre-hybridised for 3 hours at 65°C in a rotating oven (Hybaid).

2.4.5.5 Hybridisation of membranes

Following pre-hybridisation the radioactively labelled probes were denatured by boiling for 10 min, and added to the hybridisation solution. The probes were hybridised to the membranes overnight at 65°C in the rotating hybridisation oven. Next day the

membrane was washed with preheated wash solution (0.1X SSC, 1% SDS) for 2X 30min at 65°C. Membranes were sealed in Clingfilm whilst still damp and subjected to autoradiography. Membranes were placed in to an autoradiograph cassette with Medical X-ray film (Super RX, Fuji). The cassette was then stored at -70°C and the film developed 24 hours later using a hyperprocesser (Amersham). A new film was added if it was necessary to give a longer exposure.

2.4.6 Polymerase Chain Reaction (PCR)

The PCR master-mix proportions and reagents were the same for all PCRs unless otherwise stated. PCR primer sequences are shown in the table 2.1. PCR conditions were as follows. In a reaction volume of 50µl, the 10X PCR buffer (Life Technologies) was diluted to 1X buffer, $MgCl_2$ (Life Technologies) was added to a final concentration of 1.5mM. dNTPs (Amersham Pharmacia Biotech Inc) were used at 200µM each. The primers (Genosys, Sigma) were used at 1.0µM each. Taq DNA polymerase (Life Technologies) was used at 1 unit per reaction. The remaining volume was made up with sterile water. A master reaction mix was made up enough for all samples to reduce pipetting errors and then aliquoted into sterile 0.5ml eppendorf tubes. To each tube an equal volume of liquid paraffin was layered on top, to stop evaporation during thermocycling. The template DNA was added at 1ul per tube through the liquid paraffin layer. Positive and negative controls were set up for each PCR. The negative control had water added in place of DNA template to act as a control for possible contamination of the PCR master mix with foreign DNA. The positive control had DNA that was known to show the expected result and therefore confirm that the PCR conditions were optimal. The PCR reactions were carried out in a thermocycler (Hybaid). Positive displacement pipettes (Microman, Gilson) were used to reduce the risk of cross contamination due to aerosols. The cycle conditions and the expected product sizes for each primer pair are shown in the table 2.1.

Table 2.1 PCR primer sequences, primer targets, expected product sizes and the PCR cycle conditions used.

Primer	Primer Sequence 5'→3'	Target DNA	Product Size	PCR conditions
Px3S	GACTCTGAAGATGTGCCTATGGTCC	K-*ras* exon 3	125 bp	1 cycle of 94°C for 4min and then 30 cycles of 94°C for 30 sec and 58°C for 30 sec
Px3A	GCTGAGGTCTCAATGAACGGAATCC			
Px4AS	CATTGGTGAGAGAGATCCGACAGTAC	K-*ras* exon 4A	72 bp	
Px4AA	TCACACAGCCAGGAGTCTTTTCTTC			
Neo 52	GATGCCTGCTTGCCGAATATCATGG	*neo*^{r}	206bp	
Neo 22	CGATAGAAGGCGATGCGCTGCGAAT			

2.4.7 Colony PCR

A PCR strategy was developed to increase the speed of screening for homologous recombination, which meant that only targeted cells were harvested (as described above 2.3.2).

This method was adapted from McMahon and Bradley, (1990). Cells were targeted, selected and picked as before, with the exception that when the colonies were picked they were added to 400µl of medium containing 300µg/ml G418. Cell colonies were dissociated by pipetting and then split ¼ and ¾ into corresponding wells of two 24 well plates, and 1ml of medium containing G418 was layered on top. When the well containing ¾ of the colony was confluent it was harvested by scraping the cells into 1ml of medium, which was transferred to an Eppendorf tube and centrifuged at 13,000rpm for 5 min (Microcentaur, MSE) and the supernatant removed. The pellet was briefly centrifuged again to remove any remaining medium (which could inhibit the PCR reaction) and resuspended in 80µl of 1X PCR/PK buffer (see appendix I). The samples were incubated at 65°C for 2hr and then the PK was heat inactivated at 90°C for 15 min. This crude cell lysate was then used directly in the PCR reaction. The primer sequence, expected product size and cycle conditions are shown in table 2.2 below. The PCR master mix was made up as above with a few minor alterations as follows; 5µl of DNA template were used instead of 1µl. $MgCl_2$ was not added separately as it was contained in the 10X Colony PCR buffer (Appendix I) and EDTA (10mM) was added to the

reaction. The volume of water was adjusted accordingly to give a final reaction volume of 50μl as before.

Table 2.2 Table shows the PCR primer sequences, primer targets, expected product sizes and the PCR cycle conditions used in the colony PCR

Primer	Primer Sequence 5'→3'	Target DNA	Product size	PCR conditions
Neo 2	AAGCGTCGCGTAGCGGAA	Targeting vector *neo*^{r} cassette to K-*ras* exon 4B	2.1kb	1 cycle of 94°C for 4min followed by 45 cycles 1 min 94°C, 1 min 58°C and 2 min 30 sec 72°C
Px4BA	ATAACTGTACACCTTGTCCTTGACT			

2.5 Manipulation of the mouse embryo

2.5.1. Collection of Blastocysts for Microinjection

Mice were superovulated by injections of pregnant mares serum (PMS) on day 1 and of human chorionic gonadotrophin (HCG) on day 3, which was followed by mating. On day 3.5 post coitum the mice were sacrificed and the uterine horns removed. Using a fine gauge needle blastocysts were flushed out using cell culture medium 9without LIF or β-mercaptoethanol) into a petri dish. The embryos were collected and placed in a fresh petri dish in a small drop of medium under mineral oil (Sigma) and maintained at 37°C in a 5% CO_2 incubator until microinjection.

2.5.2. Production of chimaeras by blastocyst injection

Dr Charles Patek, Jan Ure and Jennifer Doig performed the blastocyst injections on my behalf. Targeted ES cells were injected into, either day 3.5pp F_2 (C57BL/6 x CBA), or day 3.5pp C57 BL/6 blastocysts. Approximately 10-12 ES cells were injected into each blastocyst and implanted into the uteri of, either day 2.5pp F_1(C57BL/6 x CBA), or CD1 pseudopregnant recipients. Vasectomised males were used to generate pseudopregnant females. The chimaeric offspring were identified on the basis of coat colour analysis.

2.6 Detection of protein expression in tissue sections

Immunohistochemistry was performed using a K-Ras 4A rabbit polyclonal antibody (Santa Cruz) and a K-Ras 4B rabbit polyclonal antibody (Santa Cruz). Antibody dilution curves were performed to establish the correct concentration of antibody to be used in each case.

The samples collected for analysis were treated as follows: The embryos were fixed for approximately 8hrs in 10% formal buffered saline to prevent over fixation, and the neonatal and adult tissue samples were fixed in 10% formal buffer saline overnight. All samples were processed for paraffin embedding. The embryos were all mounted so that the sectioning would be transverse.

2.6.1 Immunhistochemistry: Paraffin embedded sections

From paraffin blocks 5μm thick sections were cut and attached to polylysine coated slides (BDH). The sections were de-waxed using Histoclear (National Diagnostics) for 2x 5min and then rehydrated by immersion in a series of graded alcohols 100% 2x 2min, 90% 2x 2min, 70% 2x 2min, finally immersing the slides in tap water. Then a method of antigen retrieval was used. Several were tried in order to optimise the signal strength for each antibody used

1) Citrate buffer pH6.6 antigen retrieval solution (Vector) 1% in deionised water. The antigen retrieval solution (400ml) was pre-warmed in the microwave (950W) for 5min on full power. Then the slides were heated in the microwave for 2x 5min on full power. Topping up the solution as necessary to ensure that the sections remain submerged. The slides were then immediately removed to running tap water.

2) The pepsin (Sigma)/ saponin (Sigma) method was also used. The sections were incubated for 15min in a 5μg/ml in 0.01M HCl buffer pH2.5 pepsin solution at room temperature. The sections were washed twice in deionised water. The sections were then incubated for 30min in a saponin solution (5μg/ml in deionised water) at room temperature and washed 3x in PBS.

3) The urea antigen retrieval method was used. A solution of 0.8M urea pH6.4 was heated up for 5min prior to the sections being added and then 2x 5min with the sections and the levels topped up as necessary. Sections were washed in running water.

Endogenous peroxidase was blocked using a solution of 3% hydrogen peroxide (Sigma) in water for 15min at room temperature. The sections were washed in 1X PBS. The signal was visualised by the avidin biotin complex method using Vector Elite goat anti-rabbit ABC kit (Vector Labs). The blocking serum (normal goat serum) was diluted to 1.5% in 1X PBS and added to the sections for 20 min in a humid chamber. The excess was serum was removed and the primary antibody added at the required dilution (diluted in 0.01% BSA) for, either 2 hour in the humid chamber at room temperature, or overnight at 4°C. The negative control had the primary antibody omitted and was incubated in 0.01% BSA. The slides were then washed for 5 min in 1X PBS and the goat anti-rabbit secondary antibody (Vector Labs) added for 30 min and followed by washing in 1X PBS. The ABC reagent (Vector Labs) was added for 30 min and the sections washed in PBS. Finally, the DAB substrate (Vector Labs) was added for 5 min and the sections washed in running water. Sections were then counterstained with 50% haematoxylin (BDH) for 30 seconds, dehydrated through graded alcohols and placed into xylene. The coverslips were mounted with DPX (BDH).

The use of blocking peptides was included as an additional control to ensure that signals produced were the result of the specific binding of the K-Ras 4A and K-Ras 4B rabbit polyclonal primary antibodies to their epitopes. The amount of primary antibody needed for the experiment was calculated and for neutralisation a volume of blocking peptide was added to give 50-100 the weight (w/w) of peptide to primary antibody, and then a small volume of PBS was added to the tube (~100µl). The mixture was incubated on a rocking platform overnight at 4°C, and then centrifuged for 15 min at 4°C to pellet any immune complexes. The primary antibody/peptide mixture was diluted to the final working concentration of antibody required and used as described above.

2.7 RNA Analysis

2.7.1 RNA Extraction

To avoid RNase contamination all lab ware and reagents were set aside for RNA work only. The water used was DEPC treated and autoclaved. Surfaces and equipment were cleaned with RNase Away (Life Technologies) and gloves and a clean lab coat were worn at all times.

RNA was extracted from cells and tissues using the Trizol (Life Technologies) method. For tissues 1ml of Trizol reagent was used per 50-100mg of tissue and homogenised using a power homogeniser (Ultra-Turrax T25, Janke-Kunkel IKA Labortechnik). ES cells were lysed directly in the culture dish using 1ml of Trizol reagent per $10cm^2$ of tissue culture area. The cells were then scraped from the surface and the lysate was transferred to a 15ml Falcon tube. It was possible to store the lysates at this stage at -70°C. If the samples were to be used immediately they were incubated at room temperature for 5 mins to permit the complete dissociation of the nucleoprotein complexes. For every 1ml of Trizol reagent used 0.2ml of chloroform was added and the samples shaken vigorously, incubated at room temperature for several minutes and then centrifuged at 12,000xg for 15 mins at 4°C (Sorvall). The upper aqueous phase was transferred to a fresh tube and the RNA precipitated using 0.5ml of isopropanol per 1ml of Trizol reagent used for the initial homogenisation. Samples were incubated at room temperature for 10 mins and then centrifuged at 12,000xg for 10 mins at 4°C. The supernatant was removed and the RNA pellet washed once with 75% ethanol (made with DEPC treated water) using at least 1ml of 75% ethanol per 1ml of Trizol. Samples were mixed and centrifuged at 7,500xg for 5 mins at 4°C. The supernatant was discarded and the RNA briefly air-dried before redissolving in DEPC-treated water. Samples were incubated for 10mins between 55-60°C to help the RNA redissolve. The $A_{260/280}$ and concentration were determined by spectral analysis.

2.7.2 First-strand cDNA synthesis

First-strand cDNA synthesis was performed using the SuperScript™ preamplification system for first strand cDNA synthesis (Life Technologies) according to manufacturers guidelines.

RNA/primer mixtures were made up with an aliquot of RNA (1-5μg), 1μl of Oligo(dT)$_{12-18}$ (0.5μg/μl) and DEPC-treated water to a final volume of 12μl. Duplicate samples were prepared for plus and minus RT controls. Each sample was incubated at 70°C for 10 mins and then on ice for at least 1 minute. A master reaction mix was prepared containing 2μl 10X PCR buffer, 2μl 25mM $MgCl_2$, 1μl 10mM dNTP mix and 2μl 0.1M DTT for each sample. This was then mixed and 7μl was added to each RNA/primer mixture. This was mixed, collected by brief centrifugation and incubated at 42°C for 5 min. To the plus RT samples 1μl (200 units) of SuperScript II RT was added, tubes were mixed and then all samples were incubated at 42°C for 50 min. Reactions were terminated at 70°C for 15 min and then chilled on ice. Reactions were collected by brief centrifugation and 1 μl of RNase H was added to each tube and reactions were incubated for 20 min at 37°C.

2.7.3 Amplification of target cDNA

The first strand cDNA obtained above was then amplified directly using PCR. Only 10% of the first strand reaction was used, since larger amounts decreased the amount of product synthesised. The PCR reaction mixture was made up as previously described excepted that 2μl of cDNA template were used. The primer sequences, expected product sizes and cycle conditions are shown in the table below.

Table 2.3 PCR primers and conditions for amplification from cDNA

Primer	Primer Sequence 5'→3'	Target DNA	Product size	PCR conditions
KRF	GGAATTCCGCCTGCTGAA ATGACTGAGT	K-*ras* cDNA exon 1	K-*ras* 4A 687bp	30 cycles of 94°C for 1 min and 55°C for 1 min followed by a 10min 72°C final extension
KRR	CGGGATCCCGTGTACACC TTGTCCTTGACTT	K-*ras* cDNA exon 4B	K-*ras* 4B 565bp	

KRF and KRR are as previously published (Pells *et al.*, 1997).

2.8 *In vitro* analysis of ES cell proliferation, differentiation and apoptosis

2.8.1 Proliferation assay

Cells were grown in 75cm^2 flasks to approximately 80% confluence, trypsinised and counted using a Coulter particle count and size analyser (Beckman-Coulter), and seeded at ~7.5x10^5 cells/90mm petri dish. Dishes were set up in triplicate for each time point. Cells were harvested at 24, 36, 48, 72, 84 and 96 hours after seeding. At each time point the cells were harvested by trypsinisation (as previously described) and cell pellets were resuspended in 1ml of cell culture medium and diluted 1 in 20 in Isoton II balanced electrolyte solution (Beckman-Coulter) and cell numbers were counted as above.

2.8.2 Stem cell renewal assay

Cells were grown to subconfluence in 75cm^2 tissues culture flasks, trypsinised and counted (as described above). The cells were seeded at 1x10^3 cells per well of a gelatinised 6 well plate. The cells were cultured in normal growth medium that contained different levels of LIF either, 250U, 100U, 10U, 1U or in the absence of LIF for 5 days. At which time they were stained for the presence of alkaline phosphatase activity.

The alkaline phosphatase activity was detected using an alkaline phosphatase kit (Sigma Diagnostics). The volumes of solutions required were calculated according to the number of wells to be analysed, with 1ml of solution sufficient for one well of a 6 well plate. Proportions were as follows: 0.2ml of sodium nitrite and 0.2ml of FRV-alkaline solution were mixed, allowed to stand for 2 mins and added to 9ml of deionised water. To this solution 0.2ml of Naphthol AS-BI alkaline solution was added. The growth medium was removed and the cells were fixed for 30 sec and then rinsed with water for 45 sec. The stain solution was then added to the cells and incubated in the dark at room temperature for 15 mins. After removal of the stain the cells rinsed with water and allowed to air dry. ES cell colonies stained intensely pink.

2.8.3 Treatment of ES cells with apoptosis inducing agents

Cells were treated with etoposide (Sigma), TNF alpha (Cambridge bioscience), Fas monoclonal antibody (Jo2) (BD PharMingen) or recombinant Fas ligand (Upstate biotechnology).

Cells were grown to subconfluence in $75cm^2$ tissue culture flasks, trypsinised and seeded at, either $2x10^6$ cells/90mm petri dish for etoposide treatment, or $9x10^5$ cells/ well of a 6 well plate for TNF alpha, Fas monoclonal antibody and Fas ligand treatments. Cells were allowed to attach overnight in normal growth medium. Next day the medium was replaced with medium containing the apoptosis-inducing agent.

Etoposide was dissolved to a stock concentration of 100mM in DMSO for long-term storage. A working stock of 20mM etoposide was prepared in DMSO, which was further diluted to give final concentrations of between 5-40μM. All plates received DMSO to a final concentration of 0.02%. Untreated controls and controls with DMSO alone were used to control for the effect of DMSO and etoposide on the system. Cells were treated with etoposide for between 6 to 48hrs and then harvested for analysis as described below.

TNF alpha was dissolved to a stock concentration of 1μg/ml in medium containing 5% FCS (normal growth medium). This was diluted further to treatment concentrations of 10ng/ml, 50ng/ml and 100ng/ml in growth medium. Cells were incubated in the presence of TNF alpha for 24 and 48hr and then harvested for analysis.

Fas monoclonal antibody (Jo2) was provided at a concentration of 1mg/ml and was diluted to the required concentration in normal growth medium.

In the case of Fas ligand, the lyophilised powder was resuspended in 50μl of sterile water to give a concentration of 100μg/ml. The stock solution was then further diluted to the required concentrations with normal growth medium.

2.8.3.1 Treatment of ES cells with signal transduction pathway inhibitors

ES cells were treated with the MEK inhibitor PD98059 (Promega) and the PI-3Kinase inhibitor LY294002 (Promega). Both inhibitors were provided as lyophilised powders, which were reconstituted with DMSO to give 20mM stock concentrations. The stock solutions were then diluted to the required concentration with culture medium.

2.8.4 Flow-cytometry (Vindelov analysis)

The DNA content of ES cells was analysed by flow-cytometry (adapted from Vindelov *et al.*, 1983). Cells were trypsinised and resuspended to a concentration of $2x10^6$ cells/ml in cell culture medium, of which 0.5ml was transferred to a Eppendorf tube and centrifuged for 30 sec at 4,000rpm (MSE, Microcentaur). The supernatant was discarded and the cell pellet was resuspended in 100µl of citrate buffer (appendix I). To the cell/citrate buffer suspension 450µl of solution A containing a strong trypsin (0.3mg/ml) (appendix I) was added and the sample was mixed by inversion and incubated at room temperature for 10 min. To this 325µl of solution B containing a trypsin inhibitor (0.5mg/ml) and ribonuclease A (0.1mg/ml) (appendix I) was added, and the sample incubated at room temperature for 10 min following mixing by inversion. Finally, 250µl of solution C containing 0.4mg/ml propidium iodide (appendix I) was then added to the sample, mixed and incubated at 4°C in the dark for 10 min. The samples were run through a Coulter EPICS XL flow-cytometer, and the DNA content of the sample was analysed by the EPICS software.

2.8.5 Detection of phosphatidyl serine by annexin V

Annexin V detects the presence of phosphatidyl serine, which is externalised to the outer surface of the plasma membrane as an early event in apoptosis. Cells were treated with apoptosis inducing agents, harvested and washed once with ice cold PBS and then gently resuspended in 100µl of annexin V/propidium iodide buffer (R&D Systems) (0.35µg/ml annexin V and 0.25µg/ml PI) per $1x10^5$-$1x10^6$ cells for 15 min at room temperature in the dark. Then 400µl of 1X binding buffer was added and the samples were analysed immediately on a Coulter EPICS XL flow-cytometer.

2.8.6 Immunofluorescent staining with Hoechst 33342 and propidium iodide

Hoechst 33342 and propidium iodide immunofluorescence was used for morphological analysis to detect nuclear changes consistent with apoptosis. The culture medium was aspirated into a universal tube and the cell monolayer was washed with PBS, which was then aspirated into the same universal. Trypsin was added to the monolayer, and the cells were transferred to the same universal tube. This ensured that the whole cell population was collected. The cell suspension was centrifuged at 1,000rpm for 5 min (MSE Mistral 1000) and the pellet was resuspended in 1X PBS to ~$5x10^5$ cells/200µl. This was transferred to an Eppendorf to which 8µl of 200µg/ml Hoechst 33342 (Molecular Probes) was added. This cell suspension was incubated at 37°C for 10 min. Then 2µl of 1mg/ml propidium iodide (Molecular Probes) was added just prior to analysis and the samples were incubated on ice in the dark until needed, to reduce the fading of the stains. Slides were prepared with 30µl of cell suspension, which was added to the slide immediately prior to analysis, a cover slip was placed on top and the sample analysed by immunofluorescence using a UV microscope (Axioskop, Zeiss). For each sample 250 cells were scored from at least two random fields, and classified as either viable, apoptotic, late apoptotic or necrotic and expressed as a percentage of the total number of cells counted (representative pictures are shown in chapter 6.3).

Chapter 3

The Generation Of K-*ras* 4A Mutants By Gene Targeting

Introduction

Recent years have seen an emerging body of evidence for differential signalling amongst Ras protein isoforms. Far from being a highly homologous functionally redundant family of proteins, it is now becoming increasingly clear that the Ras proteins weave a complex web of interactions with exchange factors and signal transduction pathways, which is determined at least in part by the subcellular localisation of the proteins. Therefore, it is of interest to investigate the relative importance of the expression of the K-*ras* 4A and 4B isoforms during embryonic development and in adult tissues, to elucidate further their contribution to the phenotype associated with the complete deletion of both K-Ras proteins (Johnson *et al.*, 1997; Koera *et al.*, 1997).

The study of transgenic animals derived using ES cells heterozygous for the deletion of K-*ras* exon 4A, and examination of ES cells homozygous null for this deletion provides a model system with which to explore the role of K-*ras* 4A *in vitro* and *in vivo*. This system also dissects the relationship between the K-*ras* 4A and 4B isoform and could address vital questions regarding their interaction during mouse development. ES cells with a heterozygous deletion of the K-*ras* 4A exon had previously been derived by this laboratory (E14 Δ4A 73). Nevertheless, the aim of this work was to generate a new independent heterozygous null cell line for the deletion of exon 4A and then generate homozygous null cell lines from both of these. This was of importance, since it was necessary to establish the reproducibility of any observed phenotypes between independent clones of the same genotype.

3.1 Generation of ES cells heterozygous for the deletion of exon 4A

3.1.1 Characterisation of targeting vector pPTKiNKiΔ4A

The targeting vector pPTKiNKiΔ4A used in these experiments was designed and constructed by Dr James Williamson. A diagrammatic representation of the vector is shown in figure 3.1. The targeting vector comprises an upstream and a downstream arm

of homology designated KRI4 and KRI5 respectively, which were isolated from a pBR322 plasmid containing an *EcoR1* fragment of K-*ras* (George *et al.*, 1985) encompassing the region immediately upstream of exon 3 to just upstream of exon 4B. KRI4 was excised from the plasmid by *HindIII* digestion, and KRI5 was isolated by a *EcoRI/XbaI* digest. Therefore, the arms of homology are segments of intronic sequence flanking exon 4A. The vector contains a Herpes simplex virus (HSV)- *thymidine kinase* (*tk*) cassette to enable negative selection by ganciclovir, and a *neomycin* resistance (*neo*^{r}) cassette driven by a phosphoglycerate kinase (PGK) promoter to enable positive selection of targeted clones in the presence of geneticin (G418). The integration site of the targeting vector and the expected alterations to the K-*ras* gene are shown schematically in figure 3.2. The targeting vector replaces exon 4A with the *neo*^{r} cassette, generating a targeted allele, which is designated K-*ras*$^{+/tm\Delta 4A}$. Prior to carrying out the electroporation of the ES cells with the targeting vector, diagnostic cuts were performed to confirm the identity of the plasmid. The 12.2Kb targeting vector was linearised by digestion with the *EcoR1* restriction enzyme, and a triple digest with *EcoR1*, *Xba1* and *NotI* produced the four bands of ~1.3Kb, ~1.9kb, ~3.5Kb and ~4.5Kb (figure 3.3).

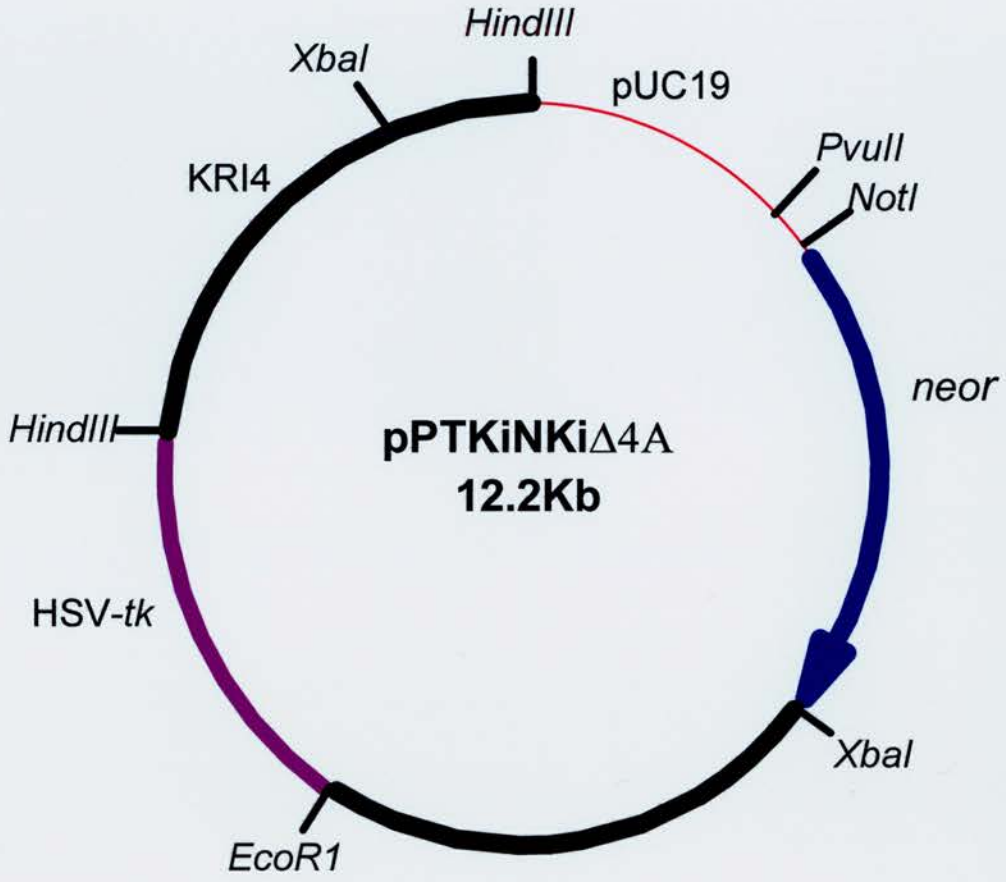

Figure 3.1 Diagrammatic representation of pPTKiNKiΔ4A. The targeting vector was constructed using the pUC19 plasmid. The vector was linearised by digestion with *EcoR1*. The positions of the restriction enzyme sites for diagnostic digest are indicated (*EcoRI*, *NotI* and *XbaI*). KRI4 is the upstream arm of homology and KRI5 is the downstream arms of homology corresponding to intronic sequence adjacent to K-*ras* exon 4A.

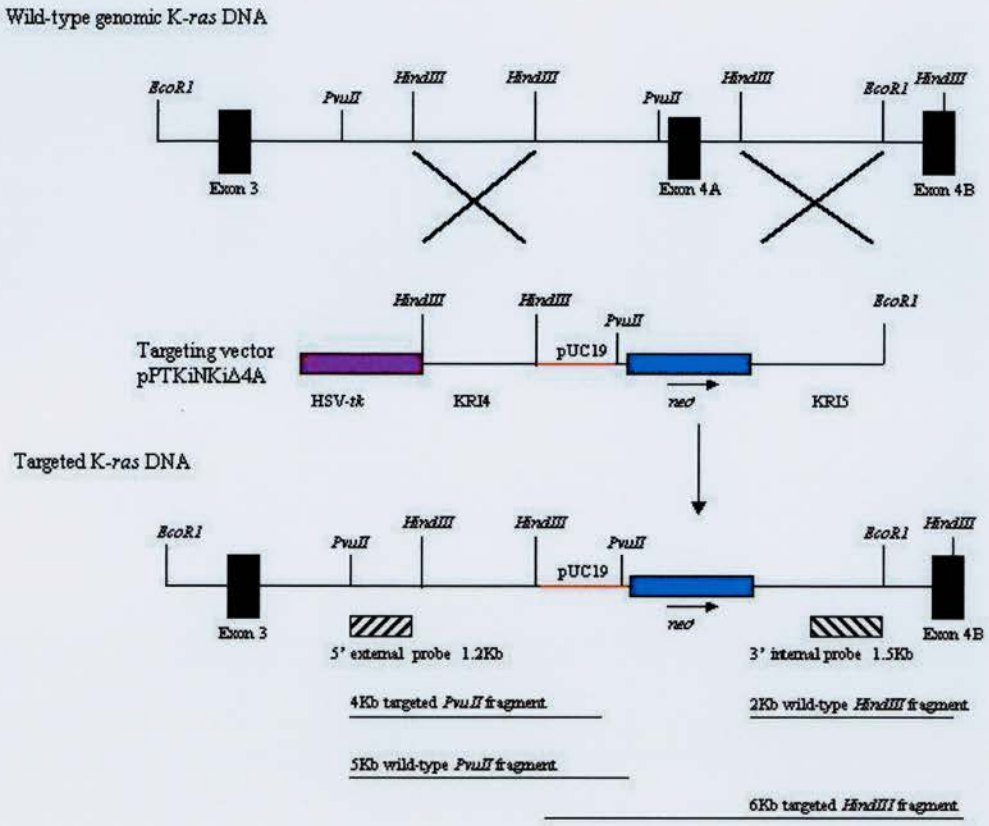

Figure 3.2 Schematic representation of the targeting strategy used to delete exon 4A. Wild-type genomic DNA shows exons 3, 4A and 4B of the K-*ras* gene with the relevant restriction sites. The targeting vector was designed to delete exon 4A by the insertion of the *neomycin* resistance (*neo*^{r}) cassette. The probes used to screen for homologous recombination by Southern analysis are shown with the expected product sizes.

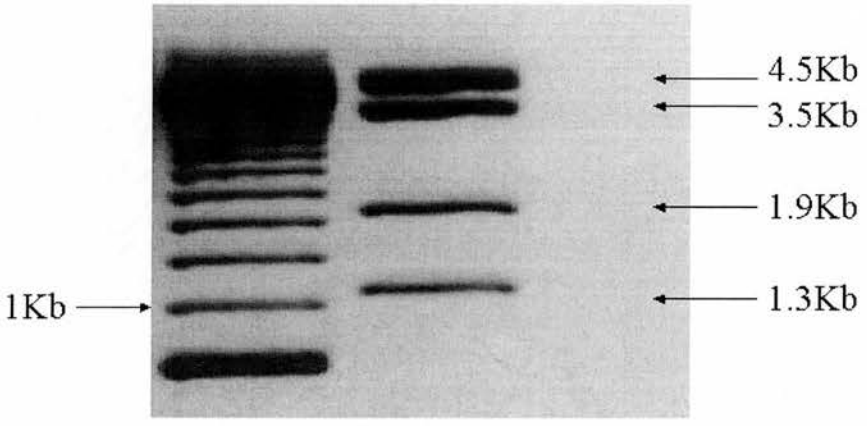

Figure 3.3 Diagnostic triple digest of pPTKiNKiΔ4A. The plasmid pPTKiNKiΔ4A was digested using a triple digest with *EcoR1*, *Xba1* and *Not1* to produce four bands of approximately 1.3, 1.9, 3.5 and 4.5Kb. The DNA marker is a 250bp ladder (Life Technologies).

3.1.2 Electroporation of E14 IV embryonic stem cells

The pPTKiNKiΔ4A targeting vector has previously been used successfully by Dr James Williamson to generate the E14 Δ4A 73 cell line. However, since only one K-*ras*$^{+/tm\Delta 4A}$ cell line was isolated it was important to generate further independent cell lines with a heterozygous deletion of exon 4A. Therefore, E14 IV ES cells (kindly gifted by Dr Julia Doran) were electroporated with 150μg of the targeting vector, which had been linearised with *EcoR1*. Following electroporation the ES cells were plated down overnight in normal growth medium then cultured in the presence of 150μg/ml geneticin for four days. The concentration of geneticin had been pre-determined by a dose response analysis of wild-type ES cells. The concentration used was the minimum required to cause total cell death over a period of approximately one week. After four days of positive selection by geneticin, negative selection was begun by the addition of ganciclovir to the media. One of the petri dishes was maintained in the presence of geneticin alone to analyse the additional selection caused by the ganciclovir treatment. The selection was carried out for 14 days as described in section 2.4.2, at which time the surviving colonies were picked and expanded. The negative selection with ganciclovir caused an approximate 2-fold increase in selection, compared to geneticin alone. The plate receiving geneticin alone had 82 colonies, whereas the plate receiving geneticin and ganciclovir had 45 colonies.

Surviving clones were screened by Southern analysis for homologous recombination (figure 3.4). In total 306 clones were screened with the internal probe, this identified both homologous and non-homologous recombinants, since the probe hybridised to a region within the targeting vector. Following digestion of genomic DNA with *HindIII*, the internal probe identified a 2Kb band in wild-type DNA, and a 2Kb to 6Kb transition following homologous recombination, due to the loss of the *HindIII* restriction site upstream of exon 4A by the integration of the *neo*^{r} cassette (figure 3.2). Of the 306 clones screened with the internal probe 22 colonies were identified that showed the correct band pattern.

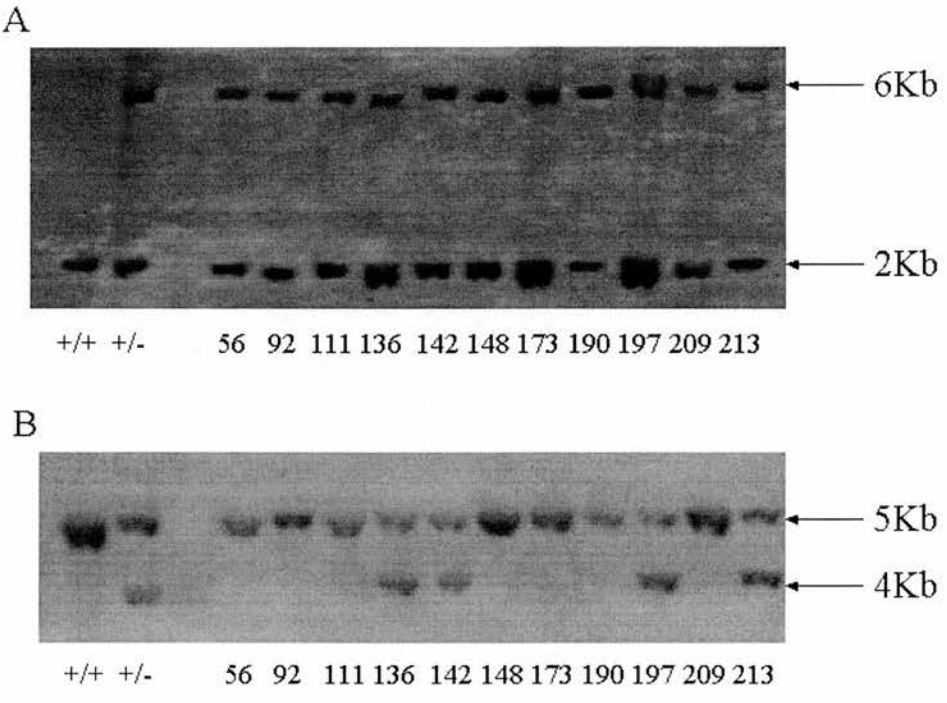

Figure 3.4 Detection of targeted clones by Southern analysis following homologous recombination with the targeting vector pPTKiNKiΔ4A. A) Repeat Southern analysis with the internal probe of 11 of the 22 clones isolated following the initial screen of all 306 clones with this probe. Homologous recombination results in the detection of a 6Kb band as well as the wild-type 2Kb band. B) Southern analysis using the external probe. Homologous recombination results in a 5kb to 4Kb transition. The use of this probe showed that only 4 of the 22 clones analysed had undergone homologous recombination.

These clones were then screened with the external probe; which identified only those clones that had undergone homologous recombination. DNA was digested with *PvuII* to identify a 5Kb band in wild-type DNA and a 5Kb to 4Kb transition following homologous recombination. Of the 22 clones analysed only 4 clones showed the correct band pattern with the external probe and an approximate 1:1 ratio of band intensity (figure 3.4).

The low percentage of homologous recombination (1.3%) observed in this targeting strategy was not unexpected, since the arms of homology used to create the targeting vector were non-isogenic, as the ES cells were derived from the 129/Ola strain of mice and the homology arms were from CBA mice. The heterozygous clones (K-*ras*$^{+/tm\Delta 4A}$) that were identified following Southern analysis were designated E14 IV 136, 142, 197 and 213. These clones were then expanded into cell lines for further analysis.

3.1.3 Analysis of ES cell chromosome number

Due to the potential for ES cells to undergo spontaneous chromosomal trisomy and other abnormalities (Liu *et al.*, 1997) in culture it was important to ensure that the targeted clones had the correct chromosome number, since chromosomal abnormalities have been shown to reduce ES cells contribution to the germline. A representative number of metaphase spreads (~25) were counted for each of the 4 clones. Clones that had more then 70% of the metaphase spreads containing 40 chromosomes were considered to be normal. In all four heterozygous cell lines approximately 80% of the metaphases counted had 40 chromosomes (Table 3.1).

Table 3.1 Percentage of chromosomally normal metaphase spreads

Cell line	Passage number	% chromosomally normal
E14 IV (+/+)	+20	81%
E14 IV 136 (+/*tmΔ4A*)	+10	78%
E14 IV 142 (+/*tmΔ4A*)	+6	85%
E14 IV 197 (+/*tmΔ4A*)	+8	75%
E14 IV 213 (+/*tmΔ4A*)	+8	83%

Wild-type (+/+) parental E14 IV cell line and the four cell lines with heterozygous deletions of exon 4A (+/*tmΔ4A*). The passage numbers at which the chromosome numbers were counted are also indicated. For the +/*tmΔ4A* cell lines the passage number represents the number of passages since isolation of the targeted cell line.

3.2 Isolation of K-*ras*$^{tm\Delta4A/tm\Delta4A}$ ES cells

3.2.1 Attempt to isolate K-*ras*$^{tm\Delta4A/tm\Delta4A}$ ES cells from clone E14 Δ4A 73

High G418 selection (section 2.4.3.) selects for cells that have undergone spontaneous loss of heterozygosity (LOH) (Mortensen *et al.*, 1992). These cells have a duplication of the *neo*^{r} cassette and can be selected for by culturing of heterozygous cells in high concentrations of geneticin. The mechanism of duplication is believed to be either, mitotic recombination or, chromosome loss and duplication (Lefebvre *et al.*, 2001).

The K-*ras*$^{+/tm\Delta4A}$ cell line designated E14 Δ4A 73 (as described above), as it was already available was used initially to generate K-*ras*$^{tm\Delta4A/tm\Delta4A}$ cell lines. This cell line had been characterised previously and been shown to have the correct genotype by Southern analysis with the internal and external probes and the correct chromosome number by metaphase spread analysis. Several high G418 selections were performed on the E14 Δ4A 73 cell line, but all proved unsuccessful. Extremely high concentrations of geneticin (Life Technologies) were used (up to 7mg/ml) and these did not cause significant cell death, and following 14 days of growth under these conditions it was not possible to identify individual colonies.

3.2.1.1 Investigation of the geneticin resistant nature of E14 Δ 4A 73

There were two possible reasons for this: firstly, that the E14 Δ 4A 73 cell line contained a mixed population of targeted cells and cells that contained a second random integration, or alternatively that a secondary event had occurred in some cells of the original clone. Both hypotheses would lead to a subpopulation of cells containing two *neo*^{r} cassettes, resulting in those cells surviving selection. If either of the above hypotheses were correct it predicts that subcloning this population should result in the isolation of cells that contain only the desired genotype. Therefore, to investigate this further E14 Δ 4A 73 cells were used for single cell cloning.

For the subcloning of E14 Δ 4A 73 a dilution was calculated to give less than 1 cell per well of a 96 well plate. Cells were grown for several days and only those wells that were deemed to have colonies derived from a single cell were harvested. A total of 62

clones were derived and screened by Southern analysis with a probe that detected the *neo*^{r} cassette. The 2.7Kb *neo* probe was generated by an *XhoI* digest of the pUHD172-*neo* plasmid (Gossen *et al.*, 1995). A 6Kb band was expected in cells containing the homologously recombined targeting vector following digestion of genomic DNA with *HindIII*. The detection of an additional 9Kb band in some clones confirmed the existence of a mixed cell population (figure 3.5 A). These same clones were subsequently screened with the internal and external probes as previously described (section 3.1.2), which also confirmed the presence of a mixed cell population, identifying the same abnormal clones as the *neo* probe (Figure 3.5 B and C).

Therefore, using this method it was possible to isolate clones that had the correct genotype. One of these was E14 Δ4A 73/39. The chromosome number of this clone was analysed following its isolation to ensure that a chromosomally abnormal clone had not been selected (table 3.2). The chromosome number was found to be comparable to its parental cell line. Therefore, using single cell cloning it was possible to isolate a new cell line containing the correct genotype with the correct chromosome number.

Table 3.2. The percentage of metaphase spreads counted containing 40 chromosomes

Cell line	passage number	% chromosomally correct
E14Δ 4A 73 (+/*tmΔ4A*)	+12	72%
E14Δ 4A 73/39 (+/*tmΔ4A*)	+2	70%

Analysis of the chromosome number of the parental K-*ras*$^{+/tm\Delta 4A}$ cell line E14 Δ4A 73 and the heterozygous cell line re-derived from it by subcloning E14 Δ 4A 73/39 by metaphase spread analysis. Passage numbers indicated are passages since isolation of the targeted clone.

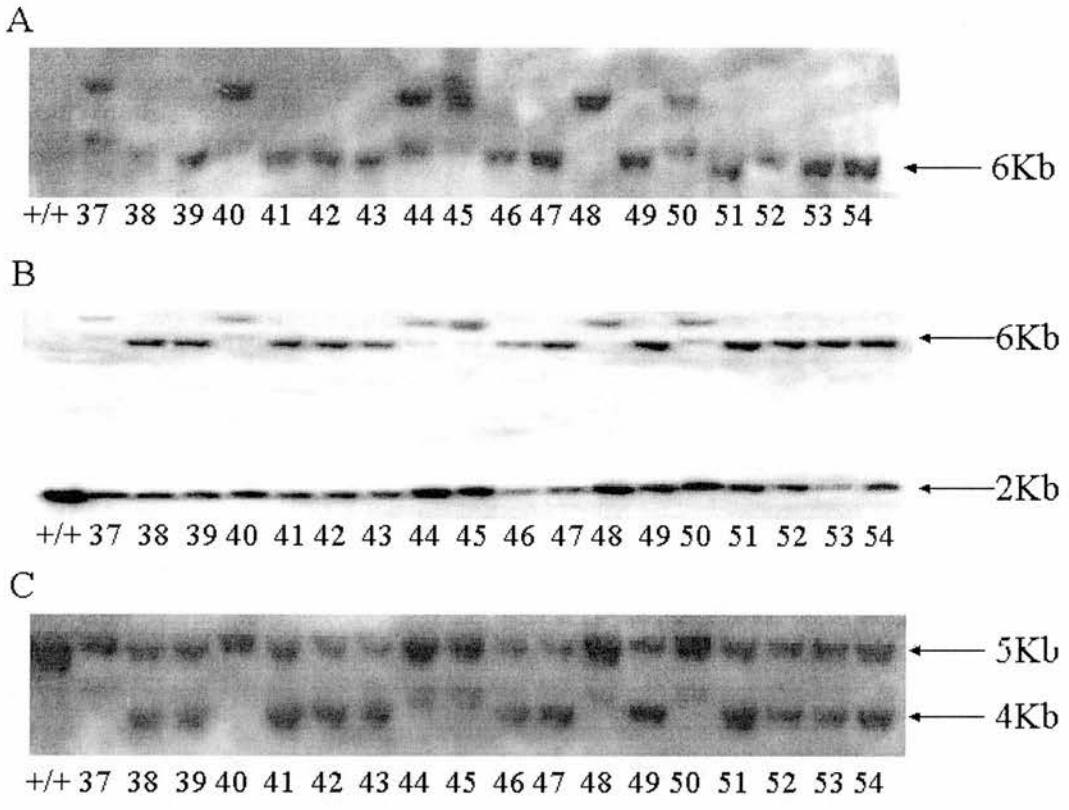

Figure 3.5 Southern analysis of K-*ras*$^{+/tm\Delta 4A}$ clones derived from single cell cloning. DNA extracted from the cell lines isolated following single cell cloning was analysed by Southern analysis. A) *neo* probe. B) Internal probe. C) External probe. These probes clearly show a mixed cell population. The correct band sizes expected for each probe are indicated.

3.2.2 Isolation of K-*ras*$^{tm\Delta4A/tm\Delta4A}$ clones from E14Δ4A 73/39 ES cells

Following the isolation of the E14 Δ4A 73/39 cell line high G418 selections (1-3mg/ml) were carried out on this and other cell lines containing the heterozygous deletion of exon 4A, (E14 IV 136, 197 and 213, as described previously (3.2.1)). The cells were grown for 14 days under these conditions changing the media regularly to maintain selective pressure. Significant cell death was observed with the formation of discrete colonies. The surviving colonies were picked and screened for the lose of exon 4A using primers in exon 4A and primers in either exon 3 or 4B as a control to confirm that DNA was present and of the appropriate quality for PCR. However, only the heterozygous cell line E14 Δ4A 73/39 produced ES cells homozygous for the deletion of exon 4A designated K-*ras*$^{tm\Delta4A/tm\Delta4A}$, these were termed E14 Δ4A 73/39/9 and E14 Δ4A 73/39/22. The PCR analysis confirmed that these clones lacked the 72bp exon 4A product (figure 3.6), but that they were still able to produce the exon 3 PCR product.

However, when the chromosome numbers of these two clones were counted, they were found to be abnormal. The majority of metaphase spreads counted had 42 instead of 40 chromosomes (Table 3.3). Therefore, a further high G418 selection was performed using the E14 Δ4A 73/39 heterozygous cell line and two more homozygous clones (E14 Δ4A 73/39/137 and E14 Δ4A 73/39/145) were identified by PCR analysis (figure 3.6). The relative efficiency of the high G418 selection for the various heterozygous cell lines used is shown in table 3.4. However, these cell lines were also determined to be chromosomally abnormal by metaphase spread analysis (Table 3.3), with the predominant chromosome number again being 42 instead of the expected 40.

Table 3.3 Proportion of metaphase spreads counted containing 40 chromosomes

Cell line	passage number	% chromosomally normal
E14 Δ 4A 73/39 (*+/tmΔ4A*)	+2	70%
E14 Δ 4A 73/39/9 (*tmΔ4A/tmΔ4A*)	+7	38%
E14 Δ 4A 73/39/22 (*tmΔ4A/tmΔ4A*)	+7	5%
E14 Δ 4A 73/39/137 (*tmΔ4A/tmΔ4A*)	+7	0%
E14 Δ 4A 73/39/145 (*tmΔ4A/tmΔ4A*)	+7	0%

The parental K-*ras*$^{+/tm\Delta4A}$ cell line E14 Δ4A 73/39 and the four K-*ras*$^{tm\Delta4A/tm\Delta4A}$ cell lines derived by high G418 selection. Passage numbers indicate passages since isolation of targeted clone.

The reasons for this are unknown, but the E14 Δ4A 73/39 cell line had been through several rounds of selection and extensive cell culture, which may have led to the selection of a chromosomally unstable subpopulation, although this was not apparent when this cell line was isolated. The generation of such low percentages of homozygous null ES cell clones from this procedure was unexpected. However, the percentage of homozygous null colonies derived by this procedure has been shown to vary greatly (Mortensen *et al.*, 1992). The failure of the heterozygous E14 IV clones to generate any homozygous null clones suggested that the conditions were not optimal for these cell lines.

Table 3.4 Percentage of K-*ras*$^{tm\Delta4A/tm\Delta4A}$ clones derived from K-*ras*$^{+/tm\Delta4A}$ cell lines following high G418 selection.

Cell line	Number of colonies screened by PCR	Number of homozygous clones identified	Percentage
E14 Δ4A 73/39	71	2	2.8
E14 Δ4A 73/39	75	2	2.7
E14 IV 136	146	0	0
E14 IV 197	96	0	0
E14 IV 213	96	0	0

The two entries for E14 Δ4A 73/39 refer to the two independent high G418 selections performed on this cell line described in the text.

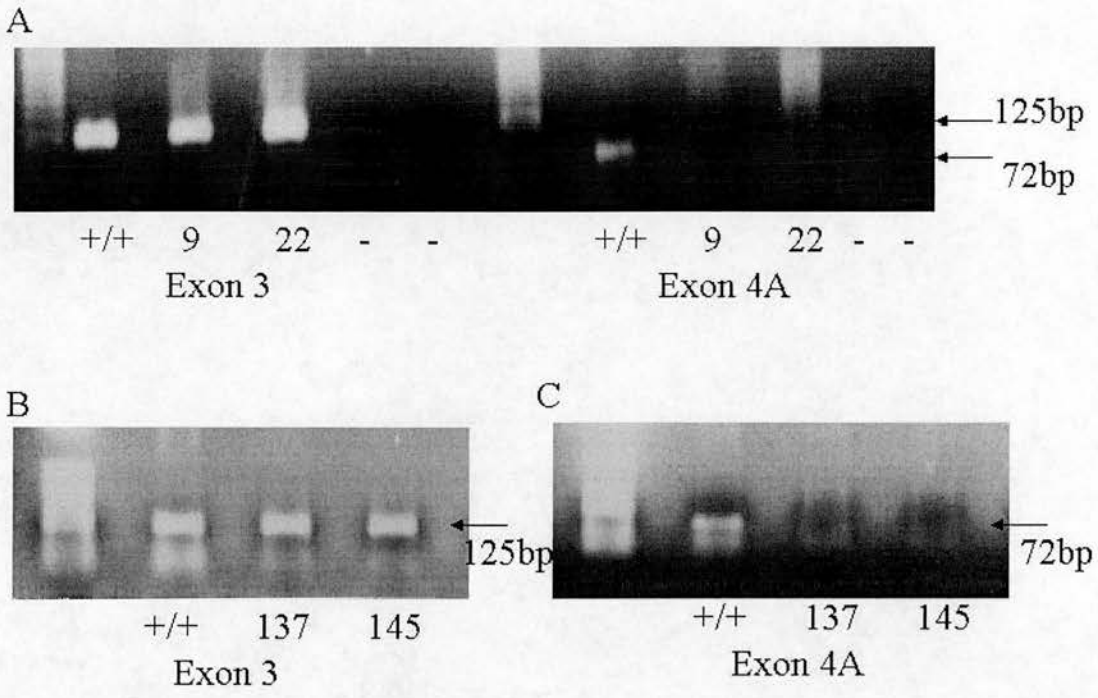

Figure 3.6 Detection of K-*ras*$^{tm\Delta4A/tm\Delta4A}$ ES cell clones by PCR analysis. The figure shows the identification of the 4 K-*ras*$^{tm\Delta4A/tm\Delta4A}$ clones generated by high G418 selection. The presence of PCR quality DNA is established by primers in exon 3, which produce a 125bp PCR product. Deletion of exon 4A was established by the absence of the 72bp exon 4A PCR product. The PCR negative controls are designated (-). A) Identification of clones E14 Δ4A 73/39/9 and E14 Δ4A 73/39/22 showing absence of the 72bp exon 4A product. B) Shows presence of exon 3 PCR products in E14 Δ4A 73/39/137 and E14 Δ4A 73/39/145 cell lines. C) Shows absence of exon 4A PCR product in the E14 Δ4A 73/39/137 and E14 Δ4A 73/39/145 cell lines.

3.2.3 RT-PCR establishing correct splicing to exon 4B in K-*ras* $^{tm\Delta4A/tm\Delta4A}$ cells

Due to the nature of the targeting event it was important to establish that the homologous recombination of the vector did not interfere with the correct splicing to exon 4B, as this would result in a K-*ras* homozygous null genotype. Therefore, once K-*ras*$^{tm\Delta4A/tm\Delta4A}$ ES cells had been isolated the mRNA splicing of these was analysed.

RNA was extracted from wild-type and K-*ras*$^{tm\Delta4A/tm\Delta4A}$ ES cells and RT-PCR was performed. The primers were positioned in exon 1 and exon 4B and PCR conditions were as previously described (Pells *et al.*, 1997). The use of these particular primers meant that both the K-*ras* 4A and K-*ras* 4B transcripts were amplified in the same reaction. The result showed that both of the K-*ras*$^{tm\Delta4A/tm\Delta4A}$ cell lines analysed were capable of producing the K-*ras* 4B transcript, demonstrating that the targeting vector did not compromise the splicing to exon 4B. This also showed that while wild-type ES cells produce the K-*ras* 4A mRNA transcript, K-*ras*$^{tm\Delta4A/tm\Delta4A}$ ES cells do not, so confirming that the cell do not expression the K-*ras* 4A isoform (figure 3.7 A). This result was confirmed by the analysis of K-*ras*$^{tm\Delta4A/tm\Delta4A}$ mice (figure 3.7 B).

3.2.4 Microinjection of blastocysts with K-*ras*$^{+/tm\Delta4A}$ ES cell lines

Having successfully isolated K-*ras*$^{+/tm\Delta4A}$ ES cells with the desired genotype and the correct chromosome number and proved that the targeting strategy resulted in deletion of K-*ras* 4A mRNA, but not K-*ras* 4B mRNA, the ES cells were used for blastocyst injection. Initially cells were grown in the presence of LIF. However, following the failure to generate chimaeras the cells were grown on a feeder layer of mitomycin C treated STO fibroblasts to ensure a proper ES cells morphology, as experiments have shown that ES cells showing non-ES cell morphology failed to contribute to embryos (Rathjen *et al.*, 1999). Two independent clones were injected by Dr Charles Patek (Molecular Medicine Centre) and a further two clones were injected by Jan Ure (Centre for Genome Research). The creation of chimaeras following blastocyst injection was monitored by coat colour. However, the maintenance of ES cells upon the feeder layer did not improve contribution to blastocysts. Despite extensive efforts no coat colour chimaeras were produced (Table 3.5).

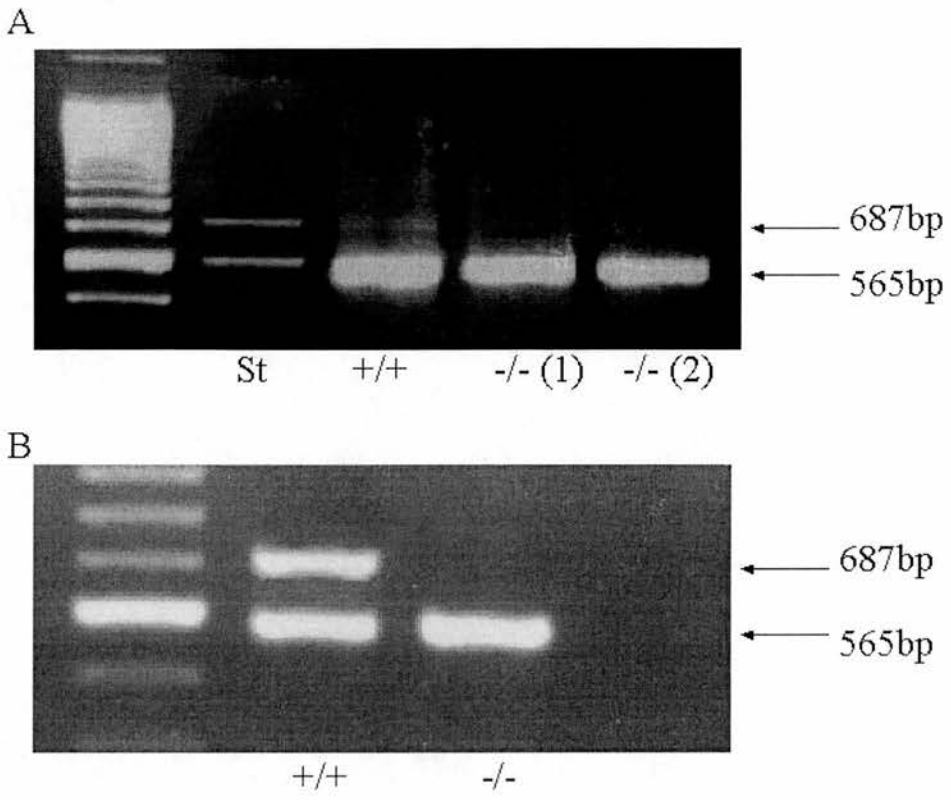

Figure 3.7. Detection of K-*ras* isoform mRNA by RT-PCR. A) Wild-type adult stomach (St) cDNA was used as a positive control. Wild-type ES cells (+/+) show both the K-*ras* 4A (687bp) and the K-*ras* 4B (565bp) mRNA products. The K-$ras^{tm\Delta 4A/tm\Delta 4A}$ ES cell lines show the K-*ras* 4B product only. The marker is a 1Kb ladder. -/- (1) E14 Δ 4A 73/39/9 -/- (2) E14 Δ 4A 73/39/22. B) Wild-type (+/+) adult mouse large intestine showing the K-*ras* 4A (687bp) and the K-*ras* 4B (565bp) mRNA products and K-$ras^{tm\Delta 4A/tm\Delta 4A}$ (-/-) adult mouse large intestine showing only the K-*ras* 4B (565bp) mRNA product, confirming that the targeting strategy results in the deletion of the K-*ras* 4A (687bp) mRNA.

Table 3.5 Results of the injection sessions performed by Jan Ure (CGR).

+/tmΔ4A cell line injected	# recipients (C57 BL/6)	# offspring	# coat colour chimaeras
E14 IV 136	2	11	0
E14 Δ 4A 73/39	2	9	0

Of the 20 animals produced by these two injection sessions no coat colour chimaeras were identified from either of the independent K-*ras*$^{+/tm\Delta 4A}$ cell lines used.

3.2.5 *Mycoplasma* testing

A possible reason for the failure to generate chimaeras was *Mycoplasma* infection. This was tested using a *Mycoplasma* PCR test (Stratagene). The test was performed using medium that cells had been cultured in. An internal control producing a product of 1Kb was included to confirm that the PCR conditions were optimal and the template DNA was amplifiable. The positive control of 874bp corresponded to the expected product size produced by *Mycoplasma* infection. The investigation confirmed that *Mycoplasma* was not infecting the cells at levels detectable by this method (Figure 3.8). Therefore, while *Mycoplasma* infection could not be completely ruled out, as it could have been infecting cells at levels undetectable by this method, it appeared unlikely that this was the reason that the cell lines were not contributing to chimaeras.

The failure to generate chimaeras, the negative *mycoplasma* status and the presence of a good chromosome number, suggested that the ES cells may have been compromised due to the length of time in culture. Extensive cell culture may have lead to an inability to form chimaeras possibly due to the ES cells being overgrown by variants, compromised in their ability to contribute to the tissues of chimaeras, that had a selective growth advantage as a result of suboptimal culture conditions. Although measures had been taken to try and avoid this by growing the ES cells on a feeder layer of mitomycin C treated STO fibroblasts. Therefore, due to these difficulties and problems encountered with the production of K-*ras*$^{tm\Delta 4A/tm\Delta 4A}$ ES cells, it was decided that further heterozygous ES cell for the deletion of exon 4A should be generated using a different parental ES cell line.

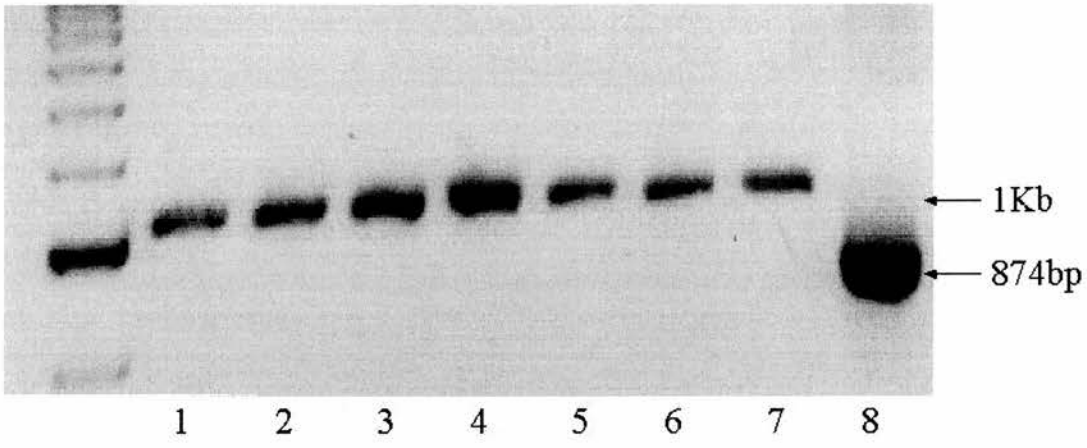

Figure 3.8. Test for *Mycoplasma* infection by PCR analysis. The internal control product (1Kb) confirmed that PCR conditions were correct and the positive control (874bp) showed the expected product size corresponding to *Mycoplasma* infection. There are no bands of corresponding size in the test lanes 1) E14 (+/+), 2) HM-1 (+/+) wild-type ES cell line, 3) E14 Δ4A 73/39, 4) E14 IV 136, 5) STO *neo* fibroblasts, 6) E14 Δ4A 73/39/9, 7) E14 Δ4A 73/39/22, 8) positive control.

3.3 Generation of HM-1 K-*ras* $^{+/tm\Delta 4A}$ ES cells

In order to try and improve the results from the electroporation of wild-type ES cells with the pPTKiNKiΔ4A targeting vector and because of the limited time span available, several alterations were made to the targeting strategy and screening methods for identifying homologous recombination. A new cell line was used for the electroporation. HM-1 ES cells were kindly gifted by Professor David Melton. These ES cells are an HPRT deficient cell line (Magin *et al.*, 1992), which were only 14 passages from their original isolation and it was hoped that this would overcome problem encountered with failure to generate coat colour chimaeras. HM-1 ES cells contribute with high frequency to the germline of chimaeric animals (Selfridge *et al.*, 1992). In addition, in order to increase the rapidity of the screening for homologous recombinants a PCR strategy was developed to replace the initial screen by Southern analysis carried out previously.

3.3.1 Development of PCR strategy to detect homologous recombination

To improve the rapidity of the isolation of putative heterozygous clones a PCR screen was to be carried out on a crude DNA extract from half the picked colony following selection (method described in section 2.4.8), while the other half of the colonies were expanded in 24 well plates (adapted from McMahon and Bradley, 1990). In this way the genotype of the colonies could be confirmed before they required expanding.

The development of the PCR method was made possible by the publication of the mouse chromosome 6 sequence in the region around the K-*ras* gene, as previously the intronic sequence had not been available. This allowed the identification of the exact start and end points of the arms of homology within the intron and therefore possible primer positions. However, because the downstream arm of homology terminated ~300bp from the 5' end of exon 4B it was decided to position the reverse primer in exon 4B to minimise any possible problems associated with divergence in intronic sequence between mouse species. The forward primer was designed to anneal to the 3' end of the *neo*^{r} gene, resulting in the amplification of a 2.1Kb PCR product (Figure 3.9) only in cells that had undergone homologous recombination.

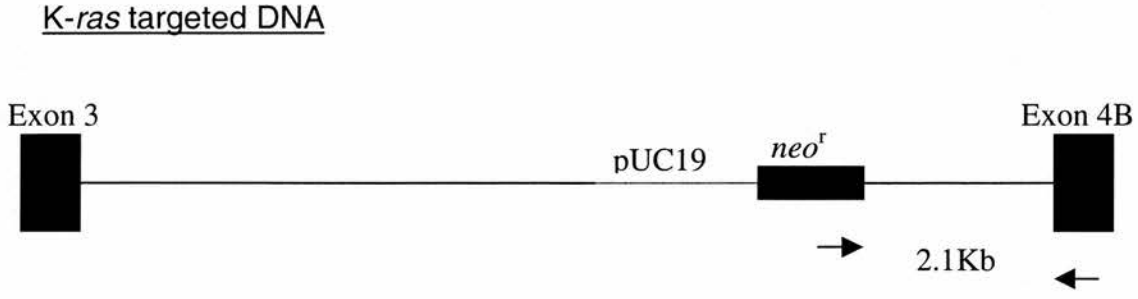

Figure 3.9. Diagrammatic representation of the PCR strategy to identify homologous recombinants. The figure shows a portion of the K-*ras* DNA following the homologous recombination event and the position of the PCR primers used to screen for heterozygous clones. Primers are positioned at the 3' end of the neomycin resistance cassette and at the 5' end of exon 4B and in heterozygous clones this resulted in a PCR product of 2.1 Kb in length.

The PCR method was validated on DNA extracted from the K-*ras*$^{+/lm\Delta 4A}$ cell line E14 Δ4A 73/39 by phenol/ chloroform extraction. The expected 2.1Kb product was produced. The PCR was then optimised on small quantities of crude DNA extract to ensure that the PCR product could be generated under these conditions. Therefore, the PCR was worked up on crude cell lysates from cell numbers ranging from 100 – 10000 to represent the likely range of cells present in half a colony. However, despite varying annealing temperature and cycle numbers the 2.1Kb product could not be amplified under these conditions. Therefore, ES cells were plated at a variety of seeding densities and grown in 24 well plates to different levels of confluency, ranging from 30%-90%. The cells were processed to make a crude lysate, which was then used for PCR analysis. The 2.1Kb targeted band was present in all the samples under these conditions (figure 3.10), suggesting that this method could be used for the screening of homologous recombination with this modification.

3.3.2 Electroporation of HM-1 ES cells with the pPTKiNKiΔ4A targeting vector

To optimise the selection for homologous recombination after electroporation two cell densities of $1.25x10^5$ and $2.5x10^5$ cells per 100mm petri dish were used and the cells were treated with, either 200μg/ml, or 300μg/ml geneticin. However, selection was increased to 300μg/ml geneticin for all petri dishes after several days to eliminate background colonies persisting on control plates that had not undergone electroporation with the targeting vector. Geneticin and ganciclovir treatment gave approximately a 2-fold increase in selection compared to geneticin alone. The plates of unelectroporated cells had no surviving colonies, suggesting that the selection was successful.

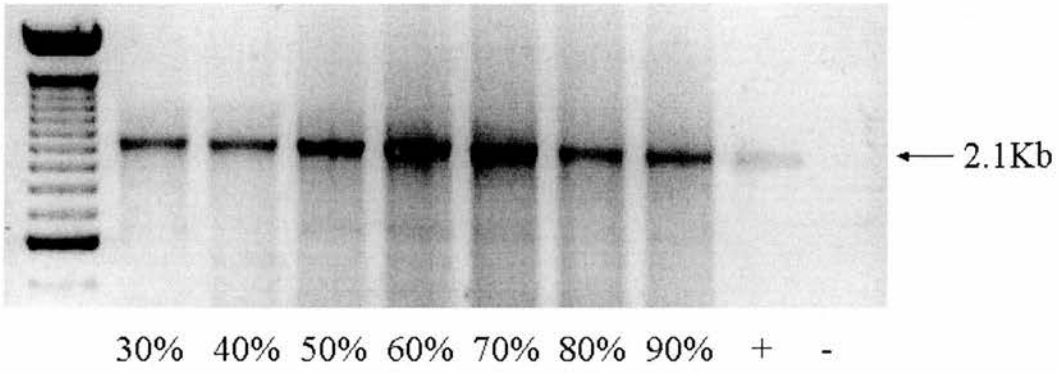

Figure 3.10 Development of a colony PCR to detect K-*ras*$^{+/tm\Delta 4A}$ targeted clones. E14 Δ4A 73/39 cells were grown in 24 well plates to different levels of confluence as indicated and harvested for colony PCR to determine the approximate destiny of cells needed to provide enough material to detect the 2.1Kb PCR product. The positive control (+) is E14 Δ4A 73/39 DNA that had been extracted by phenol/chloroform extraction; whilst a product is detectable these conditions are clearly not optimal for amplification of this sample. The PCR water negative control is designated (-).

Each plate was used once for picking colonies, which minimised the risk of re-picking colonies that may have re-seeded following this procedure. Picked colonies were resuspended in medium and ¼ was placed in a well of a 24 well plate and the remaining ¾ was placed in the corresponding well of a separate 24 well plate. Since PCR amplification had shown that there was enough material when the well was only 30% confluent well, this allowed cells to be analysed by PCR several days before the remainder of the cell population required subculturing. The use of separate plates reduced the risk of potentially targeted clones becoming infected and therefore lost, due to the disturbance caused by harvesting the other well for PCR. The picking was also staggered over several days to allow time for the PCRs to be carried out.

Table 3.6. Percentage of homologously recombined clones identified under the different selection conditions.

Cell density	Number of plates	Number colonies picked	Percentage homologously recombined clones identified
$1.25x10^6$	11	156	(10) 6%
$2.5x10^6$	10	168	(7) 4%

Following PCR screening only those clones that were shown to be targeted by the PCR were subcultured into $25cm^2$ flasks. Of the 324 colonies screened 17 (~5%) were found to have the 2.1Kb PCR product corresponding to the targeting event (table 3.6). The percentage of homologous recombination was improved in this new electroporation, although the number of positive colonies is fairly evenly spread between the two selection conditions (Table 3.6).

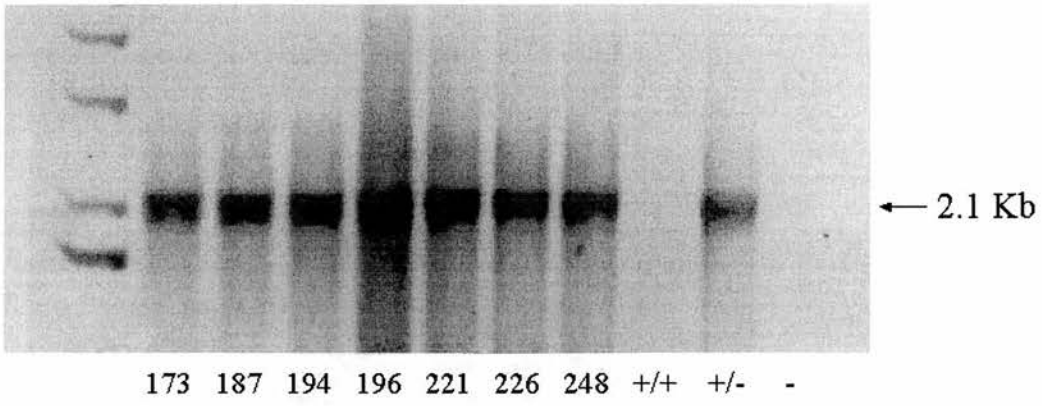

Figure 3.11. Detection of 2.1Kb targeted band by PCR. The gel shows seven targeted clones that were isolated and grown up into cell lines following the electroporation. Wild-type (+/+) and previously targeted heterozygous DNA (E14 IV 73/39) (+/-) was included as a control. Wild-type DNA did not produce the PCR product as expected. The negative control (-) had water added in place of DNA and as expected there is no PCR product.

Fresh DNA was isolated from seven of the clones (173, 187, 194, 196, 221, 226, 248) and the PCR repeated, which confirmed the result of the initial screen (Figure 3.11). Southern analysis was then performed to ensure that there were no additional non-homologous events present within the genome (using the internal probe) and that the targeting vector had integrated correctly within the genome by use of the external probe, since this detected only homologous recombination. Therefore, by using the external probe, the PCR strategy and the internal probe it was possible to show that the flanking regions around the site of the targeting vector's integration were correct.

The results of the Southern analysis with the internal and external probes confirm the PCR results. All seven heterozygous clones identified following the selection had the correct band pattern of a 2Kb wild type and a 6Kb targeted band with the internal probe, and a 5Kb wild type and 4Kb targeted band with the external probe (Figure 3.12). The Southern analysis also showed that the bands were roughly in a 1:1 ratio.

3.4 Generation of K-*ras*$^{tm\Delta4A/tm\Delta4A}$ ES cells from HM-1 K-*ras*$^{+/tm\Delta4A}$ cell line

Following the successful generation of K-*ras*$^{+/tm\Delta4A}$ ES cells with using the HM-1 ES cell line, generation of K-*ras*$^{tm\Delta4A/tm\Delta4A}$ ES cells by high G418 selection was undertaken. It was necessary to generate an independent K-*ras*$^{tm\Delta4A/tm\Delta4A}$ cell line with the proper chromosome number to corroborate any *in vitro* data generated. One heterozygous cell line, HM-1 R42 #248, was used for a high G418 selection.

Following 14 days selection in geneticin, 48 colonies were picked and split half and half into two wells of separate 24 well plates and grown to expand the colony. Once confluent one well was harvested for DNA extraction and PCR analysis. The cells growing in the corresponding well were subcultured into 6 well plates. Analysis with primers in exon 4A found that approximately 60% of the clones did not have the 72bp product resulting from amplification of exon 4A with these primers, and where therefore homozygous.

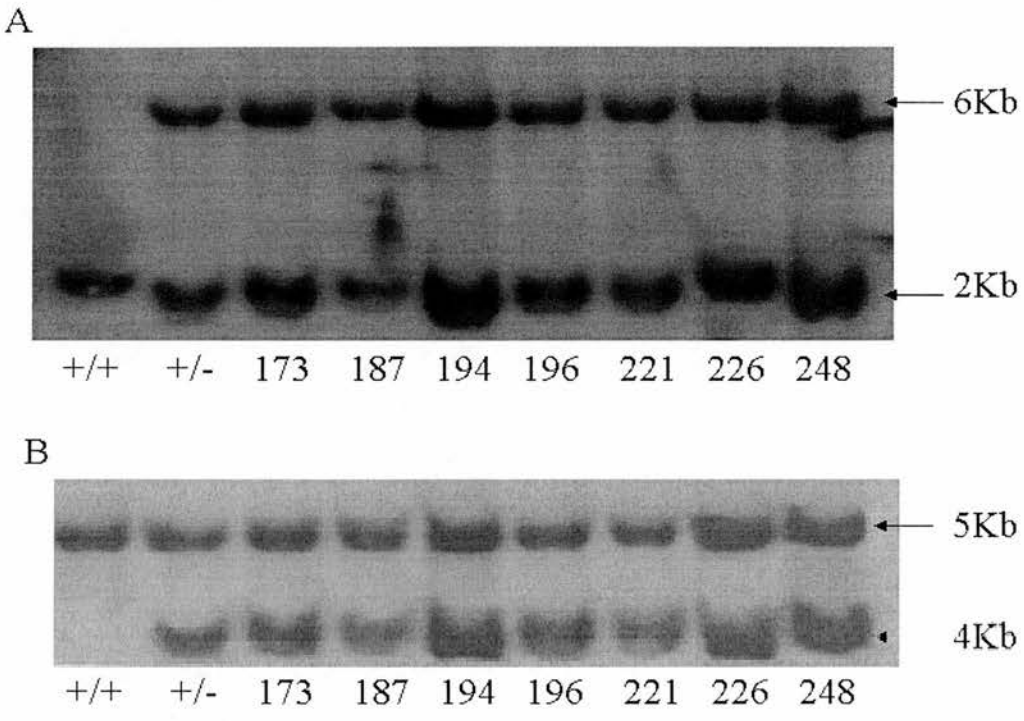

Figure 3.12 Southern analysis of targeted K-*ras*$^{+/tm\Delta 4A}$ clones. A) Southern analysis with the internal probe. Genomic DNA digest with *HindII* produces a 2Kb band with wild-type DNA (+/+) and a 2Kb to 6Kb shift in heterozygous DNA. B) Southern analysis with the external probe. Genomic DNA digest with *PvuII* results in a 5Kb band in wild-type DNA and a 5Kb to 4Kb transition in heterozygous DNA. Wild-type (+/+) and K-*ras*$^{+/tm\Delta 4A}$ DNA (+/-) from previously targeted E14 Δ4A 73/39 cell line were included as controls.

Six of these clones were expanded into 25cm^2 flasks and DNA extracted. PCR analysis was then repeated which confirmed that clones 8, 12, 16, 18 and 24 were homozygous null for the deletion of exon 4A (figure 3.13), demonstrating that selection for LOH had occurred successfully in these clones. Clone 4 was used as a positive control confirming that some of the cells picked from the selection retained the 4A exon. This finding was further confirmed by Southern analysis (figure 3.14), since only the targeted bands were detected using the internal and external probes.

3.4.1 Analysis of HM-1 K-*ras*$^{tm\Delta4A/tm\Delta4A}$ ES cell chromosome number

Previously isolated K-*ras*$^{tm\Delta4A/tm\Delta4A}$ cell lines had been found to be chromosomally abnormal, highlighting the possibility that, either the mutation, or the selection process may affect the genomic stability of K-*ras*$^{tm\Delta4A/tm\Delta4A}$ cell lines. However, metaphase spread analysis performed on the five newly isolated cell lines showed that these had the correct chromosome number (table 3.7).

Table 3.7 Percentage of metaphase spreads analysed with 40 chromosomes.

Cell line	passage number	% of metaphase spreads analysed with 40 chromosomes
HM-1 R42 #248/8	32	83%
HM-1 R42 #248/12	32	83%
HM-1 R42 #248/16	32	77%
HM-1 R42 #248/18	32	80%
HM-1 R42 #248/24	32	82%

Passage number refers to passages from HM-1 isolation rather than isolation of the targeted clone.

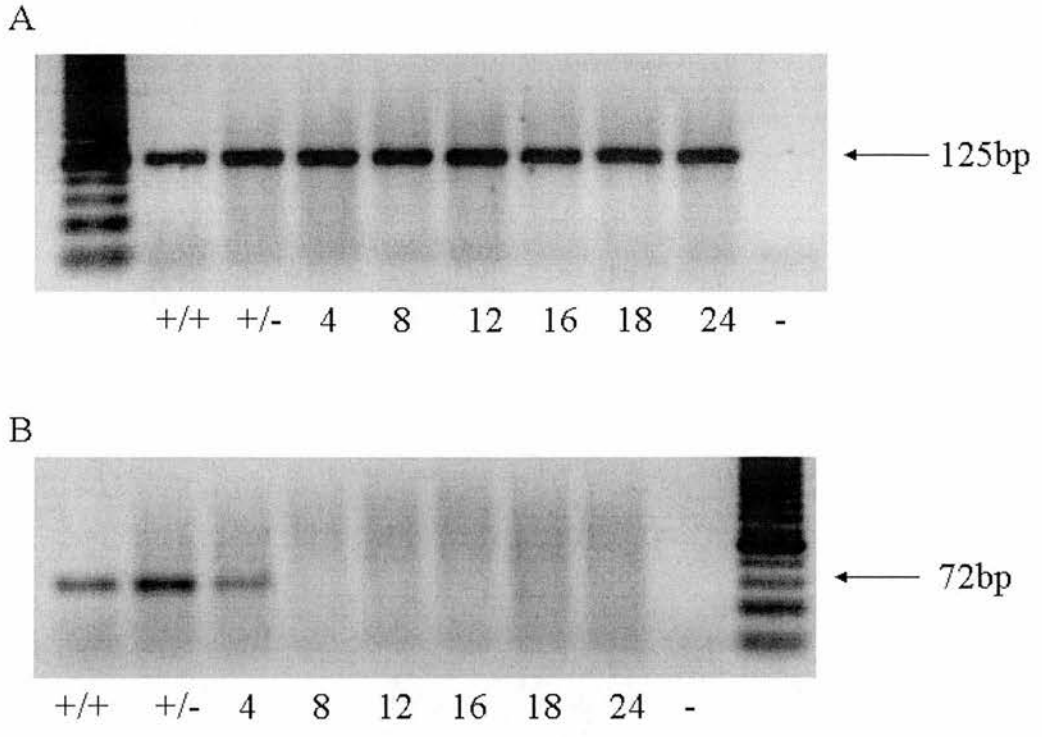

Figure 3.13 Isolation of K-*ras*$^{tm\Delta 4A/tm\Delta 4A}$ ES cell lines. The figure shows the PCR strategy to identify those clones that had undergone LOH following high G418 selection. A) Primers in exon 3 resulting in 125bp product confirming that DNA was of PCR amplification quality. B) Primers in exon 4A resulting in 72bp product present in wild-type (+/+) cells, HM-1 R42 #248 K-*ras*$^{+/tm\Delta 4A}$ (+/-) cells used for the selection and clone 4 produced in this selection. Clones 8, 12,16,18 and 24 do not have the exon 4A product, indicating that they have undergone LOH, and duplication of the mutant allele.

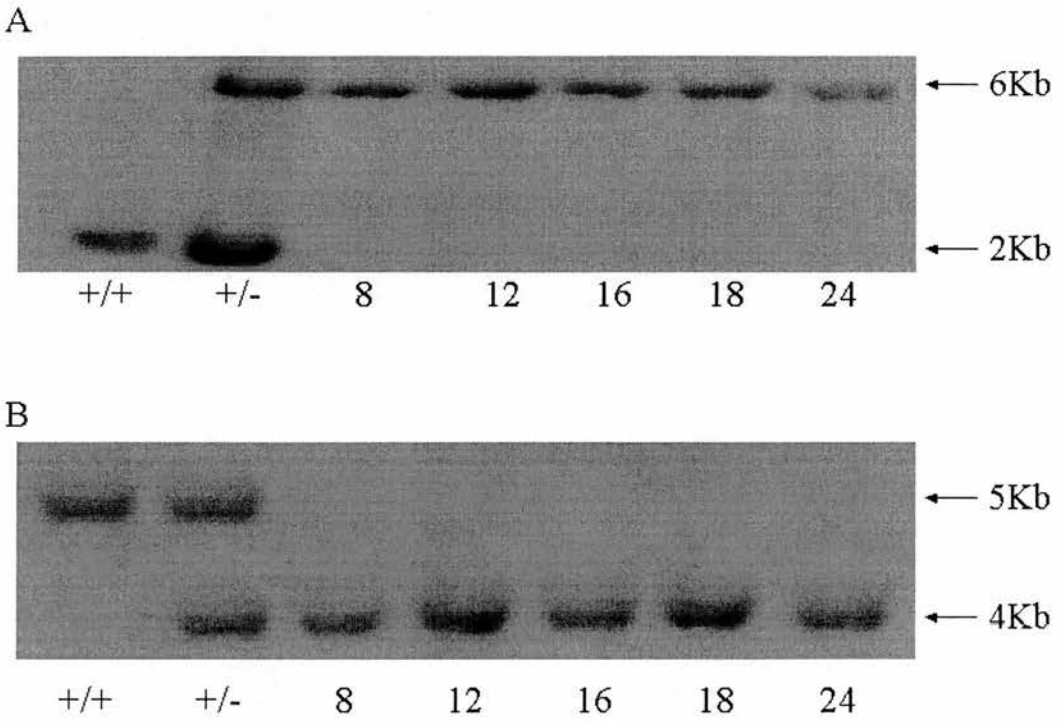

Figure 3.14. Southern analysis of putative K-*ras*$^{tm\Delta4A/tm\Delta4A}$ cell lines. Analysis of five putative K-*ras*$^{tm\Delta4A/tm\Delta4A}$ cell lines with the internal and external probes. A) Probing with the internal probe, +/+ cells contain a 2Kb band, *+/tmΔ4A* contain a 2Kb and 6Kb band and K-*ras*$^{tm\Delta4A/tm\Delta4A}$ cells contain only the targeted 6Kb band. B) Probing with the external probe, +/+ DNA contains the 5Kb wild-type band, *+/tmΔ4A* DNA contains a 5-4Kb transition and the putative K-*ras*$^{tm\Delta4A/tm\Delta4A}$ cell lines contain only the targeted 4Kb band.

3.5 Blastocyst injection of ES cells heterozygous for the deletion of exon 4A

All Five of the targeted clones (HM-1 R42 #173, 187, 194, 226 and 248) were used for blastocyst injection. The ES cells were maintained in the presence of LIF and absence of a feeder layer. Each of the K-*ras*$^{+/tm\Delta 4A}$ ES cell lines were used to inject approximately 24 blastocysts, which were returned to two recipient females, except clones 187 and 226, which were used to inject 12 blastocysts and which were returned to one recipient female. Jennifer Doig performed the injections on my behalf. For each injection 8-12 ES cells were injected into C57 BL/6 blastocysts generated either by superovulation or by natural mating and they were returned to recipient psuedo pregnant female CD1 mice. In conjunction wild-type HM-1 ES cells were also used to inject 12 blastocysts, which were returned to one recipient mouse to act as a control to ensure that any lack of coat colour chimaeras was not as a result of problems with the parental ES cell line.

In total nine coat colour chimeras were generated from three of the K-*ras*$^{+/tm\Delta 4A}$ ES cell lines used for microinjection, the results are shown in table 3.8 and pictures of the animals are shown in figure 3.15.

Table 3.8. Number of coat colour chimaeras derived from ES cell lines used for microinjection.

Cell line injected	Litter size (surviving birth)	Coat colour chimaeras
HM-1 R42 #194	6 (3)	3M
HM-1 R42 #226	5 (5)	1M/3F
HM-1 R42 #248	4 (3)	2M
HM-1	9 (8)	4M/3F

The number of male (M) and female (F) coat colour chimaeras are indicated.

3.6 Transmission of the K-*ras*$^{+/tm\Delta 4A}$ mutation through the germline

The coat colour chimaeras produced by blastocyst injection were then used to generate K-*ras*$^{+/tm\Delta 4A}$ animals. The coat colour chimaeras were mated with wild-type 129/Ola and C57 BL/6 mice. Germline transmission of the mutation was assessed by the coat

colour of the offspring following these crosses. Mice from ES cell-derived germ cells were predicted to be light yellow with pink eyes, when crossed with 129/Ola mice. In contrast, blastocyst derived germ cells would result in offspring with agouti coats and black eyes. Animals derived from crossing to C57 BL/6 mice were predicted to have an agouti coat colour and black eyes if ES cell-derived, and a black coat colour and black eyes if host blastocyst-derived. Crosses with C57 BL/6 mice were performed in order to increase the speed at which germline transmitters were identified, since 129/Ola mice have small litter sizes. The results of breeding the heterozygous chimaeras are shown in table 3.9. To the date of writing this thesis 4 male chimaeras and 1 female chimera have, produced litters containing germline animals. The male chimaera designated SP 7 was found to be a total transmitter.

3.6.1 Identification of K-*ras*$^{+/tm\Delta 4A}$ animals

Germline animals identified by coat colour were genotyped by analysis of tail tip DNA to assess whether they had the heterozygous mutation. The genotyping of these animals was initially performed using the *neo*^{r} to exon 4B PCR used to identify K-*ras*$^{+/tm\Delta 4A}$ ES cells as described in section 3.3.1. However, this PCR method was found to be inefficient at amplifying the 2.1Kb product from the tail DNA. Therefore, a new PCR strategy was designed using two primers within the *neo*^{r} cassette, and the details of the primer sequences and PCR conditions can be found in chapter 2.4.6. Figure 3.16 shows the result obtained from screening some of the germline offspring derived from the founder SP-7. Both male and female K-*ras*$^{+/tm\Delta 4A}$ animals were identified on both the inbred 129/Ola and outbred backgrounds. It was possible to determine that the correct ratio of heterozygous animals (50%) was resulting following germline transmission (table 3.9).

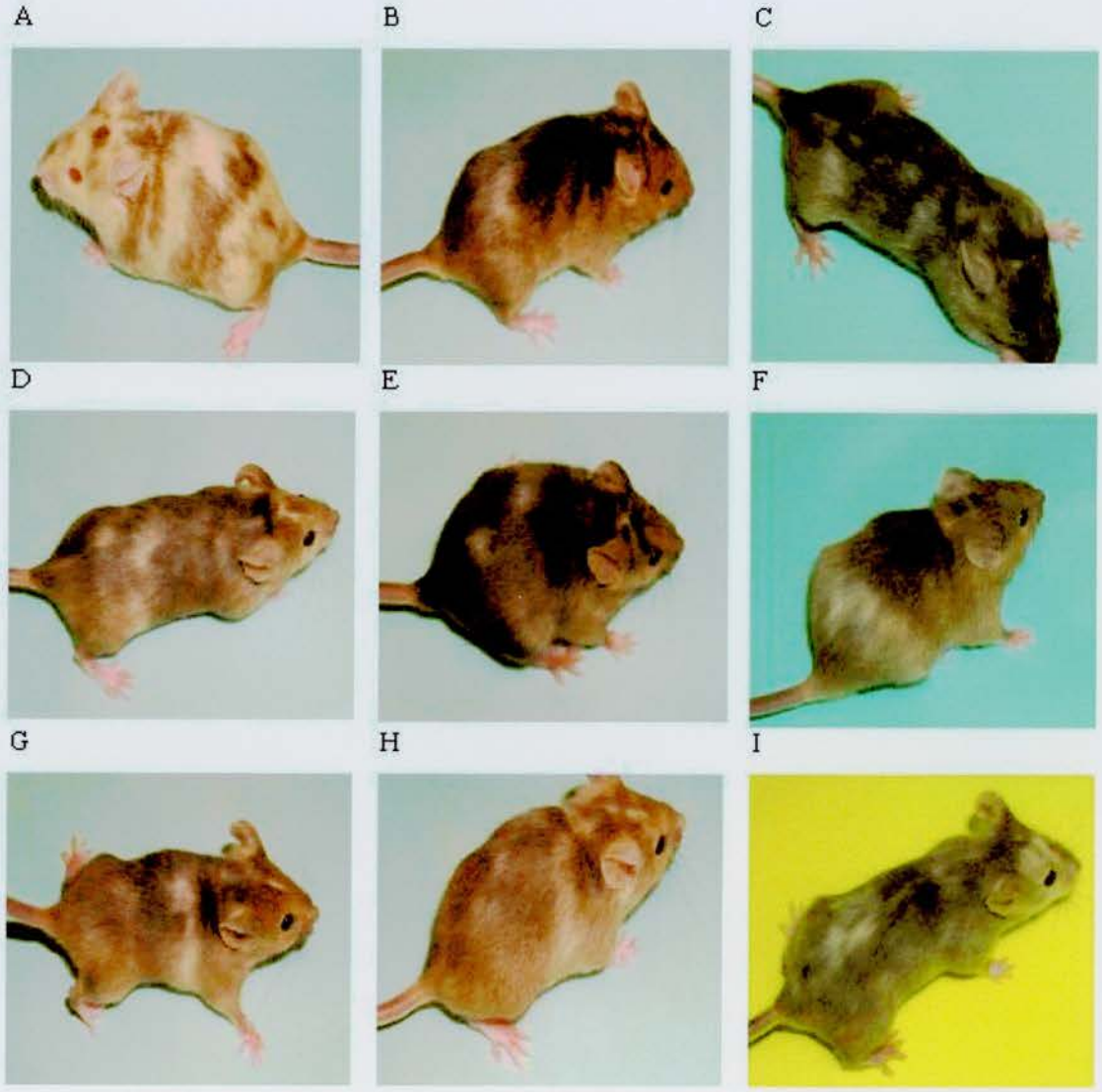

Figure 3.15. Coat colour chimaeras generated by blastocyst injection. The coat colour chimaeras produced by injection of C57 BL/6 blastocysts with K-*ras*$^{+/tm\Delta 4A}$ 129/Ola ES cells (A-H). Coat colour chimaera produced by injection of wild-type HM-1 129/Ola ES cells into C57 BL/6 blastocysts (I).

At the time of writing the K-*ras*$^{+/tm\Delta 4A}$ animals are viable at the age of 17 weeks and both males and females are fertile. Presently, K-*ras*$^{+/tm\Delta 4A}$ animals on both the inbred and outbred backgrounds are being mated to generate K-*ras*$^{tm\Delta 4A/tm\Delta 4A}$ animals in order to assess the phenotype of these animals and therefore the effect of this mutation *in vivo*.

Table 3.9. Coat colour chimaeras transmitting the ES cell derived genes through the germ line.

Founder designation (heterozygous ES cell line generated from)	Number of offspring	Number of germ line transmissions	Number of heterozygous animals
SP 1 (248) male	21	0	0
SP 2 (248) male	50	1	1/1
SP 3 (226) female	22	0	0
SP 4 (226) female	2	0	0
SP 5 (226) female	27	2	0/2
SP 6 (226) male	39	24	13/24
SP 7 (194) male	47	47	13/29
SP 8 (194) male	0	0	0
SP 9 (194) male	35	7	4/7

3.7 Characterisation of K-Ras 4A expression in ES cells

It was previously reported that K-*ras* 4A mRNA was not expressed in ES cells and that the transcript only became detectable following differentiation of these cells into embryoid bodies (Pells *et al.*, 1997). However, here using the same primers low levels of K-*ras* 4A mRNA were found to be detectable in wild-type ES cells growing under normal culture conditions (figure 3.7).

Due to the low level of expression of the K-*ras* 4A isoform mRNA detected in wild-type ES cells, a pilot study was performed to determine whether expression was indeed linked with differentiation by treatment with retinoic acid (RA). RA treatment of ES cells has previously been reported to induce differentiation, which was accompanied by

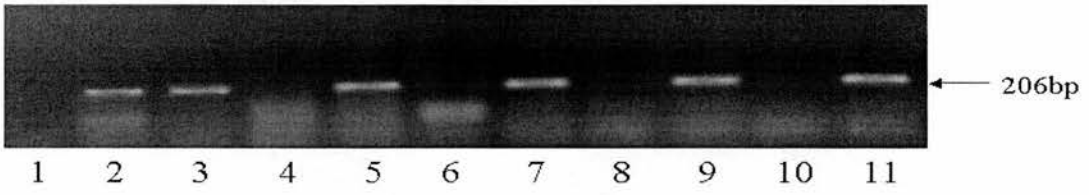

Figure 3.16. Identification of K-*ras*$^{+/tm\Delta 4A}$ animals following transmission of the mutation through the germline. The primers within the *neo*^{r} cassette amplified a 206bp product, which is only detectable in animals harbouring the mutant allele. The samples analysed here were from a litter sired by the male chimaera SP 7 that was a total transmitter, which demonstrate the correct ratio of heterozygous offspring (5/9). 1) +/+, 2) 1-SP7, 3) 2-SP7, 4) 3-SP7, 5) 4-SP7, 6) 5-SP7, 7) 6-SP7, 8) 7-SP7, 9) 8-SP7 10) negative control, 11) HM-1 R42 #248 heterozygous DNA which was included as a positive control.

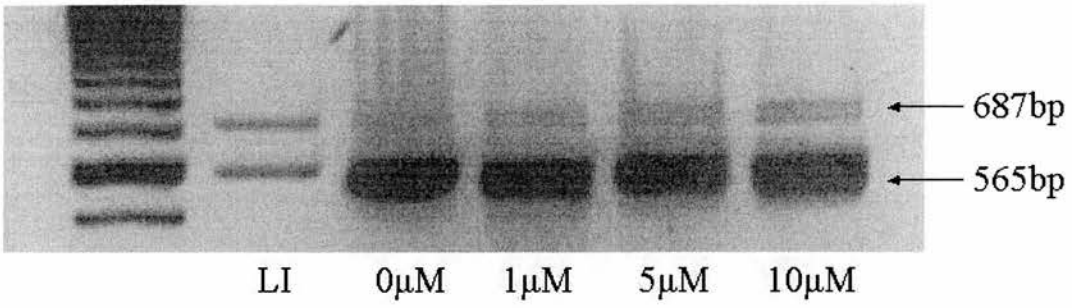

Figure 3.17. RA differentiation of ES cells. ES cells were differentiated in the presence of the indicated concentrations of all trans-retinioic acid for 5 days. RT-PCR was performed with primers in exon 1 and exon 4B to show the relative K-*ras* 4A/4B ratio after this treatment. Amplification of the K-*ras* 4A mRNA produces a 687bp product, and the K-*ras* mRNA a 565bp product. RNA from adult mouse large intestine (LI) is included as a positive control. All cultures were maintained in the absence of LIF.

the up-regulation of expression from some genes (Scharnhorst *et al.*, 1997). Cultures were treated with 1μM, 5μM or 10μM RA and in the absence of LIF for 5 days. Controls cultures, either containing DMSO and no LIF, or no LIF without DMSO were set up.

Following five days of treatment the cultures were deemed to be differentiated by morphological analysis. RNA was extracted and RT-PCR was performed using primers that amplified both the K-*ras* isoforms, as described previously. This analysis of K-*ras* isoform mRNA expression showed that under all treatment conditions the ratio observed between the K-*ras* 4A and K-*ras* 4B mRNA was similar to that observed in the control cultures, demonstrating that the presence of RA does not cause an up-regulation of the K-*ras* 4A mRNA (Figure 3.17). Thus, absence of K-*ras* 4A mRNA in the K-$ras^{tm\Delta 4A/tm\Delta 4A}$ cell lines shown in figure 3.7 results from the deletion of this exon rather than absence of differentiation in this culture, since culturing wild-type ES cells in the absence of LIF does not up-regulate the expression.

3.8 Discussion

The study reports the successful isolation of cells heterozygous for the deletion of the K-*ras* 4A exon. These cells were generated following electroporation of ES cells with the targeting vector pPTKiNKiΔ4A. Heterozygous cell lines were derived from two different parental ES cell lines (E14 and HM-1). Homologous recombination of the targeting vector into the mouse genome was confirmed using PCR and Southern analysis. These methods clearly demonstrated that the flanking regions surrounding the site of integration were correct and that non-homologous integrations had not occurred elsewhere within the genome of these cells.

The primary aim of the experiments detailed in this chapter was the generation of chimaeras heterozygous for the deletion of K-*ras* exon 4A. Three independent HM-1 K-$ras^{+/tm\Delta 4A}$ ES cell lines were successfully used to generate 9 coat colour chimaeras. This observation was important for two reasons; firstly it demonstrated that altering the genome of the ES cells in this way did not hamper their ability to contribute to developing blastocysts. Secondly, ES cells could be isolated by this selection procedure

and maintain the ability to differentiate into many cell lineages. Since, abnormal chromosome numbers and *Mycoplasma* infection were not implicated in the failure of the four E14 derived heterozygous ES cells lines to contribute to developing embryos these observations indicate that this may have resulted from the outgrowth of a variant sub population of cells with a growth advantage that were compromised in their ability to contribute to the tissues of chimaeras, possibly due to sub-optimal culture conditions.

The chimaeras were used subsequently for breeding studies, which identified 5 chimaeras that transmitted the mutation through the germline. Of the germline offspring produced, wild-type and K-*ras*$^{+/tm\Delta 4A}$ animals were present in a 1:1 ratio, which indicated that no embryonic lethality was associated with this mutation. The K-*ras*$^{+/tm\Delta 4A}$ animals were outwardly healthy at 5 months of age. Importantly, both male and female K-*ras*$^{+/tm\Delta 4A}$ animals were found to be fertile and currently breeding studies are underway to generate K-*ras*$^{tm\Delta 4A/tm\Delta 4A}$ animals. These mice will prove a powerful tool to investigate the role of the K-*ras* 4A isoform in development and tissue function.

Further experiments led to the successful isolation of ES cells with the K-*ras*$^{tm\Delta 4A/tm\Delta 4A}$ genotype. These cell lines were generated for two main purposes: firstly, to screen for the loss of the K-*ras* 4A mRNA and to ensure that this mutation did not interfere with splicing to exon 4B, and secondly, to use this cell line for analysing the effect of deleting of this protein isoform in culture. The K-*ras*$^{tm\Delta 4A/tm\Delta 4A}$ cell lines were derived by high G418 selection. This method selects cells that have undergone spontaneous loss of heterozygosity (LOH) (Mortensen *et al.*, 1992). The loss of the wild-type allele and duplication of the mutant allele meant that cells could be selected for by resistance to geneticin. The mechanism of duplication is believed to involve, either chromosome loss and duplication, or mitotic recombination (Lefebvre *et al.*, 2001). Since, this results in extensive LOH in regions surrounding the area of targeting this has implications if for example these areas contain imprinted gene. However, this may not apply to the present work, since previous studies by this laboratory have shown that transfection of a minigene expressing wild-type K-*ras* can rescue the phenotype in culture of K-*ras*$^{-/-}$ ES cells that were generated by high G418 selection (Brooks *et al.*, 2001). Therefore, phenotypes resulted from the specific mutation and not altered/inappropriate expression of genes within the chromosomal region affected by the

duplication of the transgene. Therefore, this should also apply for the targeting experiments described here, as the same gene and chromosomal region are involved.

The K-*ras*$^{tm\Delta4A/tm\Delta4A}$ cell lines were generated from two independent K-*ras*$^{+/tm\Delta4A}$ cell lines. Approximately 60% of the clones isolated following the high G418 selection using a HM-1 K-*ras*$^{+/tm\Delta4A}$ cell line were positive for the duplication of the transgene. Five of these clones were expanded into cell lines. When analysed by metaphase spread analysis these cell lines all had the correct chromosome number. Therefore, this selection produced roughly the expected proportion of clones having undergone LOH, although proportions are known to vary (Mortensen *et al.*, 1992). However, only 4 K-*ras*$^{tm\Delta4A/tm\Delta4A}$ clones (~2%) were derived following high G418 selection using the E14 Δ4A 73/39 cell line and these were all determined to be chromosomally abnormal by metaphase spread analysis. In addition, no K-*ras*$^{tm\Delta4A/tm\Delta4A}$ clones were derived from the three E14 IV heterozygous cell lines used. The problems generating the E14 K-*ras*$^{tm\Delta4A/tm\Delta4A}$ cell lines were most likely due to unknown intrinsic problems with the parental cell K-*ras*$^{+/tm\Delta4A}$ lines. These problems may also relate to their failure to contribute to developing embryos. Thus, neither the K-*ras*$^{tm\Delta4A/tm\Delta4A}$ mutation, nor the selection process appears to have an adverse affect on the genomic stability of ES cells as seen grossly by metaphase spread analysis. Furthermore, the isolation of several chromosomally normal K-*ras*$^{tm\Delta4A/tm\Delta4A}$ cell lines, demonstrates that K-*ras* 4A is not essential for the viability of ES cells in culture.

Importantly, analysis of the K-*ras* mRNA expressed in the K-*ras*$^{tm\Delta4A/tm\Delta4A}$ cell lines demonstrated that the targeting strategy had been successful. These cells were no longer able to generate the K-*ras* 4A mRNA. Therefore, the use of the pPTKiNKiΔ4A targeting vector allowed the specific deletion of the K-*ras* 4A splice form. Furthermore, from the construction of the targeting vector and the known positions of the canonical splice acceptor sequences, which occur at the 3' boundary of exon 3 and the 5' boundaries of exon 4A and 4B (McGrath *et al.*, 1983) it was predicted that the pPTKiNKiΔ4A targeting vector would not have an adverse affect upon splicing to exon 4B. Importantly, analysis of the K-*ras*$^{tm\Delta4A/tm\Delta4A}$ cell lines by RT-PCR confirmed that the size and production of the alternative K-*ras* 4B splice form was indeed not affected by the introduction of the targeting vector. This was an extremely important result, as

adverse effects upon the K-*ras* 4B splice isoform following homologous recombination of the targeting vector would have generated a K-*ras* homozygous null genotype.

Whilst it was previously reported that the K-*ras* 4A transcript was not present in ES cells (Pells *et al.*, 1997) it was detected in the present study albeit at low levels. This discrepancy could be due to the fact that Pells *et al.*, (1997) used radioactive isotopes to visualise the RT-PCR products, and therefore it is possible that the strong signal of the K-*ras* 4B transcript masked the much weaker signal of the K-*ras* 4A transcript. However, this discrepancy is unlikely to reflect the presence of differentiated cells within the cultures examined, since differentiation induced by, either LIF withdrawal, or RA treatment failed to up-regulate the expression of the K-*ras* 4A transcript in relation to the K-*ras* 4B transcript. In addition, the presence of a generally more differentiated culture would have an adverse effect upon the ability of the ES cells to contribute to the developing inner cell mass of a blastocyst. The data presented here indicates that this is not the case, since both wild-type and K-$ras^{+/tm\Delta 4A}$ ES cells contribute to developing embryos, confirming their pluripotent nature. In addition, Pells and co-workers did not detect the K-*ras* 4A transcript until the second differentiation stage, indicating that the level of differentiation reported to be needed to induce K-*ras* 4A expression is unlikely to be seen in a ES cell culture.

In conclusion, the aims and of objectives of this part of the research project were successfully completed with the generation of K-$ras^{+/tm\Delta 4A}$ coat colour chimaeras, which were capable of transmitting the mutation through the germline, and the generation of K-$ras^{tm\Delta 4A/tm\Delta 4A}$ ES cells. These model systems can now be used for the analysis of K-Ras isoforms during development, and their effects on growth, differentiation and apoptosis *in vitro*.

Chapter 4

Expression of K-Ras during mouse embryonic development

Introduction

Transgenic studies have shown that the K-*ras* gene products are essential for embryonic development (Johnson *et al.*, 1997; Koera *et al.*, 1997). However, due to the failure of these two studies to identify consistent abnormalities, the critical sites of K-*ras* gene expression during embryonic development remain unclear.

Analysis of the expression of the Ras proteins during embryonic development has until now relied almost exclusively upon analysis of the relative level of transcription. Therefore, while several studies have shown differential regulation of Ras transcription during mouse development (Muller *et al.*, 1983; Leon *et al.*, 1987; Pells *et al.*, 1997) the regulation of protein expression and the sites of expression within embryonic and neonatal tissues are unknown. Therefore, the aim of this study was to examine the expression pattern of the K-Ras isoforms during mouse development using wax embedded sections.

4.1. Development of Immunohistochemical analysis using the K-Ras isoform specific polyclonal antibodies on wax sections.

Balb/c mice were examined, since this strain has been used previously to assess mRNA levels and for limited analysis of K-Ras 4A and 4B protein expression in adult tissues (Pells *et al.*, 1997).

Balb/c mice were mated and checked for plugs. Embryonic mice were harvested at embryonic day 12.5 (E12.5), E14.5, E16.5, E18.5 post cotium using ethically approved methods. Tissues from neonatal mice were harvested at day 8 pp and those from adult mice at 10-12 weeks of age. The embryos were analysed from E12.5 onwards, since the embryonic lethal phenotype of K-*ras*$^{-/-}$ mice occurred between E12.5 and E14.5 (Johnson *et al.*, 1997).

The K-Ras 4A and 4B protein isoforms have been detected previously in adult mouse tissues using cryostat sections with rabbit polyclonal antibodies (Santa Cruz) (Pells *et al.*, 1997). However, since poor histology is a problem with cryostat sections, the aim was to use these same two antibodies to investigate the observed temporal and spatial differences in expression pattern detected at the RNA level during mouse development, using wax embedded sections (Pells *et al.*, 1997).

To develop this technique various antigen retrieval methods were tested, including citrate buffer, enzymatic retrieval (i.e pepsin digestion) and urea treatment. The citrate buffer antigen retrieval method gave the strongest signal with the least tissue degradation. Antibody dilution curves were performed to assess the appropriate concentration of antibody, to give the strongest signal possible without incurring non-specific staining. Problems were encountered with background staining on negative control sections from embryonic samples (incubated in the presence of the antibody diluent 0.01% BSA). However, this was overcome by using a biotin-blocking reagent. While this procedure was found to work well for the K-Ras 4B polyclonal antibody, no signal was evident with the K-Ras 4A antibody.

The failure of the K-Ras 4A antibody to detect expression in mouse tissues may have been due to a low level of expression, which was below the sensitivity of this detection method. However, this seems unlikely, as Pells and co-workers found that in certain embryonic and adult tissues the expression of K-*ras* 4A mRNA equalled that of K-*ras* 4B mRNA (Pells *et al.*, 1997). In addition, the K-Ras 4A protein was expressed at sufficient levels to be detectable in adult human colon (see chapter 5). The K-Ras 4A antibody was raised against human K-Ras 4A using a peptide mapping to the carboxy terminus. However, the single amino acid difference between the human and mouse protein sequence is unlikely to explain the lower affinity of this antibody for the mouse epitope. An amino acid sequence comparison between human and mouse exon 4A is shown below.

Human	RVEDAFYTLVREIRQYRLKKISKEEKTPGCVKIKKCI I M
Mouse	RVEDAFYTLVREIRQYRLKKISKEEKTPGCVKIKKCVIM

Therefore, there is no apparent explanation for this result other than the possibility of differences occuring in the posttranslational modifications of this protein in mouse and humans.

Thus, only expression of the K-Ras 4B protein was investigated. The K-Ras 4B primary antibody was used at 1/6400 dilution and the sections were incubated in the presence of the primary antibody overnight at 4°C. Negative controls were included for all samples analysed where the primary antibody was omitted and the sections were instead incubated in the presence of the primary antibody diluent (0.01% BSA). No staining was detected on any of the negative control sections analysed in this chapter (data not shown).

To confirm that the staining pattern produced was due to the specific interaction of the primary antibody with its epitope, a blocking peptide was used (figure 4.1). Following pre-treatment of the primary antibody with the blocking peptide no signal was detected, confirming that the immunoreactivity detected resulted from the association of the primary antibody with its specific epitope.

To enable direct comparison of the staining intensity the same tissue from different stages of development were analysed together, to minimise the possibility that any differences in the intensity of staining observed were attributable to experimental variations. The results presented here were found to be reproducible between experiments.

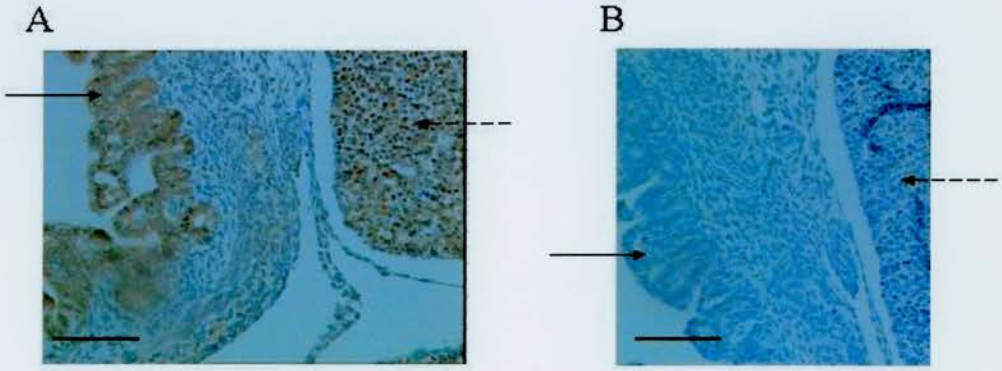

Figure 4.1 Neutralisation of K-Ras 4B polyclonal antibody with a blocking peptide. The figure shows transverse sections through an E16.5 embryo stained with the K-Ras 4B polyclonal antibody. A) Section stained with K-Ras 4B, showing immunoreactivity of the surface epithelium of the developing intestine (solid arrow) and the hepatocytes of the developing liver (broken arrow) B) Section stained with K-Ras 4B polyclonal antibody pre-incubated overnight with blocking peptide. The intestine (solid arrow) and liver (broken arrow) are indicated and show no staining. Bar represents 50μm.

4.2 Analysis of K-Ras 4B protein expression in mouse tissues

4.2.1. Examination of K-Ras 4B expression in the developing liver

In liver, K-Ras 4B is expressed strongly in the hepatocytes from E12.5 (figure 4.2 A). A general decrease in the intensity of expression was observed from E12.5 to E18.5 (figure 4.2 A-D). The level of protein expression in the 8 day old animal appears to be greater than that of the adult liver and the stain was cytoplasmic in nature, compared to the more obviously membrane associated stain of the adult tissue.

4.2.2 Expression of K-Ras 4B in the developing intestine

In colon, the epithelium of the large intestine showed strong immunoreactivity for the K-Ras 4B antibody at all stages examined and expression increased throughout embryonic development to the adult stage (figure 4.3 A-D). No gradient of expression was detected in colonic crypts as all cells stained equally strongly. K-Ras 4B protein expression was not detected within, either the smooth muscle of the intestine, or the lamina propria. Therefore, within the developing large intestine the expression of K-Ras 4B was restricted to the epithelium, a pattern that was maintained in the neonatal and adult tissues.

In small intestine, the expression of K-Ras 4B showed a more regulated pattern. Expression of K-Ras 4B in the epithelium was high in the E16.5 intestine, but was greatly reduced by the E18.5 stage, suggesting that the K-Ras 4B protein was important for earlier stages of development (figure 4.4 A-B). The expression in the neonatal small intestine was increased compared to the E18.5 section (Figure 4.4 B-C) and showed a gradient of expression, with stronger signal detected in the crypts, compared with the villi. The expression in the adult small intestine was intense. The gradient of expression detected in the neonatal small intestine was no longer evident, which led to the overall impression of increased expression (figure 4.4 C-D). The smooth muscle layers and lamina propria showed no immunoreactivity. The data suggest that, in contrast to colon, there are two peaks of K-Ras 4B expression the in mouse small intestine, one occurring before E18.5 and the second following neonatal development.

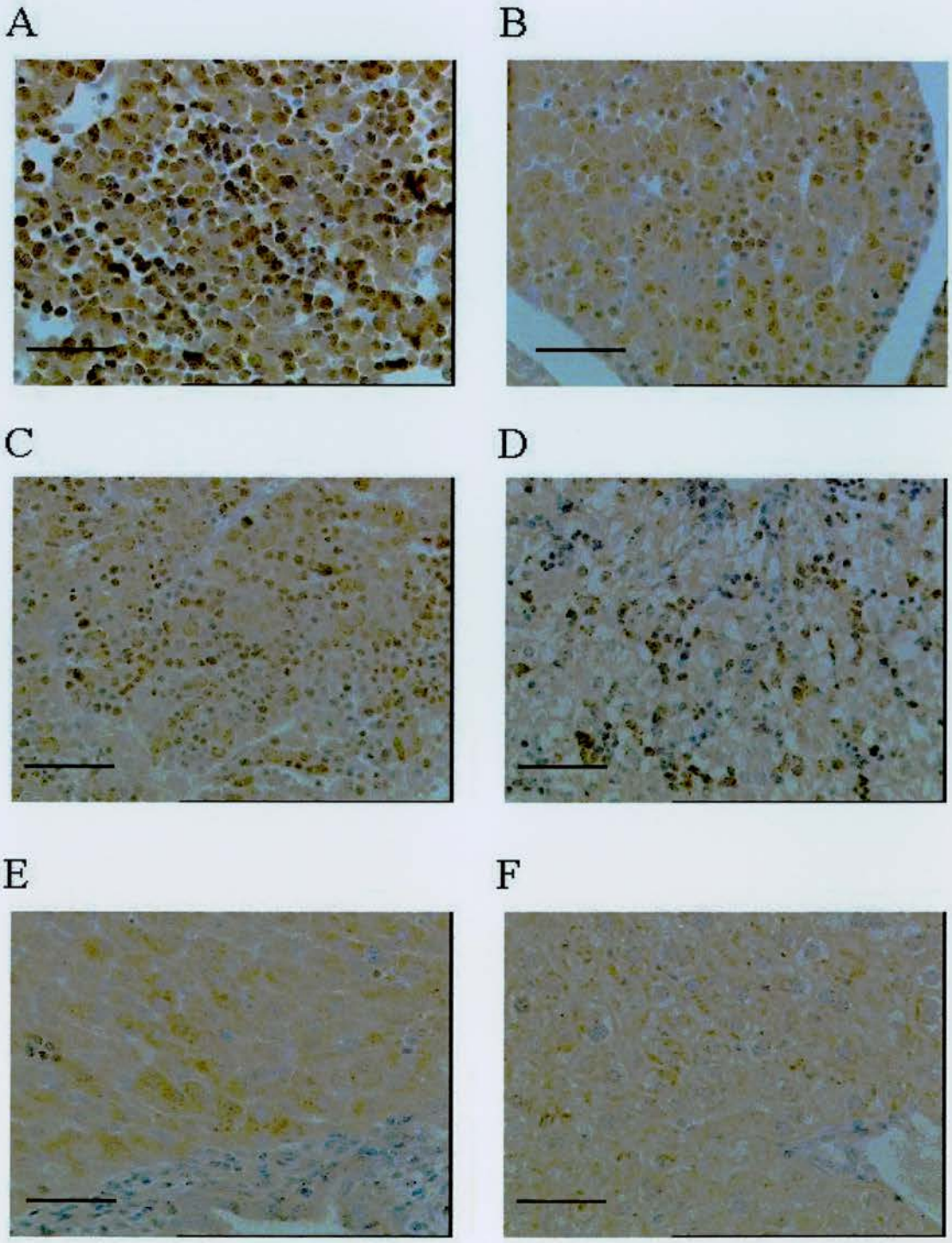

Figure 4.2 Expression of K-Ras 4B in embryonic, neonatal and adult mouse liver. K-Ras 4B immunoreactivity is present in hepatocytes of all stages examined. A) E12.5 foetal liver showing strong stain. B) E14.5 hepatocytes. C) E16.5 hepatocytes. D) E18.5 hepatocytes. E) Day 8pp hepatocytes showing moderate cytoplasmic stain. F) Adult hepatocytes showing weak membrane-associated stain. The bar represents 50μm.

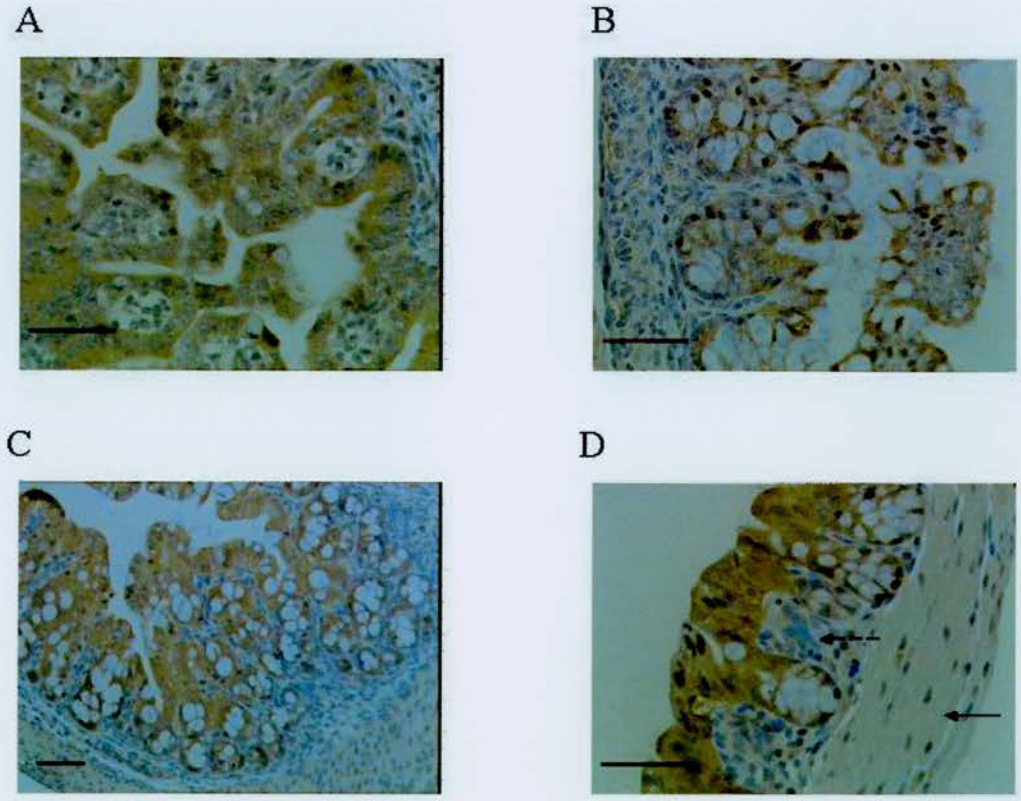

Figure 4.3 Expression of the K-Ras 4B protein during embryonic development and in neonatal and adult sections of large intestine. The surface epithelium of all stages examined show intense immunoreactivity. A) E16.5 large intestine. B) Large intestine of an E18.5 foetus. C) Day 8 pp large intestine showing specific staining of the surface epithelium. D) Adult colon. The smooth muscle (solid arrow) and lamina propria (broken arrow) show no staining. Bar represents 50μm.

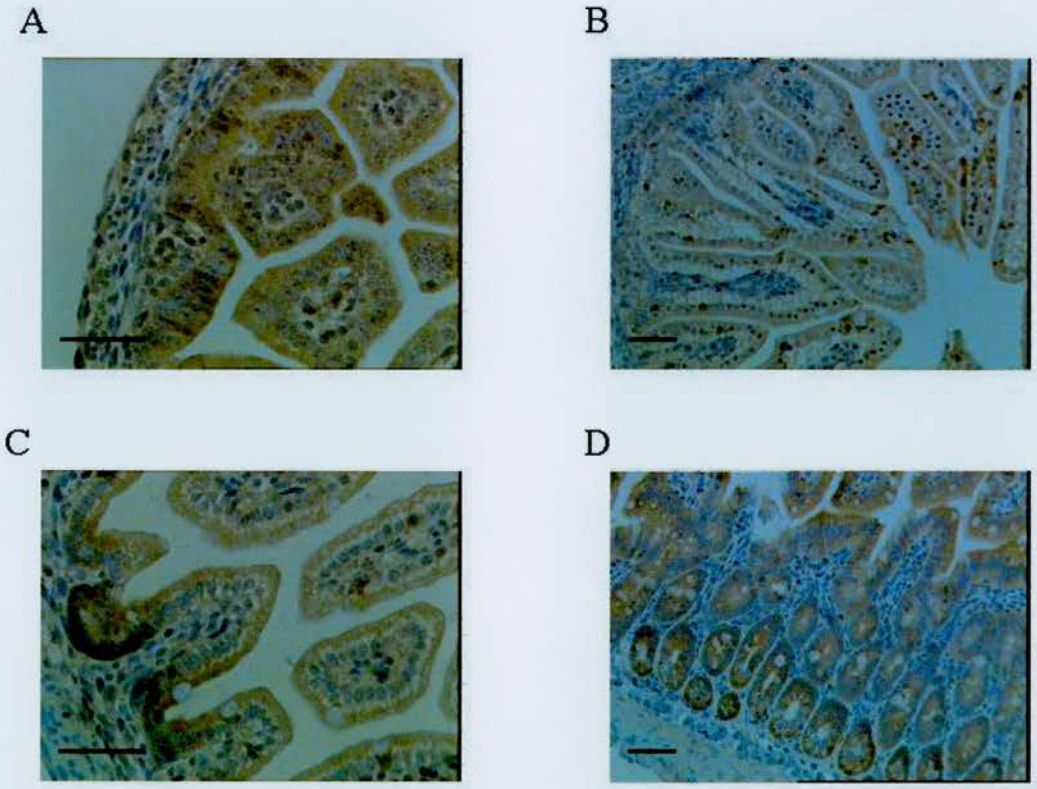

Figure 4.4 Expression of K-Ras 4B isoform in embryonic, neonatal and adult small intestine. The expression pattern appears to vary markedly depending upon the stage examined. A) E16.5 intestine showing strong stain of surface epithelium B) E18.5 small intestine, which shows weak staining. C) Day 8pp, showing strong stain in the crypts but weak stain in the villus. D) Adult mouse small intestine. Intense staining is uniformly detected in the cells of the crypt and villus. Bar represents 50μm.

4.2.3 Analysis of K-Ras 4B expression in the mouse pancreas

The expression of the K-Ras 4B protein was examined at the following stages E16.5, E18.5, day 8 pp and in 10-12 week old adults. In the pancreas, the acinar cells of the exocrine portion show immunoreactivity at all stages analysed (figure 4.5 A-D). The expression of the K-Ras 4B protein in the embryonic and neonatal pancreas was very similar, but was higher in the adult pancreas, suggesting an up-regulation of expression later in neonatal development. Interestingly, K-Ras 4B expression was not detected in the pancreatic ducts or islets examined. This is an important observation since pancreatic tumours are derived from duct and islet cells, suggesting that K-Ras 4B expression may not be important in the development of this tumour type at least in the mouse. Analysis of K-Ras 4A expression in this tissue could lend further insight into this finding.

4.2.4 Analysis of K-Ras 4B expression in the adult stomach

Immunohistochemistry was performed on adult mouse stomach showing K-Ras 4B protein was expressed in the basal part of the gastric gland and the level of expression was intense (figure 4.6 A–B). The expression appeared to be specific to the chief (zymogenic) cells of this region, whereas the parietal cells were not immunoreactive, identified by PAS staining of a corresponding section (figure 4.6 C). Staining was also evident in the surface columnar epithelium, but the muscularis mucosae and lamina propria were negative.

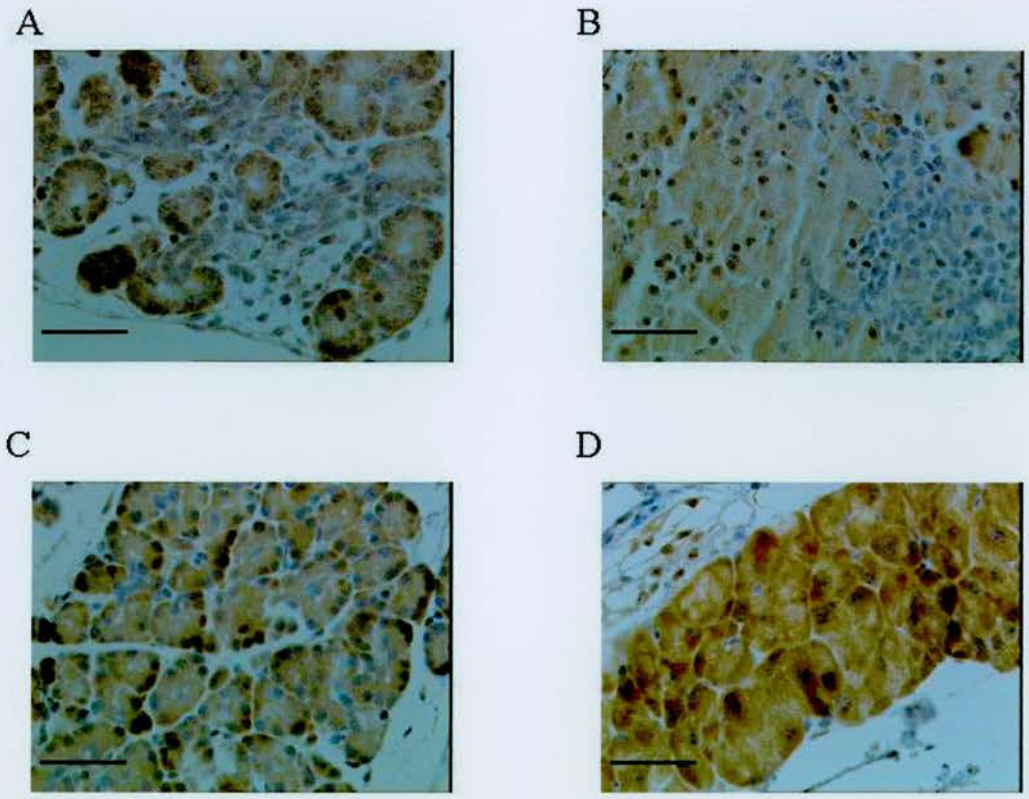

Figure 4.5 Expression of the K-Ras 4B protein in sections of E16.5, E18.5, 8 day old and 10-12 week old mouse pancreas. Strong expression of the K-Ras 4B protein is detected in acinar cells at all stages examined. A) E16.5 pancreas. B) E18.5 pancreas. C) Day 8pp pancreas. D) Adult pancreas showing intense staining of the acinar cells. Bar represents 50μm.

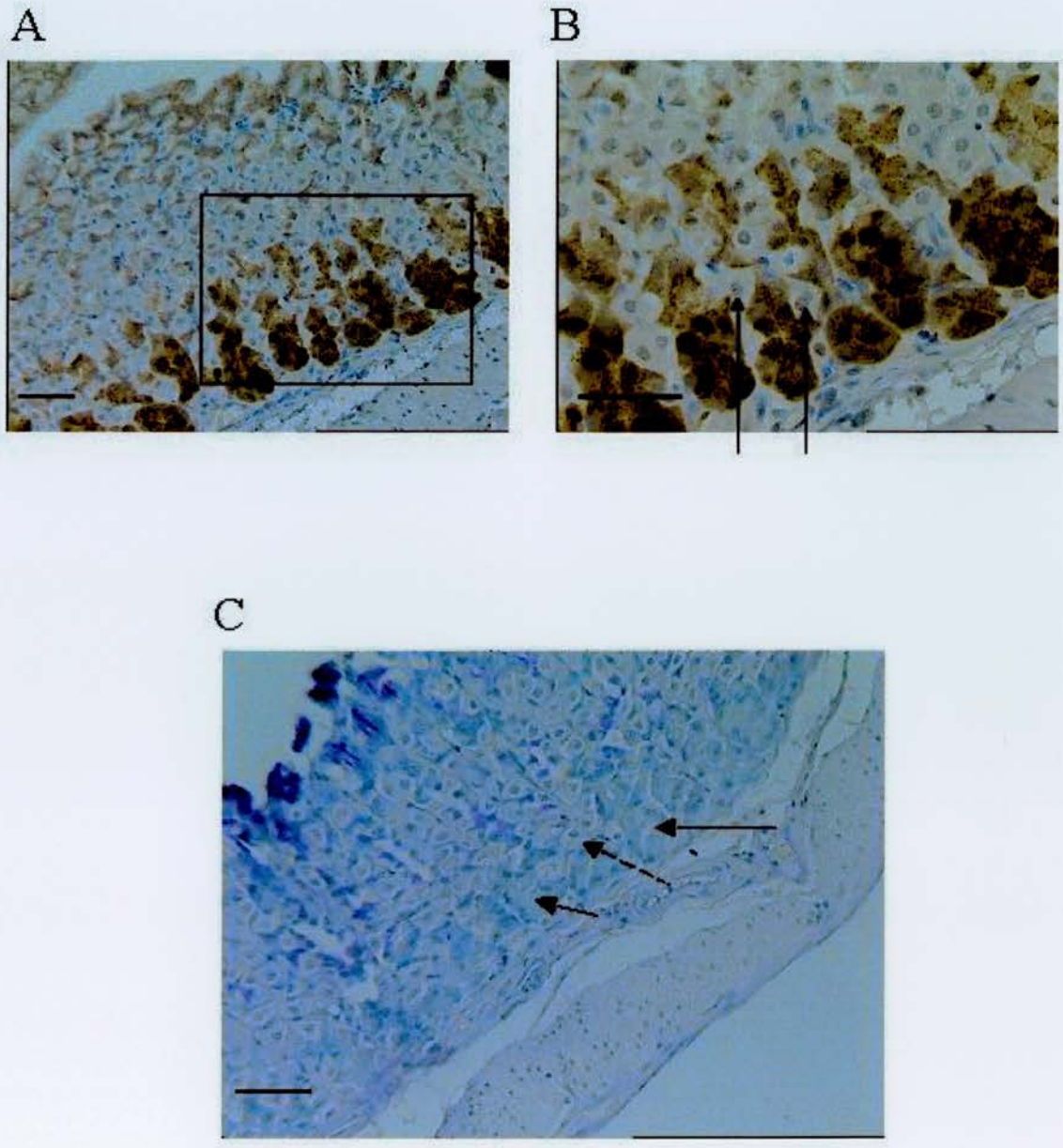

4.6 Expression of the K-Ras 4B isoform in the adult stomach. The expression of the K-Ras 4B protein was detected in the chief (zymogenic) cells in the base of the gastric gland. A) Adult stomach. B) Area of adult stomach indicated in A at higher magnification. Parietal cells (solid arrows) are negative. C) PAS staining of adult stomach. Zymogenic cells (solid arrows) and parietal cells (broken arrow) are indicated. Bar represents 50μm

4.2.5 Examination of K-Ras 4B expression in the mouse lung

The expression of the K-Ras 4B protein was examined in E14.5, E16.5, E18.5, neonatal and adult mouse lungs. The expression pattern was well defined and restricted to the respiratory epithelium lining the airways. (figure 4.7 A-D). No difference in the level of K-Ras 4B expression was detected in the embryonic sections analysed. In the bronchi and bronchioles of neonatal and adult lungs there was an up-regulation of K-Ras 4B expression, compared to embryonic sections. However, the level of expression was of a similar intensity for neonatal and adult mouse lung. The expression appeared to be specific to the epithelium of the bronchi and bronchioles, as neither the alveoli, nor the linings of the blood vessels showed immunoreactivity. In addition, the smooth muscle surrounding the bronchioles did not show immunoreactivity (figure 4.7 D). The results indicate an up-regulation of the K-Ras 4B protein levels in the epithelial lining of the airways following embryonic development in neonatal and adult stages.

4.2.6 Examination of K-Ras 4B expression in the kidney

K-Ras 4B protein expression was analysed in the developing kidney. Strong expression was detected in the developing glomerulus as early as E16.5 (Figure 4.8 A). There was a down-regulation of protein expression detected in the developing kidney at the E18.5 stage, compared to the intensity of expression observed at the E16.5 stage. The strongest expression was detected in the neonatal kidney, suggesting that there is postnatal up-regulation of this protein in the kidney (Figure 4.8 C). The expression appears to be associated with the tubules, but also cells of the glomerulus, which may be podocytes based upon their position within the glomerulus, the expression of K-Ras 4B remains high within the adult glomerulus and tubules (Figure 4.8 D). The medulla of the neonatal and adult kidney showed no immunoreactivity (data not shown).

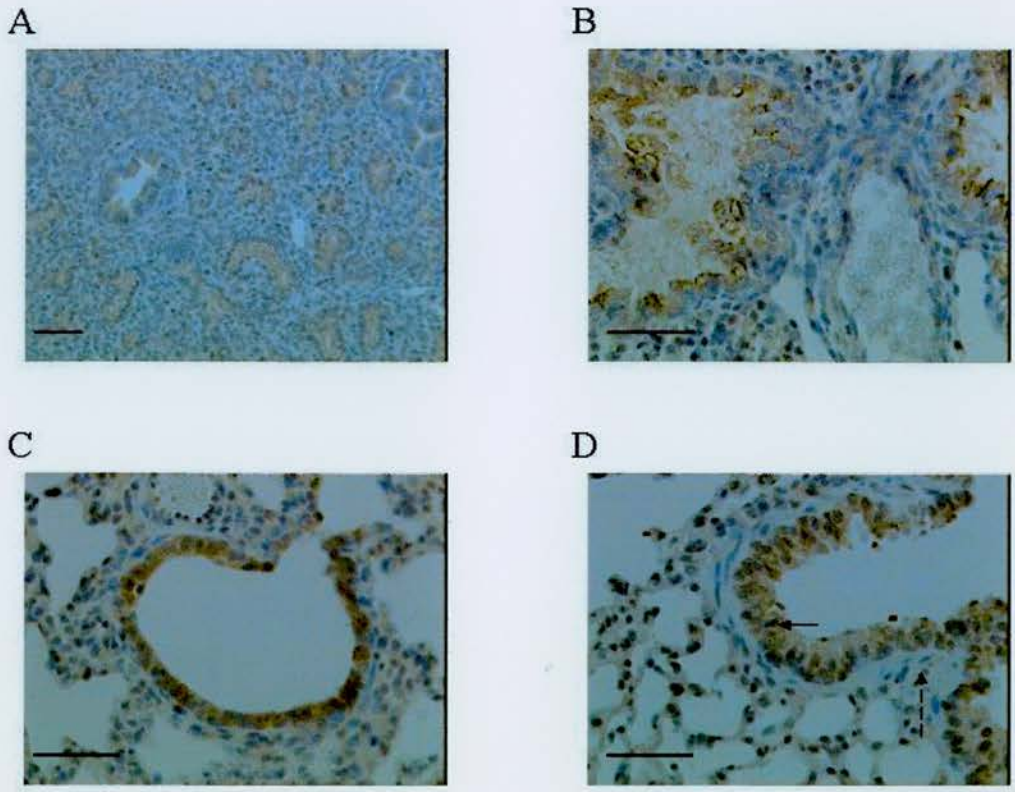

Figure 4.7. Immunohistochemical detection of K-Ras 4B protein in embryonic, neonatal and adult lung. The expression of the K-Ras 4B protein increases through development. The highest levels appear to be achieved by the neonatal stage and these levels are maintained in the adult lung. A) E16.5 lung. B) E18.5 lung. C) Neonatal lung showing immunoreactivity of the respiratory epithelium lining the bronchiole. D) Adult lung showing immunoreactivity of the respiratory epithelium lining (solid arrow) the bronchiole. The alveoli and the smooth muscle layer (dashed arrow) are not immunoreactive. Bar represents 50μm.

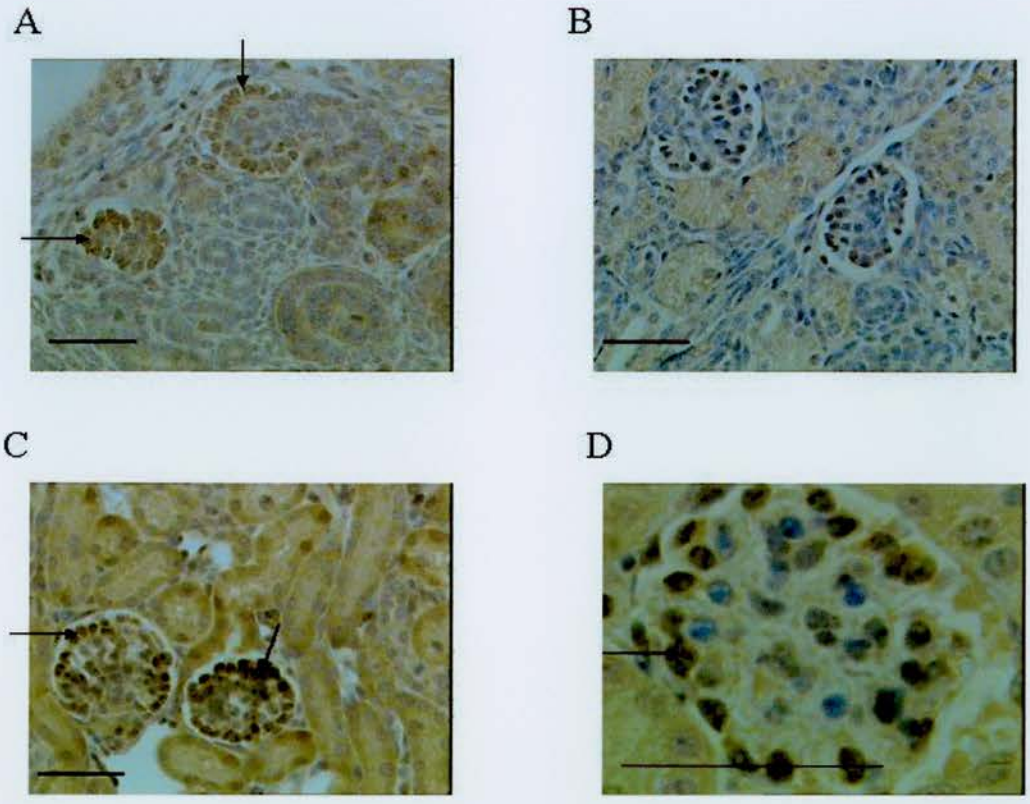

Figure 4.8 Immunohistochemical detection of the K-Ras 4B protein in embryonic, neonatal and adult kidney. The K-Ras 4B protein is strongly expressed in the neonatal and adult tissues, and particularly in the glomerulus. A) E16.5 kidney. Arrows indicate areas of strong stain present in the developing glomerulus. B) E18.5 foetal kidney. C) Neonatal kidney. Intense immunoreactivity is detected in tubular and glomerular structures. Arrows indicate cells within the glomerulus that are showing particularly strong staining. D) Adult kidney showing the staining pattern observed in the glomerulus. The arrow indicates a cell within the glomerulus that is strongly immunoreactive, which may be a podocyte. Bar represents 50μm.

4.2.7 Examination of K-Ras 4B expression in the heart

K-Ras 4B was found to be expressed in the mouse heart from E12.5 (figure 4.9 A). The expression appeared to peak about E18.5 (figure 4.9 B) and then declined following postnatal development to barely detectable levels in the adult myocardium (figure 4.9 D). This staining was specific to the myocardium, since the endothelium and smooth muscle lining of the veins and arteries showed no immunoreactivity.

4.2.8 Examination of K-Ras 4B expression in the nervous system

The analysis of the developing embryos showed that K-Ras 4B was expressed strongly in the ganglia and peripheral nerves from E14.5 onwards with no apparent alteration in intensity or location of expression during this period (figure 4.10 A-B). There was no evidence of expression at any embryonic stage in cells within the spinal cord (figure 4.10 C). The expression was not analysed in adult mice therefore it is unknown whether this pattern persists in the adult mouse. K-*ras*$^{-/-}$ embryos were reported to have increased apoptosis of motoneurones in the medulla and cervical spinal cord from E11.5, suggesting that K-*ras* has a role in the development of the nervous system (Koera *et al.*, 1997). Therefore the lack of K-Ras 4B expression implies that the defect observed in the spinal cord may result from a lack of K-Ras 4A expression in the K-*ras*$^{-/-}$ embryos. This is an important observation that points to the potential for the development of neurological defects in K-*ras*$^{tm\Delta4A/tm\Delta4A}$ mice.

Whilst examining the embryonic sections cytoplamic K-Ras 4B expression was also observed within the chondrocytes of the cartilage and the osteocytes of the bone at all stages analysed (figure 4.10 D-E). The intensity and localisation of expression did not alter during the embryonic stages analysed. However, whether this pattern persists in adult mice is unknown, since these stages were not examined.

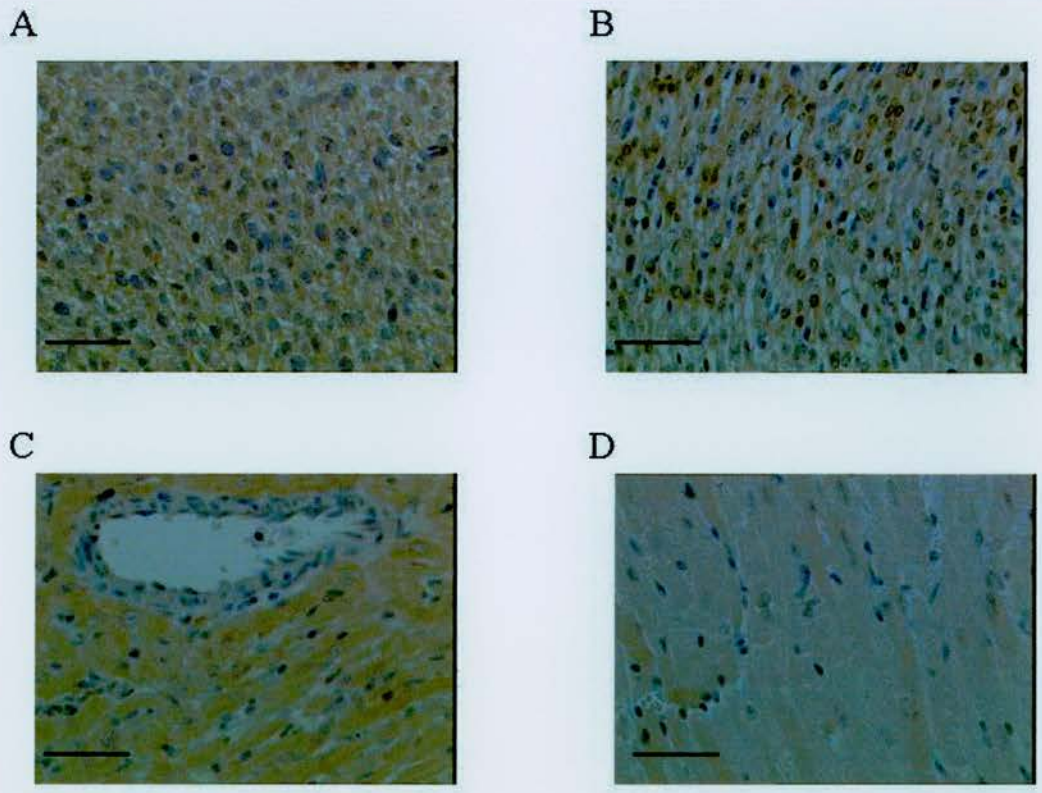

Figure 4.9. Analysis of the expression of the K-Ras 4B protein in the developing mouse heart. Immunohistochemistry was performed on hearts from E12.5, E14.5, E16.5, E18.5, and neonatal and adult mice. Immunoreactivity was detected at all stages examined, but declined during postnatal development to very low levels in the adult stage. A) E12.5. B) E18.5. C) Day 8 pp. D) Adult cardiomyocytes showing weak stain only. Bar represents 50μm.

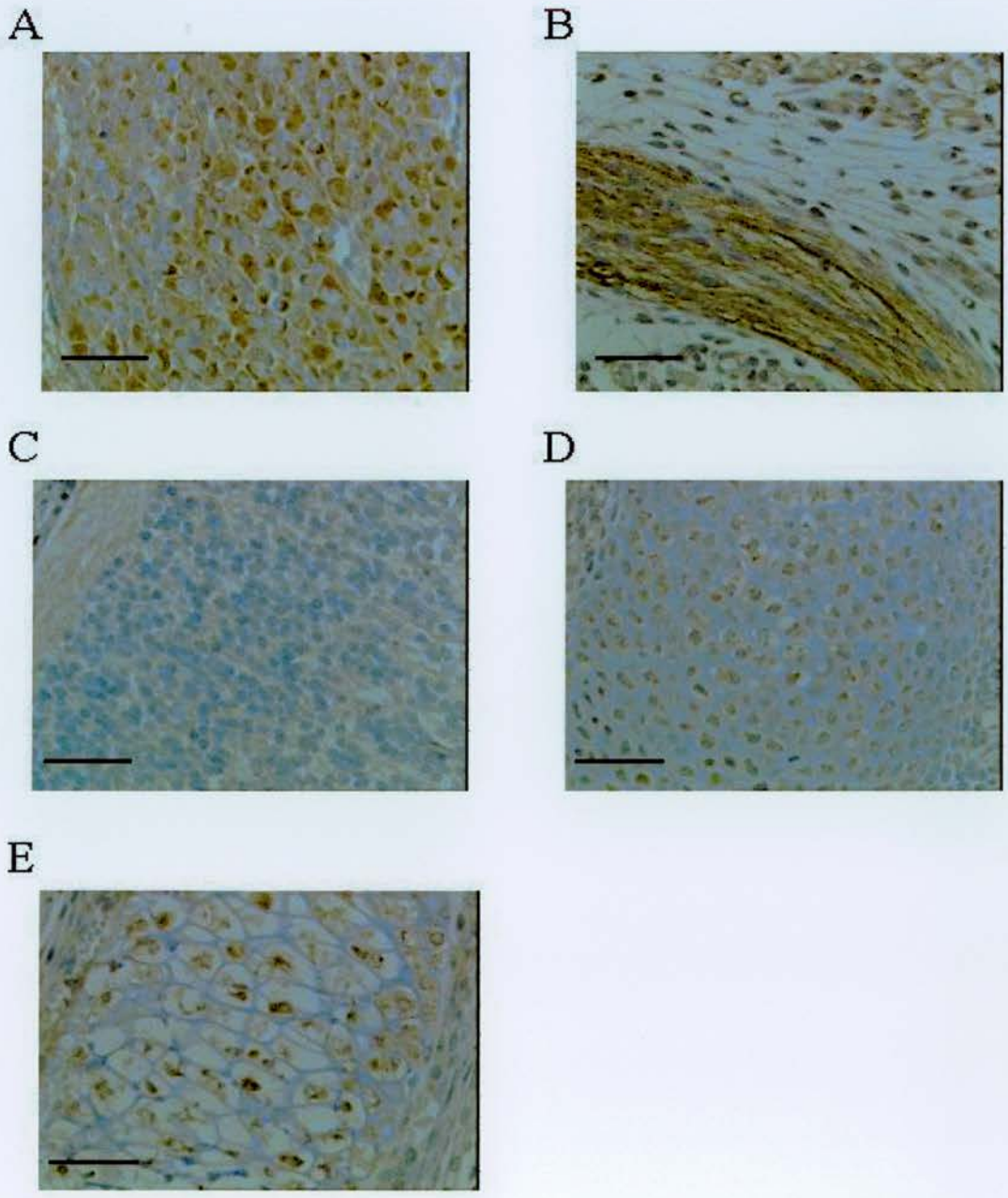

Figure 4.10. Analysis of the expression of the K-Ras 4B protein in the peripheral nervous system, spinal cord and in cartilage and bone. The expression of the K-Ras 4B protein was detected in the ganglia and peripheral nerves at all stages examined from E14.5 onwards with no alteration in intensity or location of expression. Therefore the pictures are representative. A) E14.5 ganglia. B) E14.5 peripheral nerve. C) Section showing the E16.5 spinal cord with no immunoreactivity. D) E14.5 chondrocytes showing cytoplasmic stain. E) E14.5 osteocytes showing cytoplasmic immunoreactivity. Bar represents 50μm.

4.3 Discussion

Previous studies using Northern analysis have reported changes in K-*ras* mRNA expression during embryonic and postnatal development (Muller *et al.*, 1983: Leon *et al.*, 1987). However, these studies give no information regarding which cell types express K-*ras*. In view of reports the K-*ras* homozygous null mice die between E12.5 and term due to liver, heart and motoneuron abnormalities (Johnson *et al.*, 1997; Koera *et al.*, 1997), and that K-*ras* activating mutations are linked with particular types of cancer (Bos *et al.*, 1989) the analysis of K-Ras 4B protein expression, which is the major K-*ras* isoform expressed (Pells *et al.*, 1997), can shed valuable insight in identifying which cell types express K-Ras, and therefore where K-*ras* null and activating mutations might act.

In the liver, the K-Ras 4B protein was detected in the hepatocytes with the strongest expression observed at E12.5. This time point coincided with the occurrence of liver abnormalities in K-*ras*$^{-/-}$ mice (Johnson *et al.*, 1997). These observations indicate the importance of K-Ras 4B expression for the early development of the mouse liver. The overall decline in K-Ras 4B protein expression from E16.5 to low levels in adult liver is in agreement with reported changes in K-*ras* transcription as determined by Northern analysis (Muller *et al.*, 1983; Leon *et al.*, 1987). Hence, K-*ras* 4B expression may be important for the development of embryonic and neonatal mouse liver, with a reduced requirement for K-Ras 4B protein expression in adult mouse liver.

In the heart, K-Ras 4B expression was detected in the cardiomyocytes from E12.5, and this early expression, combined with higher expression in embryonic than adult heart, suggests that expression of the K-Ras 4B protein plays an important role during the early stages of heart development. Expression of K-Ras 4B in the developing heart agrees with the finding the K-*ras*$^{-/-}$ embryos display heart defects; including decreased heart size and thin ventricular walls, compared to wild-type littermates (Koera *et al.*, 1997). Therefore, the expression of the K-Ras 4B protein appears to be important for the development of the mouse heart. However, reduced expression in the adult heart indicates that there may be decreased requirement for this protein following neonatal development. The detection of only low levels of K-Ras 4B protein in adult mouse heart is supported by previous observations using this antibody on cryostat sections (Pells *et al.*, 1997)

K-*ras* mutations have recently been shown to be associated with the progression of lung tumours in mouse models of oncogenic K-*ras* action (Fisher *et al.*, 2001; Jackson *et al.*, 2001; Johnson *et al.*, 2001). Furthermore, the study of chimaeric mice composed of wild-type and K-*ras*$^{-/-}$ cells found that the latter colonised the lung poorly (Johnson *et al.*, 1997). The result suggests that K-*ras* has an important role in both lung development and function. The present work found that the K-*ras* 4B isoform was detected in the lung from E12.5 and that the expression was confined to the respiratory epithelium. However, postnatal development was marked by an increase in expression, culminating with highest levels in the adult lung. Importantly, transcriptional analyses also indicate that K-*ras* is expressed at high levels in adult lung (Leon *et al.*, 1987; Pells *et al.*, 1997).

Previous findings, which detected high levels of K-*ras* gene transcription in the kidneys of 8-day-old-mice (Muller *et al.*, 1983), support the observations made here that the strongest expression of the K-Ras 4B protein was detected in the neonatal kidney. The down-regulation of K-Ras 4B expression detected in the kidney late in embryonic development may reflect the general decrease in K-*ras* transcription observed at this stage (Muller *et al.*, 1983; Leon *et al.*, 1987).

K-Ras 4B protein was detected in the epithelium of both the large and small intestine. The highest level of expression was detected in the adult tissues. These observations are supported by the analysis of K-*ras* transcription showing an increase from day 5 to day 30 of postnatal development and high levels in the adult mouse gut (Leon *et al.*, 1987: Pells *et al.*, 1997). The K-Ras 4B protein was also detected most strongly in the acinar cells of the adult pancreas following an up-regulation of protein expression during embryonic and neonatal development in this tissue. The strong up-regulation of K-Ras 4B expression during development of the gut, lung and pancreas, suggests that this isoform may play an important role in the homeostasis in these tissues, which give rise to tumours that contain a high proportion of K-*ras* mutations (Bos *et al.*, 1989).

The stomach has previously been identified as a specific site of strong K-Ras 4B expression (Pells *et al.*, 1997) here it was found that K-Ras 4B protein was strongly expressed in the chief (zymogenic) cells of the gastric glands. This site of expression

could reflect functional involvement of the K-Ras 4B protein in the production of the precursors of the enzymes pepsin, rennin and lipase. Similarly, the strong expression of K-Ras 4B in the acinar cells of the adult mouse pancreas may also suggest a functional role in the production and/or secretion of digestive enzymes, since the acinar cells contain zymogenic granules and secrete digestive enzymes.

In conclusion, the general trends observed in the patterns of immunoreactivity are as follows: The expression of K-Ras 4B decreases following embryonic development in the liver and heart. The expression increases during the development of the lung, small intestine, large intestine, pancreas and kidney. Finally, the expression is strong and remains so in the ganglia, peripheral nerves, chondrocytes and osteocytes during embryonic development. Thus, the expression of the K-Ras 4B protein is differentially regulated during mouse development.

Chapter 5

The expression of the K-Ras isoforms in human colorectal and cervical neoplasia

Introduction

K-*ras* mutations are associated with 40-50% of sporadically occurring human colon cancers (Bos *et al.*, 1989). The most common mutations are point mutations found in codon 12, 13 and 61, which lead to constitutive activation of the Ras proteins (reviewed Lowy and Willumsen, 1993). However, K-*ras* mutations are rarely associated with the progression of some other types of epithelial derived cancers, such as cervical tumours (Stenzel *et al.*, 2001). Activating mutations affect both K-*ras* isoforms, since they share their first three coding exons. Therefore, the possibility arises that both isoforms may be activated in colon cancer, which could in part explain the prevalence of K-*ras* activating mutations in some human cancers, compared to H-*ras* and N-*ras* mutations. The aim of this study was to investigate whether both K-*ras* isoforms are indeed expressed at elevated levels in colon cancer. For comparison, the expression patterns of the K-Ras protein isoforms were examined in cervical intraepithelial neoplasia, which are not normally associated with K-*ras* mutations.

5.1 Analysis of expression of K-Ras protein isoforms in human colon

Analysis of the expression of Ras proteins in normal and neoplastic tissues by immunohistochemistry has been studied previously using a variety of pan-Ras antibodies that detect all four Ras proteins (Garin Chesa *et al.*, 1987; Jansson et al., 1990; Visca *et al.*, 1999). These studies found a progressive increase of Ras protein expression in all phases of the sequence of colorectal carcinogenesis (Visca *et al.*, 1999). Whilst this has provided a useful insight into the expression of Ras proteins in these tissues interpretation of these results is limited by the general reactivity to all Ras proteins of the antibodies used in these studies. Therefore, it was of interest to clarify these observations by using antibodies that specifically detect the K-Ras 4A and K-Ras 4B proteins.

Specimens were anonymised archival samples that had previously been screened and known to have K-*ras* mutations, either by direct sequencing, or by RFLP analysis (details were published as part of a larger study (Andreyev *et al.*, 1998)). Twenty-two tumour blocks containing adenocarcinomas were selected for analysis that had normal colon adjacent to the area of tumour. The normal tissue acted as an internal control, which allowed direct comparison between the intensity of staining in the tumour, compared to normal colon. The tumours were stained using the K-Ras isoform specific rabbit polyclonal antibodies described in the previous chapter (chapter 4). Dr Maureen O'Sullivan performed the analysis of the histopathological features of the samples.

Since the antibodies had only previously been used on cryostat sections (Pells *et al.*, 1997), it was necessary to optimise the technique for use on wax embedded sections. Antibody dilution curves were performed to determine the correct concentration of primary antibody required to give specific signal. Various antigen retrieval methods were tested to find the conditions that gave maximal specific staining. The conditions that were selected for the immunohistochemical analysis with the rabbit polyclonal antibodies were the citrate antigen retrieval method and a 1/2000 dilution of the primary antibody, with the sections incubated overnight at 4°C in the presence of the primary antibody (chapter 2.6.1). These conditions were used for all analyses described in this chapter. Negative controls were performed for each sample. The negative controls had the primary antibody omitted and were incubated in the presence of the antibody diluent (0.01% BSA) alone. In all cases no background staining was observed (data not shown).

The staining intensity for the K-Ras 4A and 4B isoforms was scored independently. All staining was compared to the normal colonic mucosa within the same section. The intensity of expression of the protein within the tumour was scored on an arbitrary scale of (+1) for minimal increase in staining intensity to (+4) for strong increase in intensity of staining. No increase in staining intensity was indicated by (0) and a reduction in staining intensity by (–1) to (-4). The scoring for these sections is shown in the table 5.1. Representative images are shown for K-Ras 4A (figure 5.1) and K-Ras 4B (figure 5.2).

Table 5.1 Scoring of colorectal tumours for expression of the K-Ras isoforms

Block	Tumour stage	Mutation	K-Ras 4A	K-Ras 4B
13216	Moderately differentiated adenocarcinoma Duke's stage B	Codon 12	+3	0
8872	Moderately differentiated adenocarcinoma Duke's stage B	Codon 12	+1	0
22335	Moderately differentiated adenocarcinoma Duke's stage B	Codon 12	+3	+1
15144	Poorly differentiated adenocarcinoma Duke's stage D	Codon 12	+2	-1
9379	Moderately to poorly differentiated adenocarcinoma. Duke's stage B	Codon 12	+3	+1
21314	Rectal carcinoma. No data	Codon 12	+4	+1
12462	Moderately differentiated adenocarcinoma. Duke's stage B	Codon 12	+1	0
3180	Poorly differentiated adenocarcinoma. Duke's stage B	Codon 12	+3	0
2877	Moderately differentiated adenocarcinoma. Duke's stage B	Val 12	+1	0
2461	Moderately differentiated adenocarcinoma. Duke's stage B	Codon 12	+1	+1
3676	Moderately differentiated adenocarcinoma. Duke's stage C	Codon 12	+1	+2
4382	Early invasive adenocarcinoma. Duke's stage A	Codon 12	+3	0
6999	Moderately differentiated adenocarcinoma. Duke's stage B	Asp 13	+3	+1
4465	Moderately differentiated adenocarcinoma. Duke's stage B	Codon 12	+2	+2
20910	Moderately differentiated adenocarcinoma. Duke's stage B	Val 12	+1	0
4692	Moderately differentiated adenocarcinoma. Duke's stage B	Codon 12	+2	+1
9865	Poorly differentiated adenocarcinoma. Locally advanced Duke's stage B	Codon 12	+3	+3
1493	Moderately differentiated adenocarcinoma. Duke's stage C	Codon 12	0	-2
82-4345	Moderately differentiated adenocarcinoma. Duke's stage B	Val 12	0	+2
5203	Moderately differentiated adenocarcinoma. Duke's stage B	Conservative codon 13	+1	0
1352	Moderately differentiated adenocarcinoma. Duke's stage B	Ala 12	+2	+2
24571	Moderately differentiated adenocarcinoma. Duke's stage B	Codon 12	+2	0
2028	Moderately differentiated adenocarcinoma.	None	0	0
21352	Moderately differentiated adenocarcinoma.	None	+1	0
23749	Moderately differentiated adenocarcinoma.	None	0	0
1551	Moderately differentiated adenocarcinoma.	None	0	0
25643	Moderately differentiated adenocarcinoma.	None	+2	0
4634	Moderately differentiated adenocarcinoma.	None	+1	0
5391	Moderately differentiated adenocarcinoma.	None	0	0

Mutations in codon 12 and 13 were screened for using either, RFLP analysis or, direct sequencing. Unless the specific mutation is stated the codon that the mutation occurs at is indicated. The intensity of the staining was scored against the intensity of staining seen in the normal colonic mucosa within the same section as either, +1-+4 or, -1- -4. No change in the intensity of staining is indicated by 0. Duke's stage A, tumours that have not breached the muscularis propria. Duke's stage B, tumours that have breached the muscularis propria. Duke's stage C, Lymph node involvement and Dukes stage D are tumours with distal metastases.

The staining pattern with the K-Ras 4A antibody was as follows: in the normal colonic mucosa the cells of the crypt had a diffuse light cytoplasmic stain, which appeared to be evenly distributed throughout the crypt showing no evidence of a gradient of expression (figure 5.1 A and B). The muscle layer and the lamina propria showed no immunoreactivity, demonstrating that the immunoreactivity was specific to the epithelial cells of the crypt.

Whilst the staining seen in adenocarcinomas shows the same specificity of immunoreactivity, the staining intensity compared to the normal colonic mucosa described above was in general more intense (figure 5.1 C and D). The figure shows images of sections that are representative for most cases examined. The section from sample 9379 shows normal and abnormal crypts adjacent to each other. Here direct comparison shows that the staining in the abnormal crypts is more intense then the staining in the normal crypt (Figure 5.1 E and F).

The staining pattern in the normal colonic mucosa visualised with the K-Ras 4B antibody was similar to that observed with the K-Ras 4A antibody. The epithelium of the colonic crypts shows moderate staining, which was evenly distributed from the base of the crypt to the luminal surface (block 13216) showing that the stem cell compartment did not preferentially stain with K-Ras 4B. As in the case of K-Ras 4A the immunoreactivity was specific for epithelial cells of the crypt, with the muscle layers and lymph and blood vessels negative (Figure 5.2 A and B).

The abnormal crypts of adenocarcinomas from the same section, while showing the same expression pattern, do not however show the expected increase in staining observed with K-Ras 4A. The staining is still localised to the epithelial derived cells, but the staining intensity remains moderate (block 13216), although there is possibly a minor increase, but this is less marked than for K-Ras 4A (Figure 5.2 C and D). This observation is confirmed by the images from another case (block 9379) showing adjacent normal and abnormal colonic crypts where the intensity of staining is very similar (Figure 5.2 E and F).

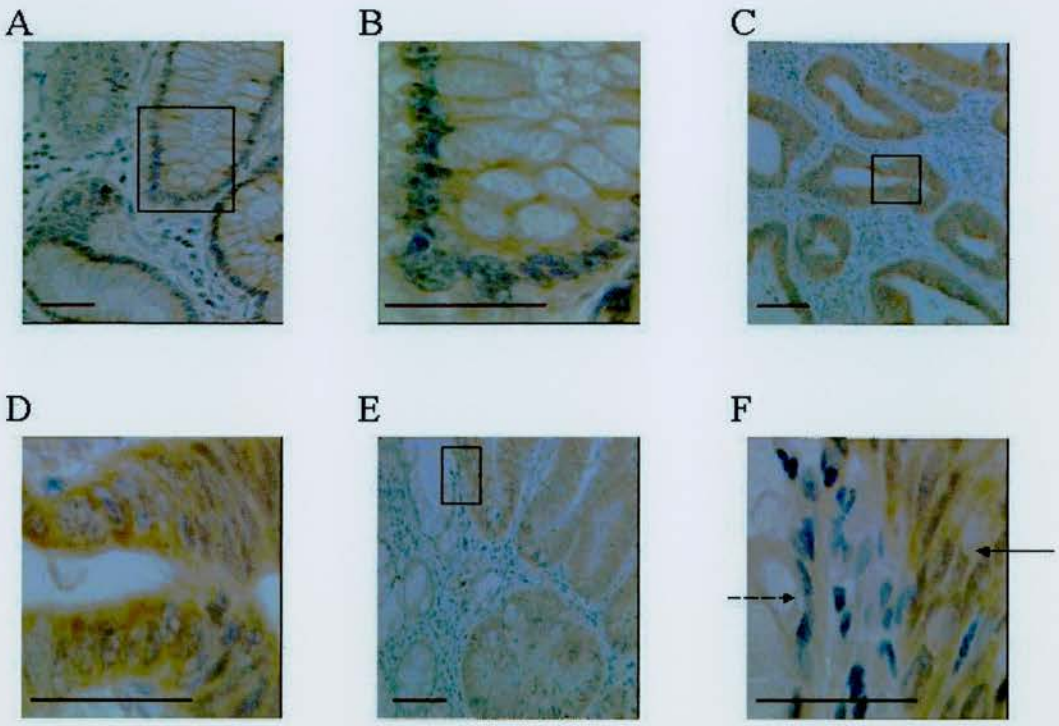

Figure 5.1 Expression of the K-Ras 4A protein in normal human colon and adenocarcinomas. Shows representative pictures of immunohistochemical staining with an antibody to detect the K-Ras 4A protein. A) Normal colonic crypts indicated by an arrow (sample 13216). B) Magnified view of normal colonic crypt as indicated in A. C) Adenocarcinoma of the colon (sample 13216). D) Magnified view of area indicated in C. E) Adjacent areas of normal colon and adenocarcinoma (sample 9379). F) Magnified view of area indicated in E, a solid arrow indicates the neoplastic crypt; the adjacent normal colonic crypt is indicated with a broken arrow. The bar represents 50μm.

An additional control was used in these experiments to confirm that the staining pattern observed with the K-Ras 4A and K-Ras 4B antibodies was the result of interaction with their specific epitopes. The primary antibodies were pre-incubated with blocking peptides and then used for the immunohistochemistry as described previously. The absence of stain (figure 5.3) indicated that the staining observed resulted from the binding of the primary antibodies to their specific epitopes, since the sections stained with the antibodies that had been pre-incubated in the presence of the blocking peptides did not show stain.

The scoring of the tumour sections showed that in general there appeared to be a greater increase in the expression of the K-Ras 4A protein isoform in moderately differentiated adenocarcinomas, when compared to the normal colon crypts, than for the K-Ras 4B isoform. Of the 22 tumours analysed 20 showed an increase in K-Ras 4A intensity, whereas only 11 of the tumours showed an increased intensity in K-Ras 4B staining, compared to the normal colon. Of those tumours that had increased staining with K-Ras 4A, 13 out of the 20 showed a difference of +2 or more compared to normal colon. In the case of K-Ras 4B the intensity of only five of the sections increased by +2 or more compared to normal colon. Two of the sections analysed with K-Ras 4A and 9 of the sections analysed with K-Ras 4B showed no change. None of the sections analysed with K-Ras 4A had decreased staining in the tumour compared to the normal colon. However, in 2 of the sections the K-Ras 4B staining was reduced in the tumour compared to the normal colon. The comparison between normal colon and areas of moderately differentiated adenocarcinomas was used as a way of controlling the observations and therefore the results only show the overall increase or decrease in staining observed in the tumour, rather than the level of staining originally seen in the normal crypt.

Additional samples were analysed that had been screened for K-*ras* mutations at codons 12 and 13 and had been found to have none. However, some (3/7) of these cases were also shown to have up-regulated K-Ras 4A expression (Table 5.1) resulting possibly from undetected K-*ras* mutations, or overexpression or amplification of the K-*ras* gene. Alternatively, the upregulation may have occurred as a result of mutations in other genes within the tumours that affect K-*ras* expression.

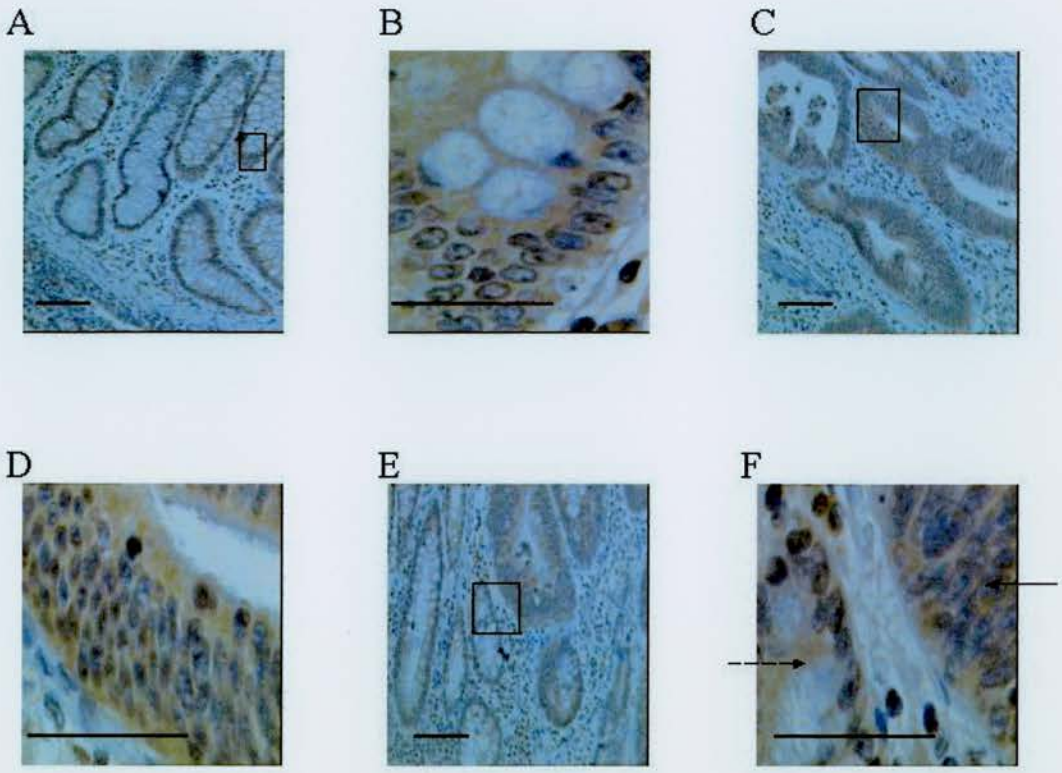

Figure 5.2 Expression of the K-Ras 4B protein in normal human colon and in moderately differentiated adenocarcinomas. Representative pictures of immunohistochemical staining with an antibody to detect the K-Ras 4B protein. A) Normal colonic crypts (block 13216). B) Magnified view of area indicated in A. C) Moderately differentiated adenocarcinoma (block 13216). D) Magnified view of area indicated in C. E) Adjacent areas of normal conic crypts and moderately differentiated adenocarcinoma (block 9379). F) Magnified view of area indicated in E. The solid arrow indicates an area of tumour; the broken arrow indicates the adjacent normal colonic crypt. Bar represents 50μm.

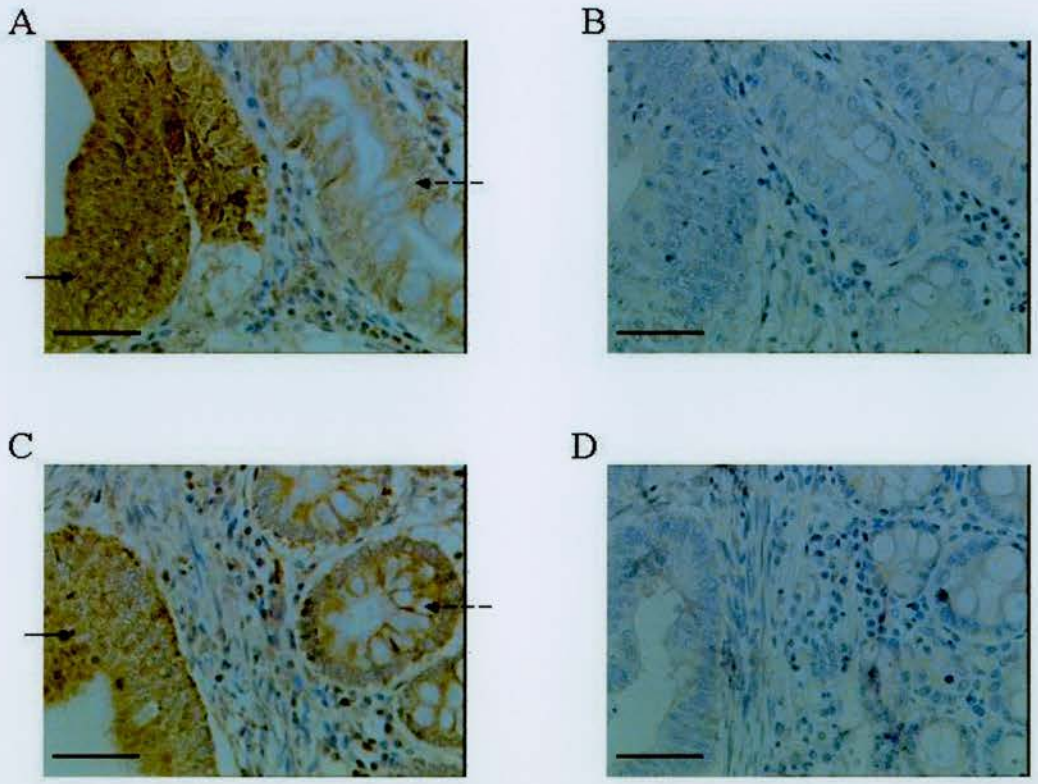

Figure 5.3 Neutralisation of the activity of K-Ras 4A and K-Ras 4B rabbit polyclonal antibodies with a specific blocking peptide. This was performed as a control to confirm the staining patterns observed were due to the specific interaction of the primary antibody with its epitope. A) K-Ras 4A primary antibody (block 4465). The solid arrow indicates an area of intensely staining tumour. The broken arrow indicates normal lightly staining crypt. B) K-Ras 4A primary antibody neutralised following incubation with specific blocking peptide (block 4465). C) K-Ras 4B primary antibody (block 4465). The solid arrow indicates an area of strongly staining tumour. The broken arrow indicates an adjacent normal crypt strongly staining. D) K-Ras 4B primary antibody neutralised following incubation with specific blocking peptide (block 4465).

5.2 Analysis of the expression of K-Ras proteins in cervical intraepithelial neoplasia

Due to the difficulty of interpreting the observations in colon adenocarcinomas with no detected K-*ras* mutations, another tumour type was sought that was known to be rarely associated with K-*ras* mutations. It was hoped that such a tumour type would act as a control to confirm that the up-regulation of expression detected in the adenocarcinomas of the colon resulted from the specific up-regulation of K-*ras* expression associated with the activating mutation, rather than a general consequence of the dysplastic changes occurring within the tissue.

Normal cervix has a stratified squamous epithelium. The epithelium is composed of three layers of cells, which differ in their differentiation status. The basal cells are the most undifferentiated type, which mature through parabasal cells and are the proliferative compartment. As cells progress further up the epithelium they become more differentiated, until they are terminally differentiated and eventually sloughed off. Cervical intraepithelial neoplasia (CIN) is believed to be the precursor lesion to squamous cell carcinoma of the cervix and is rarely associated with K-*ras* mutations (Parker *et al.*, 1997; Ferguson *et al.*, 1999). Immunohistochemistry was performed as described above using the K-Ras isoform specific polyclonal antibodies.

The five anonymised archival cervical samples analysed were obtained from women who had undergone resection following detection of CIN abnormalities. Only samples that had normal cervical epithelium and CIN within the same section were used for this analysis. The K-*ras* mutational status of these samples is not known. Dr Maureen O'Sullivan again performed the histopathological analysis of these sections.

The staining pattern observed using the K-Ras 4A antibody is as follows: there is very minimal staining in the basal area of the normal cervical epithelium. Staining is observed approximately three quarters of the way up the epithelium in the terminally differentiated cells (Figure 5.4 A). The areas of CIN compared to the areas of normal cervix from three separate blocks clearly show that the K-Ras 4A protein is not expressed in CIN (Figure 5.4 B-D).

The K-Ras 4B antibody showed a different pattern of expression, compared with the K-Ras 4A antibody. In the normal epithelium of the cervix the expression of the K-Ras 4B is most intense in the basal cells of the epithelium. The staining is intense and cytoplasmic. The K-Ras 4B staining shows a clear gradient of expression, with the intensity of expression decreasing as the cells become more differentiated (figure 5.5 A and B). The expression of the K-Ras 4B isoform is specific to the epithelium of the cervix, as the muscle layers do not show any immunoreactivity. The expression of the K-Ras isoforms therefore appears to be compartmentalised in this tissue.

Examination of the areas of CIN within the same sections show that there is a dramatic reduction in the amount and intensity of staining (Figure 5.5 C, D and E). The areas of CIN examined in general showed either no immunoreactivity, or minimal residual staining in the basal area of the epithelium.

In conclusion, the results indicate that K-*ras* expression is not associated with CIN. This observation shows that up-regulation of K-*ras* 4A expression is not a general consequence of dysplastic change and coupled with the use of blocking peptides, shows that the up-regulation of the K-Ras 4A isoform expression in colon adenocarcinomas is likely to reflect a genuine increase in protein expression resulting from specific activation of K-*ras* gene by mutations in codons 12 and 13.

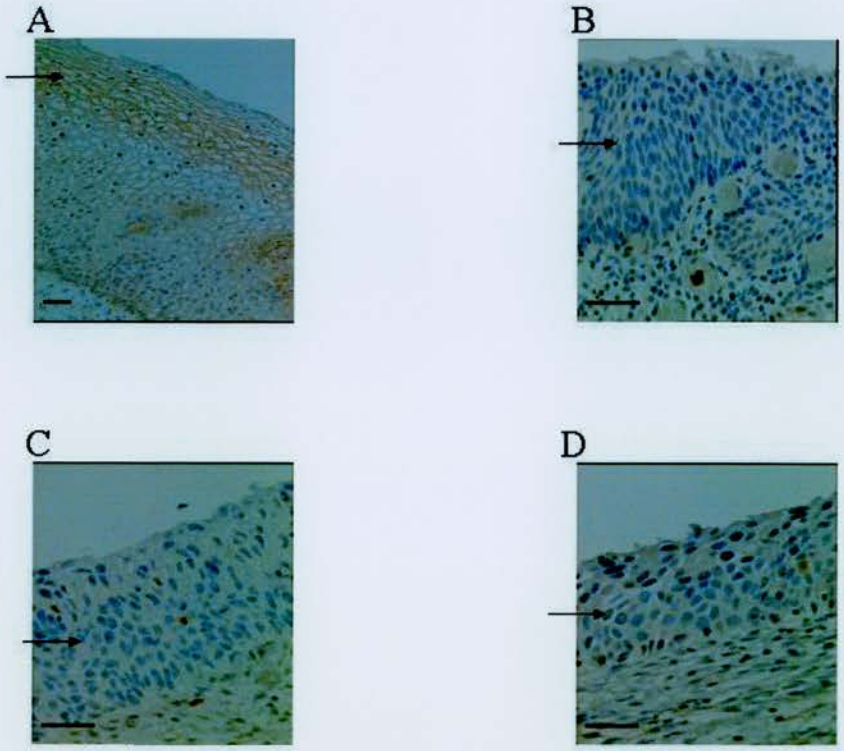

Figure 5.4 Detection of the K-Ras 4A protein in normal cervical epithelium and cervical intraepithelial neoplasia. Immunohistochemistry with the K-Ras 4A rabbit polyclonal antibody. A) Normal cervical stratified squamous epithelium (block 12832). Arrow indicates area of K-Ras 4A immunoreactivity in the upper differentiated layer of the epithelium. B) Arrow indicates area of cervical epithelium showing characteristic features of CIN (block 12829), which shows no immunoreactivity. C) Arrow indicates area of CIN that shows no staining (block 12834). D) Arrow indicates area of CIN that shows no staining (block 12832). Bar represents 50μm.

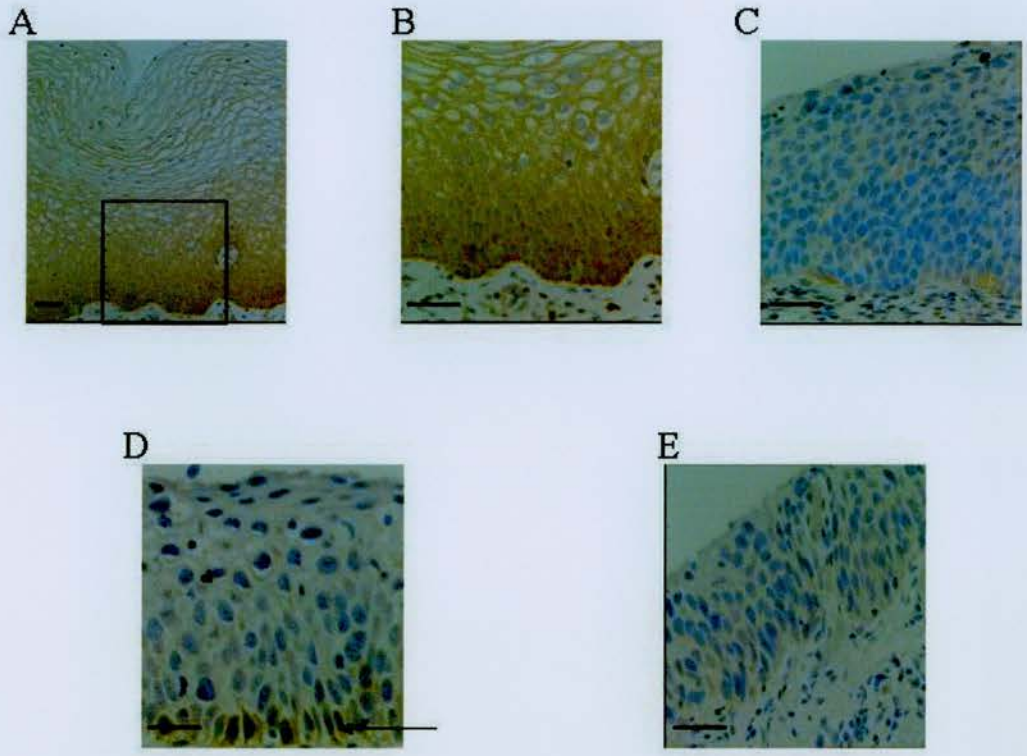

Figure 5.5 Detection of the K-Ras 4B protein in the normal cervix and in cervical intraepithelial neoplasia. A) Normal cervical stratified squamous epithelium (block 12831). The stratified epithelium shows a gradient of expression, with the highest level of expression detected in the basal cells. B) Normal cervical epithelium magnified area indicated in A. Shows more clearly the strong cytoplasmic staining of the basal cells. C) Area of CIN with weak staining in the basal region (block 12829). D) Area of CIN (block 12832). Arrow indicates area of weak residual K-Ras 4B immunoreactivity present in the basal cells of the epithelium. E) Area of CIN showing no staining (block 12834). Bar represents 50μm.

5.3 Discussion

The data presented here for the first time examines the expression of the K-Ras protein isoforms in normal and neoplastic tissues. Previous examination of the expression pattern of the Ras proteins within normal colonic mucosa identified immunoreactivity of the surface epithelium absorptive and goblet cells (Garin Chesa *et al.*, 1987; Visca *et al.*, 1999). The adenocarcinomas were associated with enhanced immunoreactivity (Visca *et al.*, 1999). The staining detected was diffuse and cytoplasmic (Hayashi *et al.*, 1994; Visca *et al.*, 1999). Therefore, the staining pattern produced with the K-Ras 4A and K-Ras 4B primary antibodies reproduced the previous observations described above, which were detected using pan-Ras antibodies. The results presented in this chapter indicate that in general the pattern of expression of the K-Ras 4A and K-Ras 4B protein isoforms is very similar in the human colon. However, the level of expression appears to be different, there is a general up regulation of the K-Ras 4A protein expression in human colonic adenocarcinomas with known K-*ras* mutations compared with normal colonic mucosa. The level of the K-Ras 4B protein does not appear to undergo this up-regulation to the same extent.

Caution was exercised in the interpretation of these results. Due to the malignant process the tissue architecture is altered, the normal colonic crypts contain little cytoplasm, as there are many globules of mucin present. However, the malignant tissue has lost this differentiated feature, which could lead to over interpretation of the results, since the cells are much more densely concentrated. Nevertheless, a general trend was observed in the sections examined, with a transition from a cytoplasmic blush stain in normal colon to a more intense cytoplasmic stain in the adenocarcinoma with the K-Ras 4A antibody.

K-Ras 4A was strongly up-regulated (+2 and above) in 13 of the 22 samples examined and showed a minor increase in a further 7 of the samples (+1). This is an important finding, since the K-Ras 4A protein has been considered to be a minor protein isoform. This is important, as the mutation present in the tumour will generate activated forms of both isoforms, since the most common mutations (codons 12, 13 and 61) occur within the first three coding exons that these two protein isoforms share. Clearly the mechanisms underlying this selective up-regulation of the 4A isoform need further investigation. The K-*ras* 4A transcript has been detected in a variety of human cancer

cell lines but at a lower level than the K-*ras* 4B transcript, the relative abundance of the two RNA species was found to be maintained in the different cell lines examined (Capon *et al.*, 1983). The authors suggest that their results indicate that the splicing pathway is not significantly altered in cell lines with activated K-*ras* transforming genes. However, it is unlikely that the K-Ras 4A protein is up-regulated as a by-product of the K-*ras* gene mutation, since its up-regulation in human adenocarcinomas is not associated with an accompanying up-regulation of the K-Ras 4B protein. While, the relevance of the selective K-Ras 4A up-regulation in colon tumorigenesis is unclear, mutant K-Ras 4A protein can induce transformed foci and growth in soft agar more efficiently than the K-Ras 4B mutant protein in a variety of cell lines; including rat intestinal epithelial cells (Voice *et al.*, 1999). Thus, suggesting possible functional relevance of the increased expression of K-Ras 4A observed in this study.

The K-Ras 4B protein was not strongly up-regulated in these tumours, which may reflect that up-regulation of K-Ras 4B protein expression, is not necessary for its tumorigenic potential. There has been relatively little investigation into the level of K-Ras protein expression, as most research has concentrated upon the presence or absence of activating mutations. In addition, those studies that have shown up-regulation of Ras proteins in colon tumours, compared to normal colon have used pan-Ras antibodies, which could have reflected the up-regulation of the K-Ras 4A protein. Therefore, the data suggests that K-Ras 4A may have a key role in the development of human colon cancer.

Analysis of expression of Ras proteins within the cervix using pan-Ras antibodies has shown discrepancies in the staining patterns observed. Furth and co-workers report that the staining was most intense in one to two layers above the basal cells (Furth *et al.*, 1987), whilst Garin Chesa and co-workers report that Ras proteins were detected in all cellular layers of the stratified epithelium (Garin Chesa *et al.*, 1987). Nevertheless, both groups agree that the patterns of expression were consistent for all stratified epithelium examined suggesting that Ras proteins have a role in the proliferation and differentiation of stratified epithelium of other tissues including the epidermis and oesophagus. This relationship has been identified recently: activation of Ras protein signalling drives proliferation of the basal cells and importantly the absence of Ras protein signalling drives differentiation (Dajee *et al.*, 2002). Disparity also exists in the

literature about the relationship between the expression of Ras proteins in CIN using pan-Ras antibodies. Sagae and co-workers showed an increase in Ras positivity associated with increasing CIN stage (Sagae *et al.*, 1990), whilst Ngan and colleagues showed no Ras immunoreactivity in normal or dysplastic cervical cells (Ngan *et al.*, 1999). Slagle and co-workers detected a similar staining pattern from normal through CIN III histology (Slagle *et al.*, 1998). However, it should be noted that Ngan and co-workers and Slagel and colleagues used the same primary antibody and yet obtained different results, suggesting that the differences may result from failure to optimise procedures or differences in experimental techniques.

Therefore, analysis of the expression of the K-Ras proteins in the cervix acts as a useful control for the observations in colon adenocarcinomas, and the isoform specific antibodies could also be used to clarify previous observations regarding the expression of Ras proteins within this tissue. The staining pattern observed in the cervix revealed a different pattern of expression, with the K-Ras 4A protein detected in the upper part of the stratified squamous epithelium and either, only staining lightly or, not at all in the basal layers, whereas the K-Ras 4B protein is detected strongly in the basal proliferative layers of the epithelium and not the upper more differentiated layers. This compartmentalisation of the protein isoforms could indicate different roles for these proteins in proliferation and differentiation of stratified squamous epithelium.

The expression of both isoforms was dramatically reduced in the regions of CIN. K-Ras 4A staining was not detected in any areas of CIN examined, and only minimal K-Ras 4B protein expression was detected in the basal areas of CIN examined. Although, only five cervical blocks were examined it is possible that the absence of K-Ras protein expression may be important for the development of CIN. Thus, the use of isoform-specific antibodies shows that compartmentalisation of Ras protein expression occurs within stratified epithelium and highlights the possibility that Ras proteins may be differentially regulated in the progression from normal cervical epithelium to CIN.

In conclusion, these observations have important implications for the development of anti-*ras* therapies and for the future direction in which investigation into the role of K-*ras* in tumorigenesis should progress.

Chapter 6

In vitro analysis of K-Ras protein function

Introduction

The role of K-*ras* in cellular proliferation, differentiation and apoptosis has been investigated extensively *in vitro*. However, despite this concerted effort there has been relatively little investigation into the role of the individual K-*ras* isoforms. However, recent evidence suggests that the individual K-*ras* isoforms may have unique functions (Pells *et al.*, 1997; Voice *et al.*, 1999), possibly mediated by association with a different subset of guanine nucleotide exchange factors (Mizuno *et al.*, 1991; Orita *et al.*, 1993; Nakanishi *et al.*, 1994). Therefore, the generation of the K-$ras^{tm\Delta 4A/tm\Delta 4A}$ ES cells provides an ideal model system to assess the functional role of the K-*ras* 4A and 4B isoforms in proliferation, differentiation and apoptosis *in vitro*. Importantly, information gained from such studies may contribute to understanding the phenotype arising from this mutation *in vivo*.

6.1 Cell Proliferation

Ras is essential for cell cycle progression (Mulcahy *et al.*, 1985; Feig and Cooper, 1988; Cai *et al.*, 1990). Studies with neutralising antibodies showed that Ras is required at multiple points throughout the G1 phase of the cell cycle in order for growth factors to stimulate quiescent cells to enter DNA synthesis, until shortly before entry into S phase (Dobrowolski *et al.*, 1994; Aktas *et al.*, 1997). Following growth factor stimulation of quiescent cells Ras signalling *via* the Raf/MAPK pathway, PI-3Kinase-PKB/Akt pathway and to a lesser extent the Rac GTPase pathway leads to up-regulation of the cyclin D1 gene product (Gille and Downward, 1999). However, deletion of the K-*ras* gene product has not been investigated in the context of cell cycle regulation. Therefore, the availability of targeted ES cells described in chapter 3 and those generated previously by this laboratory (Brooks *et al.*, 2001) permits investigation as to the effects of the K-*ras* isoforms on proliferation.

Since, the K-*ras* targeted deletions were generated in different ES cell lines i.e. E14 and HM-1, a growth curve was performed comparing E14 ES cells and HM-1 ES cells, to ensure further experiments could be interpreted correctly and any differences observed could not be attributable to intrinsic differences between the parental cell lines.

Analysis of proliferation clearly showed that the parental ES cell lines had very similar growth characteristics over time (figure 6.1). The estimated doubling times, calculated from the exponential line fitted to the graph, were 22.4hrs and 22.9hrs for E14 IV and HM-1 respectively. The similarities observed made it possible to directly compare the targeted ES cells with the knowledge that any observed growth differences were attributable to the K-*ras* mutations.

Having performed the initial experiment, the growth characteristic of wild-type, K-$ras^{tm\Delta 4A/tm\Delta 4A}$ and K-*ras* homozygous null ES cells were analysed. The results showed that the proliferation of these three genotypes was very similar, wild-type, K-$ras^{tm\Delta 4A/tm\Delta 4A}$ and K-$ras^{-/-}$ cell lines had estimated doubling times of 17.3hrs, 16.2hrs and 16.1hrs respectively (figure 6.2). The results from the 96hr time point are not included in either the graph or the calculations, as the growth of all the cell lines analysed had reached a plateau by this time point. Thus, K-*ras* is dispensable for growth in this experimental system.

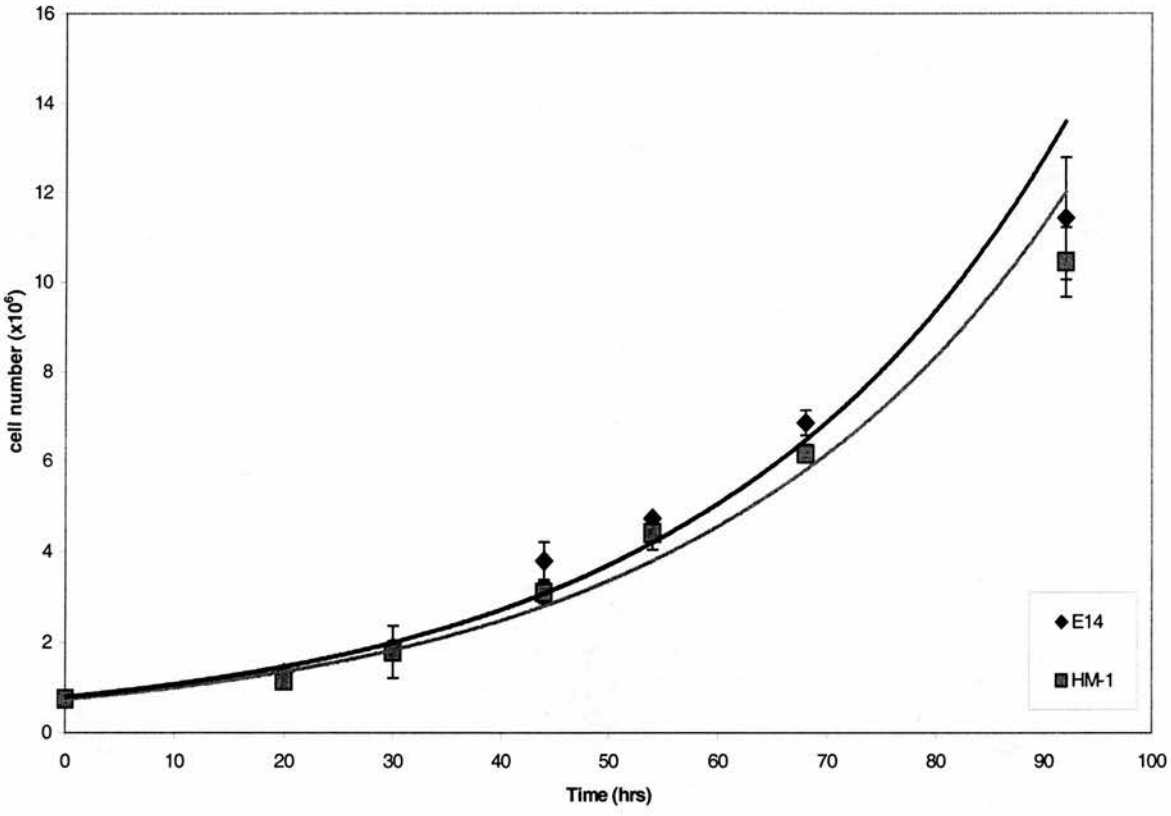

Figure 6.1 Analysis of wild-type ES cell proliferation. Cell numbers were counted at the indicated time points following seeding. The graph represents the mean of duplicate samples ± s.e.m. The trend lines were fitted to the data points using the Microsoft Excel package. The exponential equations for the lines were $y = 0.7936e^{0.0309x}$ for E14 IV and $y = 0.7423e^{0.0303x}$ for HM-1, which resulted in estimated doubling times of 22.4hrs and 22.9hrs for E14 IV and HM-1 cells respectively.

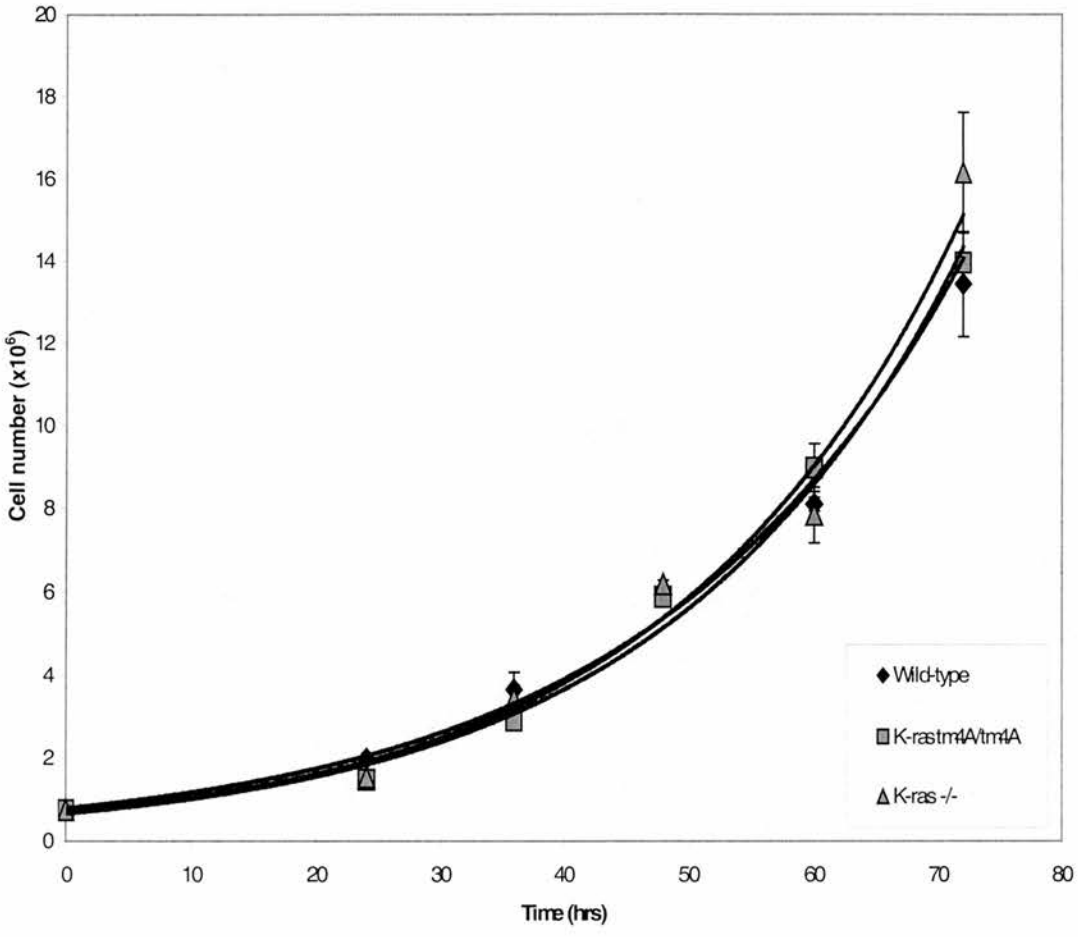

Figure 6.2 Analysis of the proliferation characteristics of targeted ES cells. Cell numbers were counted at the indicated time points following seeding. The mean number of cells for duplicate measurements ± s.e.m. are shown. The exponential trend lines were fitted to the data points using the Microsoft Excel package. The equations for the lines were $y = 0.7865e^{0.0401x}$, $y = 0.6641e^{0.0427x}$ and $y = 0.6837e^{0.043x}$ for wild-type, K-*ras*$^{tm\Delta4A/tm\Delta4A}$ and K-*ras*$^{-/-}$ cell lines respectively. The estimated doubling times calculated from these were 17.3hrs, 16.2hrs and 16.1hrs for wild-type, K-*ras*$^{tm\Delta4A/tm\Delta4A}$ and K-*ras*$^{-/-}$ cell lines respectively. The observed doubling times of the wild-type ES cells varied between experiments and this probably reflected differences in growth medium.

Activated K-*ras* causes cellular senescence in primary cell cultures, which can be overcome by the presence of other mutations in genes such as p53 and $p16^{INK4a}$ that are often present in immortalised cell lines (Serrano *et al.*, 1997). The cooperation of these mutations results in deregulated cell growth and a shortening of the G1 phase of the cell cycle (Lui *et al.*, 1995; Maher *et al.*, 1995; Winston *et al.*, 1996). Therefore, having established that K-r*as* was dispensable for normal proliferation in ES cells, it was of interest to investigate the effect of a K-*ras* activating mutation in this experimental system. Hence an additional growth curve was performed in triplicate using a K-*ras* homozygous null ES cell line that expressed an activated K-*ras* G12V minigene (Brooks *et al.*, 2001).

The estimated doubling times were ~19.5, 18.7, 19.5 and 19.5hrs for wild-type, K-$ras^{tm\Delta 4A/tm\Delta 4A}$, K-$ras^{-/-}$ and K-*ras* G12V cell lines respectively (figure 6.3). The growth curve is a representative result of the three growth curves performed. Thus, the K-*ras* G12V activating mutation does not affect the growth rate of ES cells.

However, K-*ras* G12V can alter cell-cycle kinetics while population doubling times remain unaffected (Orecchia *et al.*, 2001). Therefore, to address this possibility and to confirm the proliferation results using an independent method, the DNA profiles of wild-type, K-$ras^{tm\Delta 4A/tm\Delta 4A}$, K-$ras^{-/-}$ and K-*ras* G12V cell lines were compared by flow cytometry. Differences in the relative proportion of ES cells in each of the cell cycle phases from the genotypes analysed could indicate alteration of the cell cycle kinetics. The samples for analysis were taken at time points during the cell growth analysis above, so the DNA profiles could be directly compared. The DNA profiles show no appreciable difference between the genotypes analysed (figure 6.4.) confirming the results of the proliferation assay. In conclusion, K-*ras* is dispensable for the proliferation of ES cells, which is confirmed by the observation that the K-*ras* G12V activating mutation does not affect the growth characteristics of ES cells.

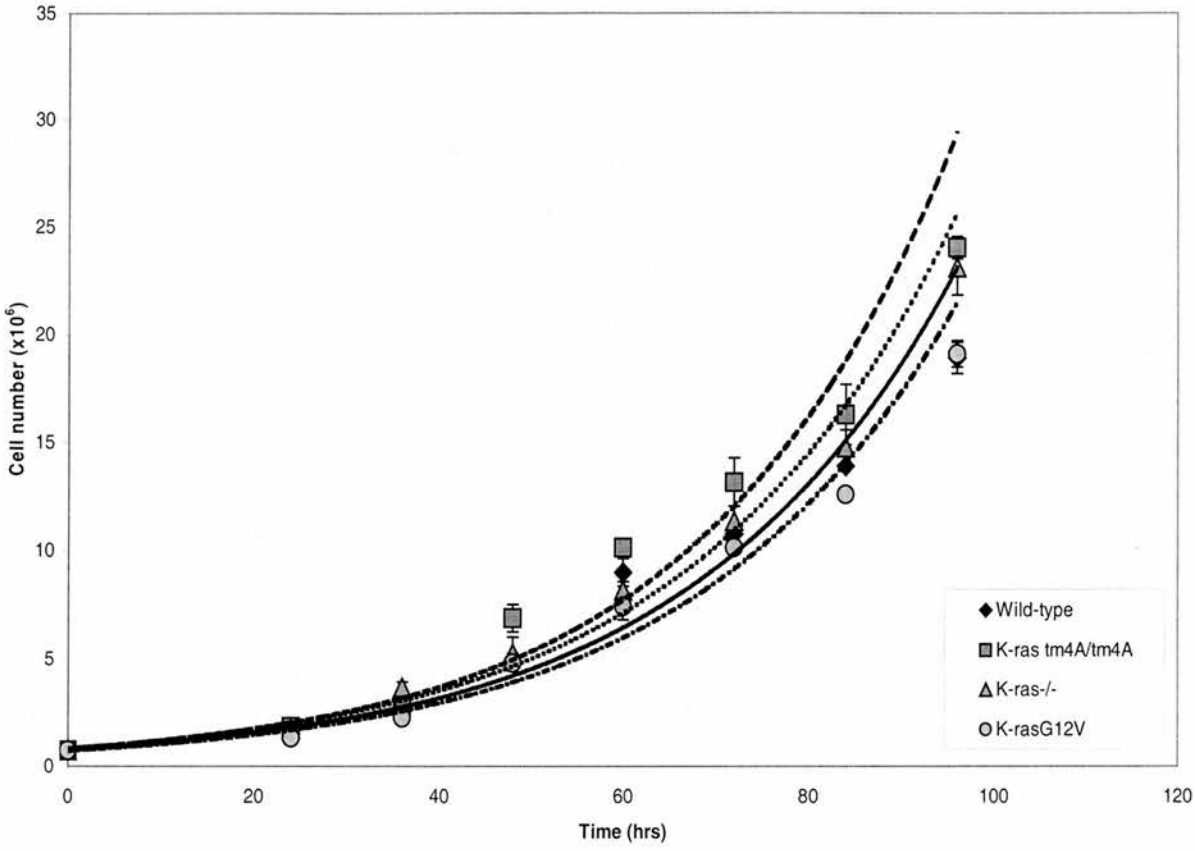

Figure 6.3 Analysis of the proliferation of wild-type, K-*ras*$^{tm\Delta4A/tm\Delta4A}$, K-*ras*$^{-/-}$ and K-*ras* G12V ES cell. The cell numbers for the four genotypes were measured at the indicated time points after seeding. The mean number of cells counted for three replicate dishes are shown ± s.e.m. The trend lines were fitted to the data points using the Microsoft Excel package. The equations for the lines are as follows: wild-type $y = 0.767e^{0.0355x}$, K-*ras*$^{tm\Delta4A/tm\Delta4A}$ $y = 0.8361e^{0.0371x}$, K-*ras*$^{-/-}$ $y = 0.8439e^{0.0356x}$ and K-*ras* G12V $y = 0.7088e^{0.0355x}$. From these the estimated doubling times were calculated as 19.5hrs, 18.7hrs, 19.5hrs and 19.5hrs respectively.

Wild-type trendline _____ K-*ras*$^{-/-}$ trendline _ _ _ _ _ _

K-*ras*$^{tm\Delta4A/tm\Delta4A}$ trendline __ __ __ K-*ras* G12V trendline __ _ __ _ __

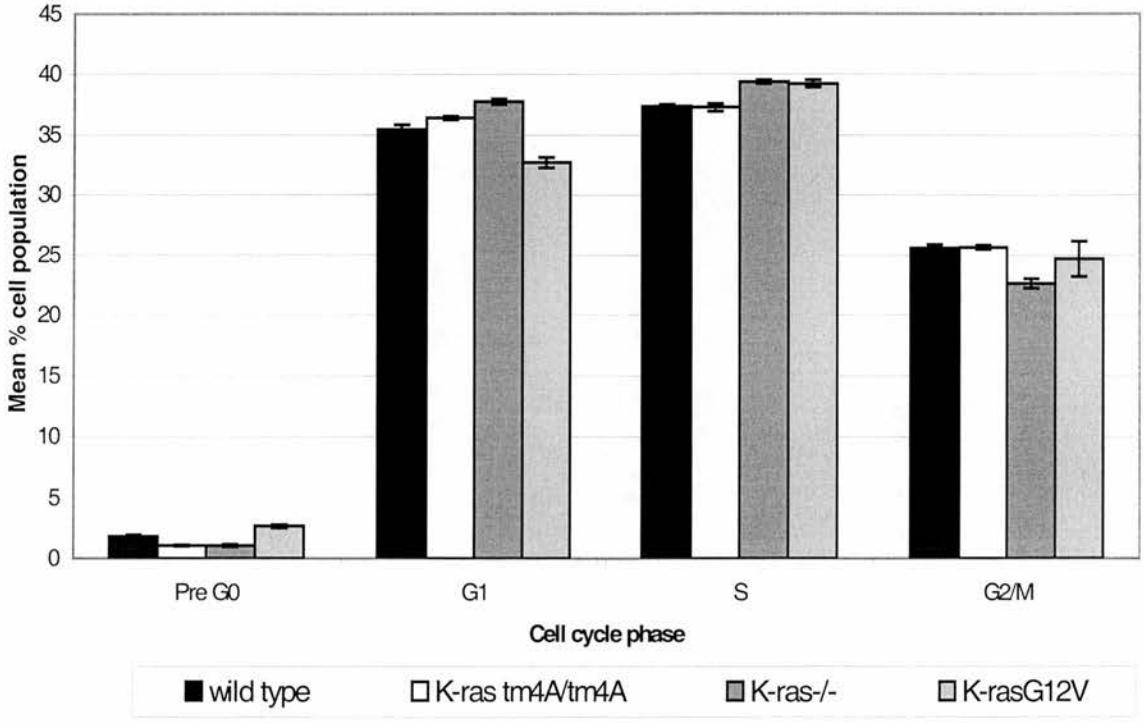

Figure 6.4 The DNA profile of ES cells growing for 24 hours following seeding. The figure shows the proportion of cells of each genotype examined in the pre G0, G1, S and G2/M phases of the cell-cycle, as measured by flow cytometry. The measurements were made 24 hours after the cells had been seeded. The samples were taken during the cell proliferation analysis, so to be directly comparable. The mean of three replicate measurements ± s.e.m. is shown.

6.2 *In vitro* differentiation of ES cells and analysis of alkaline phosphatase activity

Analysis of cell cycle parameters such as, population doubling times and DNA profile, suggested that these were not dependent upon K-*ras*. Therefore, it was of interest to investigate other cellular processes that Ras proteins may regulate using this experimental system. Ras proteins have been implicated as important regulators of differentiation in several different cell types (Szeberenyl *et al.*, 1990; Verheijen *et al.*, 1999; Dajee *et al.*, 2002). Furthermore, the Ras/MAPK pathway has a potential role in the renewal of stem cell populations by the LIF cytokine *in vitro,* as it has been linked to signalling from the gp130 receptor following LIF stimulation (Ernst *et al.*, 1996).

To investigate whether ES cell self-renewal and differentiation are dependent upon the K-*ras* gene product, wild-type, K-$ras^{tm\Delta 4A/tm\Delta 4A}$, K-$ras^{-/-}$, K-*ras* G12 and K-*ras* G12V ES cells were grown in 6 well plates in the presence of various concentrations of LIF for 5 days. Alkaline phosphatase activity has been shown to be a marker of a stem cell population (Bernstine *et al.*, 1973). Therefore, at the end of this time the cells were stained for endogenous alkaline phosphatase activity to identify those colonies that maintained a stem cell population.

The alkaline phosphatase staining identified three types of colony representative pictures of which are shown in figure 6.5. Firstly, an ES cell colony is an intensely pink staining colony of tightly grouped cells showing minimal differentiation at the colony edge (figure 6.5 A). Secondly, there was the mixed type, that still showed alkaline phosphatase activity, but the cells were less tightly grouped and the colony had a much larger proportion of differentiated cells growing out from the colony (figure 6.5 B). Finally, the third type was the differentiated colony, which showed no alkaline phosphatase activity (figure 6.5 C). For the purposes of this experiment the first two types were grouped together under the term alkaline phosphatase positive colony.

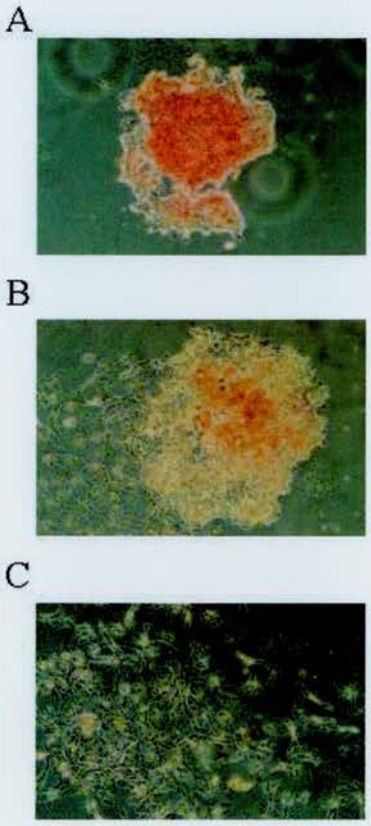

Figure 6.5 Alkaline phosphatase staining of ES cell colonies. ES cells were grown for 5 days in various concentrations of LIF then stained for the presence of alkaline phosphatase. A) Alkaline phosphatase positive ES cell colony comprised of undifferentiated cells B) Mixed ES cell colony showing some alkaline phosphatase positive undifferentiated cells but also with some differentiation ES cells C) Alkaline phosphatase negative colony comprised of differentiated ES cells.

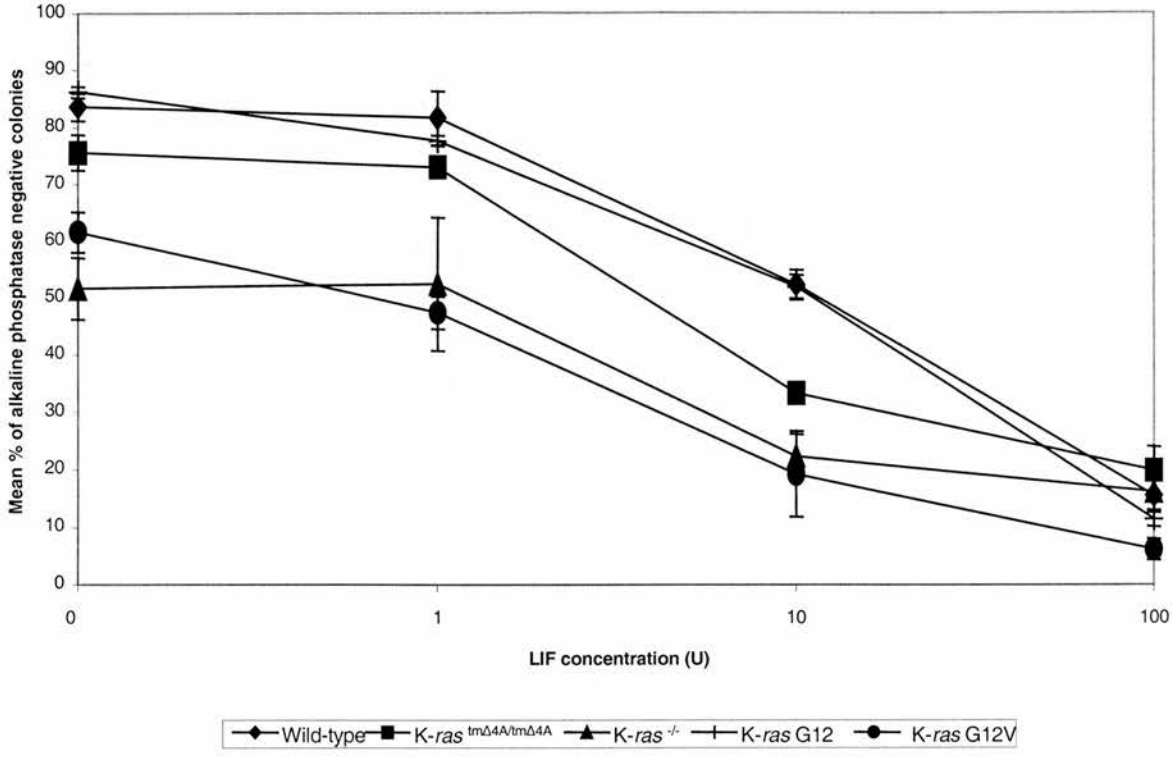

Figure 6.6 Alkaline phosphatase staining of ES cell colonies. The graph shows the percentage of alkaline phosphatase negative colonies present in each genotype after 5 days of growth in the indicated concentrations of LIF. Each data point is representative of three separate samples ± s.e.m. Under normal growth conditions there are no statistically significant differences between genotypes. In the absence of LIF K-*ras* G12 and K-*ras*$^{tm\Delta4A/tm\Delta4A}$ cells are not statistically different from wild-type. However, there are significantly fewer alkaline phosphatase negative colonies for the K-*ras*$^{-/-}$ (P=0.022 *t*-test) and K-*ras*G12V (P=0.008 *t*-test) genotypes compared to wild-type cells. The graph is representative of two experiments, which reproduce the level of sensitivity of the different genotypes examined to complete LIF withdrawal. However, the response to the intermediate concentrations of LIF showed some degree of variability, although overall trends were maintained.

All colonies were counted and scored as described and the number of alkaline phosphatase negative colonies was expressed as a percentage of the total number of colonies for each concentration of LIF used.

In the presence of 100U of LIF the majority of the colonies in all genotypes appeared to be ES cell like, as expected for optimal growth conditions. However, in the absence of LIF K-*ras* was found to be important in ES cell differentiation (Figure 6.6), since under these conditions wild-type, K-$ras^{tm\Delta 4A/tm\Delta 4A}$ and K-*ras*G12 ES cells display similar levels of differentiation, while K-$ras^{-/-}$ ES cell colonies maintain a much greater level of alkaline phosphatase activity, indicative of less differentiation. As K-$ras^{tm\Delta 4A/tm\Delta 4A}$ ES cells respond like wild-type ES cells the result indicates that the presence of the K-*ras* 4B isoform is sufficient to maintain a wild-type like response to LIF withdrawal. Thus, ES cell differentiation in the absence of LIF is controlled at least in part, by K-*ras* 4B. However, the relationship appears to be more complex, since K-*ras* homozygous null ES cells expressing a K-*ras* G12V minigene display a pattern that is similar to K-*ras* homozygous null ES cells.

6.3 Response to apoptotic stimuli

Previous work by this laboratory has found that ES cells lacking K-*ras* are more resistant to apoptosis induced by etoposide, compared to wild-type cells (Brooks *et al.*, 2001). Another investigation reported that K-$ras^{-/-}$ fibroblasts are more resistant to TNF alpha induced apoptosis (Wolfman and Wolfman, 2000). These results suggest that K-*ras* requirement for apoptosis is not a cell type specific phenomenon. In addition, K-*ras* clearly plays an integral role in the induction of apoptosis, since the apoptotic stimuli used to initiate the apoptotic pathway act by different mechanisms (Perkins *et al.*, 2000; Schmitz *et al.*, 2000). However, the role of the individual K-*ras* isoforms in this response is not known. Therefore, in the present study etoposide was used to examine the role of the individual K-*ras* isoforms in apoptosis.

Etoposide inhibits Topoisomerase II and causes major double strand DNA breaks, which lead to apoptosis by the release of cytochrome c from the mitochondria and

activation of Apaf-1 and cleavage of pro-caspase 9 (Perkins *et al.*, 2000). Since, the K-*ras* mutant ES cells under analysis were derived from two different ES cell lines (E14 and HM-1) a preliminary dose response was performed using the two wild-type ES cell lines to ensure that they responded in a similar manner to etoposide treatment. Cells were either untreated, treated with vehicle alone (DMSO), or 5μM or 15μM of etoposide for 24hrs before harvesting. The samples were analysed by flow cytometry for the percentage of events in the population having hypodiploid DNA content, using Vindelov analysis (Vindelov *et al.*, 1983). This dose response showed that the two wild-type parental cell lines E14 and HM-1 underwent similar levels of apoptosis following treatment with etoposide (figure 6.7).

The study was repeated using wild-type, K-$ras^{tm\Delta 4A/tm\Delta 4A}$ (clone 9) and K-*ras* homozygous null ES cells to investigate the role of the individual K-*ras* isoforms in response to etoposide (figure 6.8). K-$ras^{tm\Delta 4A/tm\Delta 4A}$ ES cells underwent less apoptosis in response to etoposide than wild-type and K-$ras^{-/-}$ ES cells, as measured by hypodiploid DNA content. This dose response was repeated using another K-$ras^{tm\Delta 4A/tm\Delta 4A}$ clone (clone 22) derived from the same electroporation which confirmed this result, as did a clone from a separate targeting experiment (clone HM-1 R42 #248/24). In conclusion, the expression of K-*ras* 4A was found to have an important role in the response of ES cell to etoposide treatment. Importantly, the comparison between the responsse of K-$ras^{tm\Delta 4A/tm\Delta 4A}$ ES cells and that of the K-$ras^{-/-}$ ES cells suggests that this reduced sensitivity to etoposide treatment results from an alteration of the balance between the expression of the K-Ras 4A and 4B isoforms.

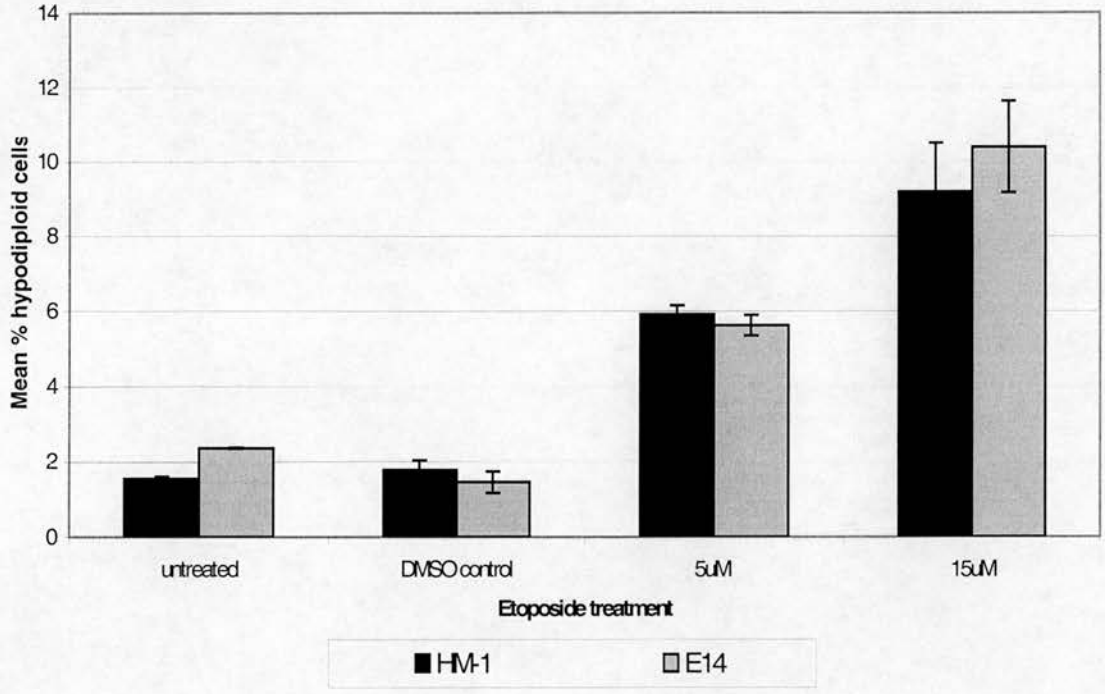

Figure 6.7 Induction of apoptosis in wild-type ES cells in response to etoposide treatment. The cells were either untreated, cultured in the presence of vehicle control (DMSO 0.02%) or with etoposide at the indicated concentrations for 24 hours before harvesting for analysis by flow cytometry using Vindelov analysis. The mean percentage of hypodiploid events for duplicate samples ± s.e.m. is shown.

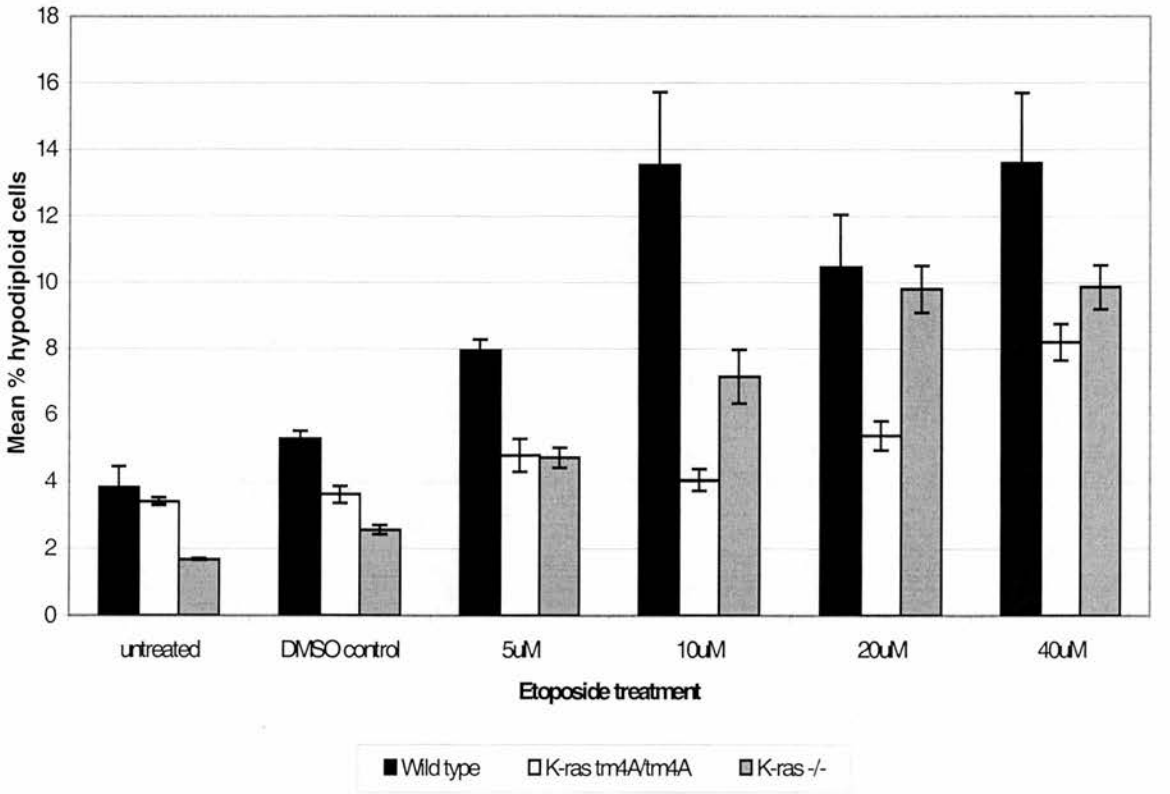

Figure 6.8 Induction of apoptosis in wild-type, K-*ras*$^{tm\Delta4A/tm\Delta4A}$ and K-*ras*$^{-/-}$ ES cells in response to etoposide treatment. The ES cells were cultured in the presence of etoposide at the indicated concentrations for 24 hours before harvesting for analysis by flow cytometry. The mean percentage of hypodiploid cells for three replicate measurements ± s.e.m. is shown. There were significantly fewer hypodiploid events detected in K-*ras*$^{tm\Delta4A/tm\Delta4A}$ (P=0.007 and 0.035 *t*-test) and K-*ras*$^{-/-}$ cells (P=0.003 and 0.049 *t*-test) treated with 5μm and 10μm of etoposide respectively compared to wild-type cells. The results are representative of three experiments performed using three different K-*ras*$^{tm\Delta4A/tm\Delta4A}$ clones E14 Δ4A 73/39/9, E14 Δ4A 73/39/22 and HM-1 R42 #248/24.

Following these observations time course studies were performed to examine in more detail the role of the K-*ras* isoforms in apoptosis. To analyse whether alteration of the expression of the K-*ras* isoforms was important for the initiation of apoptosis wild-type, K-*ras*$^{tm\Delta 4A/tm\Delta 4A}$ and K-*ras*$^{-/-}$ cells were treated with 5μM etoposide for 51 hours and analysed at different time points (figure 6.9). Increased apoptosis in wild-type and K-*ras*$^{-/-}$ ES cells (above background levels) was first detectable by hypodiploid analysis following 12-18 hours of treatment with 5μM etoposide. However, in K-*ras*$^{tm\Delta 4A/tm\Delta 4A}$ cells the apoptotic response to etoposide treatment was delayed. An increase in apoptosis above control levels was not detected until after 24 hours of treatment. This was a delay rather than an inhibition of the response, as the percentage of apoptotic events detected did increase over time. Therefore, this result indicates that the balance of expression of the K-Ras 4A and 4B proteins is critical for the proper initiation of apoptosis in response to etoposide treatment.

To determine whether K-*ras* 4A mediated effects were etoposide dose dependent a separate study was performed. A higher concentration of etoposide (20μM) was tested to investigate whether this could overcome the delayed apoptotic response observed in K-*ras*$^{tm\Delta 4A/tm\Delta 4A}$ cells. In the second time course experiment cells were treated with 20μM etoposide for 48 hours. The same genotypes as described above were also analysed in this experiment. Under these treatment conditions K-*ras*$^{-/-}$ ES cells were found to undergo apoptosis more readily than wild-type ES cells. It was also found that the K-*ras*$^{tm\Delta 4A/tm\Delta 4A}$ cells showed an increased level of apoptosis at the higher concentration of etoposide (figure 6.10).

In this experiment the phenotype of the K-*ras*$^{tm\Delta 4A/tm\Delta 4A}$ ES cells was partially overcome by the increased etoposide concentration, suggesting that the absence of K-Ras 4A and the change in the balance of expression of the K-*ras* isoforms had a reduced effect under these circumstances. Thus, higher concentrations of etoposide may induce apoptosis by a different mechanism that is not dependent upon K-Ras expression.

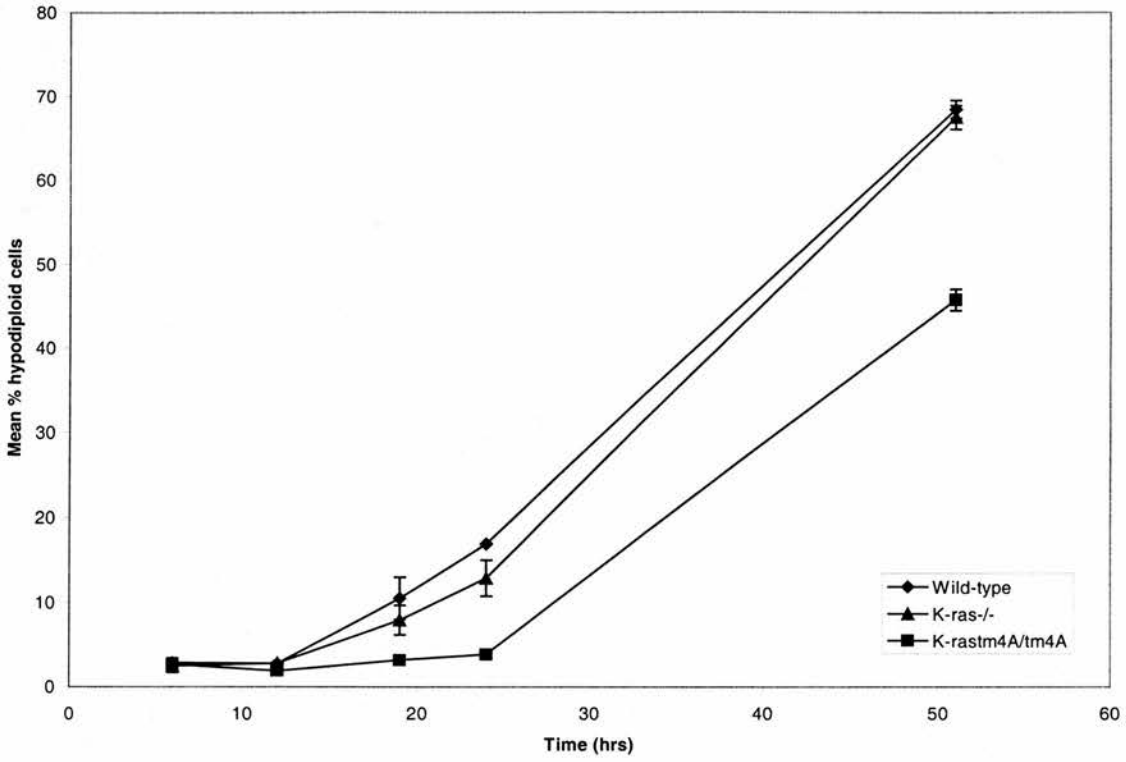

Figure 6.9 Induction of apoptosis in response to etoposide over time. ES cells were cultured in the presence of 5 μM etoposide for the indicated times before harvesting for flow cytometry by Vindelov analysis. The mean percentage of hypodiploid cells for duplicate measurements ± s.e.m. is shown. E14 Δ4A 73/39/9 (K-*ras*$^{tm\Delta 4A/tm\Delta 4A}$) ES cells were used for this analysis. Following 24 and 51hrs of treatement there were significantly fewer hypodiploid events in K-*ras*$^{tm\Delta 4A/tm\Delta 4A}$ cells (P=0.008 and 0.033 *t*-test) compared to wild-type cells.

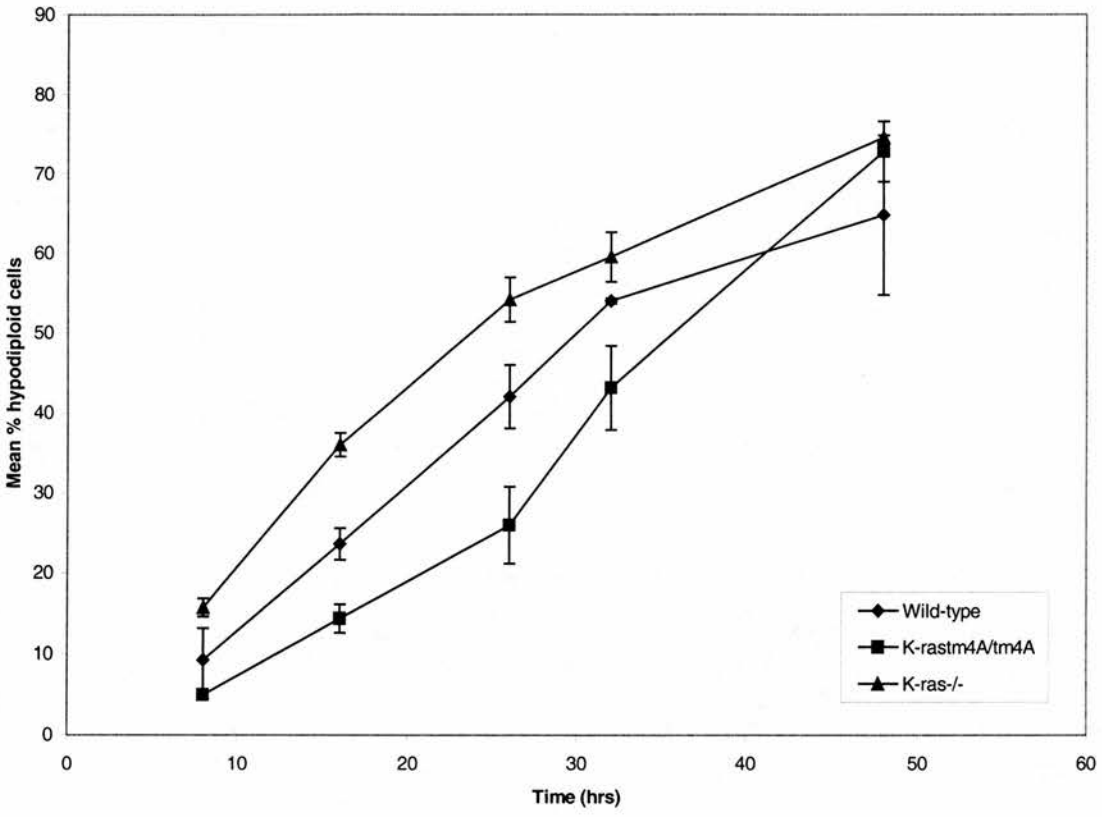

Figure 6.10 Induction of apoptosis in response to etoposide treatment over time. The ES cells were cultured in the presence of 20μM etoposide for the indicated times before harvesting for flow cytometry. The mean percentage of hypodiploid cells for duplicate measurements ± s.e.m. is shown. No significant differences were detected between genotypes analysed. E14 Δ4A 73/39/9 (K-*ras*$^{tm\Delta 4A/tm\Delta 4A}$) ES cells were used for this analysis.

To enabled direct comparison between the different etoposide treatments and to confirm the results of the time course experiments discussed above, a further experiment was performed repeating them in concert. All three genotypes were repeated, but in addition a K-*ras*$^{-/-}$ ES cell line expressing an activated K-*ras* G12V was also included in this study to confirm previous data (Brooks *et al.*, 2001) and to place the K-*ras*$^{tm\Delta 4A/tm\Delta 4A}$ ES cells in relation to this data.

The data reproduced by this analysis confirmed the results of the two earlier studies (figure 6.11). Therefore, under conditions of 5μM etoposide treatment the order of sensitivity to etoposide from the most sensitive is K-*ras* G12V then, wild-type, K-*ras*$^{-/-}$ and K-*ras*$^{tm\Delta 4A/tm\Delta 4A}$ ES cells showing the least sensitivity. Following 20μM etoposide treatment K-*ras*$^{tm\Delta 4A/tm\Delta 4A}$ cells showed a reduced level of apoptosis at 24hrs, but not following 48hrs of treatment, as found previously. Following 48hrs of treatment all the genotypes showed similar levels of apoptosis, except K-*ras* G12V ES cells which were slightly more sensitive.

Whilst the measurement of hypodiploidy is an established technique (Brooks *et al.*, 2001) for identifying apoptosis, it was important to confirm the above results by an independent method. The use of annexin V to detect phosphatidyl serine (PS) is a recognised technique for detecting apoptosis (Koopman *et al.*, 1994). The exposure of PS on the surface of apoptotic cells is a widespread and early event during apoptosis regardless of the initiating stimulus and is important for triggering specific recognition and removal by macrophages (Fadok *et al.*, 1992; Martin *et al.*, 1995).

A)

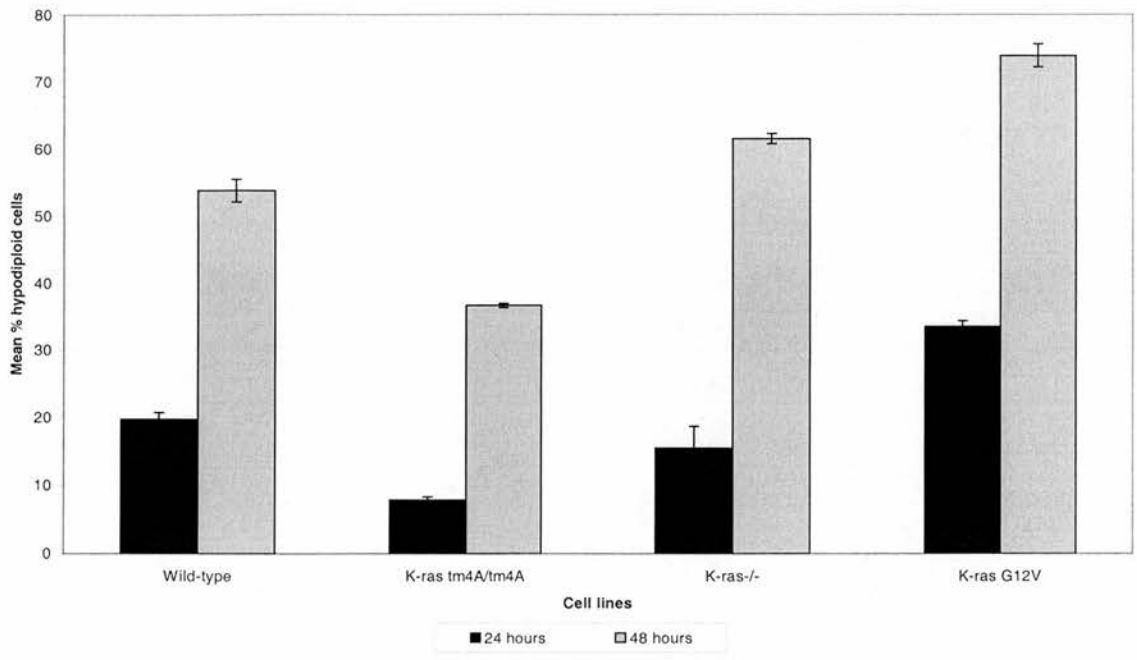

B)

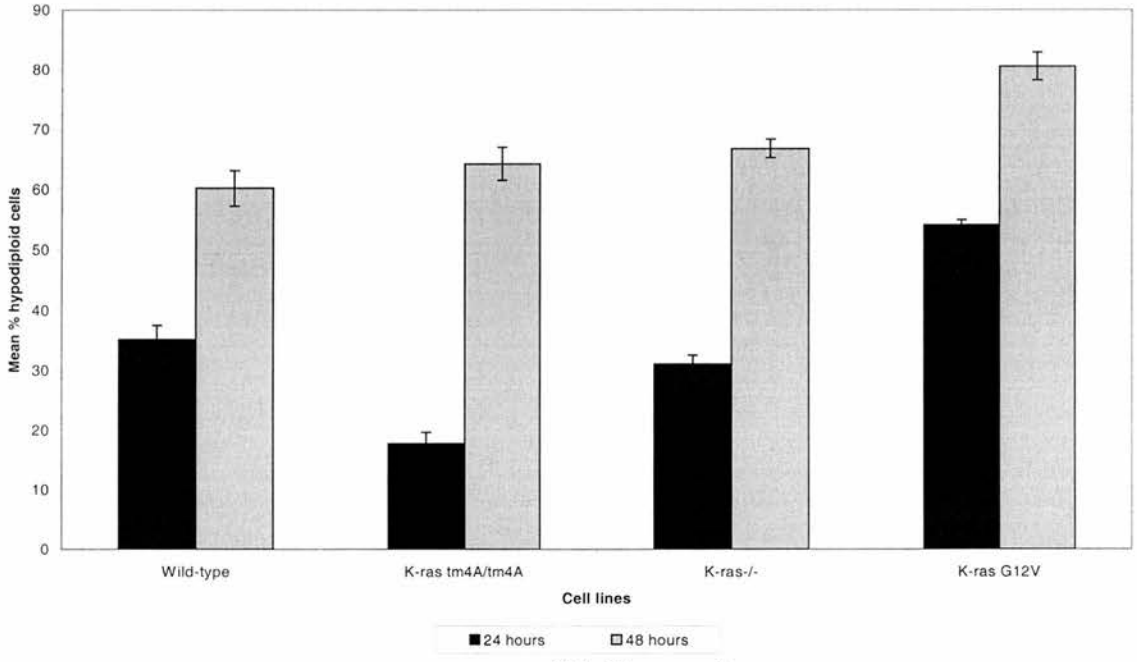

Figure 6.11 Dose responses of wild-type, K-*ras*$^{tm\Delta4A/tm\Delta4A}$, K-*ras*$^{-/-}$ and K-*ras* G12V ES cells to 5μM and 20μM etoposide treatment over time. A) 5μM etoposide for 24 and 48 hours. Following 24 and 48hrs of treatment respectively, K-*ras*$^{tm\Delta4A/tm\Delta4A}$ cells (P=0.001 and 0.006 *t*-test) and K-*ras*G12V cells (P=0.001 and 0.002 *t*-test) were significantly different to wild-type cells. K-*ras*$^{-/-}$ cells were only significantly different from wild-type following 48hrs (P=0.035 *t*-test). B) 20μM etoposide for 24 and 48hrs. Following 24hrs, K-*ras*$^{tm\Delta4A/tm\Delta4A}$ and K-*ras*G12V were significantly different to wild-type (P=0.006 and 0.012 respectively *t*-test). Following 48hrs only K-*ras*G12V cells were significantly different from wild-type (P=0.020 *t*-test). Samples were harvested for analysis by flow cytometry. The mean percentage of hypodiploid cells for triplicate measurements ± s.e.m. is shown. HM-1 R42 #248/24 (K-*ras*$^{tm\Delta4A/tm\Delta4A}$) ES cells were used for this analysis.

The annexin V assay was used in combination with propidium iodide (PI) exclusion. The inclusion of PI staining, which is a marker for necrosis, is necessary since the detection of PS alone does not confirm apoptosis, as in necrotic cells annexin V can detect PS on the inner surface of the plasma membrane, since the cells have lost membrane integrity. The system was initially optimised on wild-type HM-1 ES cells (figure 6.12).

The annexin V and PI exclusion method classifies cells into four categories determined by the staining pattern. 1) Viable cells, which are not positive for either annexin V or PI. 2) Early apoptotic cells, which are positive for annexin V but are still able to exclude PI, as the plasma membrane has not been compromised. 3) Late apoptotic cells, which are positive for annexin V and PI, i.e. membrane integrity has been compromised (this is probably an artefact of the culture system, as under *in vivo* circumstances these cells would be cleared by macrophages before reaching this stage). 4) Necrotic cells, which are those that are only positive for PI, having lost membrane integrity but not undergone the nuclear changes associated with apoptosis. .

This result clearly showed that annexin V positive cells were detectable at 5μM and 20μM etoposide following 24 and 48 hours of treatment. The percentage of annexin V positive cells increased with dose and time, as did the percentage of annexin V/ PI positive cells. Thus, in wild-type ES cells apoptosis is detectable by this method. In this analysis ~60% of the cell population was classified as apoptotic, compared to between 10-20% by hypodiploid DNA analysis. This reflects that the two methods are measuring parameters associated with different stages of apoptosis, since PS exposure is considered to be an early event in apoptosis and hypodiploid DNA content detects a later stage.

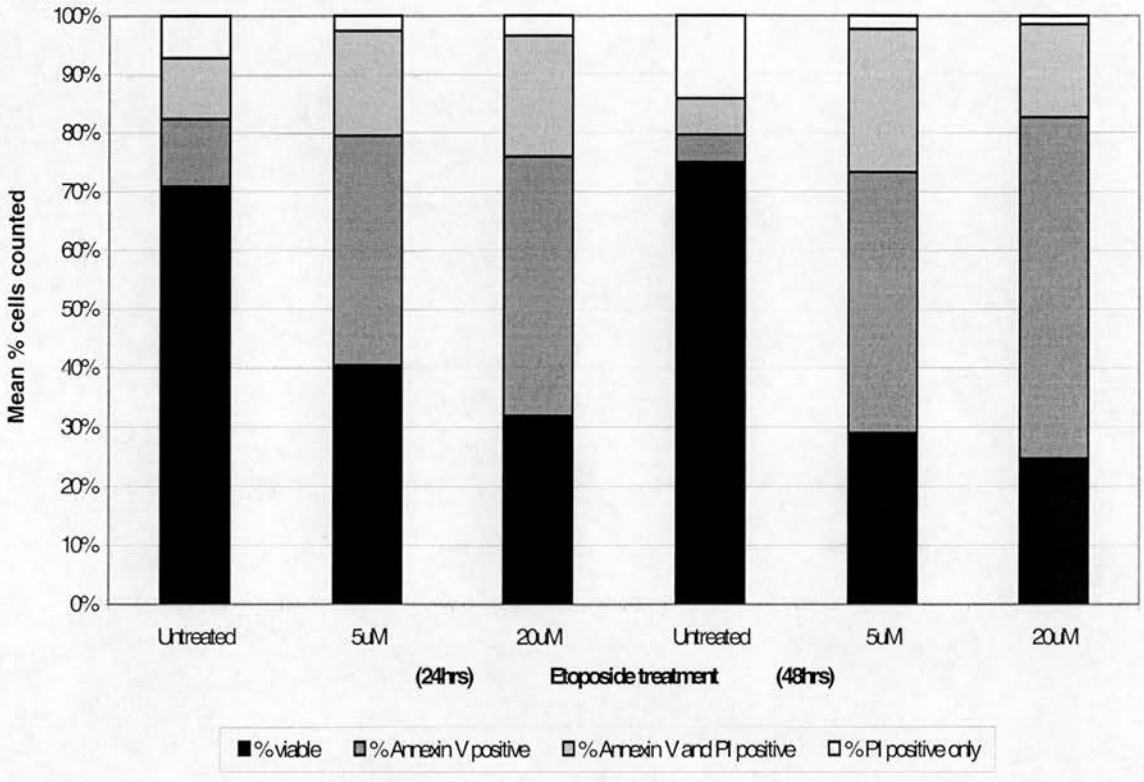

Figure 6.12 Detection of phosphatidyl serine by Annexin V staining. Cells were cultured in the presence of either 5μM or 20μM of etoposide for the indicated times and then harvested for annexin V/propidium iodide staining and detection by flow cytometry. Classification was as follows: viable, no staining; early apoptotic, annexin V staining; late apoptotic, annexin V and propidium iodide staining; and necrotic, propidium iodide staining alone.

This experiment was repeated in triplicate with wild-type, K-*ras*$^{tm\Delta 4A/tm\Delta 4A}$, K-*ras*$^{-/-}$ and K-*ras* G12V ES cells and a representative result shown in figure 6.13. Apoptosis is detectable by the presence of annexin V positive cells following treatment with etoposide. However, the detection of PS by annexin V does not reproduce the order of sensitivity to etoposide seen by hypodiploid DNA analysis of these genotypes. A study of the number of viable cells following treatment with 5μM etoposide, suggests that K-*ras*$^{-/-}$ ES cells are the most sensitive to etoposide, followed by K-*ras* G12V and wild-type ES which show very similar levels of viable cells, and finally the K-*ras*$^{tm\Delta 4A/tm\Delta 4A}$ ES cells are least sensitive. In one experiment samples were also taken for hypodiploid DNA analysis, to determine whether the data could be reproduced if the experiments were performed on the same cell populations. The hypodiploid data confirmed the results of previous experiments (data not shown), but the annexin V data gave the same pattern as shown in figure 6.13. It should be noted that the annexin V/PI populations more closely represent the hypodiploid data, suggesting that those parameters are more closely associated. In conclusion, the detection of PS by annexin V does not reproduce the hypodiploid DNA data, but analysis of annexin V/PI positive data does more closely reproduce this data.

The reasons for this discrepancy are unclear, but a possible hypothesis is as follows: PS exposure is an early event in the apoptotic process and precedes the loss of mitochondrial transmembrane potential and release of cytochrome c, both of which occur before late apoptotic events (Denecker *et al.*, 2000). Therefore, if K-*ras* is important for the initiation of mitochondrial events, or the events immediately downstream of this, early apoptotic events, such as PS externalisation may be able to occur as normal, but then there may be a delay in the continuation of the process.

A)

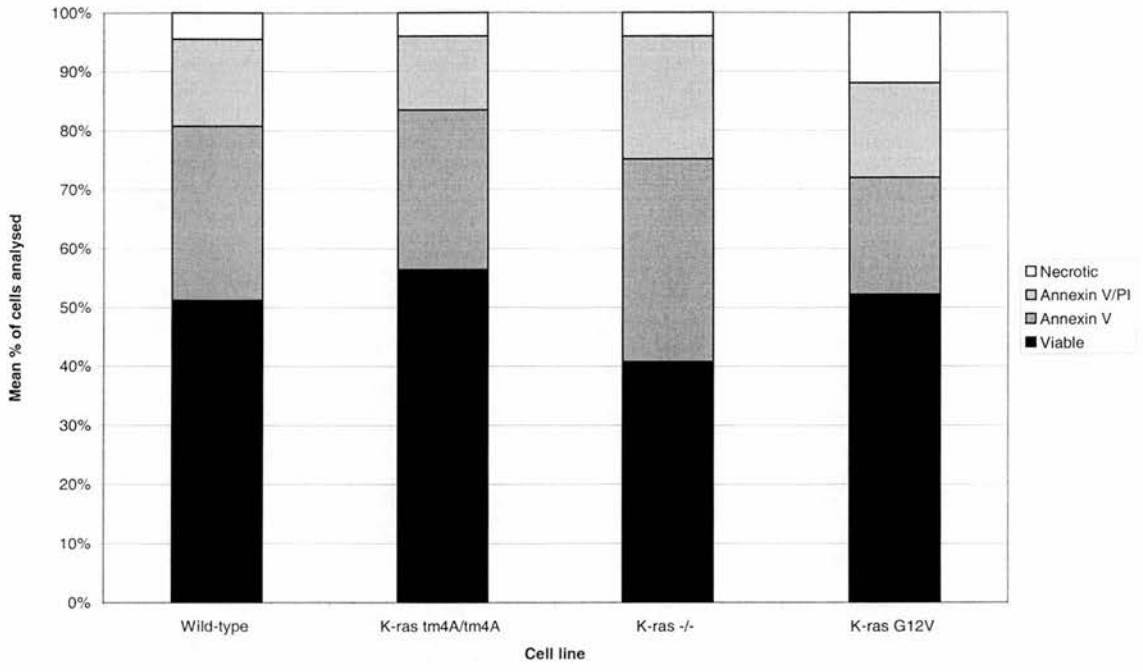

B)

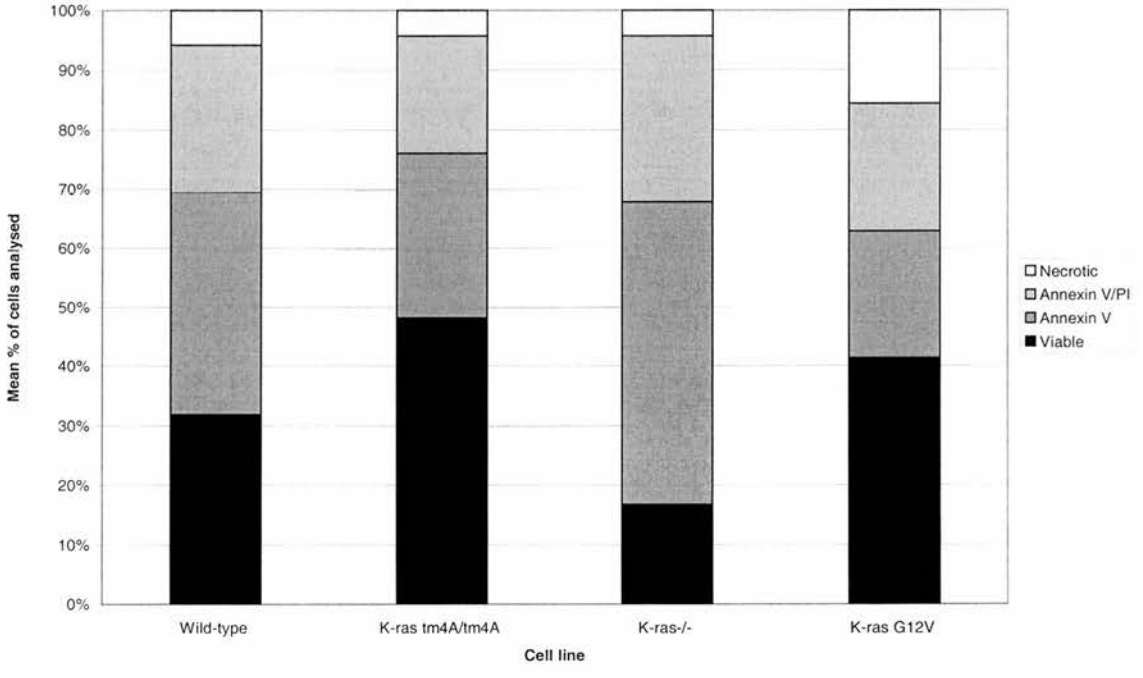

Figure 6.13 Detection of phosphatidyl serine by Annexin V in wild-type, K-*ras*$^{tm\Delta4A/tm\Delta4A}$, K-*ras*$^{-/-}$ and K-*ras* G12V ES cells. The ES cells were treated with either A) 5μM or B) 20μM of etoposide for 18 hours and then harvested for analysis by flow cytometry. Cells were stained with annexin V and propidium iodide. The mean percentages for three replicate samples of viable, annexin V positive, annexin V positive/PI positive and PI positive cells are shown. The graph is representative of three independent experiments.

Due to the discrepancy between the annexin V and hypodiploid data a third method of detecting apoptosis was sought. Analysis of morphological changes is the most direct way of assessing the occurrence of classical apoptosis, since the process is defined by the identification of these changes (Kerr *et al.*, 1972). This method was also attractive since these are also end stage changes and would allow easier comparison with the hypodiploid data. This would confirm that the hypodiploid DNA content was a direct consequence of the formation of apoptotic bodies rather than nuclear abnormalities such as, chromosome loss or the occurrence of a non-apoptotic type of cell death.

Immunofluorescent analysis of morphological changes consistent with apoptosis was performed using Hoechst 33342 and PI staining. This technique was optimised using wild-type ES cells that had been treated with 5μM and 20μM etoposide for 24 and 48hrs. The cells were classified as follows; 1) viable cells had morphologically normal Hoechst 33342 positive nuclei; 2) apoptotic cells had chromatin condensation and nuclear fragmentation; 3) late apoptotic cells had nuclear changes, but were also positive for PI and finally 4) necrotic cells had no nuclear abnormalities but were positive for PI. The data (not shown) indicated that the level of apoptosis detected measured by morphological changes such as chromatin condensation, and membrane blebbing increased with dose and time.

Having established the technique, wild-type, K-*ras*$^{tm\Delta 4A/tm\Delta 4A}$, K-*ras*$^{-/-}$ and K-*ras* G12V ES cells were treated with 5μM and 20μM etoposide for 18hrs and analysed as above, (figure 6.14) and a representative immunofluorescent image of the nuclear morphology observed is shown (figure 6.15). The data supported the overall trends detected by hypodiploid DNA analysis. K-*ras*$^{tm\Delta 4A/tm\Delta 4A}$ ES cells were scored as mainly viable under both treatment conditions. K-*ras* G12V cells had the greatest percentage of apoptotic nuclei followed by wild-type, K-*ras*$^{-/-}$ and finally K-*ras*$^{tm\Delta 4A/tm\Delta 4A}$ ES cells when treated with 5μM etoposide for 18 hours. When treated with 20μM etoposide for 18 hours the level of viability is still greatest in K-*ras*$^{tm\Delta 4A/tm\Delta 4A}$ ES cells, followed by wild-type, K-*ras*$^{-/-}$ and finally K-*ras* G12V ES cells. Importantly, this study demonstrated that the results from the hypodiploid analyses were indeed indicative of apoptosis.

A)

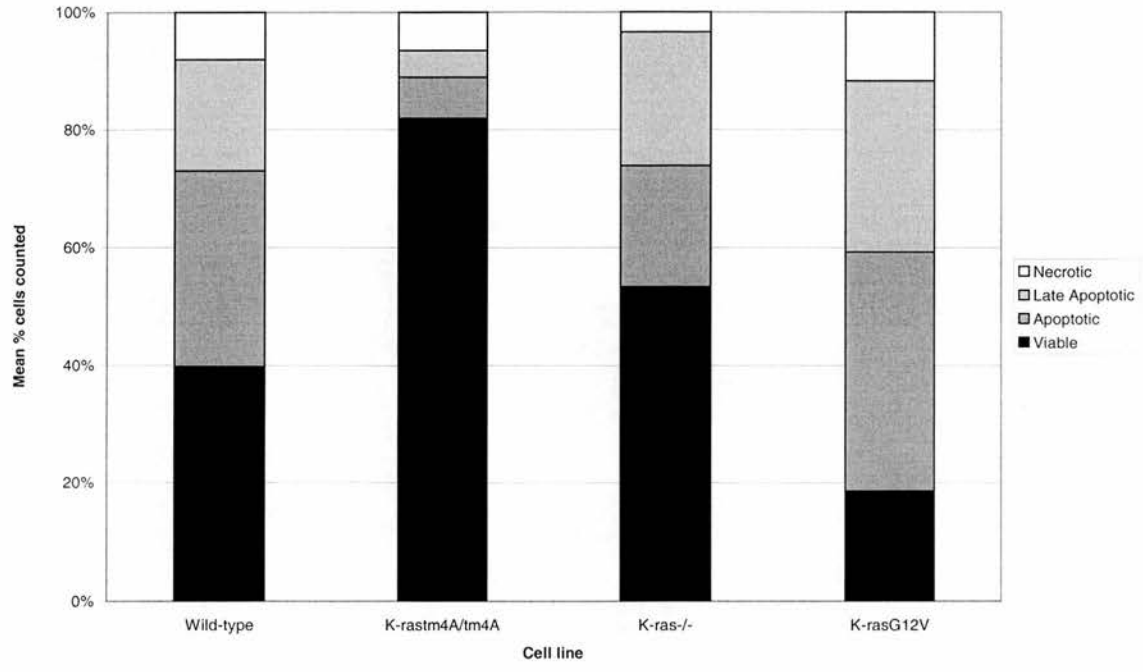

B)

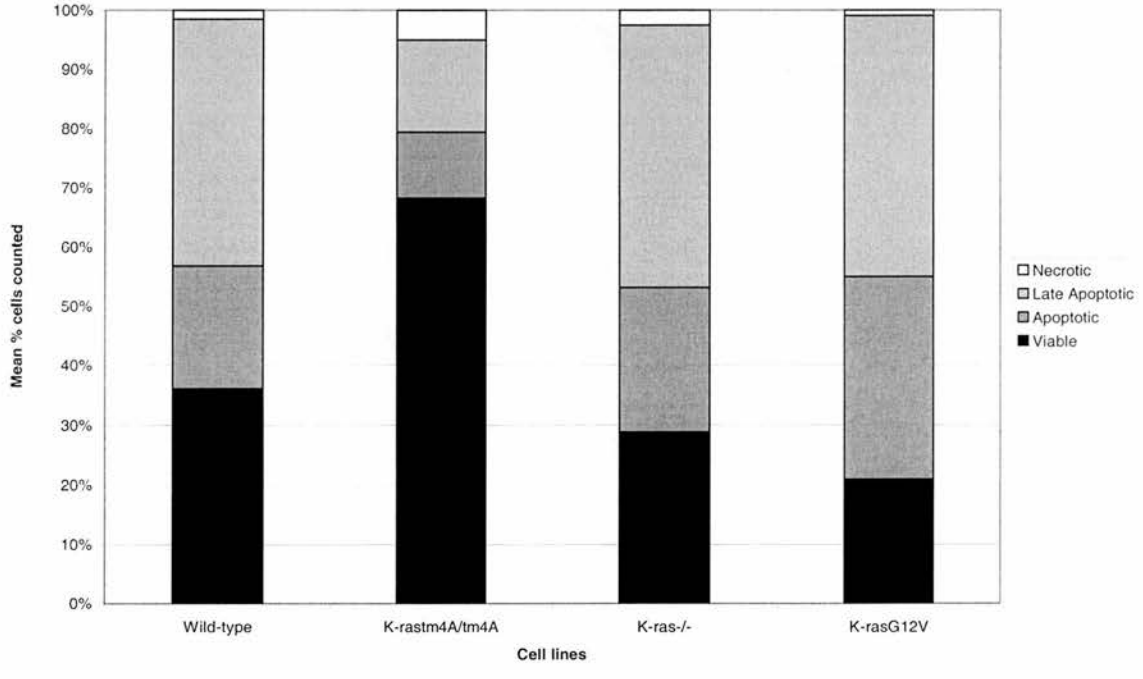

Figure 6.14 Immunofluorescent detection of apoptosis. Morphological analysis by immunofluorescent detection with Hoechst 33342 and propidium iodide. A) 5μM etoposide for 18hrs. There were significantly fewer apoptotic nuclei observed in K-*ras*$^{tm\Delta4A/tm\Delta4A}$ (P=0.022 *t*-test) than in wild-type cells. B) 20μM etoposide for 18hrs. The data represents the mean of three samples. The experiment was performed on three separate occasions using three different K-*ras*$^{tm\Delta4A/tm\Delta4A}$ clones E14 Δ4A 73/39/9, E14 Δ4A 73/39/22 and HM-1 R42 #248/24.

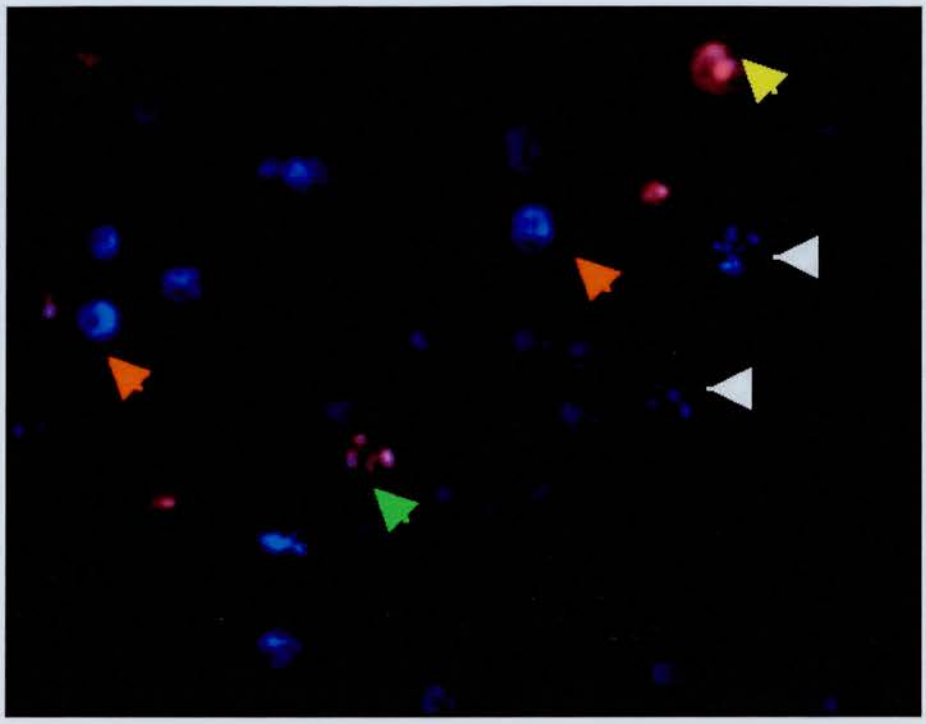

Figure 6.15. Representative image of immunofluorescent morphological analysis of ES cells following treatment with etoposide. ES cells were counted and classified according to their nuclear morphology and the presence or absence of Hoechst 33342 (blue nuclear stain) and PI immunofluorescence (red cytoplasmic stain), examples are indicated Red arrow = viable, white arrow = apoptotic, green arrow = secondary apoptotic and yellow arrow = necrotic.

6.3.1 Analysis of receptor mediated apoptosis in ES cells

Published data has implicated K-*ras* as an important mediator of TNF alpha-induced apoptosis (Wolfman and Wolfman, 2000). Therefore, since K-*ras* 4A expression was found to be critical for ES cells to undergo appropriate etoposide-induced apoptosis, it was of interest to assess its role in receptor mediated apoptosis induced by TNF alpha and Fas ligand (CD95L). Tumour necrosis factor receptor (TNFR) and CD95 (APO-1/Fas) are members of the TNF/NGF-receptor superfamily. These death receptors are activated by their ligands namely TNF alpha and CD95L (FasL) and are thought to lead to initiation of receptor mediated apoptosis by the formation of the death inducing signalling complex and cleavage of pro-caspase 8 (reviewed Schmitz *et al.*, 2000), thereby initiating apoptosis through a different mechanism from etoposide.

Since ES cells express TNFR (Wuu *et al.*, 1998) wild-type ES cells were treated with TNF alpha to assess dose response and time course of effect. However, TNF alpha treatment failed to induced apoptosis as measured by hypodiploid DNA content (figure 6.16). A further experiment was performed using TNF alpha in the presence of cycloheximide, since this had been shown to cause increased apoptosis in fibroblasts (Wolfman and Wolfman, 2000). However, co-treatment with TNF alpha and cycloheximide did not cause an increase in apoptosis detected by hypodiploid DNA content in wild-type ES cells above control levels (data not shown).

Therefore, Fas monoclonal antibody (MAb) and FasL treatment were also investigated as potential initiators of receptor mediated apoptosis in ES cells. The Fas MAb (Jo2) has been reported to induce apoptosis in ES cells (Zou *et al.*, 2000) at a concentration of 1μg/ml. However, following 24hrs of treatment with 1μg/ml, 2μg/ml or 4μg/ml Fas MAb (Jo2) apoptosis was not detectable above control levels using hypodiploid DNA content as a marker (Figure 6.17). Likewise, treatment with recombinant FasL did not cause an increase in apoptosis above control levels when used at concentrations of 50ng/ml, 100ng/ml and 150ng/ml (data not shown). The reasons for this failure are unclear, but may reflect the use of different ES cell lines and/or culture conditions.

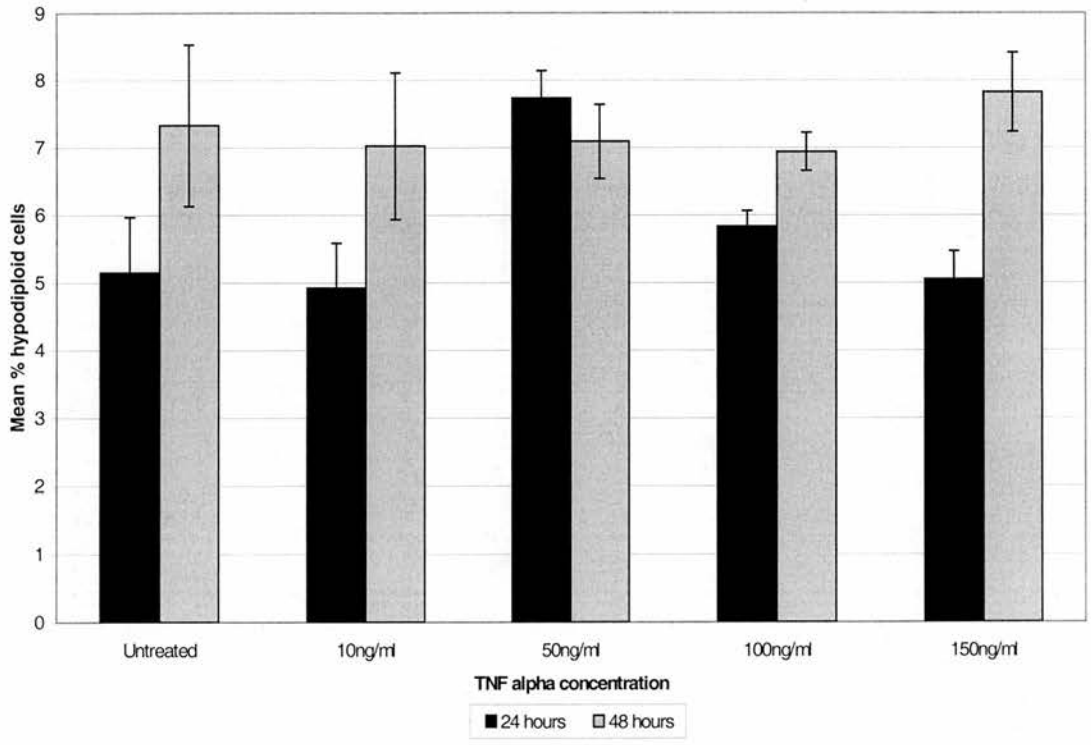

Figure 6.16 Effect of TNF alpha treatment on wild-type ES cells. Represents the response of wild-type ES cells to treatment with TNFα at the indicated concentrations for 24hrs and 48hrs. Following treatment the cells were harvested for analysis by flow cytometry using Vindelov analysis. The data represents the mean of three samples ± s.e.m.

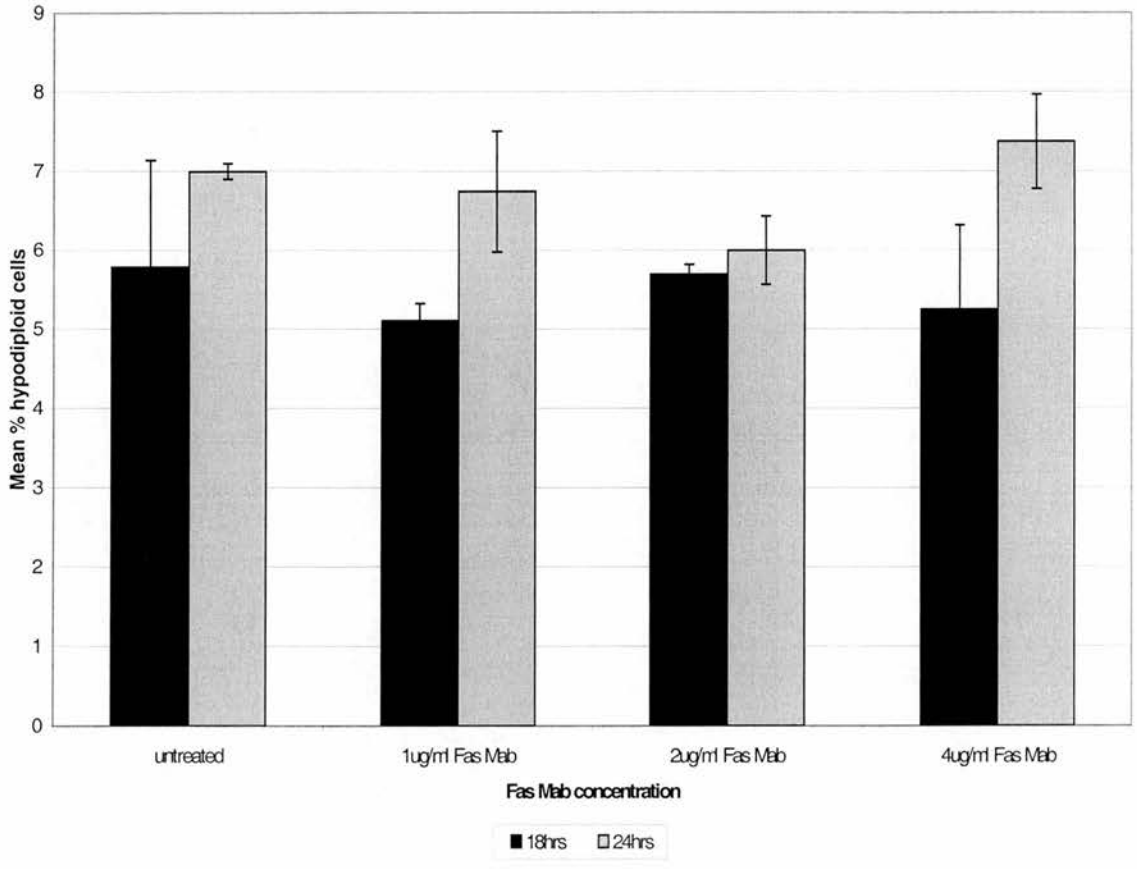

Figure 6.17 Response of wild-type ES cells to Fas MAb treatment. Represents the response of wild-type ES cells following treatment for 18hrs and 24hrs with the concentrations of FasMAb (Jo2) indicated. Following treatment the ES cells were harvested for analysis by flow cytometry using Vindelov analysis. The mean of three samples ± s.e.m. is shown.

6.3.2 Analysis of K-*ras* 4A mRNA levels in response to apoptotic stimuli

While the level of K-*ras* 4A mRNA expression is very low in ES cells compared with the K-*ras* 4B isoform (chapter 3). The ratio of K-Ras 4A and 4B protein isoforms has been shown to be critical for the response of ES cells to etoposide-induced apoptosis. Therefore, it was important to examine the possible mechanisms by which these proteins may be mediating their affects. One avenue of investigation focused on the level of K-*ras* 4A mRNA expression during apoptosis to examine the possibility that K-*ras* 4A mRNA may be up-regulated during early apoptosis.

To test this hypothesis RNA was extracted from wild-type ES cells treated with etoposide for 1, 2, 3, 4, and 8hrs and analysed by RT-PCR using primers in exon 1 and exon 4B (described previously, chapter 3) which amplifying both the K-*ras* 4A and 4B transcripts in the same reaction enabling examination of the isoform ratio. However, the ratio between the K-*ras* 4A and K-*ras* 4B isoforms was clearly not affected by the etoposide treatment (figure 6.18). Therefore, further quantitation of the level of expression of the isoform transcripts was not performed.

The results indicate that K-*ras* 4A mRNA expression is not up-regulation during the early stage of etoposide-induced apoptosis in ES cells, and that it plays an important role in the apoptotic process even though it is expressed at low levels, compared to K-*ras* 4B. However, this result does not exclude the possibility of regulation at the protein level.

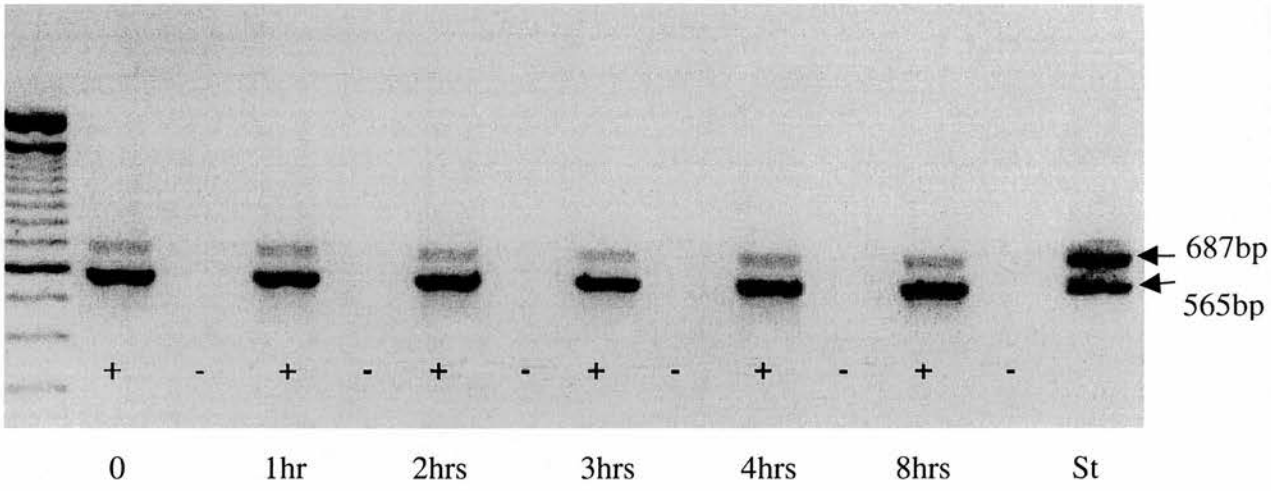

Figure 6.18 Detection of K-*ras* 4A and 4B isoform ratio following treatment with etoposide. ES cells were treated for the times indicated with 5μM etoposide and harvested for RNA extraction. The figure shows the (+) RT PCR product and the (–) RT control showing that DNA contamination is not present and adult wild-type stomach (St) was included as a positive control. All samples contain the 687bp K-*ras* 4A and 565bp K-*ras* 4B products.

6.3.3 Analysis of potential effector pathways mediating K-Ras 4A involvement in apoptosis

Ras proteins have been implicated as key regulators of several signal transduction pathways including the Raf/MAPK, PI-3Kinase and RalGDS pathways (reviewed in Downward, 1998). The Raf/MAPK and PI-3Kinase-PKB/Akt pathways have been particularly intensively studied and have been implicated as regulation of pro- and anti-apoptotic signals (reviewed Downward, 1998). The PI-3Kinase pathway has been shown to mediate survival signals *via* PKB/Akt through the phosphorylation and inactivation of Bad and other pro-apoptotic mediators and Raf/MAPK pathway has been shown to mediate both pro- and anti-apoptotic signals.

Therefore, in order to investigate the mechanisms by which K-Ras 4A mediates such a critical role in apoptosis its role in signal transduction *via* the PI-3Kinase-PKB/Akt and Raf/MAPK pathways were investigated by the use of specific inhibitors of PI-3Kinase (Vlahos *et al.*, 1994) and MEK-1 (Dudley *et al.*, 1995).

K-*ras*$^{tm\Delta4A/tm\Delta4A}$ ES cells when treated with etoposide in the presence of the PI-3Kinase inhibitor LY294002 at 20μM and 50μM had a greater percentage of hypodiploid events than K-*ras*$^{tm\Delta4A/tm\Delta4A}$ cells treated with etoposide alone (figure 6.19). The percentage of hypodiploid events seen with 50μM LY294002 is at least as great as wild-type ES cells treated with etoposide alone. Wild-type ES cells also showed an increase in apoptosis when co-treated with etoposide and 50μM LY294002; this could reflect a general sensitivity of ES cells to inhibition of the PI-3Kinase pathway, which has been reported recently (Jirmanova *et al.*, 2002). Since, the increased apoptosis detected in wild-type ES cells does not account for the total increase observed in K-*ras*$^{tm\Delta4A/tm\Delta4A}$ ES cells the result indicates that expression of K-*ras* 4A may be important for counteracting cell survival signals generated by the PI-3Kinase pathway in ES cells.

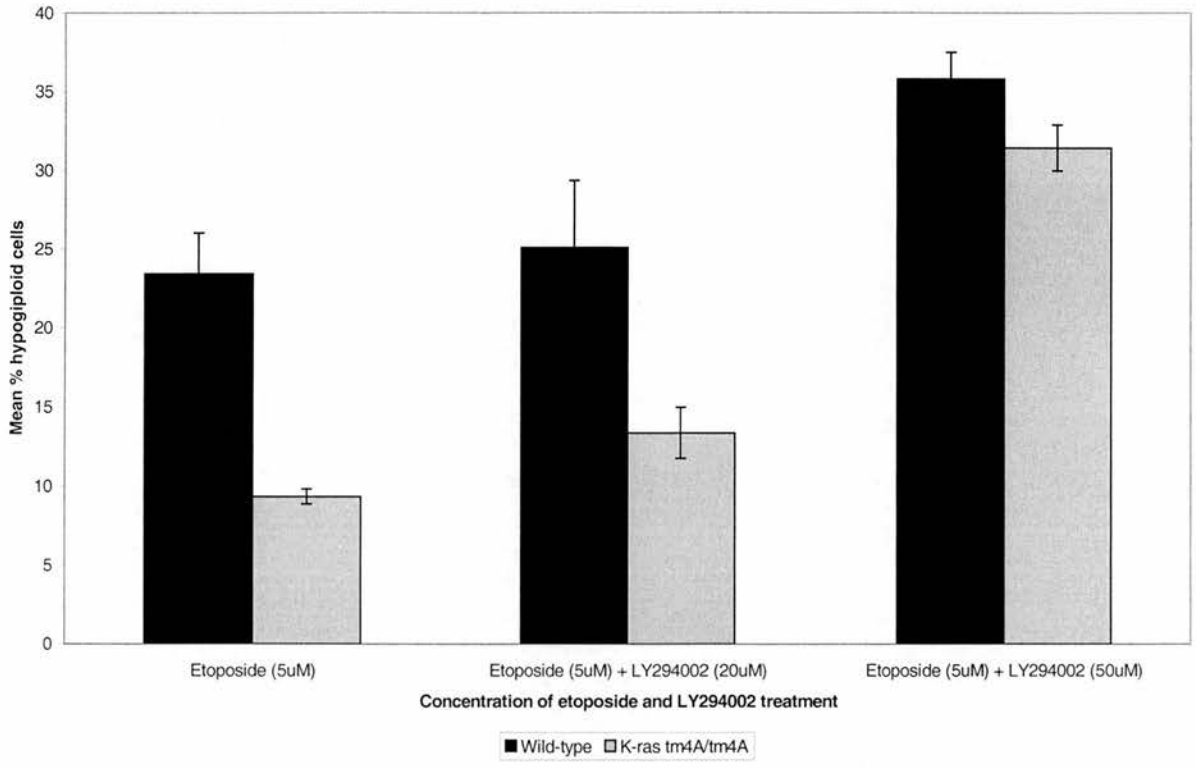

Figure 6.19 Effect of the PI-3Kinase inhibitor on ES cell response to etoposide. Response of wild-type and K-*ras*$^{tm\Delta 4A/tm\Delta 4A}$ ES cells to 5μM etoposide treatment for 18hrs either alone or in the presence of the PI-3Kinase inhibitor LY294002, which was added to cells at the concentrations indicated. The data points represent the mean hypodiploid events of three data sets. There was significantly more apoptosis detected in K-*ras*$^{tm\Delta 4A/tm\Delta 4A}$ ES cells (P=0.003 *t*-test) following treatment with 50μm LY294002 compared to cells treated with etoposide alone. However, this was also true for wild-type ES cells (P=0.011 *t*-test). The graph shown here is representative of two experiments using two different K-*ras*$^{tm\Delta 4A/tm\Delta 4A}$ clones E14 Δ4A 73/39/9 and HM-1 R42 #248/24.

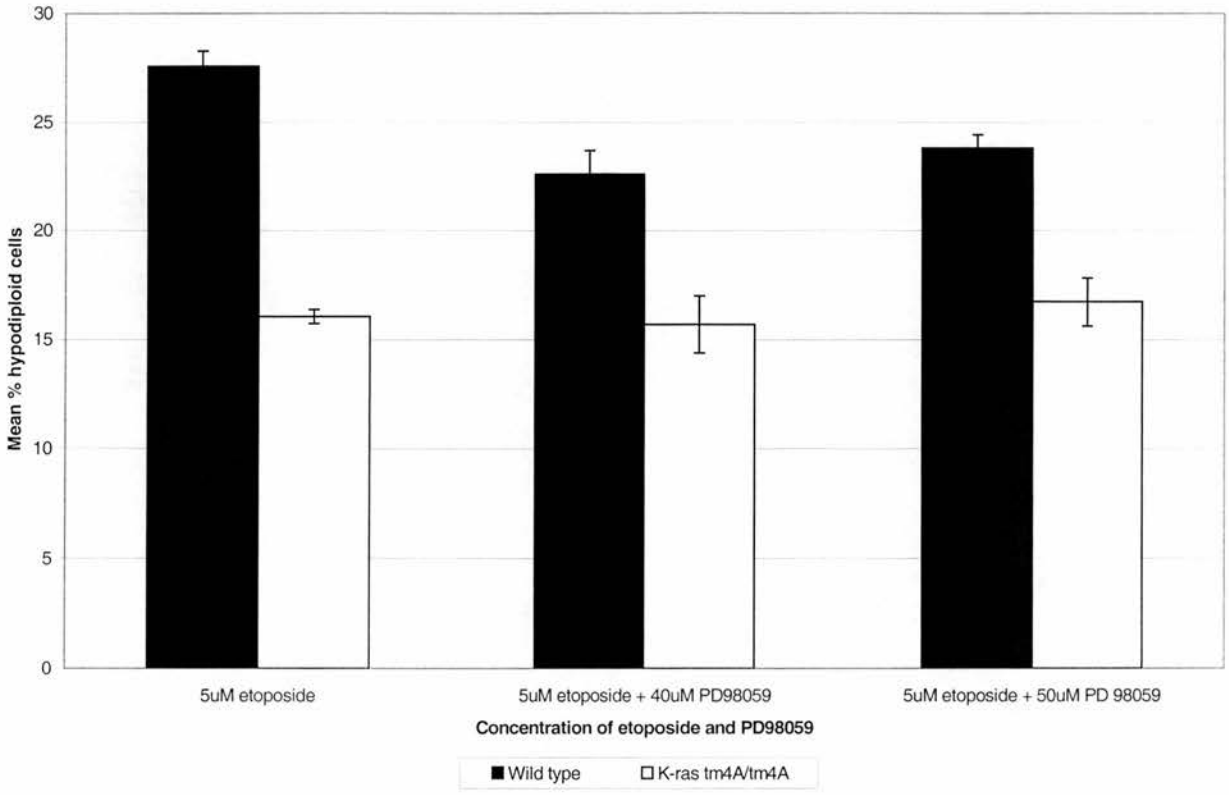

Figure 6.20 Effect of the MEK inhibitor on ES cell response to etoposide. Response of wild-type and K-*ras*$^{tm\Delta 4A/tm\Delta 4A}$ ES cells to 5μM etoposide treatment either alone or in the presence of increasing concentrations of the MEK inhibitor PD98059 as indicated for 18hrs. The data points represent the mean of three data sets ± s.e.m. The graph shown here is representative of two experiments using two different K-*ras*$^{tm\Delta 4A/tm\Delta 4A}$ clones, E14 Δ4A 73/39/9 and HM-1 R42~248/24. While the response of wild-type ES cells was significantly different to K-*ras*$^{tm\Delta 4A/tm\Delta 4A}$ ES cells under all conditions (P=0.003, 0.016 and 0.004 respectively, *t*-test). Treatment with both 40μm and 50μm PD98059 resulted in a significant decrease in the amount of apoptosis detected in wild-type ES cells (P=0.018 and 0.040 respectively, *t*-test), but not in K-*ras*$^{tm\Delta 4A/tm\Delta 4A}$ ES cells (P=0.771 and 0.551 respectively, *t*-test).

In contrast, co-treatment with etoposide and the MEK inhibitor PD98059 resulted in a different response to that seen with the PI-3Kinase inhibitor (figure 6.20). In wild-type ES cells co-treatment with PD98059 and etoposide resulted in less apoptosis than treatment with etoposide alone. However, the observed reduction did not decrease the level of apoptosis to that seen in K-*ras*$^{tm\Delta4A/tm\Delta4A}$ ES cells. The level of apoptosis observed in K-*ras*$^{tm\Delta4A/tm\Delta4A}$ cells was not affected by co-treatment with PD98059 and etoposide, compared to etoposide alone. These findings indicate that K-*ras* 4A may mediate some of its effect through the MAPK pathway, although clearly other pathways are involved, since inhibition of MEK in wild-type ES cells did not cause the same level of resistance to etoposide observed in K-*ras*$^{tm\Delta4A/tm\Delta4A}$ ES cells. In conclusion, the data suggest that the altered balance of expression of the K-Ras 4A and 4B proteins may result in reduced pro-apoptotic and increased anti-apoptotic signal transduction in these cells following etoposide treatment resulting in an inappropriate response to apoptotic stimuli.

6.4 Discussion

Gene targeting studies and mutational analyses indicate that K-*ras* plays an important role in development and tumorigenesis. To gain insight as to how K-*ras* may affect these processes, effects on cell proliferation, differentiation and apoptosis were investigated using ES cells harbouring different K-*ras* mutations, including the K-*ras*$^{tm\Delta4A/tm\Delta4A}$ mutation generated in the present study, and ES cells with a homozygous K-*ras* null mutation or K-*ras* null ES cells transfected with minigenes that express, either wild-type K-*ras,* or an activating (G12V) K-*ras* mutation (Brooks *et al.*, 2001). Importantly, K-*ras* mutant ES cells generated by homologous recombination offer a unique and valuable system to analyse the role of K-*ras* and its individual isoforms, since interpretation of the results is not complicated by, either chromosomal abnormalities, or mutations in other genes.

Ras activity is required at multiple points throughout G0/G1 progression until just before entry into S phase for mitogen stimulated quiescent cells to undergo DNA synthesis (Mulcahy *et al.*, 1985; Feig and Cooper, 1988; Cai *et al.*, 1990; Dobrowolski

et al., 1994; Aktas *et al.*, 1997). K-*ras* in particular modulates both positive and negative regulators of the cell cycle; including up-regulation of cyclins A, D3 and E and the E2F transcription factors and down-regulation of $p27^{kip1}$ (Fan and Bertino, 1997). In addition, the fact that K-*ras* homozygous null embryos displayed growth retardation, reduced cell numbers in foetal livers and had smaller hearts (Johnson *et al.*, 1997; Koera *et al.*, 1997) implies that K-*ras* may have a key role in cell proliferation *in vivo*. Therefore, using the ES cell model system it was possible to investigate whether these defects were mirrored by a decreased rate of proliferation *in vitro*. However, comparison between wild-type, K-$ras^{tm\Delta 4A/tm\Delta 4A}$ and K-*ras* homozygous null ES cells demonstrated that K-*ras* is dispensable for cell cycle progression under normal growth conditions. Although this appears to contradict the *in vivo* observations there are several possible explanations for this discrepancy. ES cells, unlike somatic cells, do not exit from the cell cycle following serum withdrawal, but instead continue to proliferate (Schratt *et al.*, 2001). The activation of the immediate early gene (IEG) response by serum response factor (SRF) following signal transduction through the MAPK pathway is dispensable for ES cell growth. Thus, K-*ras* may be dispensable for the growth of ES cells, because they lack normal cell cycle controls and do not require signal transduction *via* the MAPK pathway to proliferate. However, K-*ras* may affect more committed cell types in which these controls exist, since signal transduction *via* MEK is important for ES cell proliferation following differentiation with retinoic acid (Jirmanova *et al.*, 2002) and embryonic abnormalities in K-$ras^{-/-}$ mice are not observed until the onset of organogenesis (Johnson *et al.*, 1997; Koera *et al.*, 1997). Therefore, it would be of interest to investigate proliferation in other cell types with these genotypes. Alternatively, the failure of K-*ras* to influence the growth of ES cells may be because they are cultured under optimal growth conditions. Finally, it is also possible that the reduced cell numbers in foetal liver and thin ventricular walls in K-*ras* homozygous null embryos are due to effects of the K-*ras* mutation upon differentiation or apoptosis rather than proliferation.

In immortalised cell lines, such as the NIH3T3 fibroblasts expression of activated H-, N- and K-*ras* genes causes transformation and deregulated growth (Maher *et al.*, 1995), which is accompanied by shortening of the G1 phase of the cell cycle (Lui *et al.*, 1995; Winston *et al.*, 1996). In contrast, expression of oncogenic *ras* in primary cells resulted in premature G1 cell cycle arrest that resembled senescence. This effect was mediated

via an induction of $p21^{cip1}$ and subsequent inhibition of CDK (Lloyd *et al.*, 1997; Sewing *et al.*, 1997; Woods *et al.*, 1997), accumulation of p53 and $p16^{INK4a}$ (Serrano *et al.*, 1997), alteration in the activity of the members of the RB family (Peeper *et al.*, 2001) and ubiquitin dependent degradation of cyclin D1 (Shoa *et al.*, 2000).

ES cells have the characteristics of an immortal cell line. As such ES cells cycle rapidly and have a short G1 phase with an absence of hypophosphorylated retinoblastoma (Rb) protein, and an apparent reduction in the overall level of this protein following the exit from mitosis (Savatier *et al.*, 1994). In addition, ES cells express very low levels of cyclin E/CDK2 complexes, $p21^{cip1}$ and $p27^{kip1}$ CDK inhibitors (Savatier *et al.*, 1996). Furthermore, over expression of $p16^{INK4a}$, which is associated with activated *ras* induced cell cycle arrest (Serrano *et al.*, 1997) did not cause growth arrest in ES cells (Savatier *et al.*, 1996). Therefore, the effect of the K-*ras* activating mutation was investigated in this cell line to assess the response of a stem cell population.

However, here it was found that expression of the activating K-*ras* G12V mutation did not alter the cell cycle kinetics of ES cells. Thus, the immortalised nature of ES cells was not sufficient to cooperate with the K-*ras* G12V mutation in deregulating the cell cycle and the lack of the normal G1 cell cycle controls in ES cells, which are present in more differentiated cell types, may account for the absence of cellular senescence in K-*ras* homozygous null ES cells over expressing K-*ras* G12V.

Differentiation has been identified as a Ras regulated process in several studies. The differentiation of F9 embryonal carcinoma cells into primitive endoderm (PrE) and then to parietal endoderm (PE), was demonstrated to be a *ras* dependent process (Verheijen *et al.*, 1999), since differentiation to PrE requires Ras up-regulation and the further differentiation to PE requires down-regulation of Ras. The expression of activated Ras was capable of blocking PrE to PE differentiation (Verheijen *et al.*, 1999). In addition, activated *ras* caused sustained proliferation and failure to differentiate when expressed by a keratin 14 promoter in the basal dermal layers (Dajee *et al.*, 2002), whereas expression of dominant negative *ras* resulted in decreased proliferation and a thin layer of terminally differentiated cells. Activation of the MAPK pathway following cytokine stimulation of the gp130 receptor (Boulton *et al.*, 1994; Ernst *et al.*, 1996; Sheng *et al.*,

1997; Yin and Yang, 1994), suggests that *ras* might be important in the maintenance of ES cell renewal.

The analysis of ES cell differentiation following LIF withdrawal highlighted the importance of K-*ras* for ES cell renewal as assessed by alkaline phosphatase activity (Bernstine *et al.*, 1973). K-$ras^{-/-}$ ES cells were found to have a reduced requirement for LIF, and importantly the reduced level of differentiation was rescued by the introduction of a minigene expressing wild-type K-*ras*. This demonstrated that the phenotype was due to the deletion of K-*ras* rather than, either the selection of a differentiation insensitive clone, or a detrimental effect of the targeting strategy. Importantly, the finding that K-$ras^{tm\Delta 4A/tm\Delta 4A}$ ES cells respond as wild-type cells indicates that the K-*ras* 4B isoform plays a critical role in ES cell differentiation and, therefore, in maintaining stem cell renewal. However, some redundancy is evident in the pathway responsible for exit from the stem cell population, since the K-$ras^{-/-}$ genotype causes only partial insensitivity to LIF. Indeed, this redundancy may explain why K-$ras^{-/-}$ ES cells contribute to tissues in mouse chimaeras (Johnson *et al.*, 1997). Importantly, the failure of these cells to colonise efficiently some lineages; including lung and haematopoietic tissues, support the current *in vitro* findings that K-*ras* has a role in differentiation.

However, the finding that K-$ras^{-/-}$ ES cells are insensitive to LIF withdrawal is difficult to reconcile with the finding that this also applies to ES cells expressing K-*ras* G12V. Importantly, ES cells that express v-H-*ras* also show a reduced requirement for LIF (Ernst *et al.*, 1996). Furthermore, Verheijen and co-workers demonstrated that in ES cells oncogenic Ras induced a PrE-like morphology (Verheijen *et al.*, 1999). Therefore, expression of the activated K-*ras* G12V minigene may be inducing differentiation to a PrE-like morphology, but preventing further differentiation to PE-like cells. Therefore, reduced requirement for LIF in the K-$ras^{-/-}$ ES cells may reflect the need for Ras signalling for differentiation to PrE and in K-*ras* G12V ES cell lines differentiation to PrE, but failure to differentiate further into PE. However, further experiments would be required to identify if the specific markers for these differentiation stages were present.

Previous work by this laboratory reported that ES cells with activating K-*ras* mutations were more susceptible to apoptosis induced by etoposide, whereas cells lacking K-*ras*

were less susceptible (Brooks *et al.*, 2001). Furthermore, K-*ras* homozygous null fibroblasts were also less susceptible to receptor mediated cell death than wild-type fibroblasts (Wolfman and Wolfman, 2000). This suggests that K-*ras* may be an integral component of the apoptotic pathway, as both these types of cell death signal are dependent upon its presence. Research has also indicated that different *ras* genes may have different roles in apoptosis, while K-*ras* appears to promote apoptosis, N-*ras* appears to be important for preventing apoptosis (Wolfman and Wolfman, 2000; Wolfman *et al.*, 2002). Therefore, the role of the individual K-*ras* isoforms was investigated. In the present study apoptosis was measured using flow cytometry and Hoechst 33342 staining, and it was found that the deletion of K-Ras 4A results in an ES cell population with a reduced sensitivity to apoptosis induced by etoposide, compared to wild-type ES cells. At low doses of etoposide apoptosis was not detected in K-$ras^{tm\Delta 4A/tm\Delta 4A}$ ES cells until after 24 hours of treatment, compared to the detection of apoptosis at 18 hours in wild-type ES cells. Indicating that this resistance occurs in the form of a delay in the initiation of this process. Clearly expression of the K-*ras* 4B isoform in these cells is not sufficient for normal apoptotic responses to occur. Furthermore, K-$ras^{tm\Delta 4A/tm\Delta 4A}$ ES cells are less sensitive to etoposide than K-*ras* homozygous null ES cells. Importantly, this observation suggests the possibility that the greater sensitivity of K-$ras^{-/-}$ ES cells to etoposide than K-$ras^{tm\Delta 4A/tm\Delta 4A}$ ES cells may result from a skewing of the ratio of K-Ras 4A and 4B protein expression in the K-$ras^{tm\Delta 4A/tm\Delta 4A}$ ES cells, indicating that the control of this balance of expression may determine the apoptotic response.

The DNA damaging agent etoposide acts by inhibiting topoisomerase II, which results in double-strand breaks that are lethal to the cell. Induction of apoptosis by this agent has been shown to result in cytochrome c release from the mitochondria by two distinct mechanisms, which are determined by the concentration of etoposide used (Robertson *et al.*, 2000). Since, caspase inhibitors can prevent cytochrome c release caused by low, but not high doses of etoposide this could in part explain the finding that the delay in the initiation of apoptosis shown by K-$ras^{tm\Delta 4A/tm\Delta 4A}$ cells was evident only when treated with the lower dose of etoposide. Therefore, K-*ras* 4A may play a role in the caspase-dependent release of cytochrome c from the mitochondria or steps immediately downstream of this in response to etoposide treatment.

Therefore, the presence of the K-*ras* gene products are essential for proper apoptotic responses when cells are exposed to DNA damaging agents such as etoposide. This data indicates that K-*ras* functions as a protective mechanism by which to clear cells with DNA damage. Over-expression of an activated K-*ras* G12V minigene in K-*ras*$^{-/-}$ cells confirmed this, since elevated levels of apoptosis were detected when these cells were challenged with etoposide, compared to wild-type ES cells. This result confirms the previously published data (Brooks *et al.*, 2001). However, it was important to note that there was no increase in apoptosis under normal growth conditions, as published data has shown that the introduction of an activated *ras* gene can promote cell death without other stimuli in certain cell types (Shao *et al.*, 2000).

The data indicates that K-*ras* 4A/4B ratio plays a crucial role in the initiation of apoptosis. Therefore, in order to investigate the underlying mechanisms K-*ras* 4A mRNA levels were examined to assess whether the induction of apoptosis was preceded by an up-regulation. However, no alteration in the level of K-*ras* 4A mRNA was apparent up to 8 hours after etoposide treatment. However, since this does not address the question of possible increased protein stability or other such mechanisms of up-regulation these cannot be excluded. Nevertheless, there is no evidence to suggest that K-Ras 4A is up-regulated in relation to K-Ras 4B by a transcriptional method.

To examine further the role of the K-Ras 4A and 4B proteins in apoptosis, signal transduction *via* the PI-3K and MAPK pathways was analysed using specific inhibitors. These pathways have been implicated in Ras mediated signal transduction effects upon apoptosis (reviewed Downward *et al.*, 1998). The PI-3Kinase pathway mediates anti-apoptotic signals (Kauffmann-Zeh *et al.*, 1997; Xue *et al.*, 2000), whereas the Raf/MAPK pathway can mediate, either pro- or anti-apoptotic effects depending upon the cell type and apoptotic stimulus (Kauffmann-Zeh *et al.*, 1997; Xue *et al.*, 2000). The results presented indicated that there are two apparently paradoxical mechanisms involved. However, this effect is not entirely without precedent, as in fibroblasts and rat thyroid cell activated Ras caused both survival signals from PI-3Kinase and pro-apoptotic signals *via* the Raf/MAPK pathway (Kauffmann-Zeh *et al.*, 1997; Cheng and Meinkoth, 2001) clearly demonstrating that the outcome of apoptotic signals is dependent on the synergistic effect of these signal transduction pathways determining

the cell fate. In this context, it appears that expression K-*ras* 4A may be needed to signal *via* the MAPK pathway to promote apoptosis, since the MEK inhibitor caused a reduction in apoptosis in wild-type ES cells, but not in K-$ras^{tm\Delta 4A/tm\Delta 4A}$ ES cells when co-treated with etoposide. However, it is clear that this is only partly responsible for the effects mediated by K-Ras 4A, as the MEK inhibitor does not inhibit apoptosis to the same extent as the absence of the K-*ras* 4A gene. Conversely, co-treatment with etoposide and the PI-3Kinase inhibitor LY294002 caused an increase in apoptosis in K-$ras^{tm\Delta 4A/tm\Delta 4A}$ ES cells, suggesting that K-*ras* 4A may be needed to act as an antagonist to this pathway. However, this observation was complicated by the increased apoptosis detected in wild-type ES cells with this co-treatment, which although not as great, suggested that these observations may reflect a general sensitivity of ES cells to inhibition of the PI-3Kinase pathway, which has been reported recently (Jirmanova *et al.*, 2002). Therefore, further analysis is required to determine the involvement of K-Ras 4A in PI-3Kinase signal transduction. However, this preliminary analysis of these signal transduction pathways suggests a possible mechanism by which perturbation of the K-Ras 4A/4B ratio may result in inappropriate apoptotic responses.

In conclusion, the work presented in this chapter provides a preliminary insight into the differential regulation of cellular functions by the K-Ras protein isoforms, identifying for the first time a critical role for the K-Ras 4A protein in the regulation of apoptosis and cell survival.

Chapter 7

General Conclusions And Future Directions

The data presented in this thesis represents an investigation into the role of the K-*ras* isoforms in development and neoplasia. This took the form of identifying differential roles for the K-*ras* isoforms, which may in part explain the high incidence in tumours of mutations in K-*ras* relative to mutations in other members of the *ras* family.

The aim was achieved by examination of K-*ras* expression in human tumours and mouse embryos using isoform specific antibodies, and by analysing targeted ES cells harbouring K-*ras* gene mutations. The K-$ras^{+/tm\Delta 4A}$ ES cells were generated during the course of the present work by homologous recombination, following electroporation of the pPTKiNKiΔ4A targeting vector. ES cells homozgous for the mutation, K-$ras^{tm\Delta 4A/tm\Delta 4A}$, were derived from heterozygous cells by high G418 selection. Importantly, K-$ras^{tm\Delta 4A/tm\Delta 4A}$ ES cells continued to express the K-*ras* 4B isoform. Comparative analyses between wild-type and K-*ras* mutant ES cells enabled detailed investigation of the role of the K-*ras* isoforms in cell proliferation, differentiation and apoptosis. It was found that K-*ras* was dispensible for cell proliferation, and that K-Ras 4B was implicated in stem cell renewal and differentiation, and K-Ras 4A in apoptosis. Importantly, the different roles assigned to each isoform were confirmed by analysing K-*ras* mutant clones derived from independent parental ES cell lines. While many past studies have used transformed cell lines to examine the function of K-Ras, the gene targeted ES cells used here have the advantage in that they harbour only defined K-*ras* mutations, and therefore interpretation of the data is not complicated by mutations in other genes.

Expression of the K-*ras* 4B isoform was implicated in ES cell renewal, since while K-$ras^{-/-}$ ES cells showed reduced requirement for LIF K-$ras^{tm\Delta 4A/tm\Delta 4A}$ and wild-type ES cells showed comparable levels. However, these analyses indicated that K-*ras* might exert opposing functions within the processes determining, either stem cell renewal, or differentiation, since expression of activated K-*ras* G12V within K-$ras^{-/-}$ ES cells also

results in a reduced requirement for LIF. Therefore, signal transduction *via* K-*ras* may be important for the maintenance of a stem cell population, but also for signalling stem cells to differentiate following withdrawal of renewal signals. Further analysis of the mechanisms underlying this apparently contradictory regulation could be of value. Since, these findings appear to agree with the observations that the differentiation into primitive endoderm (PrE) requires up-regulation of Ras signal transduction and differentiation of PrE to parietal endoderm (PE) requires down-regulation of this (Verheijen *et al.*, 1999), it would be of interest to analyse whether markers for these differentiation stages are present following withdrawal of LIF. Importantly, since signal transduction *via* MEK has been implicated in regulating stem cell renewal (Burdon *et al.*, 1999), it would be interesting to determine if this involves signal transduction *via* K-*ras*.

ES cell proliferation and cell cycle kinetics were similar regardless of whether they expressed K-*ras*. The introduction of an activated K-*ras* G12V minigene into K-*ras*$^{-/-}$ ES cells confirmed these observations, as constitutive activation of this gene did not deregulate proliferation. Thus, K-*ras* is dispnesible for the proliferation of ES cells. Clearly, the regulation of the cell cycle in ES cells differs from somatic cells; therefore this result does not preclude the involvement of the K-*ras* gene products as critical regulators of the somatic cell cycle, but serves to highlight the importance of investigation of the ES cell cycle. Further investigation is warranted in the light of a recent publication (Jirmanova *et al.*, 2002), which demonstrated that following differentiation of ES cells with retinoic acid (RA) the proliferation of these cells was dependent upon MEK activity. Since, this raises the possibility that proliferation of differentiated cells is dependent upon Ras it would be interesting to determine whether K-*ras* is involved by comparing the proliferation of wild-type and K-*ras* mutant ES cells following treatment with RA.

Previously, it has been reported that K-*ras* expression is important for pro-apoptotic signals in ES cells and fibroblasts (Brooks *et al.*, 2001; Wolfman and Wolfman, 2000). The present study demonstrated that K-*ras* 4A is a key regulator of ES cell apoptosis in response to DNA damage, since K-*ras*$^{tm\Delta 4A/tm\Delta 4A}$ cells were more resistant to apoptosis induced by etoposide. The absence of both K-*ras* isoforms results in a slight decrease in sensitivity, but this is not as marked. Therefore, the expression of the K-*ras* 4B

isoform alone is not sufficient for the cells to respond like wild-type ES cells. Indeed, the lack of K-*ras* 4A expression results in a more dramatic phenotype than the deletion of both K-*ras* isoforms, indicating a possible skewing of the balance between the expression of the isoforms during this process. Therefore, the possibility arises that the pro-apoptotic effects of K-Ras 4A and the possible anti-apoptotic effects of K-Ras 4B may ultimately decide the cellular fate.

Investigation of the mechanisms involved indicated that K-*ras* 4A mRNA was not up-regulated in response to apoptotic stimuli. However, analysis of the signal transduction pathways involved in known Ras pro- or anti-apoptotic responses showed different sensitivity to inhibitors of these pathways in K-$ras^{tm\Delta4A/tm\Delta4A}$ versus wild-type ES cells. The increased apoptosis elicited by the PI-3Kinase inhibitor in K-$ras^{tm\Delta4A/tm\Delta4A}$ cells, suggested that this pathway may be over stimulated in these cells, explaining at least part of the reduced sensitivity of these cells to DNA damage. The decreased apoptosis elicited by the MEK inhibitor in wild-type, but not K-$ras^{tm\Delta4A/tm\Delta4A}$ ES cells, indicated that K-*ras* 4A might be important for signal transduction *via* the MAPK pathway in response to DNA damage. These observations while appearing contradictory are supported by data from effector mutant studies, which show that the Ras proteins can activate both the PI-3Kinase and MAPK pathway in response to apoptotic stimuli and that the balance of this activation determines the cellular response (Kauffman-Zeh *et al.*, 1997; Cheng and Meinkoth, 2001). In the light of these observations it would be of interest to investigate further the pathways involved in K-Ras 4A mediated apoptosis. These analyses could address several further questions; including whether the level of activity of the downstream effectors of the Raf/MAPK and PI-3Kinase are altered in response to etoposide treatment. This investigation would clarify whether the effects observed with the pathway inhibitors reflected a genuine alteration in the level of activity associated with these signal transduction pathways in the K-$ras^{tm\Delta4A/tm\Delta4A}$ cells in response to etoposide treatment, compared to wild-type cell. Furthermore, since K-Ras 4A appears to be important for the initiation of apoptosis in response to low, but not high doses of etoposide, analysis of caspase activation in these cells could provide useful insight into the underlying mechanisms involved in K-Ras 4A control of apoptosis. Since, the apoptotic response to low, but not high doses of etoposide have previously been demonstrated to be caspase dependent (Robertson *et al.*, 2000).

Finally, it may be of interest to examine the level of expression of anti-apoptotic factors, such as Bcl-2 to investigate whether these are inappropriately up-regulated in K-*ras*$^{tm\Delta 4A/tm\Delta 4A}$ ES cells, compared to wild-type cells.

K-*ras* activating mutations occur in approximately 40-50% of colon cancers (Bos *et al.*, 1989). Since, these mutations primarily affect codons 12 or 13 the mutation can affect both isoforms, and therefore both K-Ras 4A and 4B have the potential to contribute to tumours. Analysis of the role of K-*ras* isoforms in cancer was performed by immunohistochemical analysis of the expression patterns of both isoforms in colon tumours, which had been screened previously (published as part of a larger study (Andreyev *et al.*, 1998)) and been shown to contain a mutation in the K-*ras* gene. The results clearly demonstrated that both protein isoforms were expressed in the normal and neoplastic colon. K-Ras 4A inparticular was strongly up-regulated in the neoplastic colon. Therefore, K-*ras* 4A has the potential to be involved in colon tumorigenesis. Importantly, up-regulation was not detected in pre-malignant cervical intraepithelial neoplasia, which is not normally associated with K-*ras* mutations. The fact that both isoforms are expressed in colorectal cancer and therefore have the potential for combined or synergistic interactions may, at least in part, account for the higher incidence of activating K-*ras* mutations, compared to either N- or H-*ras*. This is supported by the present data, which shows that the K-*ras* isoforms are capable of differential regulation of apoptosis and differentiation, but also by previously published data, which demonstrated that the K-*ras* isoforms had different transforming abilities and could activate the downstream signalling molecule Raf with varying efficiencies (Voice *et al.*, 1999).

While studies with cultured ES cells suggest that the different K-*ras* isoforms have distinct roles in differentiation and apoptosis, information about their function in cellular processes *in vivo* is crucial to understanding their contribution to development and tumorigenesis.

In the first step to achieve this goal K-*ras*$^{+/tm\Delta 4A}$ mice were developed as part of this thesis. The mice are viable and show no overt abnormalities at 5 months of age on, either inbred, or outbred backgrounds. Furthermore, analysis of K-*ras*$^{tm\Delta 4A/tm\Delta 4A}$

offspring derived from the mating of the K-*ras*$^{+/tm\Delta 4A}$ animals will provide a unique opportunity to investigate the contribution of each of the isoforms to the developmental phenotype seen in K-*ras* homozygous null animals (Koera *et al.*, 1997: Johnson *et al.*, 1997). Immunohistochemical analysis of developing mouse embryos has shown that K-*ras* 4B is expressed in many cell lineages and is present even at early stages of development, as has RNA analysis (Pells *et al.*, 1997). However, importantly the results detailed in this thesis show that differential regulation of K-Ras 4B protein levels occurs during embryonic and neonatal development. Expression of this protein is closely associated with those tissues that are thought to contribute to the lethality associated with the complete deletion of both K-*ras* gene products, which may have important implication for the developmental phenotype of K-*ras*$^{tm\Delta 4A/tm\Delta 4A}$ mice.

In addition, future analyses of the K-*ras*$^{+/tm\Delta 4A}$ mice will investigate whether the heterozygous deletion of exon 4A results in an altered ratio of expression between the two K-*ras* isoforms. This analysis will be of importance to investigate whether regulatory processes exist *in vivo* to ensure the correct level of K-*ras* 4A mRNA transcription occurs. An absence of regulation and an absence of a phenotype in the K-*ras*$^{+/tm\Delta 4A}$ animals may reflect that a skewing of the balance of expression of these two isoforms is unimportant *in vivo*.

Importantly, while TNF alpha and FasL failed to induce apoptosis in ES cells these agents could be tested on K-*ras*$^{tm\Delta 4A/tm\Delta 4A}$ embryonic fibrobalsts to estalish whether K-Ras 4A has a role in receptor mediated apoptosis.

Should K-*ras*$^{tm\Delta 4A/tm\Delta 4A}$ mice prove to be viable and survive to adulthood it will be possible to examine the importance of this mutaion on cell growth using tissues that normally express high levels of K-*ras* 4A, including intestinal epithelial cells. A crucial role for K-Ras 4A initiating apoptosis could be confirmed in gut epithelial cells following whole body γ-irradiation, where a reduction in apoptosis might be expected. These animals could also be used to analyse the importance of the contribution of K-*ras* 4A to the development of tumours in such tissues, as the lung and colon by carcinogen studies. Since K-*ras* 4A is expressed highly in these tissues (Pells *et al.*, 1997) it is tempting to speculate that under such conditions the incidence of tumour development

may be decreased, compared to wild-type controls if the hypothesised requirement for combined or synergistic activation of both isoforms for tumorigenesis is correct.

Importantly, these data have demonstrated that functional redundancy between the K-Ras protein isoforms does not occur in at least two cellular processes, which has important implications for development and tumorigenesis. Therefore, in conclusion the data presented as part of this thesis has added to the current understanding of the differential regulation of cellular functions by the K-Ras isoforms.

REFERENCES

AKTAS H., CAI H. & COOPER G.M. (1997) Ras links growth factor signaling to the cell cycle machinery via regulation of cyclin D1 and the Cdk inhibitor p27KIP1. *Mol.Cell Biol.* **17**, 3850-3857.

AL MULLA F., GOING J.J., SOWDEN E.T., WINTER A., PICKFORD I.R. & BIRNIE G.D. (1998) Heterogeneity of mutant versus wild-type Ki-ras in primary and metastatic colorectal carcinomas, and association of codon-12 valine with early mortality. *J.Pathol.* **185**, 130-138.

ALESSI D.R., ANDJELKOVIC M., CAUDWELL B., CRON P., MORRICE N., COHEN P. & HEMMINGS B.A. (1996) Mechanism of activation of protein kinase B by insulin and IGF-1. *EMBO J.* **15**, 6541-6551.

ALESSI D.R., DEAK M., CASAMAYOR A., CAUDWELL F.B., MORRICE N., NORMAN D.G., GAFFNEY P., REESE C.B., MACDOUGALL C.N., HARBISON D., ASHWORTH A. & BOWNES M. (1997) 3-Phosphoinositide-dependent protein kinase-1 (PDK1): structural and functional homology with the Drosophila DSTPK61 kinase. *Curr.Biol.* 7, 776-789.

ANDREYEV H.J., NORMAN A.R., CUNNINGHAM D., OATES J.R. & CLARKE P.A. (1998) Kirsten ras mutations in patients with colorectal cancer: the multicenter "RASCAL" study. *J.Natl.Cancer Inst.* **90**, 675-684.

ANTON M. & GRAHAM F.L. (1995) Site-specific recombination mediated by an adenovirus vector expressing the Cre recombinase protein: a molecular switch for control of gene expression. *J.Virol.* **69**, 4600-4606.

APOLLONI A., PRIOR I.A., LINDSAY M., PARTON R.G. & HANCOCK J.F. (2000) H-ras but not K-ras traffics to the plasma membrane through the exocytic pathway. *Mol.Cell Biol.* **20**, 2475-2487.

ARENDS J.W. (2000) Molecular interactions in the Vogelstein model of colorectal carcinoma. *J.Pathol.* **190**, 412-416.

ARENDS M.J., MCGREGOR A.H., TOFT N.J., BROWN E.J. & WYLLIE A.H. (1993) Susceptibility to apoptosis is differentially regulated by c-myc and mutated Ha-ras oncogenes and is associated with endonuclease availability. *Br.J.Cancer* **68**, 1127-1133.

ASHBY M.N. (1998) CaaX converting enzymes. *Curr.Opin.Lipidol.* **9**, 99-102.

AUSTIN S., ZIESE M. & STERNBERG N. (1981) A novel role for site-specific recombination in maintenance of bacterial replicons. *Cell* **25**, 729-736.

BAR-SAGI D. & FERAMISCO J.R. (1985) Microinjection of the ras oncogene protein into PC12 cells induces morphological differentiation. *Cell* **42**, 841-848.

BARBACID M. (1987) ras genes. *Annu.Rev.Biochem.* **56**, 779-827.

BENITO M., PORRAS A., NEBREDA A.R. & SANTOS E. (1991) Differentiation of 3T3-L1 fibroblasts to adipocytes induced by transfection of ras oncogenes. *Science* **253**, 565-568.

BERSTINE E.G., HOOPER M.L., GRANDCHAMP S. & EPHRUSSI B. (1973) Alkaline phosphatase activity in mouse teratoma. *Proc.Natl.Acad.Sci.U.S.A* **70**, 3899-3903.

BOGUSKI M.S. & MCCORMICK F. (1993) Proteins regulating Ras and its relatives. *Nature* **366**, 643-654.

BOLLAG G. & MCCORMICK F. (1991) Regulators and effectors of ras proteins. *Annu.Rev.Cell Biol.* **7**, 601-632.

BOLLAG G. & MCCORMICK F. (1991) Differential regulation of rasGAP and neurofibromatosis gene product activities. *Nature* **351**, 576-579.

BONNI A., BRUNET A., WEST A.E., DATTA S.R., TAKASU M.A. & GREENBERG M.E. (1999) Cell survival promoted by the Ras-MAPK signaling pathway by transcription-dependent and -independent mechanisms. *Science* **286**, 1358-1362.

BOS J.L. (1989) ras oncogenes in human cancer: a review. *Cancer Res.* **49**, 4682-4689.

BOSCH M., GIL J., BACHS O. & AGELL N. (1998) Calmodulin inhibitor W13 induces sustained activation of ERK2 and expression of p21(cip1). *J.Biol.Chem.* **273**, 22145-22150.

BOULTON T.G., STAHL N. & YANCOPOULOS G.D. (1994) Ciliary neurotrophic factor/leukemia inhibitory factor/interleukin 6/oncostatin M family of cytokines induces tyrosine phosphorylation of a common set of proteins overlapping those induced by other cytokines and growth factors. *J.Biol.Chem.* **269**, 11648-11655.

BOYER B., ROCHE S., DENOYELLE M. & THIERY J.P. (1997) Src and Ras are involved in separate pathways in epithelial cell scattering. *EMBO J.* **16**, 5904-5913.

BREWER L.M. & BROWN N.A. (1992) Distribution of p21ras in postimplantation rat embryos. *Anat.Rec.* **234**, 443-451.

BROOK F.A. & GARDNER R.L. (1997) The origin and efficient derivation of embryonic stem cells in the mouse. *Proc.Natl.Acad.Sci.U.S.A* **94**, 5709-5712.

BROOKS D.G., JAMES R.M., PATEK C.E., WILLIAMSON J. & ARENDS M.J. (2001) Mutant K-ras enhances apoptosis in embryonic stem cells in combination with DNA damage and is associated with increased levels of p19(ARF). *Oncogene* **20**, 2144-2152.

BRUGAL G., DYE R., KRIEF B., CHASSERY J.M., TANKE H. & TUCKER J.H. (1992) HOME: highly optimized microscope environment. *Cytometry* **13**, 109-116.

BRUNET A., BONNI A., ZIGMOND M.J., LIN M.Z., JUO P., HU L.S., ANDERSON M.J., ARDEN K.C., BLENIS J. & GREENBERG M.E. (1999) Akt promotes cell survival by phosphorylating and inhibiting a Forkhead transcription factor. *Cell* **96**, 857-868.

BURDON T., STRACEY C., CHAMBERS I., NICHOLS J. & SMITH A. (1999) Suppression of SHP-2 and ERK signalling promotes self-renewal of mouse embryonic stem cells. *Dev.Biol.* **210**, 30-43.

CAI H., SZEBERENYI J. & COOPER G.M. (1990) Effect of a dominant inhibitory Ha-ras mutation on mitogenic signal transduction in NIH 3T3 cells. *Mol.Cell Biol.* **10**, 5314-5323.

CANTOR S.B., URANO T. & FEIG L.A. (1995) Identification and characterization of Ral-binding protein 1, a potential downstream target of Ral GTPases. *Mol.Cell Biol.* **15**, 4578-4584.

CAPON D.J., SEEBURG P.H., MCGRATH J.P., HAYFLICK J.S., EDMAN U., LEVINSON A.D. & GOEDDEL D.V. (1983) Activation of Ki-ras2 gene in human colon and lung carcinomas by two different point mutations. *Nature* **304**, 507-513.

CARDONE M.H., ROY N., STENNICKE H.R., SALVESEN G.S., FRANKE T.F., STANBRIDGE E., FRISCH S. & REED J.C. (1998) Regulation of cell death protease caspase-9 by phosphorylation. *Science* **282**, 1318-1321.

CARPENTER C.L. & CANTLEY L.C. (1996) Phosphoinositide kinases. *Curr.Opin.Cell Biol.* **8**, 153-158.

CEROTTINI J.P., CAPLIN S., SARAGA E., GIVEL J.C. & BENHATTAR J. (1998) The type of K-ras mutation determines prognosis in colorectal cancer. *Am.J.Surg.* **175**, 198-202.

CHANG E.H., FURTH M.E., SCOLNICK E.M. & LOWY D.R. (1982) Tumorigenic transformation of mammalian cells induced by a normal human gene homologous to the oncogene of Harvey murine sarcoma virus. *Nature* **297**, 479-483.

CHEN C.Y. & FALLER D.V. (1995) Direction of p21ras-generated signals towards cell growth or apoptosis is determined by protein kinase C and Bcl-2. *Oncogene* **11**, 1487-1498.

CHEN C.Y. & FALLER D.V. (1996) Phosphorylation of Bcl-2 protein and association with p21Ras in Ras- induced apoptosis. *J.Biol.Chem.* **271**, 2376-2379.

CHEN C.Y., LIOU J., FORMAN L.W. & FALLER D.V. (1998) Differential regulation of discrete apoptotic pathways by Ras. *J.Biol.Chem.* **273**, 16700-16709.

CHEN C.Y., JUO P., LIOU J.S., LI C.Q., YU Q., BLENIS J. & FALLER D.V. (2001) The recruitment of Fas-associated death domain/caspase-8 in Ras-induced apoptosis. *Cell Growth Differ.* **12**, 297-306.

CHEN X. & RESH M.D. (2001) Activation of mitogen-activated protein kinase by membrane-targeted Raf chimeras is independent of raft localization. *J.Biol.Chem.* **276**, 34617-34623.

CHEN Z., OTTO J.C., BERGO M.O., YOUNG S.G. & CASEY P.J. (2000) The C-terminal polylysine region and methylation of K-Ras are critical for the interaction between K-Ras and microtubules. *J.Biol.Chem.* **275**, 41251-41257.

CHENG G. & MEINKOTH J.L. (2001) Enhanced sensitivity to apoptosis in Ras-transformed thyroid cells. *Oncogene* **20**, 7334-7341.

CHESA P.G., RETTIG W.J., MELAMED M.R., OLD L.J. & NIMAN H.L. (1987) Expression of p21ras in normal and malignant human tissues: lack of association with proliferation and malignancy. *Proc.Natl.Acad.Sci.U.S.A* **84**, 3234-3238.

CHIANG J.M., CHOU Y.H. & CHOU T.B. (1998) K-ras codon 12 mutation determines the polypoid growth of colorectral cancer. *Cancer Res.* **58**, 3289-3293.

CHIU V.K., BIVONA T., HACH A., SAJOUS J.B., SILLETTI J., WIENER H., JOHNSON R.L., COX A.D. & PHILIPS M.R. (2002) Ras signalling on the endoplasmic reticulum and the Golgi. *Nat.Cell Biol.* **4**, 343-350.

CHOY E., CHIU V.K., SILLETTI J., FEOKTISTOV M., MORIMOTO T., MICHAELSON D., IVANOV I.E. & PHILIPS M.R. (1999) Endomembrane trafficking of ras: the CAAX motif targets proteins to the ER and Golgi. *Cell* **98**, 69-80.

CODONY C., GUIL S., CAUDEVILLA C., SERRA D., ASINS G., GRAESSMANN A., HEGARDT F.G. & BACH-ELIAS M. (2001) Modulation in vitro of H-ras oncogene expression by trans-splicing. *Oncogene* **20**, 3683-3694.

COHEN G.M. (1997) Caspases: the executioners of apoptosis. *Biochem.J.* **326 (Pt 1)**, 1-16.

COOPERSMITH C.M., CHANDRASEKARAN C., MCNEVIN M.S. & GORDON J.I. (1997) Bi-transgenic mice reveal that K-rasVal12 augments a p53-independent apoptosis when small intestinal villus enterocytes reenter the cell cycle. *J.Cell Biol.* **138**, 167-179.

DAI Q., CHOY E., CHIU V., ROMANO J., SLIVKA S.R., STEITZ S.A., MICHAELIS S. & PHILIPS M.R. (1998) Mammalian prenylcysteine carboxyl methyltransferase is in the endoplasmic reticulum. *J.Biol.Chem.* **273**, 15030-15034.

DAJEE M., TARUTANI M., DENG H., CAI T. & KHAVARI P.A. (2002) Epidermal Ras blockade demonstrates spatially localized Ras promotion of proliferation and inhibition of differentiation. *Oncogene* **21**, 1527-1538.

DATTA S.R., DUDEK H., TAO X., MASTERS S., FU H., GOTOH Y. & GREENBERG M.E. (1997) Akt phosphorylation of BAD couples survival signals to the cell- intrinsic death machinery. *Cell* **91**, 231-241.

DEBORTOLI M.E., ABOU-ISSA H., HALEY B.E. & CHO-CHUNG Y.S. (1985) Amplified expression of p21 ras protein in hormone-dependent mammary carcinomas of humans and rodents. *Biochem.Biophys.Res.Commun.* **127**, 699-706.

DENECKER G., DOOMS H., VAN LOO G., VERCAMMEN D., GROOTEN J., FIERS W., DECLERCQ W. & VANDENABEELE P. (2000) Phosphatidyl serine exposure during apoptosis precedes release of cytochrome c and decrease in mitochondrial transmembrane potential. *FEBS Lett.* **465**, 47-52.

DENHARDT D.T. (1996) Signal-transducing protein phosphorylation cascades mediated by Ras/Rho proteins in the mammalian cell: the potential for multiplex signalling. *Biochem.J.* **318 (Pt 3)**, 729-747.

DOBROWOLSKI S., HARTER M. & STACEY D.W. (1994) Cellular ras activity is required for passage through multiple points of the G0/G1 phase in BALB/c 3T3 cells. *Mol.Cell Biol.* **14**, 5441-5449.

DOETSCHMAN T., GREGG R.G., MAEDA N., HOOPER M.L., MELTON D.W., THOMPSON S. & SMITHIES O. (1987) Targetted correction of a mutant HPRT gene in mouse embryonic stem cells. *Nature* **330**, 576-578.

DOWNWARD J. (1998) Ras signalling and apoptosis. *Curr.Opin.Genet.Dev.* **8**, 49-54.

DUDLEY D.T., PANG L., DECKER S.J., BRIDGES A.J. & SALTIEL A.R. (1995) A synthetic inhibitor of the mitogen-activated protein kinase cascade. *Proc.Natl.Acad.Sci.U.S.A* **92**, 7686-7689.

ERNST M., OATES A. & DUNN A.R. (1996) Gp130-mediated signal transduction in embryonic stem cells involves activation of Jak and Ras/mitogen-activated protein kinase pathways. *J.Biol.Chem.* **271**, 30136-30143.

ESTEBAN L.M., VICARIO-ABEJON C., FERNANDEZ-SALGUERO P., FERNANDEZ-MEDARDE A., SWAMINATHAN N., YIENGER K., LOPEZ E., MALUMBRES M., MCKAY R., WARD J.M., PELLICER A. & SANTOS E. (2001) Targeted genomic disruption of H-ras and N-ras, individually or in combination, reveals the dispensability of both loci for mouse growth and development. *Mol.Cell Biol.* **21**, 1444-1452.

EVANS M.J. & KAUFMAN M.H. (1981) Establishment in culture of pluripotential cells from mouse embryos. *Nature* **292**, 154-156.

FADOK V.A., VOELKER D.R., CAMPBELL P.A., COHEN J.J., BRATTON D.L. & HENSON P.M. (1992) Exposure of phosphatidylserine on the surface of apoptotic lymphocytes triggers specific recognition and removal by macrophages. *J.Immunol.* **148**, 2207-2216.

FAN J. & BERTINO J.R. (1997) K-ras modulates the cell cycle via both positive and negative regulatory pathways. *Oncogene* **14**, 2595-2607.

FANG X., YU S., EDER A., MAO M., BAST R.C., Jr., BOYD D. & MILLS G.B. (1999) Regulation of BAD phosphorylation at serine 112 by the Ras-mitogen- activated protein kinase pathway. *Oncogene* **18**, 6635-6640.

FEARON E.R. & VOGELSTEIN B. (1990) A genetic model for colorectal tumorigenesis. *Cell* **61**, 759-767.

FEIG L.A. & COOPER G.M. (1988) Inhibition of NIH 3T3 cell proliferation by a mutant ras protein with preferential affinity for GDP. *Mol.Cell Biol.* **8**, 3235-3243.

FERGUSON A.W., SVOBODA-NEWMAN S.M. & FRANK T.S. (1998) Analysis of human papillomavirus infection and molecular alterations in adenocarcinoma of the cervix. *Mod.Pathol.* **11**, 11-18.

FISHER G.H., WELLEN S.L., KLIMSTRA D., LENCZOWSKI J.M., TICHELAAR J.W., LIZAK M.J., WHITSETT J.A., KORETSKY A. & VARMUS H.E. (2001) Induction and apoptotic regression of lung adenocarcinomas by regulation of a K-Ras transgene in the presence and absence of tumor suppressor genes. *Genes Dev.* **15**, 3249-3262.

FRANKE T.F., KAPLAN D.R. & CANTLEY L.C. (1997) PI3K: downstream AKTion blocks apoptosis. *Cell* **88**, 435-437.

FRANZA B.R., Jr., MARUYAMA K., GARRELS J.I. & RULEY H.E. (1986) In vitro establishment is not a sufficient prerequisite for transformation by activated ras oncogenes. *Cell* **44**, 409-418.

FROST J.A., XU S., HUTCHISON M.R., MARCUS S. & COBB M.H. (1996) Actions of Rho family small G proteins and p21-activated protein kinases on mitogen-activated protein kinase family members. *Mol.Cell Biol.* **16**, 3707-3713.

FROST J.A., STEEN H., SHAPIRO P., LEWIS T., AHN N., SHAW P.E. & COBB M.H. (1997) Cross-cascade activation of ERKs and ternary complex factors by Rho family proteins. *EMBO J.* **16**, 6426-6438.

FURTH M.E., ALDRICH T.H. & CORDON-CARDO C. (1987) Expression of ras proto-oncogene proteins in normal human tissues. *Oncogene* **1**, 47-58.

GALLICK G.E., KURZROCK R., KLOETZER W.S., ARLINGHAUS R.B. & GUTTERMAN J.U. (1985) Expression of p21ras in fresh primary and metastatic human colorectal tumors. *Proc.Natl.Acad.Sci.U.S.A* **82**, 1795-1799.

GEORGE D.L., SCOTT A.F., TRUSKO S., GLICK B., FORD E. & DORNEY D.J. (1985) Structure and expression of amplified cKi-ras gene sequences in Y1 mouse adrenal tumor cells. *EMBO J.* **4**, 1199-1203.

GILLE H. & DOWNWARD J. (1999) Multiple ras effector pathways contribute to G(1) cell cycle progression. *J.Biol.Chem.* **274**, 22033-22040.

GOSSEN M. & BUJARD H. (1992) Tight control of gene expression in mammalian cells by tetracycline-responsive promoters. *Proc.Natl.Acad.Sci.U.S.A* **89**, 5547-5551.

GOSSEN M., FREUNDLIEB S., BENDER G., MULLER G., HILLEN W. & BUJARD H. (1995) Transcriptional activation by tetracyclines in mammalian cells. *Science* **268**, 1766-1769.

GOTOH T., TIAN X. & FEIG L.A. (2001) Prenylation of target GTPases contributes to signaling specificity of Ras-guanine nucleotide exchange factors. *J.Biol.Chem.* **276**, 38029-38035.

GU H., MARTH J.D., ORBAN P.C., MOSSMANN H. & RAJEWSKY K. (1994) Deletion of a DNA polymerase beta gene segment in T cells using cell type-specific gene targeting. *Science* **265**, 103-106.

GUAN K.L., FIGUEROA C., BRTVA T.R., ZHU T., TAYLOR J., BARBER T.D. & VOJTEK A.B. (2000) Negative regulation of the serine/threonine kinase B-Raf by Akt. *J.Biol.Chem.* **275**, 27354-27359.

HAMAD N.M., ELCONIN J.H., KARNOUB A.E., BAI W., RICH J.N., ABRAHAM R.T., DER C.J. & COUNTER C.M. (2002) Distinct requirements for Ras oncogenesis in human versus mouse cells. *Genes Dev.* **16**, 2045-2057.

HAMILTON M. & WOLFMAN A. (1998) Ha-ras and N-ras regulate MAPK activity by distinct mechanisms in vivo. *Oncogene* **16**, 1417-1428.

HANCOCK J.F., MAGEE A.I., CHILDS J.E. & MARSHALL C.J. (1989) All ras proteins are polyisoprenylated but only some are palmitoylated. *Cell* **57**, 1167-1177.

HANCOCK J.F., PATERSON H. & MARSHALL C.J. (1990) A polybasic domain or palmitoylation is required in addition to the CAAX motif to localize p21ras to the plasma membrane. *Cell* **63**, 133-139.

HANCOCK J.F., CADWALLADER K., PATERSON H. & MARSHALL C.J. (1991) A CAAX or a CAAL motif and a second signal are sufficient for plasma membrane targeting of ras proteins. *EMBO J.* **10**, 4033-4039.

HAND P.H., VILASI V., THOR A., OHUCHI N. & SCHLOM J. (1987) Quantitation of Harvey ras p21 enhanced expression in human breast and colon carcinomas. *J.Natl.Cancer Inst.* **79**, 59-65.

HAYASHI Y., WIDJONO Y.W., OHTA K., HANIOKA K., OBAYASHI C., ITOH K., IMAI Y. & ITOH H. (1994) Expression of EGF, EGF-receptor, p53, v-erb B and ras p21 in colorectal neoplasms by immunostaining paraffin-embedded tissues. *Pathol.Int.* **44**, 124-130.

HOFFMAN E.K., TRUSKO S.P., FREEMAN N. & GEORGE D.L. (1987) Structural and functional characterization of the promoter region of the mouse c-Ki-ras gene. *Mol.Cell Biol.* 7, 2592-2596.

HOSHINO R., CHATANI Y., YAMORI T., TSURUO T., OKA H., YOSHIDA O., SHIMADA Y., ARI-I S, WADA H., FUJIMOTO J. & KOHNO M. (1999) Constitutive activation of the 41-/43-kDa mitogen-activated protein kinase signaling pathway in human tumors. *Oncogene* **18**, 813-822.

HOULSTON R.S. (2001) What we could do now: molecular pathology of colorectal cancer. *Mol.Pathol.* **54**, 206-214.

HUSER M., LUCKETT J., CHILOECHES A., MERCER K., IWOBI M., GIBLETT S., SUN X.M., BROWN J., MARAIS R. & PRITCHARD C. (2001) MEK kinase activity is not necessary for Raf-1 function. *EMBO J.* **20**, 1940-1951.

IKEDA M., ISHIDA O., HINOI T., KISHIDA S. & KIKUCHI A. (1998) Identification and characterization of a novel protein interacting with Ral-binding protein 1, a putative effector protein of Ral. *J.Biol.Chem.* **273**, 814-821.

JACKSON E.L., WILLIS N., MERCER K., BRONSON R.T., CROWLEY D., MONTOYA R., JACKS T. & TUVESON D.A. (2001) Analysis of lung tumor initiation and progression using conditional expression of oncogenic K-ras. *Genes Dev.* **15**, 3243-3248.

JACKSON J.H., LI J.W., BUSS J.E., DER C.J. & COCHRANE C.G. (1994) Polylysine domain of K-ras 4B protein is crucial for malignant transformation. *Proc.Natl.Acad.Sci.U.S.A* **91**, 12730-12734.

JAMES G., GOLDSTEIN J.L. & BROWN M.S. (1996) Resistance of K-RasBV12 proteins to farnesyltransferase inhibitors in Rat1 cells. *Proc.Natl.Acad.Sci.U.S.A* **93**, 4454-4458.

JAMES G.L., GOLDSTEIN J.L. & BROWN M.S. (1995) Polylysine and CVIM sequences of K-RasB dictate specificity of prenylation and confer resistance to benzodiazepine peptidomimetic in vitro. *J.Biol.Chem.* **270**, 6221-6226.

JANSSEN K.P., EL MARJOU F., PINTO D., SASTRE X., ROUILLARD D., FOUQUET C., SOUSSI T., LOUVARD D. & ROBINE S. (2002) Targeted expression of oncogenic K-ras in intestinal epithelium causes spontaneous tumorigenesis in mice. *Gastroenterology* **123**, 492-504.

JANSSON D.S., RADOSEVICH J.A., CARNEY W.P., ROSEN S.T., SCHLOM J., STAREN E.D., HYSER M.J. & GOULD V.E. (1990) An immunohistochemical analysis of ras oncogene expression in epithelial neoplasms of the colon. *Cancer* **65**, 1329-1337.

JEN J., POWELL S.M., PAPADOPOULOS N., SMITH K.J., HAMILTON S.R., VOGELSTEIN B. & KINZLER K.W. (1994) Molecular determinants of dysplasia in colorectal lesions. *Cancer Res.* **54**, 5523-5526.

JIRMANOVA L., AFANASSIEFF M., GOBERT-GOSSE S., MARKOSSIAN S. & SAVATIER P. (2002) Differential contributions of ERK and PI3-kinase to the regulation of cyclin D1 expression and to the control of the G1/S transition in mouse embryonic stem cells. *Oncogene* **21**, 5515-5528.

JOHNSON L., GREENBAUM D., CICHOWSKI K., MERCER K., MURPHY E., SCHMITT E., BRONSON R.T., UMANOFF H., EDELMANN W., KUCHERLAPATI R. & JACKS T. (1997) K-ras is an essential gene in the mouse with partial functional overlap with N-ras. *Genes Dev.* **11**, 2468-2481.

JOHNSON L., MERCER K., GREENBAUM D., BRONSON R.T., CROWLEY D., TUVESON D.A. & JACKS T. (2001) Somatic activation of the K-ras oncogene causes early onset lung cancer in mice. *Nature* **410**, 1111-1116.

JONES M.K. & JACKSON J.H. (1998) Ras-GRF activates Ha-Ras, but not N-Ras or K-Ras 4B, protein in vivo. *J.Biol.Chem.* **273**, 1782-1787.

JONESON T., WHITE M.A., WIGLER M.H. & BAR-SAGI D. (1996) Stimulation of membrane ruffling and MAP kinase activation by distinct effectors of RAS. *Science* **271**, 810-812.

JONESON T. & BAR-SAGI D. (1999) Suppression of Ras-induced apoptosis by the Rac GTPase. *Mol.Cell Biol.* **19**, 5892-5901.

JULLIEN-FLORES V., DORSEUIL O., ROMERO F., LETOURNEUR F., SARAGOSTI S., BERGER R., TAVITIAN A., GACON G. & CAMONIS J.H. (1995) Bridging Ral GTPase to Rho pathways. RLIP76, a Ral effector with CDC42/Rac GTPase-activating protein activity. *J.Biol.Chem.* **270**, 22473-22477.

JULLIEN-FLORES V., MAHE Y., MIREY G., LEPRINCE C., MEUNIER-BISCEUIL B., SORKIN A. & CAMONIS J.H. (2000) RLIP76, an effector of the GTPase Ral, interacts with the AP2 complex: involvement of the Ral pathway in receptor endocytosis. *J.Cell Sci.* **113 (Pt 16)**, 2837-2844.

KAUFFMANN-ZEH A., RODRIGUEZ-VICIANA P., ULRICH E., GILBERT C., COFFER P., DOWNWARD J. & EVAN G. (1997) Suppression of c-Myc-induced apoptosis by Ras signalling through PI(3)K and PKB. *Nature* **385**, 544-548.

KAWAMURA M., KAIBUCHI K., KISHI K. & TAKAI Y. (1993) Translocation of Ki-ras p21 between membrane and cytoplasm by smg GDS. *Biochem.Biophys.Res.Commun.* **190**, 832-841.

KAZAMA H. & YONEHARA S. (2000) Oncogenic K-Ras and basic fibroblast growth factor prevent Fas-mediated apoptosis in fibroblasts through activation of mitogen-activated protein kinase. *J.Cell Biol.* **148**, 557-566.

KELLENDONK C., OPHERK C., ANLAG K., SCHUTZ G. & TRONCHE F. (2000) Hepatocyte-specific expression of Cre recombinase. *Genesis.* **26**, 151-153.

KERKHOFF E., HOUBEN R., LOFFLER S., TROPPMAIR J., LEE J.E. & RAPP U.R. (1998) Regulation of c-myc expression by Ras/Raf signalling. *Oncogene* **16**, 211-216.

KERR J.F., WYLLIE A.H. & CURRIE A.R. (1972) Apoptosis: a basic biological phenomenon with wide-ranging implications in tissue kinetics. *Br.J.Cancer* **26**, 239-257.

KHOKHLATCHEV A., RABIZADEH S., XAVIER R., NEDWIDEK M., CHEN T., ZHANG X.F., SEED B. & AVRUCH J. (2002) Identification of a novel Ras-regulated proapoptotic pathway. *Curr.Biol.* **12**, 253-265.

KIM B.Y., GAYNOR R.B., SONG K., DRITSCHILO A. & JUNG M. (2002) Constitutive activation of NF-kappaB in Ki-ras-transformed prostate epithelial cells. *Oncogene* **21**, 4490-4497.

KIM K., CAI J., SHUJA S., KUO T. & MURNANE M.J. (1998) Presence of activated ras correlates with increased cysteine proteinase activities in human colorectal carcinomas. *Int.J.Cancer* **79**, 324-333.

KIMMELMAN A., TOLKACHEVA T., LORENZI M.V., OSADA M. & CHAN A.M. (1997) Identification and characterization of R-ras3: a novel member of the RAS gene family with a non-ubiquitous pattern of tissue distribution. *Oncogene* **15**, 2675-2685.

KINOSHITA T., YOKOTA T., ARAI K. & MIYAJIMA A. (1995) Regulation of Bcl-2 expression by oncogenic Ras protein in hematopoietic cells. *Oncogene* **10**, 2207-2212.

KIVINEN L., TSUBARI M., HAAPAJARVI T., DATTO M.B., WANG X.F. & LAIHO M. (1999) Ras induces p21Cip1/Waf1 cyclin kinase inhibitor transcriptionally through Sp1-binding sites. *Oncogene* **18**, 6252-6261.

KOERA K., NAKAMURA K., NAKAO K., MIYOSHI J., TOYOSHIMA K., HATTA T., OTANI H., AIBA A. & KATSUKI M. (1997) K-ras is essential for the development of the mouse embryo. *Oncogene* **15**, 1151-1159.

KOHN A.D., TAKEUCHI F. & ROTH R.A. (1996) Akt, a pleckstrin homology domain containing kinase, is activated primarily by phosphorylation. *J.Biol.Chem.* **271**, 21920-21926.

KOLCH W. (2000) Meaningful relationships: the regulation of the Ras/Raf/MEK/ERK pathway by protein interactions. *Biochem.J.* **351 Pt 2**, 289-305.

KOOPMAN G., REUTELINGSPERGER C.P., KUIJTEN G.A., KEEHNEN R.M., PALS S.T. & VAN OERS M.H. (1994) Annexin V for flow cytometric detection of phosphatidylserine expression on B cells undergoing apoptosis. *Blood* **84**, 1415-1420.

KOPS G.J., DE RUITER N.D., VRIES-SMITS A.M., POWELL D.R., BOS J.L. & BURGERING B.M. (1999) Direct control of the Forkhead transcription factor AFX by protein kinase B. *Nature* **398**, 630-634.

KOZMA L., KISS I., NAGY A., SZAKALL S. & EMBER I. (1997) Investigation of c-myc and K-ras amplification in renal clear cell adenocarcinoma. *Cancer Lett.* **111**, 127-131.

KRESSNER U., BJORHEIM J., WESTRING S., WAHLBERG S.S., PAHLMAN L., GLIMELIUS B., LINDMARK G., LINDBLOM A. & BORRESEN-DALE A.L. (1998) Ki-ras mutations and prognosis in colorectal cancer. *Eur.J.Cancer* **34**, 518-521.

KURIBARA R., KINOSHITA T., MIYAJIMA A., SHINJYO T., YOSHIHARA T., INUKAI T., OZAWA K., LOOK A.T. & INABA T. (1999) Two distinct interleukin-3-mediated signal pathways, Ras-NFIL3 (E4BP4) and Bcl-xL, regulate the survival of murine pro-B lymphocytes. *Mol.Cell Biol.* **19**, 2754-2762.

LE GALLIC L., SGOURAS D., BEAL G., Jr. & MAVROTHALASSITIS G. (1999) Transcriptional repressor ERF is a Ras/mitogen-activated protein kinase target that regulates cellular proliferation. *Mol.Cell Biol.* **19**, 4121-4133.

LEE K.Y., LADHA M.H., MCMAHON C. & EWEN M.E. (1999) The retinoblastoma protein is linked to the activation of Ras. *Mol.Cell Biol.* **19**, 7724-7732.

LEFEBVRE L., DIONNE N., KARASKOVA J., SQUIRE J.A. & NAGY A. (2001) Selection for transgene homozygosity in embryonic stem cells results in extensive loss of heterozygosity. *Nat.Genet.* **27**, 257-258.

LEON J., GUERRERO I. & PELLICER A. (1987) Differential expression of the ras gene family in mice. *Mol.Cell Biol.* **7**, 1535-1540.

LEONE G., DEGREGORI J., SEARS R., JAKOI L. & NEVINS J.R. (1997) Myc and Ras collaborate in inducing accumulation of active cyclin E/Cdk2 and E2F. *Nature* **387**, 422-426.

LERNER E.C., QIAN Y., HAMILTON A.D. & SEBTI S.M. (1995) Disruption of oncogenic K-Ras4B processing and signaling by a potent geranylgeranyltransferase I inhibitor. *J.Biol.Chem.* **270**, 26770-26773.

LESLIE A., CAREY F.A., PRATT N.R. & STEELE R.J. (2002) The colorectal adenoma-carcinoma sequence. *Br.J.Surg.* **89**, 845-860.

LIN A.W. & LOWE S.W. (2001) Oncogenic ras activates the ARF-p53 pathway to suppress epithelial cell transformation. *Proc.Natl.Acad.Sci.U.S.A* **98**, 5025-5030.

LIU J.J., CHAO J.R., JIANG M.C., NG S.Y., YEN J.J. & YANG-YEN H.F. (1995) Ras transformation results in an elevated level of cyclin D1 and acceleration of G1 progression in NIH 3T3 cells. *Mol.Cell Biol.* **15**, 3654-3663.

LIU X., WU H., LORING J., HORMUZDI S., DISTECHE C.M., BORNSTEIN P. & JAENISCH R. (1997) Trisomy eight in ES cells is a common potential problem in gene targeting and interferes with germ line transmission. *Dev.Dyn.* **209**, 85-91.

LLOYD A.C. (1998) Ras versus cyclin-dependent kinase inhibitors. *Curr.Opin.Genet.Dev.* **8**, 43-48.

LOBELL R.B., OMER C.A., ABRAMS M.T., BHIMNATHWALA H.G., BRUCKER M.J., BUSER C.A., DAVIDE J.P., DESOLMS S.J., DINSMORE C.J., ELLIS-HUTCHINGS M.S., KRAL A.M., LIU D., LUMMA W.C., MACHOTKA S.V., RANDS E., WILLIAMS T.M., GRAHAM S.L., HARTMAN G.D., OLIFF A.I., HEIMBROOK D.C. & KOHL N.E. (2001) Evaluation of farnesyl:protein transferase and geranylgeranyl:protein transferase inhibitor combinations in preclinical models. *Cancer Res.* **61**, 8758-8768.

LOWY D.R. & WILLUMSEN B.M. (1993) Function and regulation of ras. *Annu.Rev.Biochem.* **62**, 851-891.

LUCAS L., DEL PESO L., RODRIGUEZ P., PENALVA V. & LACAL J.C. (2000) Ras protein is involved in the physiological regulation of phospholipase D by platelet derived growth factor. *Oncogene* **19**, 431-437.

MADRID L.V., WANG C.Y., GUTTRIDGE D.C., SCHOTTELIUS A.J., BALDWIN A.S., Jr. & MAYO M.W. (2000) Akt suppresses apoptosis by stimulating the transactivation potential of the RelA p65 subunit of NF-kappaB. *Mol.Cell Biol.* **20**, 1626-1638.

MAGIN T.M., MCWHIR J. & MELTON D.W. (1992) A new mouse embryonic stem cell line with good germ line contribution and gene targeting frequency. *Nucleic Acids Res.* **20**, 3795-3796.

MAHER J., BAKER D.A., MANNING M., DIBB N.J. & ROBERTS I.A. (1995) Evidence for cell-specific differences in transformation by N-, H- and K-ras. *Oncogene* **11**, 1639-1647.

MALTZMAN T., KNOLL K., MARTINEZ M.E., BYERS T., STEVENS B.R., MARSHALL J.R., REID M.E., EINSPAHR J., HART N., BHATTACHARYYA A.K., KRAMER C.B., SAMPLINER R., ALBERTS D.S. & AHNEN D.J. (2001) Ki-ras proto-oncogene mutations in sporadic colorectal adenomas: relationship to histologic and clinical characteristics. *Gastroenterology* **121**, 302-309.

MANGUES R., CORRAL T., KOHL N.E., SYMMANS W.F., LU S., MALUMBRES M., GIBBS J.B., OLIFF A. & PELLICER A. (1998) Antitumor effect of a farnesyl protein transferase inhibitor in mammary and lymphoid tumors overexpressing N-ras in transgenic mice. *Cancer Res.* **58**, 1253-1259.

MANSOUR S.L., THOMAS K.R. & CAPECCHI M.R. (1988) Disruption of the proto-oncogene int-2 in mouse embryo-derived stem cells: a general strategy for targeting mutations to non-selectable genes. *Nature* **336**, 348-352.

MARTIN G.R. (1981) Isolation of a pluripotent cell line from early mouse embryos cultured in medium conditioned by teratocarcinoma stem cells. *Proc.Natl.Acad.Sci.U.S.A* **78**, 7634-7638.

MARTIN S.J., REUTELINGSPERGER C.P., MCGAHON A.J., RADER J.A., VAN SCHIE R.C., LAFACE D.M. & GREEN D.R. (1995) Early redistribution of plasma membrane phosphatidylserine is a general feature of apoptosis regardless of the initiating stimulus: inhibition by overexpression of Bcl-2 and Abl. *J.Exp.Med.* **182**, 1545-1556.

MATSUGUCHI T. & KRAFT A.S. (1998) Regulation of myeloid cell growth by distinct effectors of Ras. *Oncogene* **17**, 2701-2709.

MATSUI T., KINOSHITA T., MORIKAWA Y., TOHYA K., KATSUKI M., ITO Y., KAMIYA A. & MIYAJIMA A. (2002) K-Ras mediates cytokine-induced formation of E-cadherin-based adherens junctions during liver development. *EMBO J.* **21**, 1021-1030.

MAZZONI I.E., SAID F.A., ALOYZ R., MILLER F.D. & KAPLAN D. (1999) Ras regulates sympathetic neuron survival by suppressing the p53- mediated cell death pathway. *J.Neurosci.* **19**, 9716-9727.

MCCONKEY D.J. (1998) Biochemical determinants of apoptosis and necrosis. *Toxicol.Lett.* **99**, 157-168.

MCCORMICK F. (1994) Activators and effectors of ras p21 proteins. *Curr.Opin.Genet.Dev.* **4**, 71-76.

MCGRATH J.P., CAPON D.J., SMITH D.H., CHEN E.Y., SEEBURG P.H., GOEDDEL D.V. & LEVINSON A.D. (1983) Structure and organization of the human Ki-ras proto-oncogene and a related processed pseudogene. *Nature* **304**, 501-506.

MCMAHON A.P. & BRADLEY A. (1990) The Wnt-1 (int-1) proto-oncogene is required for development of a large region of the mouse brain. *Cell* **62**, 1073-1085.

MEADE-TOLLIN L.C., BOUKAMP P., FUSENIG N.E., BOWEN C.P., TSANG T.C. & BOWDEN G.T. (1998) Differential expression of matrix metalloproteinases in activated c-ras- Ha-transfected immortalized human keratinocytes. *Br.J.Cancer* 77, 724-730.

MEDEMA R.H., KOPS G.J., BOS J.L. & BURGERING B.M. (2000) AFX-like Forkhead transcription factors mediate cell-cycle regulation by Ras and PKB through p27kip1. *Nature* **404**, 782-787.

MEIER P. & EVAN G. (1998) Dying like flies. *Cell* **95**, 295-298.

MISSERO C., PIRRO M.T. & DI LAURO R. (2000) Multiple ras downstream pathways mediate functional repression of the homeobox gene product TTF-1. *Mol.Cell Biol.* **20**, 2783-2793.

MIZUNO T., KAIBUCHI K., YAMAMOTO T., KAWAMURA M., SAKODA T., FUJIOKA H., MATSUURA Y. & TAKAI Y. (1991) A stimulatory GDP/GTP exchange protein for smg p21 is active on the post-translationally processed form of c-Ki-ras p21 and rhoA p21. *Proc.Natl.Acad.Sci.U.S.A* **88**, 6442-6446.

MOELLING K., SCHAD K., BOSSE M., ZIMMERMANN S. & SCHWENEKER M. (2002) Regulation of Raf-Akt Cross-talk. *J.Biol.Chem.* **277**, 31099-31106.

MORTENSEN R.M., ZUBIAUR M., NEER E.J. & SEIDMAN J.G. (1991) Embryonic stem cells lacking a functional inhibitory G-protein subunit (alpha i2) produced by gene targeting of both alleles. *Proc.Natl.Acad.Sci.U.S.A* **88**, 7036-7040.

MORTENSEN R.M., CONNER D.A., CHAO S., GEISTERFER-LOWRANCE A.A. & SEIDMAN J.G. (1992) Production of homozygous mutant ES cells with a single targeting construct. *Mol.Cell Biol.* **12**, 2391-2395.

MULCAHY L.S., SMITH M.R. & STACEY D.W. (1985) Requirement for ras proto-oncogene function during serum-stimulated growth of NIH 3T3 cells. *Nature* **313**, 241-243.

MULLER R., SLAMON D.J., TREMBLAY J.M., CLINE M.J. & VERMA I.M. (1982) Differential expression of cellular oncogenes during pre- and postnatal development of the mouse. *Nature* **299**, 640-644.

MULLER R., SLAMON D.J., ADAMSON E.D., TREMBLAY J.M., MULLER D., CLINE M.J. & VERMA I.M. (1983) Transcription of c-onc genes c-rasKi and c-fms during mouse development. *Mol.Cell Biol.* **3**, 1062-1069.

NAGATA S. (1997) Apoptosis by death factor. *Cell* **88**, 355-365.

NAKANISHI H., KAIBUCHI K., ORITA S., UENO N. & TAKAI Y. (1994) Different functions of Smg GDP dissociation stimulator and mammalian counterpart of yeast Cdc25. *J.Biol.Chem.* **269**, 15085-15091.

NAKASHIMA S., MORINAKA K., KOYAMA S., IKEDA M., KISHIDA M., OKAWA K., IWAMATSU A., KISHIDA S. & KIKUCHI A. (1999) Small G protein Ral and its downstream molecules regulate endocytosis of EGF and insulin receptors. *EMBO J.* **18**, 3629-3642.

NAVARRO P., VALVERDE A.M., BENITO M. & LORENZO M. (1999) Activated Ha-ras induces apoptosis by association with phosphorylated Bcl-2 in a mitogen-activated protein kinase-independent manner. *J.Biol.Chem.* **274**, 18857-18863.

NGAN H.Y., LIU S.S., YU H., LIU K.L. & CHEUNG A.N. (1999) Proto-oncogenes and p53 protein expression in normal cervical stratified squamous epithelium and cervical intra-epithelial neoplasia. *Eur.J.Cancer* **35**, 1546-1550.

NICOLAIDES A., HUANG Y.Q., LI J.J., ZHANG W.G. & FRIEDMAN-KIEN A.E. (1994) Gene amplification and multiple mutations of the K-ras oncogene in Kaposi's sarcoma. *Anticancer Res.* **14**, 921-926.

NIV H., GUTMAN O., HENIS Y.I. & KLOOG Y. (1999) Membrane interactions of a constitutively active GFP-Ki-Ras 4B and their role in signaling. Evidence from lateral mobility studies. *J.Biol.Chem.* **274**, 1606-1613.

NOMOTO S., NAKAO A., ANDO N., TAKEDA S., KASAI Y., INOUE S., KANEKO T. & TAKAGI H. (1998) Clinical application of K-ras oncogene mutations in pancreatic carcinoma: detection of micrometastases. *Semin.Surg.Oncol.* **15**, 40-46.

NOOTER K., BOERSMA A.W., OOSTRUM R.G., BURGER H., JOCHEMSEN A.G. & STOTER G. (1995) Constitutive expression of the c-H-ras oncogene inhibits doxorubicin- induced apoptosis and promotes cell survival in a rhabdomyosarcoma cell line. *Br.J.Cancer* **71**, 556-561.

OHNISHI T., TOMITA N., MONDEN T., OHUE M., YANA I., TAKAMI K., YAMAMOTO H., YAGYU T., KIKKAWA N., SHIMANO T. & MONDEN M. (1997) A detailed analysis of the role of K-ras gene mutation in the progression of colorectal adenoma. *Br.J.Cancer* **75**, 341-347.

OHTA Y., SUZUKI N., NAKAMURA S., HARTWIG J.H. & STOSSEL T.P. (1999) The small GTPase RalA targets filamin to induce filopodia. *Proc.Natl.Acad.Sci.U.S.A* **96**, 2122-2128.

OKADA F., RAK J.W., CROIX B.S., LIEUBEAU B., KAYA M., RONCARI L., SHIRASAWA S., SASAZUKI T. & KERBEL R.S. (1998) Impact of oncogenes in tumor angiogenesis: mutant

K-ras up-regulation of vascular endothelial growth factor/vascular permeability factor is necessary, but not sufficient for tumorigenicity of human colorectal carcinoma cells. *Proc.Natl.Acad.Sci.U.S.A* **95**, 3609-3614.

OLSON M.F., PATERSON H.F. & MARSHALL C.J. (1998) Signals from Ras and Rho GTPases interact to regulate expression of p21Waf1/Cip1. *Nature* **394**, 295-299.

ORECCHIA R., INFUSINI E., SCIUTTO A., RAPALLO A., DI VINCI A., NIGRO S., GEIDO E. & GIARETTI W. (2000) Ki-ras activation in vitro affects G1 and G2M cell-cycle transit times and apoptosis. *J.Pathol.* **190**, 423-429.

ORITA S., KAIBUCHI K., KURODA S., SHIMIZU K., NAKANISHI H. & TAKAI Y. (1993) Comparison of kinetic properties between two mammalian ras p21 GDP/GTP exchange proteins, ras guanine nucleotide-releasing factor and smg GDP dissociation stimulation. *J.Biol.Chem.* **268**, 25542-25546.

OZES O.N., MAYO L.D., GUSTIN J.A., PFEFFER S.R., PFEFFER L.M. & DONNER D.B. (1999) NF-kappaB activation by tumour necrosis factor requires the Akt serine- threonine kinase. *Nature* **401**, 82-85.

PACOLD M.E., SUIRE S., PERISIC O., LARA-GONZALEZ S., DAVIS C.T., WALKER E.H., HAWKINS P.T., STEPHENS L., ECCLESTON J.F. & WILLIAMS R.L. (2000) Crystal structure and functional analysis of Ras binding to its effector phosphoinositide 3-kinase gamma. *Cell* **103**, 931-943.

PALMERO I., PANTOJA C. & SERRANO M. (1998) p19ARF links the tumour suppressor p53 to Ras. *Nature* **395**, 125-126.

PAN G., O'ROURKE K. & DIXIT V.M. (1998) Caspase-9, Bcl-XL, and Apaf-1 form a ternary complex. *J.Biol.Chem.* **273**, 5841-5845.

PARK S.H. & WEINBERG R.A. (1995) A putative effector of Ral has homology to Rho/Rac GTPase activating proteins. *Oncogene* **11**, 2349-2355.

PARKER M.F., ARROYO G.F., GERADTS J., SABICHI A.L., PARK R.C., TAYLOR R.R. & BIRRER M.J. (1997) Molecular characterization of adenocarcinoma of the cervix. *Gynecol.Oncol.* **64**, 242-251.

PAUMELLE R., TULASNE D., KHERROUCHE Z., PLAZA S., LEROY C., REVENEAU S., VANDENBUNDER B., FAFEUR V., TULASHE D. & REVENEAU S. (2002) Hepatocyte growth factor/scatter factor activates the ETS1 transcription factor by a RAS-RAF-MEK-ERK signaling pathway. *Oncogene* **21**, 2309-2319.

PEEPER D.S., DANNENBERG J.H., DOUMA S., TE R.H. & BERNARDS R. (2001) Escape from premature senescence is not sufficient for oncogenic transformation by Ras. *Nat.Cell Biol.* **3**, 198-203.

PELI J., SCHROTER M., RUDAZ C., HAHNE M., MEYER C., REICHMANN E. & TSCHOPP J. (1999) Oncogenic Ras inhibits Fas ligand-mediated apoptosis by downregulating the expression of Fas. *EMBO J.* **18**, 1824-1831.

PELLS S., DIVJAK M., ROMANOWSKI P., IMPEY H., HAWKINS N.J., CLARKE A.R., HOOPER M.L. & WILLIAMSON D.J. (1997) Developmentally-regulated expression of murine K-ras isoforms. *Oncogene* **15**, 1781-1786.

PERKINS C.L., FANG G., KIM C.N. & BHALLA K.N. (2000) The role of Apaf-1, caspase-9, and bid proteins in etopo. *Cancer Res.* **60**, 1645-1653.

PRETLOW T.P., BRASITUS T.A., FULTON N.C., CHEYER C. & KAPLAN E.L. (1993) K-ras mutations in putative preneoplastic lesions in human colon. *J.Natl.Cancer Inst.* **85**, 2004-2007.

PRIOR I.A., HARDING A., YAN J., SLUIMER J., PARTON R.G. & HANCOCK J.F. (2001) GTP-dependent segregation of H-ras from lipid rafts is required for biological activity. *Nat.Cell Biol.* **3**, 368-375.

RATHJEN J., LAKE J.A., BETTESS M.D., WASHINGTON J.M., CHAPMAN G. & RATHJEN P.D. (1999) Formation of a primitive ectoderm like cell population, EPL cells, from ES cells in response to biologically derived factors. *J.Cell Sci.* **112 (Pt 5)**, 601-612.

RAY M.K., FAGAN S.P., MOLDOVAN S., DEMAYO F.J. & BRUNICARDI F.C. (1999) Development of a transgenic mouse model using rat insulin promoter to drive the expression of CRE recombinase in a tissue-specific manner. *Int.J.Pancreatol.* **25**, 157-163.

REBOLLO A., PEREZ-SALA D. & MARTINEZ A. (1999) Bcl-2 differentially targets K-, N-, and H-Ras to mitochondria in IL-2 supplemented or deprived cells: implications in prevention of apoptosis. *Oncogene* **18**, 4930-4939.

REED J.C. (1998) Bcl-2 family proteins. *Oncogene* **17**, 3225-3236.

RIDLEY A.J., PATERSON H.F., NOBLE M. & LAND H. (1988) Ras-mediated cell cycle arrest is altered by nuclear oncogenes to induce Schwann cell transformation. *EMBO J.* **7**, 1635-1645.

RINKENBERGER J.L. & KORSMEYER S.J. (1997) Errors of homeostasis and deregulated apoptosis. *Curr.Opin.Genet.Dev.* **7**, 589-596.

RIZZO M.A., KRAFT C.A., WATKINS S.C., LEVITAN E.S. & ROMERO G. (2001) Agonist-dependent traffic of raft-associated Ras and Raf-1 is required for activation of the mitogen-activated protein kinase cascade. *J.Biol.Chem.* **276**, 34928-34933.

ROBERTSON J.D., GOGVADZE V., ZHIVOTOVSKY B. & ORRENIUS S. (2000) Distinct pathways for stimulation of cytochrome c release by etoposide. *J.Biol.Chem.* **275**, 32438-32443.

RODRIGUEZ-VICIANA P., WARNE P.H., DHAND R., VANHAESEBROECK B., GOUT I., FRY M.J., WATERFIELD M.D. & DOWNWARD J. (1994) Phosphatidylinositol-3-OH kinase as a direct target of Ras. *Nature* **370**, 527-532.

RODRIGUEZ-VICIANA P., WARNE P.H., KHWAJA A., MARTE B.M., PAPPIN D., DAS P., WATERFIELD M.D., RIDLEY A. & DOWNWARD J. (1997) Role of phosphoinositide 3-OH kinase in cell transformation and control of the actin cytoskeleton by Ras. *Cell* **89**, 457-467.

ROMASHKOVA J.A. & MAKAROV S.S. (1999) NF-kappaB is a target of AKT in anti-apoptotic PDGF signalling. *Nature* **401**, 86-90.

ROWELL C.A., KOWALCZYK J.J., LEWIS M.D. & GARCIA A.M. (1997) Direct demonstration of geranylgeranylation and farnesylation of Ki-Ras in vivo. *J.Biol.Chem.* **272**, 14093-14097.

ROY S., LUETTERFORST R., HARDING A., APOLLONI A., ETHERIDGE M., STANG E., ROLLS B., HANCOCK J.F. & PARTON R.G. (1999) Dominant-negative caveolin inhibits H-Ras function by disrupting cholesterol-rich plasma membrane domains. *Nat.Cell Biol.* **1**, 98-105.

SABBATINI P. & MCCORMICK F. (1999) Phosphoinositide 3-OH kinase (PI3K) and PKB/Akt delay the onset of p53- mediated, transcriptionally dependent apoptosis. *J.Biol.Chem.* **274**, 24263-24269.

SAGAE S., KUDO R., KUZUMAKI N., HISADA T., MUGIKURA Y., NIHEI T., TAKEDA T. & HASHIMOTO M. (1990) Ras oncogene expression and progression in intraepithelial neoplasia of the uterine cervix. *Cancer* **66**, 295-301.

SAUER B. & HENDERSON N. (1988) Site-specific DNA recombination in mammalian cells by the Cre recombinase of bacteriophage P1. *Proc.Natl.Acad.Sci.U.S.A* **85**, 5166-5170.

SAVATIER P., HUANG S., SZEKELY L., WIMAN K.G. & SAMARUT J. (1994) Contrasting patterns of retinoblastoma protein expression in mouse embryonic stem cells and embryonic fibroblasts. *Oncogene* **9**, 809-818.

SAVATIER P., LAPILLONNE H., VAN GRUNSVEN L.A., RUDKIN B.B. & SAMARUT J. (1996) Withdrawal of differentiation inhibitory activity/leukemia inhibitory factor up-regulates D-type cyclins and cyclin-dependent kinase inhibitors in mouse embryonic stem cells. *Oncogene* **12**, 309-322.

SCHARNHORST V., KRANENBURG O., VAN DER EB A.J. & JOCHEMSEN A.G. (1997) Differential regulation of the Wilms' tumor gene, WT1, during differentiation of embryonal carcinoma and embryonic stem cells. *Cell Growth Differ.* **8**, 133-143.

SCHEFFZEK K., AHMADIAN M.R., KABSCH W., WIESMULLER L., LAUTWEIN A., SCHMITZ F. & WITTINGHOFER A. (1997) The Ras-RasGAP complex: structural basis for GTPase activation and its loss in oncogenic Ras mutants. *Science* **277**, 333-338.

SCHMIDT W.K., TAM A., FUJIMURA-KAMADA K. & MICHAELIS S. (1998) Endoplasmic reticulum membrane localization of Rce1p and Ste24p, yeast proteases involved in carboxyl-terminal CAAX protein processing and amino-terminal a-factor cleavage. *Proc.Natl.Acad.Sci.U.S.A* **95**, 11175-11180.

SCHMITZ I., KIRCHHOFF S. & KRAMMER P.H. (2000) Regulation of death receptor-mediated apoptosis pathways. *Int.J.Biochem.Cell Biol.* **32**, 1123-1136.

SCHRAMM K., KRAUSE K., BITTROFF-LEBEN A., GOLDIN-LANG P., THIEL E. & KREUSER E.D. (2000) Activated K-ras is involved in regulation of integrin expression in human colon carcinoma cells. *Int.J.Cancer* **87**, 155-164.

SCHRATT G., WEINHOLD B., LUNDBERG A.S., SCHUCK S., BERGER J., SCHWARZ H., WEINBERG R.A., RUTHER U. & NORDHEIM A. (2001) Serum response factor is required for immediate-early gene activation yet is dispensable for proliferation of embryonic stem cells. *Mol.Cell Biol.* **21**, 2933-2943.

SCHWAB M., ALITALO K., VARMUS H.E., BISHOP J.M. & GEORGE D. (1983) A cellular oncogene (c-Ki-ras) is amplified, overexpressed, and located within karyotypic abnormalities in mouse adrenocortical tumour cells. *Nature* **303**, 497-501.

SCHWARTZBERG P.L., GOFF S.P. & ROBERTSON E.J. (1989) Germ-line transmission of a c-abl mutation produced by targeted gene disruption in ES cells. *Science* **246**, 799-803.

SCITA G., TENCA P., FRITTOLI E., TOCCHETTI A., INNOCENTI M., GIARDINA G. & DI FIORE P.P. (2000) Signaling from Ras to Rac and beyond: not just a matter of GEFs. *EMBO J.* **19**, 2393-2398.

SEBOLT-LEOPOLD J.S., DUDLEY D.T., HERRERA R., VAN BECELAERE K., WILAND A., GOWAN R.C., TECLE H., BARRETT S.D., BRIDGES A., PRZYBRANOWSKI S., LEOPOLD W.R. & SALTIEL A.R. (1999) Blockade of the MAP kinase pathway suppresses growth of colon tumors in vivo. *Nat.Med.* **5**, 810-816.

SEBOLT-LEOPOLD J.S. (2000) Development of anticancer drugs targeting the MAP kinase pathway. *Oncogene* **19**, 6594-6599.

SELFRIDGE J., POW A.M., MCWHIR J., MAGIN T.M. & MELTON D.W. (1992) Gene targeting using a mouse HPRT minigene/HPRT-deficient embryonic stem cell system: inactivation of the mouse ERCC-1 gene. *Somat.Cell Mol.Genet.* **18**, 325-336.

SERRANO M., LEE H., CHIN L., CORDON-CARDO C., BEACH D. & DEPINHO R.A. (1996) Role of the INK4a locus in tumor suppression and cell mortality. *Cell* **85**, 27-37.

SERRANO M., LIN A.W., MCCURRACH M.E., BEACH D. & LOWE S.W. (1997) Oncogenic ras provokes premature cell senescence associated with accumulation of p53 and p16INK4a. *Cell* **88**, 593-602.

SEWING A., WISEMAN B., LLOYD A.C. & LAND H. (1997) High-intensity Raf signal causes cell cycle arrest mediated by p21Cip1. *Mol.Cell Biol.* **17**, 5588-5597.

SHAO J., SHENG H., DUBOIS R.N. & BEAUCHAMP R.D. (2000) Oncogenic Ras-mediated cell growth arrest and apoptosis are associated with increased ubiquitin-dependent cyclin D1 degradation. *J.Biol.Chem.* **275**, 22916-22924.

SHENG Z., KNOWLTON K., CHEN J., HOSHIJIMA M., BROWN J.H. & CHIEN K.R. (1997) Cardiotrophin 1 (CT-1) inhibition of cardiac myocyte apoptosis via a mitogen-activated protein kinase-dependent pathway. Divergence from downstream CT-1 signals for myocardial cell hypertrophy. *J.Biol.Chem.* **272**, 5783-5791.

SHIELDS J.M., PRUITT K., MCFALL A., SHAUB A. & DER C.J. (2000) Understanding Ras: 'it ain't over 'til it's over'. *Trends Cell Biol.* **10**, 147-154.

SLAGLE B.L., KAUFMAN R.H., REEVES W.C. & ICENOGLE J.P. (1998) Expression of ras, c-myc, and p53 proteins in cervical intraepithelial neoplasia. *Cancer* **83**, 1401-1408.

SLAMON D.J., DEKERNION J.B., VERMA I.M. & CLINE M.J. (1984) Expression of cellular oncogenes in human malignancies. *Science* **224**, 256-262.

SMITH A.G. & HOOPER M.L. (1987) Buffalo rat liver cells produce a diffusible activity which inhibits the differentiation of murine embryonal carcinoma and embryonic stem cells. *Dev.Biol.* **121**, 1-9.

SMITH A.G., HEATH J.K., DONALDSON D.D., WONG G.G., MOREAU J., STAHL M. & ROGERS D. (1988) Inhibition of pluripotential embryonic stem cell differentiation by purified polypeptides. *Nature* **336**, 688-690.

SMITH G., CAREY F.A., BEATTIE J., WILKIE M.J., LIGHTFOOT T.J., COXHEAD J., GARNER R.C., STEELE R.J. & WOLF C.R. (2002) Mutations in APC, Kirsten-ras, and p53--alternative genetic pathways to colorectal cancer. *Proc.Natl.Acad.Sci.U.S.A* **99**, 9433-9438.

SMITH R.G. (1994) Southwestern internal medicine conference: hereditary predisposition to colorectal cancer: new insights. *Am.J.Med.Sci.* **308**, 295-308.

STENZEL A., SEMCZUK A., ROZYNSKAL K., JAKOWICKI J. & WOJCIEROWSKI J. (2001) "Low-risk" and "high-risk" HPV-infection and K-ras gene point mutations in human cervical cancer: a study of 31 cases. *Pathol.Res.Pract.* **197**, 597-603.

STEPHENS L., ANDERSON K., STOKOE D., ERDJUMENT-BROMAGE H., PAINTER G.F., HOLMES A.B., GAFFNEY P.R., REESE C.B., MCCORMICK F., TEMPST P., COADWELL J. & HAWKINS P.T. (1998) Protein kinase B kinases that mediate phosphatidylinositol 3,4,5-trisphosphate-dependent activation of protein kinase B. *Science* **279**, 710-714.

STERNBERG N., AUSTIN S., HAMILTON D. & YARMOLINSKY M. (1978) Analysis of bacteriophage P1 immunity by using lambda-P1 recombinants constructed in vitro. *Proc.Natl.Acad.Sci.U.S.A* **75**, 5594-5598.

STOKOE D., STEPHENS L.R., COPELAND T., GAFFNEY P.R., REESE C.B., PAINTER G.F., HOLMES A.B., MCCORMICK F. & HAWKINS P.T. (1997) Dual role of phosphatidylinositol-3,4,5-trisphosphate in the activation of protein kinase B. *Science* **277**, 567-570.

STOPERA S.A. & BIRD R.P. (1992) Expression of ras oncogene mRNA and protein in aberrant crypt foci. *Carcinogenesis* **13**, 1863-1868.

SUN J., QIAN Y., HAMILTON A.D. & SEBTI S.M. (1998) Both farnesyltransferase and geranylgeranyltransferase I inhibitors are required for inhibition of oncogenic K-Ras prenylation but each alone is sufficient to suppress human tumor growth in nude mouse xenografts. *Oncogene* **16**, 1467-1473.

SUN X.F., EKBERG H., ZHANG H., CARSTENSEN J.M. & NORDENSKJOLD B. (1998) Overexpression of ras is an independent prognostic factor in colorectal adenocarcinoma. *APMIS* **106**, 657-664.

SZEBERENYI J., CAI H. & COOPER G.M. (1990) Effect of a dominant inhibitory Ha-ras mutation on neuronal differentiation of PC12 cells. *Mol.Cell Biol.* **10**, 5324-5332.

TAKUWA N. & TAKUWA Y. (2001) Regulation of cell cycle molecules by the Ras effector system. *Mol.Cell Endocrinol.* **177**, 25-33.

TANG Y., ZHOU H., CHEN A., PITTMAN R.N. & FIELD J. (2000) The Akt proto-oncogene links Ras to Pak and cell survival signals. *J.Biol.Chem.* **275**, 9106-9109.

TERADA K., KAZIRO Y. & SATOH T. (2000) Analysis of Ras-dependent signals that prevent caspase-3 activation and apoptosis induced by cytokine deprivation in hematopoietic cells. *Biochem.Biophys.Res.Commun.* **267**, 449-455.

THISSEN J.A., GROSS J.M., SUBRAMANIAN K., MEYER T. & CASEY P.J. (1997) Prenylation-dependent association of Ki-Ras with microtubules. Evidence for a role in subcellular trafficking. *J.Biol.Chem.* **272**, 30362-30370.

THOMAS K.R. & CAPECCHI M.R. (1987) Site-directed mutagenesis by gene targeting in mouse embryo-derived stem cells. *Cell* **51**, 503-512.

TSUNEOKA M. & MEKADA E. (2000) Ras/MEK signaling suppresses Myc-dependent apoptosis in cells transformed by c-myc and activated ras. *Oncogene* **19**, 115-123.

TU S. & CERIONE R.A. (2001) Cdc42 is a substrate for caspases and influences Fas-induced apoptosis. *J.Biol.Chem.* **276**, 19656-19663.

UMANOFF H., EDELMANN W., PELLICER A. & KUCHERLAPATI R. (1995) The murine N-ras gene is not essential for growth and development. *Proc.Natl.Acad.Sci.U.S.A* **92**, 1709-1713.

URBAN T., RICCI S., GRANGE J.D., LACAVE R., BOUDGHENE F., BREITTMAYER F., LANGUILLE O., ROLAND J. & BERNAUDIN J.F. (1993) Detection of c-Ki-ras mutation by PCR/RFLP analysis and diagnosis of pancreatic adenocarcinomas. *J.Natl.Cancer Inst.* **85**, 2008-2012.

VERHEIJEN M.H., WOLTHUIS R.M., BOS J.L. & DEFIZE L.H. (1999) The Ras/Erk pathway induces primitive endoderm but prevents parietal endoderm differentiation of F9 embryonal carcinoma cells. *J.Biol.Chem.* **274**, 1487-1494.

VERHEIJEN M.H., WOLTHUIS R.M., DEFIZE L.H., DEN HERTOG J. & BOS J.L. (1999) Interdependent action of RalGEF and Erk in Ras-induced primitive endoderm differentiation of F9 embryonal carcinoma cells. *Oncogene* **18**, 4435-4439.

VIKIS H.G., STEWART S. & GUAN K.L. (2002) SmgGDS displays differential binding and exchange activity towards different Ras isoforms. *Oncogene* **21**, 2425-2432.

VILLALONGA P., LOPEZ-ALCALA C., BOSCH M., CHILOECHES A., ROCAMORA N., GIL J., MARAIS R., MARSHALL C.J., BACHS O. & AGELL N. (2001) Calmodulin binds to K-Ras, but not. *Mol.Cell Biol.* **21**, 7345-7354.

VINDELOV L.L., CHRISTENSEN I.J. & NISSEN N.I. (1983) A detergent-trypsin method for the preparation of nuclei for flow cytometric DNA analysis. *Cytometry* **3**, 323-327.

VISCA P., ALO P.L., DEL NONNO F., BOTTI C., TROMBETTA G., MARANDINO F., FILIPPI S., DI TONDO U. & DONNORSO R.P. (1999) Immunohistochemical expression of fatty acid synthase, apoptotic- regulating genes, proliferating factors, and ras protein product in colorectal adenomas, carcinomas, and adjacent nonneoplastic mucosa. *Clin.Cancer Res.* **5**, 4111-4118.

VLAHOS C.J., MATTER W.F., HUI K.Y. & BROWN R.F. (1994) A specific inhibitor of phosphatidylinositol 3-kinase, 2-(4- morpholinyl)-8-phenyl-4H-1-benzopyran-4-one (LY294002). *J.Biol.Chem.* **269**, 5241-5248.

VOGELSTEIN B., FEARON E.R., HAMILTON S.R., KERN S.E., PREISINGER A.C., LEPPERT M., NAKAMURA Y., WHITE R., SMITS A.M. & BOS J.L. (1988) Genetic alterations during colorectal-tumor development. *N.Engl.J.Med.* **319**, 525-532.

VOICE J.K., KLEMKE R.L., LE A. & JACKSON J.H. (1999) Four human ras homologs differ in their abilities to activate Raf-1, induce transformation, and stimulate cell motility. *J.Biol.Chem.* **274**, 17164-17170.

VOS M.D., ELLIS C.A., BELL A., BIRRER M.J. & CLARK G.J. (2000) Ras uses the novel tumor suppressor RASSF1 as an effector to mediate apoptosis. *J.Biol.Chem.* **275**, 35669-35672.

VOSS M., WEERNINK P.A., HAUPENTHAL S., MOLLER U., COOL R.H., BAUER B., CAMONIS J.H., JAKOBS K.H. & SCHMIDT M. (1999) Phospholipase D stimulation by receptor tyrosine

kinases mediated by protein kinase C and a Ras/Ral signaling cascade. *J.Biol.Chem.* **274**, 34691-34698.

WALSH A.B. & BAR-SAGI D. (2001) Differential activation of the Rac pathway by Ha-Ras and K-Ras. *J.Biol.Chem.* **276**, 15609-15615.

WANG D.Z., NUR E.K.M., TIKOO A., MONTAGUE W. & MARUTA H. (1997) The GTPase and Rho GAP domains of p190, a tumor suppressor protein that binds the M(r) 120,000 Ras GAP, independently function as anti-Ras tumor suppressors. *Cancer Res.* **57**, 2478-2484.

WANG Y., YOU M. & WANG Y. (2001) Alternative splicing of the K-ras gene in mouse tissues and cell lines. *Exp.Lung Res.* **27**, 255-267.

WARD R.L., TODD A.V., SANTIAGO F., O'CONNOR T. & HAWKINS N.J. (1997) Activation of the K-ras oncogene in colorectal neoplasms is associated with decreased apoptosis. *Cancer* **79**, 1106-1113.

WEBER C.K., SLUPSKY J.R., HERRMANN C., SCHULER M., RAPP U.R. & BLOCK C. (2000) Mitogenic signaling of Ras is regulated by differential interaction with Raf isozymes. *Oncogene* **19**, 169-176.

WEN L.P., MADANI K., MARTIN G.A. & ROSEN G.D. (1998) Proteolytic cleavage of ras GTPase-activating protein during apoptosis. *Cell Death.Differ.* **5**, 729-734.

WENNSTROM S. & DOWNWARD J. (1999) Role of phosphoinositide 3-kinase in activation of ras and mitogen- activated protein kinase by epidermal growth factor. *Mol.Cell Biol.* **19**, 4279-4288.

WESTWICK J.K., COX A.D., DER C.J., COBB M.H., HIBI M., KARIN M. & BRENNER D.A. (1994) Oncogenic Ras activates c-Jun via a separate pathway from the activation of extracellular signal-regulated kinases. *Proc.Natl.Acad.Sci.U.S.A* **91**, 6030-6034.

WIDMANN C., GIBSON S. & JOHNSON G.L. (1998) Caspase-dependent cleavage of signaling proteins during apoptosis. A turn-off mechanism for anti-apoptotic signals. *J.Biol.Chem.* **273**, 7141-7147.

WILLIAMS R.L., HILTON D.J., PEASE S., WILLSON T.A., STEWART C.L., GEARING D.P., WAGNER E.F., METCALF D., NICOLA N.A. & GOUGH N.M. (1988) Myeloid leukaemia inhibitory factor maintains the developmental potential of embryonic stem cells. *Nature* **336**, 684-687.

WINSTON J.T., COATS S.R., WANG Y.Z. & PLEDGER W.J. (1996) Regulation of the cell cycle machinery by oncogenic ras. *Oncogene* **12**, 127-134.

WOLFMAN J.C. & WOLFMAN A. (2000) Endogenous c-N-Ras provides a steady-state anti-apoptotic signal. *J.Biol.Chem.* **275**, 19315-19323.

WOLFMAN J.C., PALMBY T., DER C.J. & WOLFMAN A. (2002) Cellular N-Ras promotes cell survival by downregulation of Jun N- terminal protein kinase and p38. *Mol.Cell Biol.* **22**, 1589-1606.

WOODS D., PARRY D., CHERWINSKI H., BOSCH E., LEES E. & MCMAHON M. (1997) Raf-induced proliferation or cell cycle arrest is determined by the level of Raf activity with arrest mediated by p21Cip1. *Mol.Cell Biol.* **17**, 5598-5611.

WUU Y.D., PAMPFER S., VANDERHEYDEN I., LEE K.H. & DE HERTOGH R. (1998) Impact of tumor necrosis factor alpha on mouse embryonic stem cells. *Biol.Reprod.* **58**, 1416-1424.

XU C.W. & LUO Z. (2002) Inactivation of Ras function by allele-specific peptide aptamers. *Oncogene* **21**, 5753-5757.

XUE L., MURRAY J.H. & TOLKOVSKY A.M. (2000) The Ras/phosphatidylinositol 3-kinase and Ras ERK pathways function as independent survival modules each of which inhibits a distinct apoptotic signaling pathway in sympathetic neurons. *J.Biol.Chem.* **275**, 8817-8824.

YAMADA T., NAKAMORI S., OHZATO H., OSHIMA S., AOKI T., HIGAKI N., SUGIMOTO K., AKAGI K., FUJIWARA Y., NISHISHO I., SAKON M., GOTOH M. & MONDEN M. (1998) Detection of K-ras gene mutations in plasma DNA of patients with pancreatic adenocarcinoma: correlation with clinicopathological features. *Clin.Cancer Res.* **4**, 1527-1532.

YAMAGUCHI A., URANO T., GOI T. & FEIG L.A. (1997) An Eps homology (EH) domain protein that binds to the Ral-GTPase target, RalBP1. *J.Biol.Chem.* **272**, 31230-31234.

YAMAUCHI N., KIESSLING A.A. & COOPER G.M. (1994) The Ras/Raf signaling pathway is required for progression of mouse embryos through the two-cell stage. *Mol.Cell Biol.* **14**, 6655-6662.

YAN J., ROY S., APOLLONI A., LANE A. & HANCOCK J.F. (1998) Ras isoforms vary in their ability to activate Raf-1 and phosphoinositide 3-kinase. *J.Biol.Chem.* **273**, 24052-24056.

YAN Z., DENG X., CHEN M., XU Y., AHRAM M., SLOANE B.F. & FRIEDMAN E. (1997) Oncogenic c-Ki-ras but not oncogenic c-Ha-ras up-regulates CEA expression and disrupts basolateral polarity in colon epithelial cells. *J.Biol.Chem.* **272**, 27902-27907.

YAN Z., CHEN M., PERUCHO M. & FRIEDMAN E. (1997) Oncogenic Ki-ras but not oncogenic Ha-ras blocks integrin beta1-chain maturation in colon epithelial cells. *J.Biol.Chem.* **272**, 30928-30936.

YANG B.S., HAUSER C.A., HENKEL G., COLMAN M.S., VAN BEVEREN C., STACEY K.J., HUME D.A., MAKI R.A. & OSTROWSKI M.C. (1996) Ras-mediated phosphorylation of a conserved threonine residue enhances the transactivation activities of c-Ets1 and c-Ets2. *Mol.Cell Biol.* **16**, 538-547.

YAO R. & COOPER G.M. (1995) Regulation of the Ras signaling pathway by GTPase-activating protein in PC12 cells. *Oncogene* **11**, 1607-1614.

YIN T. & YANG Y.C. (1994) Mitogen-activated protein kinases and ribosomal S6 protein kinases are involved in signaling pathways shared by interleukin-11, interleukin-6, leukemia inhibitory factor, and oncostatin M in mouse 3T3-L1 cells. *J.Biol.Chem.* **269**, 3731-3738.

ZHA J., HARADA H., YANG E., JOCKEL J. & KORSMEYER S.J. (1996) Serine phosphorylation of death agonist BAD in response to survival factor results in binding to 14-3-3 not BCL-X(L). *Cell* **87**, 619-628.

ZHANG X., GASPARD J.P. & CHUNG D.C. (2001) Regulation of vascular endothelial growth factor by the Wnt and K-ras pathways in colonic neoplasia. *Cancer Res.* **61**, 6050-6054.

ZHU D., KEOHAVONG P., FINKELSTEIN S.D., SWALSKY P., BAKKER A., WEISSFELD J., SRIVASTAVA S. & WHITESIDE T.L. (1997) K-ras gene mutations in normal colorectal tissues from K-ras mutation- positive colorectal cancer patients. *Cancer Res.* **57**, 2485-2492.

ZOU G.M., REZNIKOFF-ETIEVANT M.F., LEON A., VERGE V., HIRSCH F. & MILLIEZ J. (2000) Fas-mediated apoptosis of mouse embryo stem cells: its role during embryonic development. *Am.J.Reprod.Immunol.* **43**, 240-248.

Appendix I- solutions

Solutions for bacterial work

L Broth

Bactotryptone (DIFCO)	10g/L
Yeast extract (DIFCO)	5g/L
NaCl (Fisher)	10g/L

In de-ionised H2O, autoclaved
Supplemented with 50µg/ml ampicillin where stated
Supplemented with 1.2% w/v Bactoagar for plates

Solutions for DNA analysis

10X TBE Buffer

TRIZMA base (Sigma)	108g
Boric Acid (Sigma)	55g
0.5M EDTA pH 8.0 (Fisher)	40ml

Make up to 1L with double distilled water

Loading Buffer

Glycerol	3ml
Bromophenol blue	50mg
10X TBE	1ml
Distilled water	6ml

DNA Lysis Buffer

IM Tris pH 7.5 (Fisher)	5ml
0.5M EDTA (Fisher)	10ml
5M NaCl (Fisher)	2ml
Spermidine phosphate (Sigma)	29mg
Dithiotheitol (DTT) (Sigma)	75mg
10% SDS (Fisher)	10ml

Make up to 100ml with double distilled water

10X TE Buffer

Tris (Fisher)	1.2g
EDTA (Fisher)	0.37g

pH 8.0 and make up to 100ml with double distilled water

20X SSC

NaCl (Fisher)	350.6g
Tri-Sodium Citrate (Fisher)	176.5g

In 2L of distilled water pH 7.2

Hybridisation solution

For each 50ml aliquot of hybridisation solution

Dextran sulphate (Amersham Pharmica), 6% solution in distilled water	30ml
20X SSC	15ml
10% SDS	5ml

Store frozen, 25ml is sufficient for 1 membrane.

10X Colony PCR Buffer

3M KCl (Fisher)	8.3ml
1M MgCl (Fisher)	0.75ml
1% Gelatin (Sigma)	5ml
1M Tris (fFisher) pH8.3	5ml
100% Triton X100 (Fisher)	2.25ml
100% Tween 20 (Fisher)	2.25ml
Distilled water	26.45ml

PK/PCR Buffer for Colony PCR

Proteinase K (ICN)	0.002g/100µl distilled water

Add 10µl to 2ml of 1X Colony PCR Buffer

Solutions for flow cytometry (Vindelov Analysis)

Citrate Buffer

Sucrose (Fisher)	85.5g
Tri-sodium citrate (Fisher)	11.76g
Double distilled water	800ml
DMSO (Sigma)	50ml

pH to 7.6 with 5M HCl

Stock solution

Tri-sodium citrate (Sigma)	2g
TRIZMA base (Sigma)	121mg
Spermidine tetrahydrochloride (Sigma)	1044mg

Nonidet P40 (Sigma)	2ml
Double distilled water	2L

Adjust pH to 7.6 with 5M HCl

Solution A

Trypsin (Sigma)	15mg

In 500ml of the stock solution, store frozen

Solution B

Trypsin inhibitor (Sigma)	250mg
Ribonuclease A (Sigma)	50mg

In 500ml of the stock solution, store frozen

Solution C

Propidium iodide	208mg
Spermidine tetrachloride (Sigma)	500mg

In 500ml of the stock solution, store frozen and protect from light

Solutions for Cell Culture

Trypsin-EDTA

Trypsin	0.25%
EDTA	0.1%

In 1X PBS pH 7.6